Smart TSO-DSO interaction schemes, market architectures and ICT Solutions for the integration of ancillary services from demand side management and distributed generation

Italian Pilot Report

D5.1

Authors:

Luca Ortolano (TERNA), Margherita Palleschi (TERNA), Giacomo della Croce (SELTA), Michele Erba (SIEMENS), Carlo Arrigoni (SIEMENS), Alessandro Bernardini (SIEMENS), Dario Colombo (SIEMENS) Alberto Bridi (EDYNA), Marco Baldini (EDYNA), Gianluigi Migliavacca (RSE)

Distribution Level	Public
Responsible Partner	Terna
Checked by WP leader **Carlos Madina**	Date: 17/06/2019
Approved by Project Coordinator **Gianluigi Migliavacca**	Date: 17/06/2019

This project has received funding from the European Union's Horizon 2020 research and innovation programme under grant agreement No 691405

Issue Record

Planned delivery date	30/06/2019
Actual date of delivery	
Status and version	0.11

Version	Date	Author(s)	Notes
0.1	28/06/2018	Terna	First Draft
0.2	30/08/2018	Terna	Second Draft
0.3	25/09/2018	Selta, Siemens	Added contributions
0.4	01/10/2018	Terna	Modified some sections and added more contributions
0.5	24/10/2018	Selta, Siemens	Added contributions
0.6	16/01/2019	Edyna	Added contributions
0.7	22/01/2019	Terna, Siemens, Selta, Edyna	Version sent to WP Leader
0.8	13/02/2019	Terna, Siemens, Selta, Edyna	Modified according to WP Leader's comments
0.9	27/03/2019	Edyna, Siemens, Selta	Added test results and modifications
0.10	30/04/2019	Siemens	Added test results
0.11	11/06/2019	Terna	Final updates to the document

About SmartNet

The project SmartNet (http://smartnet-project.eu) aims at providing architectures for optimized interaction between TSOs and DSOs in managing the exchange of information for monitoring, acquiring and operating ancillary services (frequency control, frequency restoration, congestion management and voltage regulation) both at local and national level, taking into account the European context. Local needs for ancillary services in distribution systems should be able to co-exist with system needs for balancing and congestion management. Resources located in distribution systems, like demand side management and distributed generation, are supposed to participate to the provision of ancillary services both locally and for the entire power system in the context of competitive ancillary services markets.

Within SmartNet, answers are sought for to the following questions:

- Which ancillary services could be provided from distribution grid level to the whole power system?
- How should the coordination between TSOs and DSOs be organized to optimize the processes of procurement and activation of flexibility by system operators?
- How should the architectures of the real time markets (in particular the markets for frequency restoration and congestion management) be consequently revised?
- What information has to be exchanged between system operators and how should the communication (ICT) be organized to guarantee observability and control of distributed generation, flexible demand and storage systems?

The objective is to develop an ad hoc simulation platform able to model physical network, market and ICT in order to analyse three national cases (Italy, Denmark, Spain). Different TSO-DSO coordination schemes are compared with reference to three selected national cases (Italian, Danish, Spanish).

The simulation platform is then scaled up to a full replica lab, where the performance of real controller devices is tested.

In addition, three physical pilots are developed for the same national cases testing specific technological solutions regarding:

- monitoring of generators in distribution networks while enabling them to participate to frequency and voltage regulation,
- capability of flexible demand to provide ancillary services for the system (thermal inertia of indoor swimming pools, distributed storage of base stations for telecommunication).

Partners

Table of Contents

List of Abbreviations and Acronyms

Acronym	Meaning
aFRR	automatic Frequency Restoration Reserve
AVR	Automatic Voltage Regulator
DCS	Distributed Control System
DER	Distributed Energy Resources
DG	Distributed Generation
DSO	Distribution System Operator
DSO OC	DSO Operation Center
EU	European Union
FCR	Frequency Containment Reserve
FRR	Frequency Restoration Reserve
HB	Half-band
HMI	Human-Machine Interface
HV	High Voltage
HVRS	High Voltage Regulation System
IPS	Estimation Accuracy Index
LV	Low Voltage
MV	Medium Voltage
MVRS	Medium Voltage Regulation Systems
NRA	National Regulatory Authority
OLTC	On Load Tap Changers
ORPF	Optimal Reactive Power Flow
PCR	Plant Central Regulator
PV	Photovoltaic
RES	Renewable Energy Source
SAS	Substation Automation System
SAT	Site Acceptance Test
SM	Sentinel Measurement
TSO	Transmission System Operator
TSO OC	TSO Operation Center
VPP	Virtual Power Plant

Executive Summary

The Italian pilot represents a technological application within Horizon2020 SmartNet project. It aims to find new and innovative technological solutions to promote the integration of renewable energy sources (RES) and distributed generation (DG) in smart grid systems. In particular, the purpose was to develop, implement and test in field innovative devices to demonstrate the technical feasibility of increasing the monitoring of the distribution grid and the controllability of RES connected at lower voltage levels. From the point of view of the electrical grid, the purpose was to involve DG and RES, which currently do not participate in real-time management of the grid, in the provision of ancillary services and to analyse the accuracy and the reliability of their contribution.

The pilot is located in a portion of the grid characterized by high hydro penetration connected at all voltage levels. The services considered were the voltage regulation from power plants connected at sub-transmission grid and the frequency/power regulation from DG.

The pilot project has been realized by a consortium that is made up of 5 Italian participants with wide experience and expertise in different fields:

- Terna, the Italian transmission system operator (TSO), is the pilot leader, involved mainly in the coordination of the pilot to define the executive specification of the functionalities and to organise tests to telecontrol the virtual power plant to test the functionalities of the devices;
- RSE (Ricerca sul Sistema Energetico) is expert in electro-energetic research and coordinator of the project SmartNet;
- Edyna is the distribution system operator (DSO) that manages the medium voltage (MV) grid involved in the project;
- Siemens and Selta are the technological partners that developed the devices whose functionalities are detailed in this document.

This deliverable describes in detail all the aspects of the pilot realization and it is structured as follows:

- The introduction shows the Italian energy context, the future scenarios characterized by the spread of RES and the consequent evolution in the management of the grid;
- The area where the pilot is localized is described and the main characteristics of the distribution grid involved in the pilot are illustrated in chapter 2;
- The following chapters of the document describe in detail each functionality implemented in the devices realized by the technological partners, comparing the different approaches and algorithms developed by Siemens and Selta;
- Chapter 5 contains the explanation of the tests and analysis carried out to evaluate each functionality of the project;

- Chapter 6 is dedicated to the outcomes of the tests carried out employing the three devices developed;
- At the end of the document, the report contains the conclusions focusing in particular on the future opportunities and on aspects that need to be improved in order to overcome the issues encountered in the experimentation.

1 Introduction

The Italian pilot represents a technological application within SmartNet project and it aims to implement new tools for ancillary services provision by renewable energy resources (RES) connected at both high-voltage (HV) and medium-voltage (MV).

The European Union (EU) has adopted a policy that aims to replace the fossil fuel promoting the development of renewable forms of energy. The Member States have adopted national actions in order to meet their renewables targets by 2020.

As reported in the Grid Development Plan 2019 of Terna [1], the strategy aims to further increase the renewable capacity: already reached the 2020 objective, the targets set by the National Energy Strategy provide for renewable sources reaching a level of 28% of total consumption at 2030 (in particular a 55% share of renewables in electricity consumption) and for the complete phase-out from coal by 2025. Figure 1 represents the breakdown by sector of the targets of the National Energy Strategy.

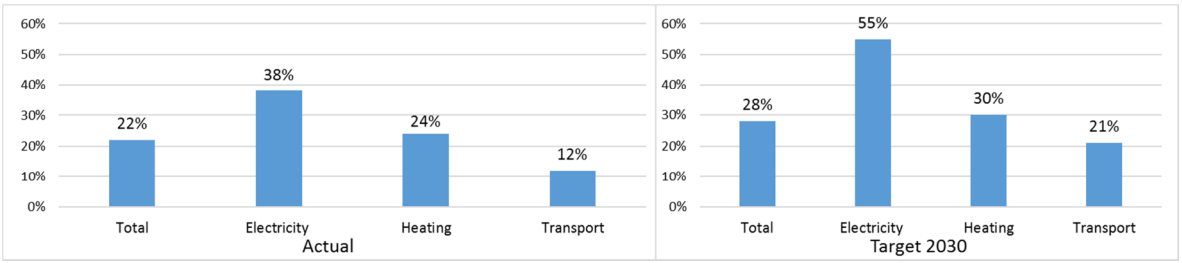

Figure 1: Penetration of renewable energy per sector

Such a policy has led to an important growth of the renewable penetration in the last 10 years: as shown in Figure 2, extracted from Grid Development Plan 2019 [1], since 2008, about 6.6 GW of wind power capacity and about 19.6 GW of solar photovoltaic (PV) power capacity have been installed.

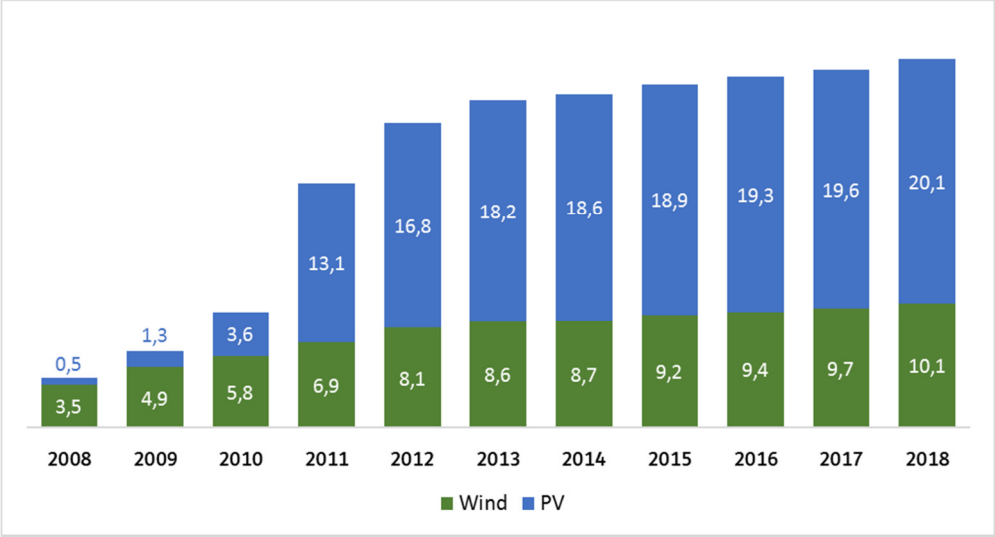

Figure 2 Wind and photovoltaic capacity installed in Italy (GW), 2008-2018 [1]

Two are the main characteristics of renewable forms of energy generation that can influence the management of the electrical system.

On one hand, they have a variable behaviour that depends on aleatory primary energy sources (wind, sun or water). On the other hand, the growth of renewable penetration is closely linked to a spread of the distributed generation because the small-sized renewable plants are often connected to the distribution network, especially PV panels and small hydro power plants.

There is then an important increase of units located at MV and low voltage (LV) levels, characterized by unpredictable generation and currently not observable and not able to provide ancillary services necessary to allow the transmission system operator (TSO) to manage the grid.

The energy framework is moving from a power generation mainly characterized by few traditional plants connected to HV transmission grid and controlled directly by the TSO to a park composed by numerous plants connected to MV and LV grids. In the past, the distribution grids were traditionally considered and planned as "passive" networks: power flows were unidirectional, from the HV grid, where generation plants were connected, to the distribution grid, composed mainly by loads. The new configuration characterized by a growing distributed generation (DG) often leads to reverse power flows. In case of local oversupply at the distribution level, i.e. when the distributed generation exceed the local consumption connected to the same substation, the power can rise-up from lower to upper voltage levels of the grid. The bidirectional nature of power flows could influence the system management and operation of the transmission grid. This scenario is particularly evident in areas where Distributed Energy Resources (DER) have high penetration, as in mountain areas where many small-sized hydro power plants are installed.

In order to quantify the problem, the growth of the number of transformers of the main Italian distribution system operator (DSO) subject to the reverse flow from distribution to transmission grid is illustrated in Figure 3, published on the Grid Development Plan 2019 of Terna [1].

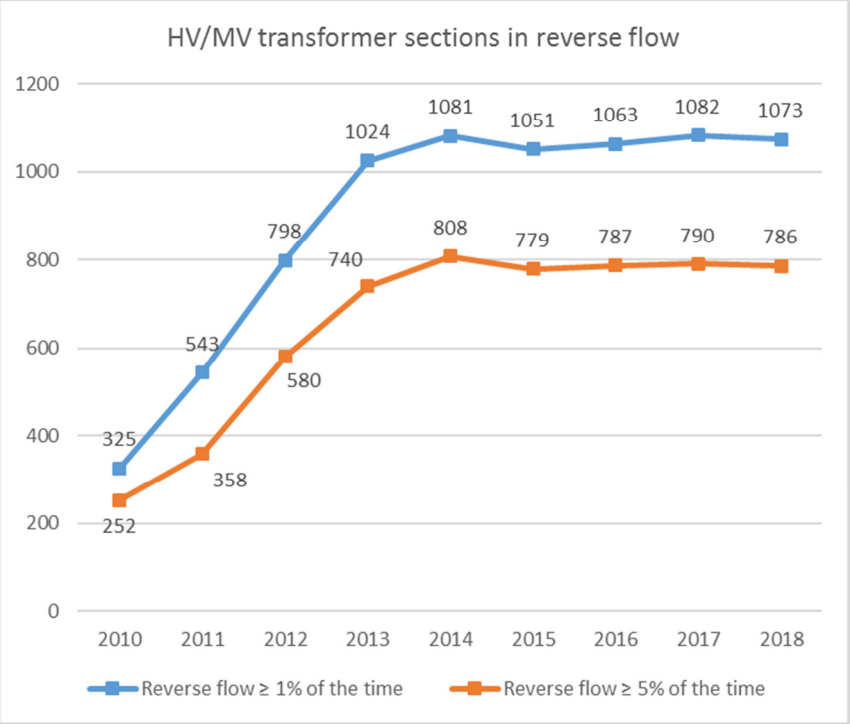

Figure 3: HV/MV transformer sections of e-distribuzione in reverse flow

The bidirectional nature of power flows could influence the system management and operation of the transmission grid. The reversal of the power flows at the HV/MV transformers of the interconnection points between TSO and DSO grid leads to:

- Increasing of the voltage in HV grid, because when the active power along a line is below the nominal value, the power line produces reactive power. This involves a consequent increasing of the need of sources to control and regulate the grid voltage, that, at present, are provided by traditional programmable big-size plants.
- The inadequacy of the current automation and monitoring devices at the HV side of the primary substation, particularly in radial networks designed for unidirectional power flow, affecting also the efficiency of the operation and of the monitoring.
- The reduction of selectivity and efficiency in the load curtailment, measure taken in case of emergency state, because the disconnection of a primary substation implies not only disconnection of demand but also of generation and the net load disconnected is lower than in the past.

Furthermore, the high penetration of non-programmable DG implies issues related to the frequency and voltage profiles regulations, because these types of generators cannot foresee and ensure a fixed power exchange with the system; furthermore these plants cannot provide ancillary services, such as frequency containment reserves (FCR), frequency restoration reserves (FRR) or reactive power control, and it means that it is necessary to maintain thermoelectric plants in operation, also at off-peak times, to provide ancillary services.

The spread of RES leads also to the reduction of the downward reserve, particularly during daylight hours when the PV generation, not controllable, is high, and of the upward reserve, particularly during periods of drought that reduce the hydroelectric generation or for peak load demand.

The Italian pilot within SmartNet aims to study opportunities and challenges of integrating renewable energy in ancillary services provision with the intent to anticipate future developments in the operation of electrical power system.

In particular, to enable DG to become active players in the electricity system, it is necessary to improve the observability of the whole grid and to allow DER and RES to provide ancillary services.

For this reason, the functionalities developed in the project are:

- The observability module, to have an accurate real time observation of the MV and LV sources. Measurements and estimations of the power of the plants located at distribution level are aggregated and provided to the TSO to achieve a continuous and adequate monitoring of the grid.
- The voltage regulation, to achieve a hierarchical control of the reactive power regulation through generators connected to both HV and MV grid;
- The power/frequency regulation, in particular, the automatic FRR (aFRR), by generators connected to MV grid, currently not included in the Italian market.

2 Grid involved in the pilot

The pilot is located in the area of Ahrntal valley (Figure 4), in northern Italy, at the border with Austria. The choice of this location is due to the availability of several generating modules of different sizes connected to different voltage levels.

Figure 4: Location of the Italian pilot

Regarding the part of the project that involves the HV grid, the project involved two hydroelectrical power plants of about 43 MW, directly connected to the TSO sub-transmission grid (132 kV).

On the other hand, part of the project involves the MV grid, powered by the primary substation of the DSO characterized by 2 HV/MV (132/20 kV) transformers of 40 MVA each. There are 9 MV feeders outgoing from this substation: 3 of them feed distributed load at LV level (mainly domestic consumers, touristic loads and small-sized industry) and the other 6 are dedicated to MV producers or local subtended DSOs. For the specific geographical characteristics of the area, the feeders are long and without counter feeding from other lines, as shown in Figure 5. At the MV grid, there are 23 producers connected, with an installed power of 29 MW (27.7 run-of-river hydroelectric, 1.5 biomass, 0.2 PV), and 5 local DSOs characterized by a small number of customers fed by one or more small-size hydroelectric plants. Due to the behavior of the subtended grid, the interconnection points with local DSOs are comparable to prosumers with 17 MW of total power consumption. Finally, there are installed 0.85 MW of generation in the LV level (0.73 MW of PV).

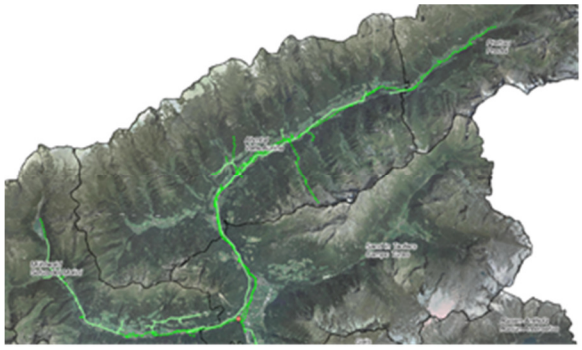

Figure 5: Topology of the distribution grid

The consequence of this installed production at MV and LV levels is that for almost the whole year in the interconnection point between TSO and DSO (Primary substation) the power rises from MV to HV, with a peak higher than 30 MW in summer. Figure 6 shows the trend of the active power flow at the primary substation: during periods of drought, the hydroelectric generation is reduced and the peak load demand causes a flow from HV to MV grid; instead, during the summer the abundant water flows lead to a high hydroelectric production that often exceeds the local load, causing reverse flow. The convention used by Terna is the passive sign convention and the power value is negative when active power is supplied to the transmission grid.

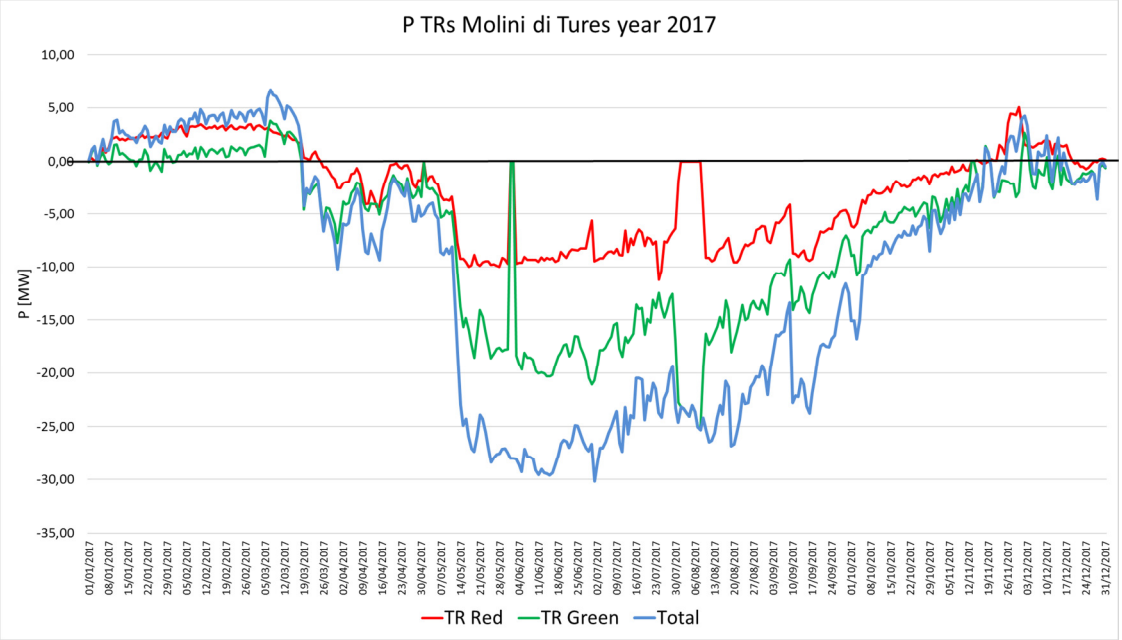

Figure 6: Trend of the active power at the HV/MV primary substation during 2017

Within this scenario, the Italian pilot is a technological project that aims to implement new devices to investigate the feasibility to integrate RES in the management of the grid by the TSO.

The High Voltage Regulation System (HVRS), developed by Siemens, has been installed in the HV substation of Molini di Tures in order to control the reactive power of the two plants that currently do not participate in hierarchical voltage regulation.

The Medium Voltage Regulation Systems (MVRSs), developed by Selta and Siemens, have been installed in the DSO Operation Center (DSO OC) in order to monitor and control the DG connected to each HV/MV transformer of the Primary Substation.

As represented in ***Figure 7***, Selta has installed in field the 28 Plant Central Regulators (PCRs) in order to monitor 16 plants and 5 interconnection points with subtended DSOs and, furthermore, to monitor and control 7 of the biggest hydroelectric plants of about 22 MW total. PCR represents the most peripheral device in the communication chain between the TSO and the plant. It plays an essential role for

observability of the DSO grid, for the Voltage Regulation and power/frequency Regulation purposes. It allows the monitoring and the control functions of the MV DERs. Indeed, when PCR interfaces a controllable DER, it makes available the functions of reactive power and cosphi modulation in V Regulation and active power modulation in the f/P regulation.

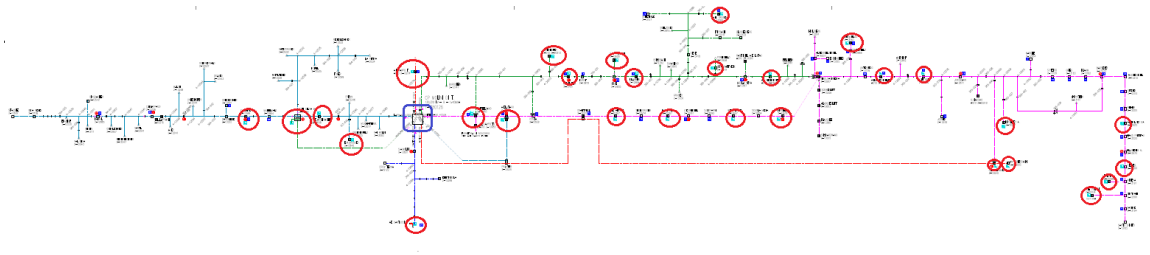

Figure 7: Localization of the PCRs installed in the distribution grid

The system architecture implemented in field and the data flow among the devices involved in the project are represented in Figure 8. The communications are based on standard protocols: IEC 60870-5-104 to communicate with the TSO and IEC 61850 to communicate with power plants.

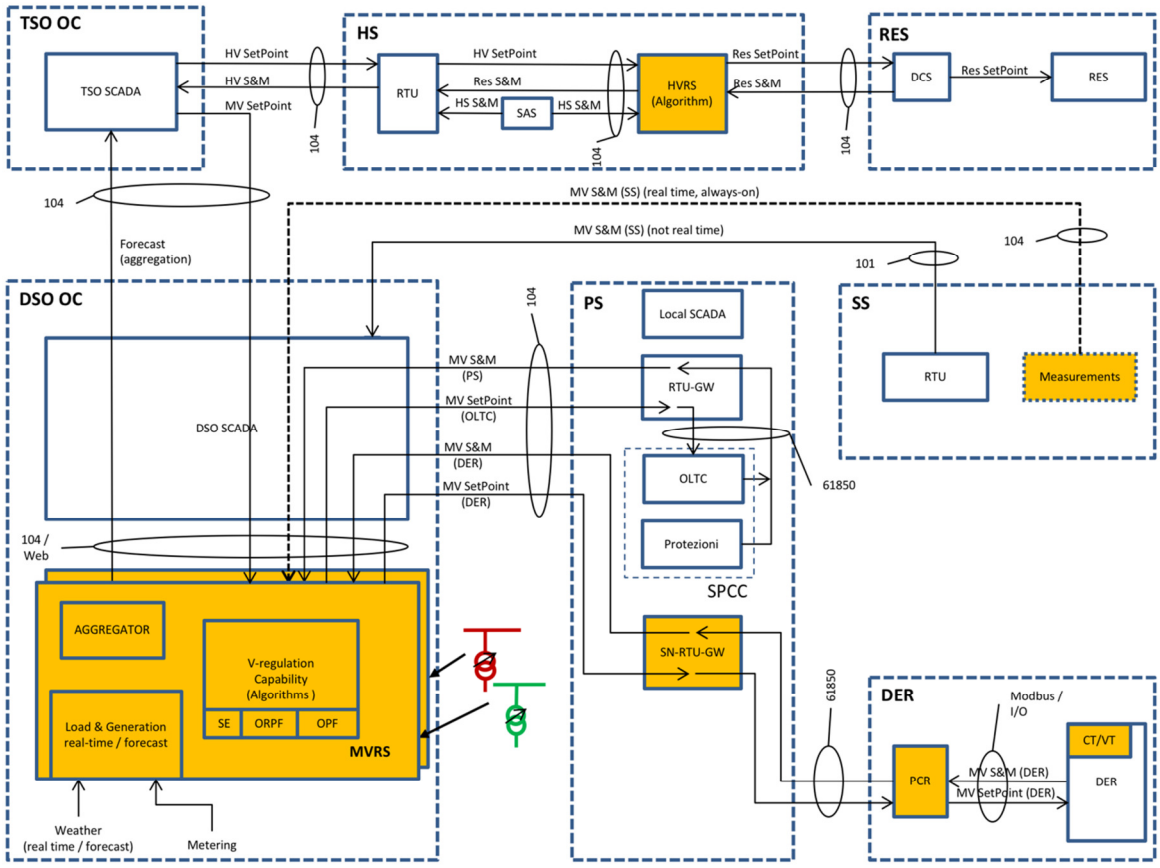

Figure 8: Architecture of the system implemented in the Italian Pilot of SmartNet: at the top is represented the HVRS system and at the bottom is represented the MVRS system

The items depicted in the figure are:

- TSO OC: TSO Operation Center
- DSO OC: DSO Operation Center
- HS: HV Substation
- PS: Primary Substation
- SS: Secondary Substation
- RES: the RES power plants connected at the sub-transmission grid
- DER: MV generators/customers
- SPCC: local protection, command and control system, a system installed in substation for the protection, command and control functions at local level
- OLTC: On Load Tap Changer
- DCS: Distributed Control System
- HVRS: High Voltage Regulation System
- MVRS: Medium Voltage Regulation System
- PCR: device to interface the power generation module control system to the MVRS
- S&M: State & Measurements
- CT/VT: Current/Voltage Transformers

3 HVRS: Functionalities developed in the project

At present, Italian regulation provides that only conventional large power plants have to be equipped with specific devices to participate in the hierarchical control voltage. The evolution of electric system introduced above will benefice by the involvement of non-programmable RES generating facilities in the operation of electric power system to guarantee the margins of security and reliability of transmission and distribution systems.

One of the purposes of the pilot is to implement and test an innovative device to enable the involvement of RES in the dispatching function, such as PV plants, wind farms and small hydroelectric plants.

In SmartNet application, the HVRS (High Voltage Regulation System), developed by Siemens, has been installed in the Molini di Tures HV substation (132 kV) to smooth the voltage fluctuations measured in the substation by means of the reactive power exchanged by two HV hydro power plants (Molini di Tures and Lappago), connected at this substation. The purpose of the HVRS is to modify the reactive power of the four synchronous generators (absorption or injection) in order to satisfy the TSO command, which can be a reactive power amount or a voltage setpoint referred to the HV busbar of the substation.

As depicted in the Figure 8, the HVRS device is connected, on one side, to the Terna operation center (TSO OC) and, on the other side, to the power plant Distributed Control System (DCS).

Regarding the data flow between the HVRS and Terna, the measurements and status related to current, voltage and power flow at the HV Substation are sent to Terna's SCADA, together with some parameters pertinent to voltage regulation. The protocol enabling this data exchange is IEC 60870-5-104. The HVRS is also linked to the digital SCADA at the substation, the so-called Substation Automation System (SAS). The communication with Lappago and Molini di Tures hydro power plants is based on the IEC 61850 protocol and it allows a hierarchical voltage control.

All this information is summarized in the main human-machine interface (HMI) of the HVRS, as shown in Figure 9. In particular, the screen contains the voltage regulation parameters (in the upper part of the screen), an orange box for each generator (which resumes the regulation operating status and the calculated setpoint) and the single-line diagram of the substation (with the indication of active and reactive power and voltage measurements).

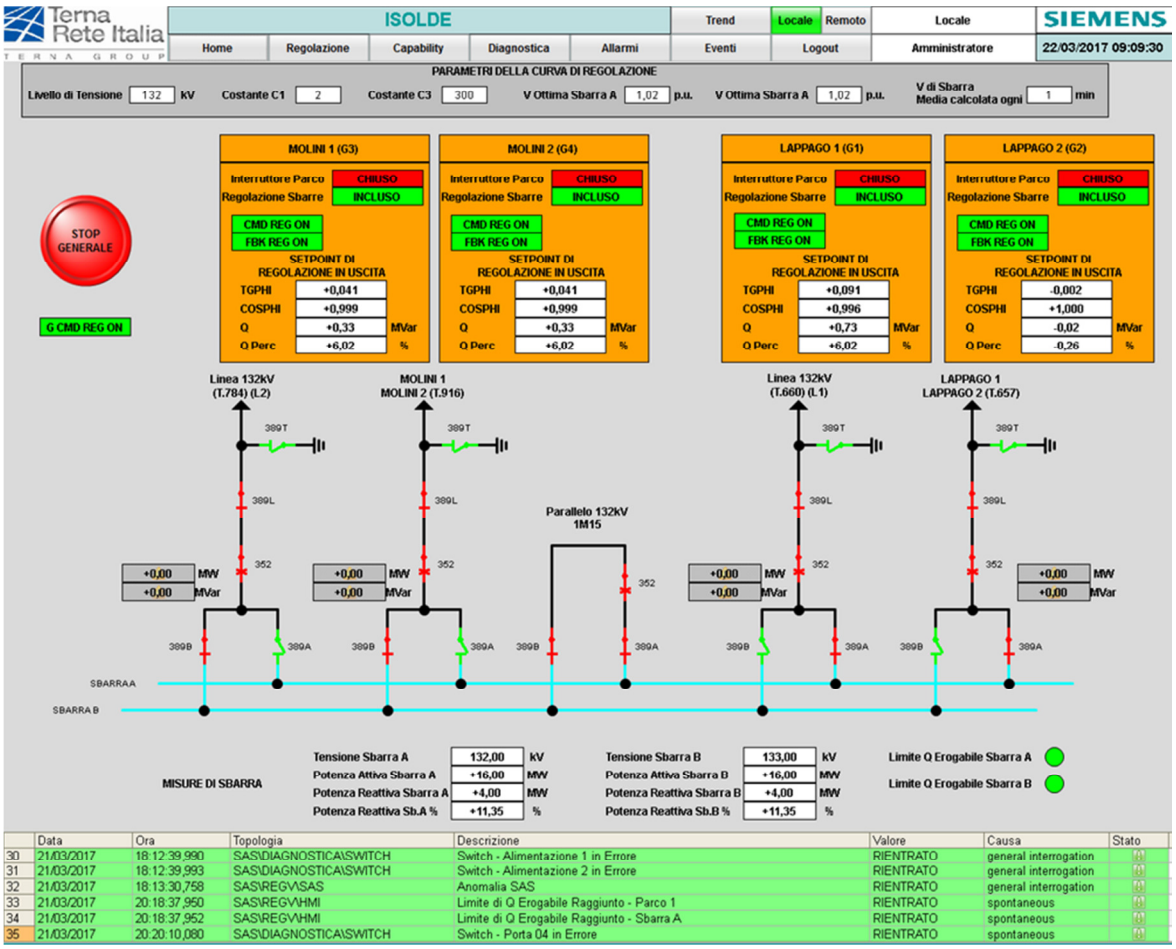

Figure 9: Main HMI of the HVRS device

The HV voltage regulation functionality implemented in the HVRS is summarized in the block diagram in Figure 10, which shows that Terna's control center can select the regulation signal between reactive power and voltage. In the first case, the reactive power (Q) setpoint is a percentage value of the capability, calculated in actual operating conditions, to be interpreted as follow:

- A value between (0, + 100%] indicates the condition of over-excitation, i.e. represents the reactive power that has to be provided by the plants in order to increase the voltage.
- A value between [-100%, 0) indicates the condition of under-excitation, i.e. represents the reactive power that has to be absorbed by the plants in order to reduce the voltage.

If a reactive power setpoint in p.u. is sent to the HVRS, the algorithm will share the desired reactive power level among the four synchronous generators and the HVRS will send the individual values to the DCS in each power plant.

In the second case, the setpoint is a voltage value expressed in kV. If Terna requires an optimal voltage value at the Molini di Tures HV busbar, the HVRS converts the setpoint in a reactive power command on the basis of the voltage error, defined as the difference between the voltage setpoint and the voltage

measurement. This is achieved through flexible and parametric correlations between the production/consumption of reactive power and the voltage error detected, and the reduction to zero of the voltage error.

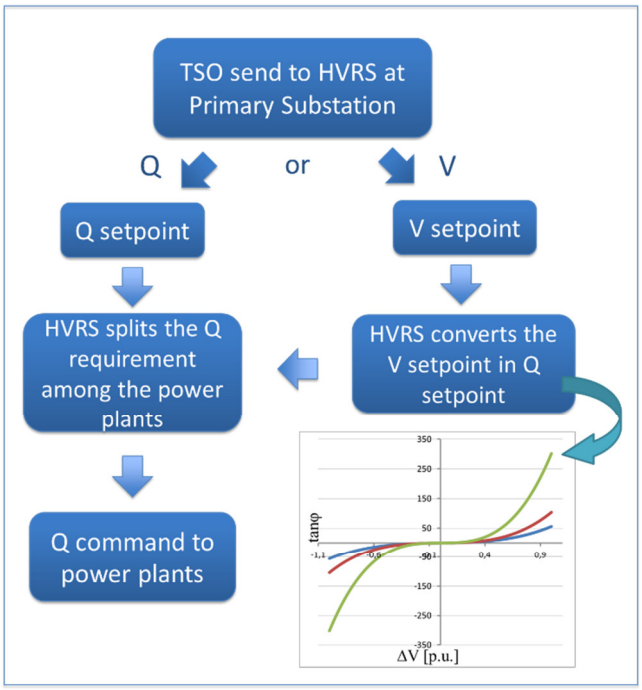

Figure 10: Diagram of operation of the HVRS

The cubic correlation law links the voltage error to the tgφ, as represented in Figure 11: the regulation sensitivity with respect to the voltage error is adjustable by acting on the coefficients c1 and c3, from a less sensible regulation (e.g.: c1 = 6 and c3 = 50 in Figure 11) up to a more consistent involvement of the regulating resources (e.g.: c1 = 2 and c3 = 300).

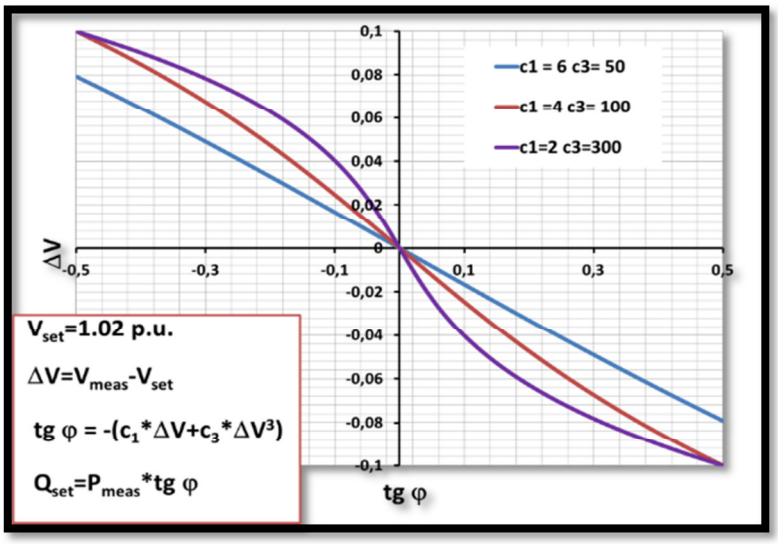

Figure 11: Cubic correlations of the control law

The capability curves of each power unit involved in the HVRS regulation (Molini di Tures and Lappago) are respectively depicted in Figure 12 and Figure 13.

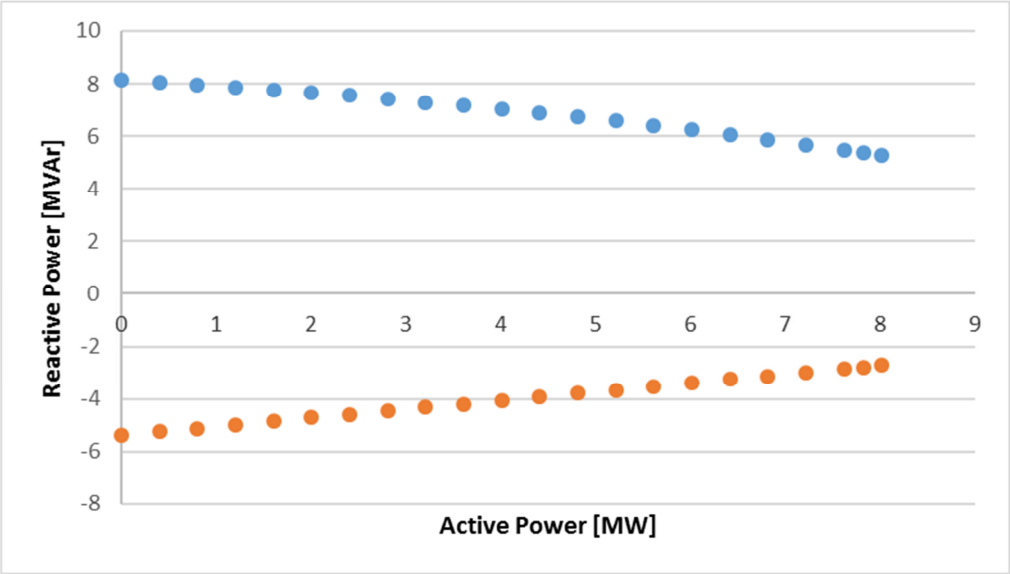

Figure 12: Capability Curve of Molini di Tures Unit

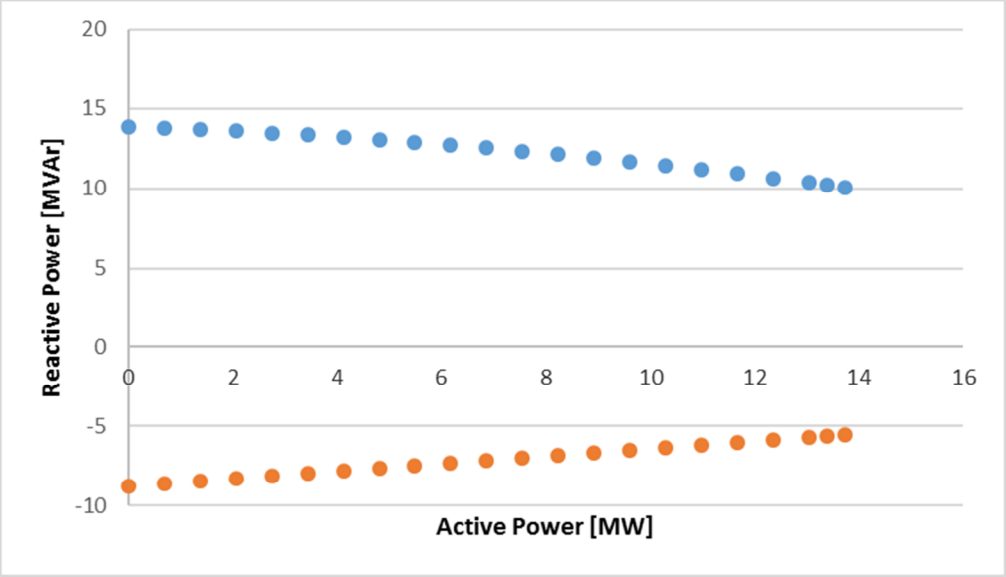

Figure 13: Capability Curve of Lappago Unit

Regardless of the type of setpoint, the HVRS splits the command amongst the controlled generators in order to obtain a homogenous distribution of the efforts and avoid undue reactive power flows between providers in the same electrical area. In order to determine the reactive power availability of the whole controlled system, the algorithm developed in the HVRS calculates the reactive capability of each generator corresponding to the operational point, computes the virtual capability of the system on the basis of the grid configuration and sends it to the TSO.

4 MVRS: Functionalities developed in the project

The second type of device developed within the project is MVRS (Medium Voltage Regulation System) that is intended to manage, monitor and control the DG connected at Edyna's grid.

The technological partners, Siemens ad Selta, have developed two different devices, each with its own algorithms and approaches. In fact, each manufacturer, both important vendors in Italian context, has applies its own experience in the development of automatisms employed in Italian electrical grid to implement innovative systems and functionalities to reach the purpose to increase the integration of DG in the power system.

Each of the functionalities implemented will be described in detail in the following sections.

4.1 Observability

The data considered in the observability function are classified in three categories:

- Nominal data, in order to represents properly the grid: nominal data regarding the active power installed at the primary substation have to be collected for the different type of energy sources (PV, wind, storage and other sources) and for the load, and shall be updated (e.g. every 3-6 months);
- Real-time data, to estimate the grid operational conditions and the availability of the resources:
    - Real-time data for observability: the MVRS is able to send the aggregations of active and reactive power to the TSO, differentiated according to the type of energy source, equivalent to the DER connected at the HV/MV transformers. The aggregations of generation are composed by measurements in field, acquired by PCRs, and estimations of unmonitored plants and LV generation. The gross amount of load is calculated as the difference between the measurement at the interconnection point and the generation. The aggregation is composed every 20 seconds and sent to the TSO every 4 seconds. The estimation algorithm is based on the available measurements of monitored plants, real-time weather data and/or historical power profiles acquired by energy meters.
    - Real-time data for capability: real-time data are used by the MVRS also to calculate the virtual capability at the TSO/DSO interconnection point in order to define the active and reactive availability for ancillary services from MV resources. The calculation of the virtual capability has to consider the capabilities of each distributed generator, taking into account the distribution grid constraints. Through the virtual capability, the TSO can send voltage or active power setpoint to the DG, considering it as a unique virtual plant comparable to a traditional plant, so allowing a centralized activation that always respects the DSO network constraints.

- Forecast data, in order to predict the future operational conditions: the DSO also has to send the active power profile forecast through the MVRS, taking into account also predicted changes in the grid configuration. The forecast must be sent to the TSO every 3 hours, with 1-hour resolution and covering the next 72 hours.

Regarding the improvement of the real-time observability of the whole electrical grid, the Italian National Regulatory Authority (NRA) ARERA issued a resolution (646/2015/R/eel) to promote the implementation of services to allow a reliable and effective management of distribution grids characterised by a high penetration of DG. The implementation of the observability refers to the principle of this NRA resolution, but (and this is one of the *lessons learnt*) the update time of 20 seconds seems not to be coherent with the aFRR activation monitoring requirements.

The aggregation of real-time data to be transmitted to the TSO OC is obtained by the following steps:

- Acquisition of power measurement, through PCRs installed in field to measure the production of all the power plants of the selected MV grid and the power exchange at the interconnection point with subtended DSOs.
- Estimation of unmonitored plants' data, through algorithms that elaborate and combine available data (e.g. weather data, neighbouring plants' measurements, "near real-time" data registered by smart energy meters, historical profiles…).
- Aggregation of measured and estimated data at the interconnection point between HV and MV grids, differentiated by energy sources.
- Transmission of the aggregated data to the TSO, to obtain a nodal representation of the equivalents connected at each HV/MV substation. The aggregation is updated every 20 seconds, in accordance with the NRA's resolution, and sent to the TSO every 4 seconds, in accordance with the sample rate of the control system.

The process is represented in Figure 14.

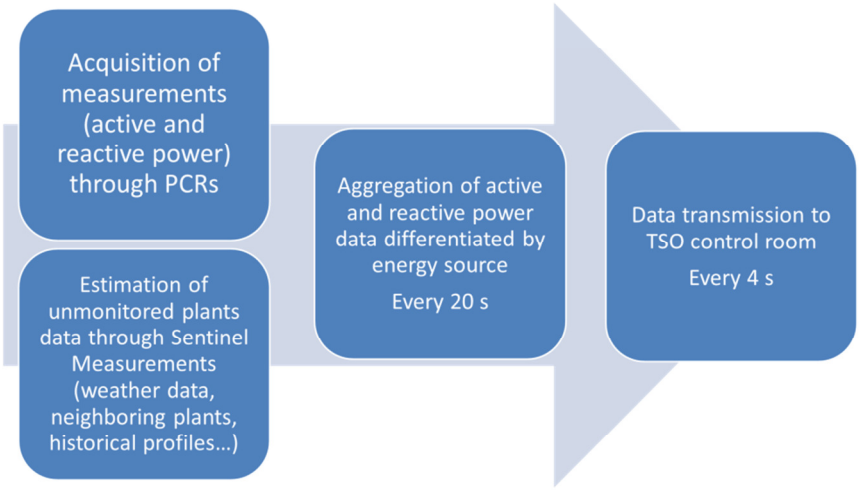

Figure 14: Diagram of operation of the observability functionality of MVRS

As anticipated, in this application, the measurements cover almost all the grid in order to obtain the required accuracy needed to test the provision of ancillary services from DG. The estimation algorithms proposed by Siemens and Selta were therefore not used for the composition of the aggregations in real-time, but for off-line analysis that aimed to assess the accuracy of the proposed approaches.

From the TSO's point of view, the possibility to know the accurate amount of the resources, split into generation and load at all times, leads to a more efficient and safe management of the transmission grid. Firstly, the observability functionality gives a better perception of the energy mix underlying the primary substation and, in particular, of the geographic allocation of the generation and the actual energy consumption of the load. It allows improving the grid calculation, where currently a gross estimate based on the installation is used, i.e. for state estimation and for static and dynamic simulations online and offline to individuate also critical constraints. It could enhance the Defence System, adapting the protection scheme of the system, and it could increase the adequacy of the Load Shedding Plan, providing the awareness of the real presumption disconnection. Moreover, it could support the TSO during the restoration of the service after a disconnection at the station.

Finally, the acquisition of real-time data could improve the algorithms to calculate the consumption forecast in different time frames, processing this type of data with appropriate probabilistic methods. It allows to predict the evolution of the active and reactive power flows, which is especially useful when a high penetration of DER can lead to reverse flow from MV to HV grids.

Another important application of this functionality is the identification of the capability of the virtual power plant connected to the primary substation and composed by MV plants. The calculation of the active and reactive power availability takes into account the distribution grid constraints. It means that

the observability provides the possibility to identify the potential contribution in the voltage and active power regulation.

Each constructor has developed its own estimation algorithm characterized by different approaches and different input. In order to evaluate the accuracy of the solution adopted, Terna has required the respect of an index of energy accuracy that will be described in section 5.2. The approaches adopted by each manufacturer are described in the following sections.

4.1.1 Selta estimation algorithm

The Selta nowcast estimation algorithm is based on the concept of Sentinel Measurements (SMs), as summarized in the scheme of Figure 15. The SMs can consist of real-time power measurements related to plants monitored by PCRs, of historical power profiles acquired by energy meters or of real time weather data (e.g. solar radiation, air temperature or river flow). Taking into account the historical data, it is possible to calculate the correlation coefficients between the unmonitored DERs and the SMs. This off-line evaluation, updated monthly, allows to find out the relationship between neighbouring plants of the same primary source (e.g. hydroelectric generators) and to assess the impact of weather variables (in particular for the PV plants). Therefore, the best SMs (3 SMs in practical applications) are selected for each unmonitored DER and appropriate weights are generated.

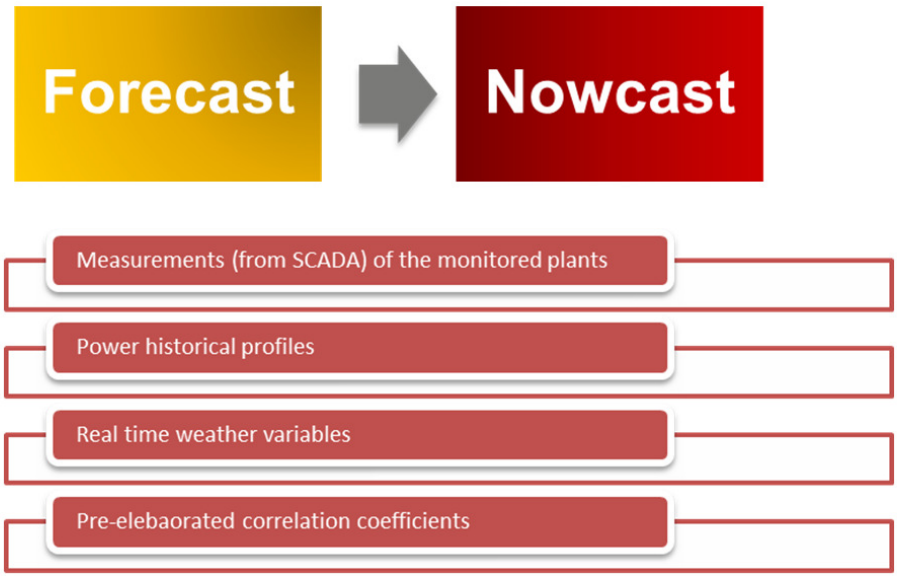

Figure 15: Sentinel Measurements for nowcast estimation

An example of the off-line comparison necessary for defining how much a SM and an unknown measurement are linked will be illustrated in paragraph 6.2.1.

A different approach is carried out for the estimation of reactive power exchanged by the unmonitored plants. Considering the historical metering, the average value of cos phi is calculated for

each generator. Therefore, the on-line evaluation of reactive power is computed as directly related to the estimation of active power through the corresponding cos phi.

4.1.2 Siemens estimation algorithm

The Siemens solution is based on an integrated architecture that is able to elaborate and combine non-homogenous raw data. The non-homogenous data is represented by MV plants monitored through field meter (PCR) and unmonitored MV plant estimated with different techniques.

In particular, to estimate the real and reactive power amount for each unmonitored MV plant and each MV/LV Secondary Substation transformer, the system is able to consider real-time weather data (solar radiation and temperature) and "near real-time" data registered by energy meters of MV plants (on a 15-minutes basis, originally used for billing purposes).

Figure 16 shows the architecture of the system and how the different data are gathered and processed.

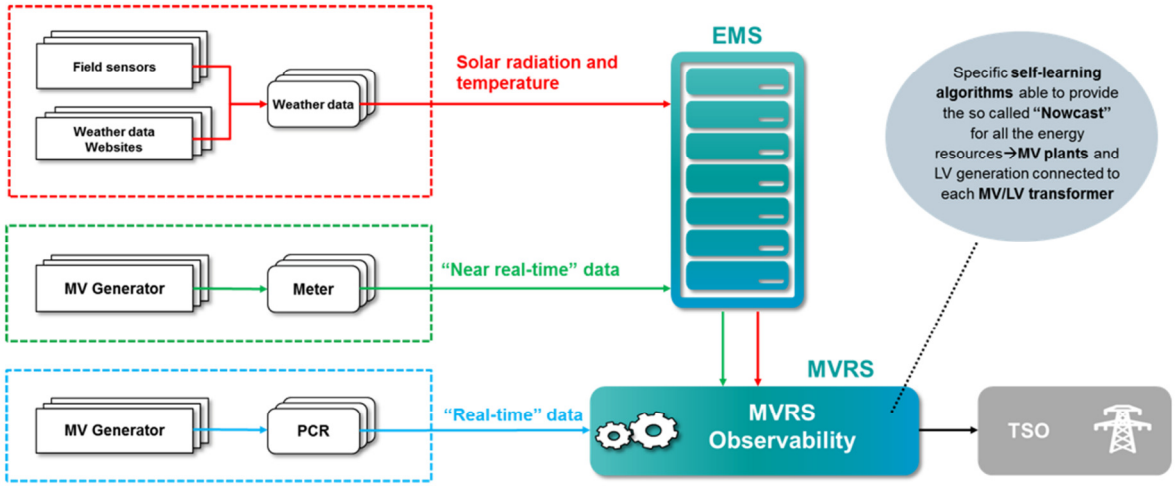

Figure 16: Observability architecture of Siemens system

Regarding the estimation of PV generation, the weather data are processed by a specific Siemens application based on a self-learning algorithm that, considering the geographical location and the physical characteristics of each plant, is able to provide the so called "nowcast" for all the PV plants connected to the DSO electrical network (MV plants and LV generation connected to each MV/LV transformer). An example of the PV estimation is shown in Figure 17.

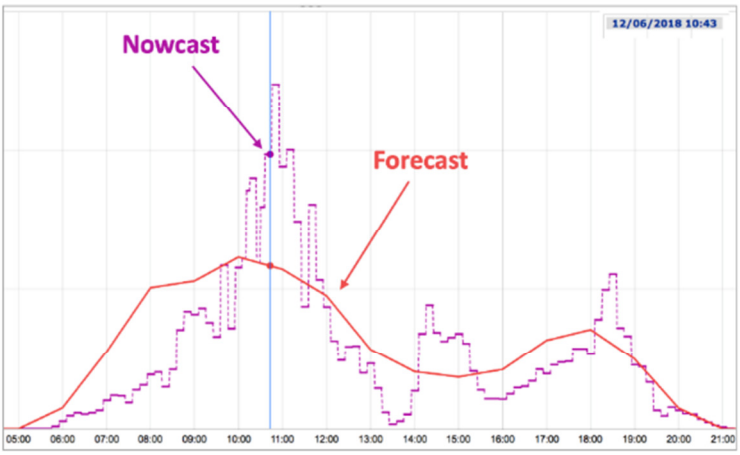

Figure 17: Nowcast estimation for PV plants

All the other energy resources (i.e. non-renewable or hydroelectric) are estimated processing the combination of historical data and available "near real-time" data registered by energy meters. Figure 18 represents an example of the results obtained with the estimation of MV hydro plants: it is possible to see how the "near real-time" data registered by the energy meter (i.e. related to the previous 15 minutes) is used to obtain the current estimated generation value.

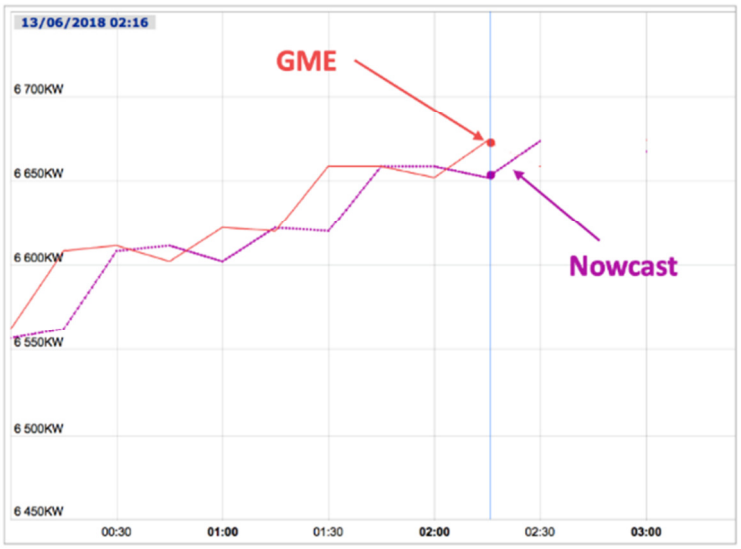

Figure 18: Nowcast estimation for hydroelectric plants

All the nowcast data is then transferred to the Siemens Monitoring & Control system, which carries out the selection and combination of this data with the real-time measurements coming from the field (PCR) to obtain the aggregated real and reactive power (HV/MV transformer level) ready to be sent to the TSO. Moreover, from this data and the HV/MV TR active power measurement, it is possible to estimate the overall load of the MV grid as the difference between the generation and the power measured at the primary substation.

4.2 Voltage regulation

In order to increase the amount of reactive power reserve, for the benefit of DSO and/or TSO, the MVRS also aims to involve DG in the voltage regulation ancillary service.

As shown in Figure 19, through the computation of the virtual capability, the MVRS provides to the TSO an instrument to command the reactive power of the plants connected to MV level of the grid considering them as a unique plant in order to regulate the HV voltage. It also considers under- and over-excitation limits, dictated by the DSO's grid constraints, and then it allows the TSO to send setpoints, while avoiding violations on the MV network. In case of constraints violation in the distribution grid, the priority of the device is to solve the violation, making the generators unavailable for the voltage regulation.

Once received the command, the algorithm provides a smart splitting of reactive power command among the controlled plants according to single DERs capability.

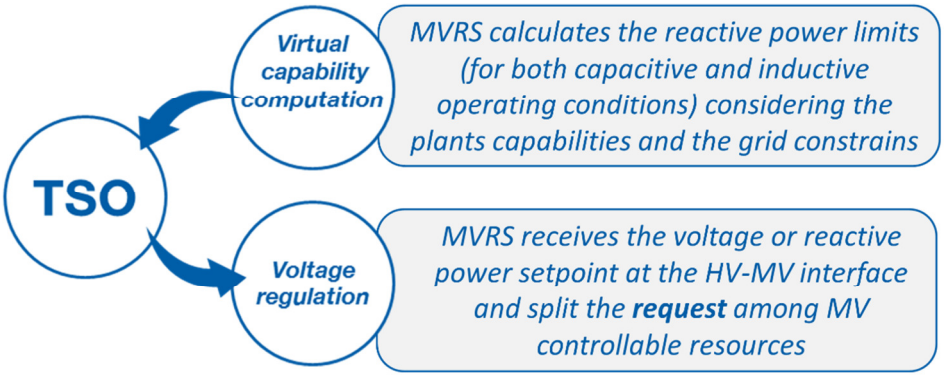

Figure 19: Diagram of operation of voltage regulation functionality of MVRS

The solutions developed by the vendors are based on the same project specification and then the phases of the computation are similar. Each approach, however, has different algorithms based on different assumptions, for instance, in the calculation of the capability and of the state estimation, or in the approximations adopted or in the command splitting. The solutions are described in the following sections.

4.2.1 Selta solution for the voltage regulation

Voltage regulation, implemented by Selta, works with a continuous, time-constant cycle and it consists in a multi-stage algorithm.

The first step is characterized by the state-estimation of the electrical parameters of the distribution grid model, corresponding to the controlled portion of the grid. Measurements from SCADA, power estimations and load-flow calculation contribute to the smart allocation of unmonitored loads, feeder by feeder. The on-line evaluation allows to check out the nodal voltages value at any time.

The algorithm needs to know:

- Structural data, which are useful to describe the grid topology:
    - connectivity between the elements and identification codes,
    - line parameters,
    - nominal values of transformers (MV/LV and HV/MV), of DGs and of loads, and
    - capability curves of the generators involved in the regulation.
- Operational data, which are useful to describe the current state of operation of the distribution grid:
    - state of the switches,
    - position of on-load tap changers (OLTC),
    - voltage referring to the MV/HV transformer,
    - active and reactive power flowing at the beginning of the feeders,
    - active and reactive power coming from the DG and possibly from the loads, and
    - active and reactive power estimations of the unmonitored DG.

Considering a normal operating range in ±7% of the nominal voltage, the second step includes the voltage regulation by OLTC and/or by DERs reactive power, in order to fix possible nodal voltage violations in the MV grid. This preliminary regulation takes into account the DERs' sensitivity to the node in violation and tries to avoid the misuse of OLTC. The specific calculated setpoints are sent to the involved controlled resources. While the violation persists, the Virtual Power Plant (VPP) is declared unavailable to participate to the ancillary services and it is reported back to TSO. Moreover, the system runs the optimization of the OLTC position two times a day.

If the program does not detect any violation, the evaluation of VPP reactive power dynamic capability represents the next step. In this part of the algorithm, several load-flows are run in order to evaluate the maximum available capability of the VPP in under- and over-excitation. The calculation includes checking of possible nodal voltage violations and, where necessary, the capability is reduced by DERs sensitivity method. Considering the capability of a plant composed by several generators, the system needs to monitor the operating state of the single machine and its nominal power. Reactive power virtual capability and operation point at the HV side of the transformer are sent to TSO, on the basis of set up and topology of the DSO network.

Figure 20 shows a typical capability curve implemented in the MVRS in order to simulate the operation of a hydroelectric power plant. This kind of capability has been provided by DSO and it is used by MVRS to calculate the VPP capability.

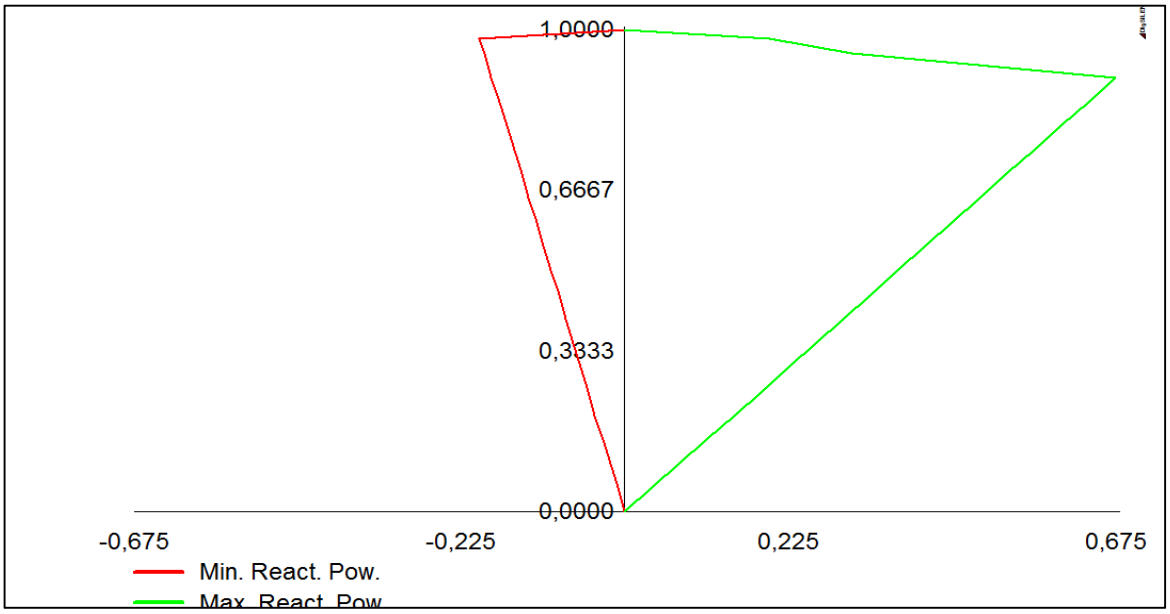

Figure 20: Capability of a single power plant connected at the MV grid

According to VPP capability, the TSO requires ancillary services to regulate the voltage value at the high-side of the TSO/DSO grid interconnection point. In this application, MVRS can receive a percentage of reactive power, referred to the last capability sent to the TSO. In other cases, if a relation between voltage and reactive power is available, the device can receive voltage setpoints and convert them into reactive power commands, through appropriate Q(ΔV) tables.

The goal of the regulation algorithm is chasing and keeping setpoint requested, adapting decisions to changing field conditions. The MVRS closed-loop control system finds a solution for the simulated model and the setpoints are sent towards MV DERs, available and controllable. This regulation step is repeated only after the real settling of the plants, working as external closed-loop control.

4.2.2 Siemens solution for the voltage regulation

The Siemens MVRS implements a control loop based on the evolution of some functionalities of the Siemens Smart Distribution Management System. In detail, to realize this SmartNet functionality three algorithms has been released.

The first one provides an accurate state estimation of the MV grid, the second one defines, on the previous state estimation, the virtual capability (reactive power reserve of the grid) and the last one is called voltage regulation, which is able to control and adjust the reactive power exchanges in the network. Figure 21 explains the process.

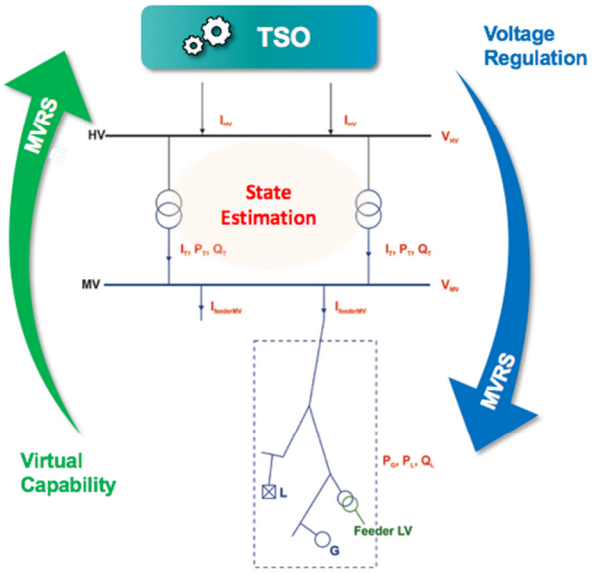

Figure 21: Elaboration flow for the Voltage Regulation of a MVRS

Siemens' MVRS is able to manage both the reactive power and the voltage setpoint.

In case of receiving from the TSO a voltage setpoint referred to the primary substation HV busbar, the MVRS pre-processes the data using specific Q(ΔV) curves (implementing the same approach used in the Siemens HVRS as described in chapter 3). Thanks to this elaboration, the voltage regulation algorithms are always run with a reactive power constraint assigned to each HV/MV transformer.

Regarding the State Estimation, this process represents the first step to manage the distribution network in real-time, before taking any control action. In distribution networks, the application of classical state-estimation methods is impossible mainly due to the reduced number of available measurements and, hence, the lack of redundancy. Therefore, depending on the available measurement points, various specially-designed state-estimation techniques have been implemented:

- simplified algorithms when only the primary substation measurements are available,
- advanced algorithm when both primary and secondary substation measurements are available.

About the control step (virtual capability computation and voltage regulation), this part of the functionality aims to apply an imposed reactive power setpoint on the HV-MV interface (the HV/MV transformer) by optimally dispatching the reactive resources available at the MV level and assuring the operational constraints of the network.

Originally, an optimization problem was designed by adapting the traditional Optimal Reactive Power Flow (ORPF) problem to an ORPF model suitable for distribution networks. Here, the goal of the ORPF was to minimize the real energy losses in the distribution network subject to the following constraints:

- power flow equations,

- generating unit's capability constraints,
- nodal voltage operating limits, and
- branch current limits.

To realize this specific SmartNet goal, the objective function of the ORPF was changed to minimizing the square of the difference between the actual reactive power flowing in the HV–MV interface and its setpoint; ideally, this is null, but if constraints are at limit then the minimum possible deviation from the setpoint is achieved.

With this new algorithm, as illustrated in Figure 22, it is possible:

- to calculate, at a given moment in time, the reactive power limits at the HV–MV interface by giving fictitious large setpoints (above the sum of the capabilities of the generating units) for both capacitive and inductive operating conditions (i.e. virtual capability computation)
- to impose, in real-time, a reactive power setpoint that lies inside the previously computed limits (i.e. voltage regulation)

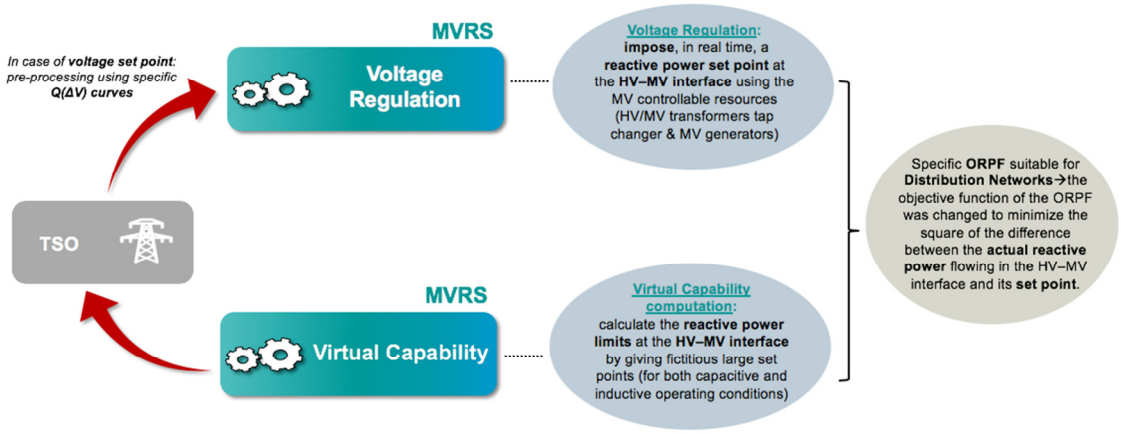

Figure 22: Relationship between Virtual Capability and Voltage Regulation

In Figure 23, there is a screenshot of the HMI of a MVRS. For each HV/MV transformer, there is a section "REG V TRx", where the main setpoint and information regarding the voltage regulation are displayed. Likewise, there is a section, namely Capability TRx, dedicated to the virtual capability of each HV/MV transformer.

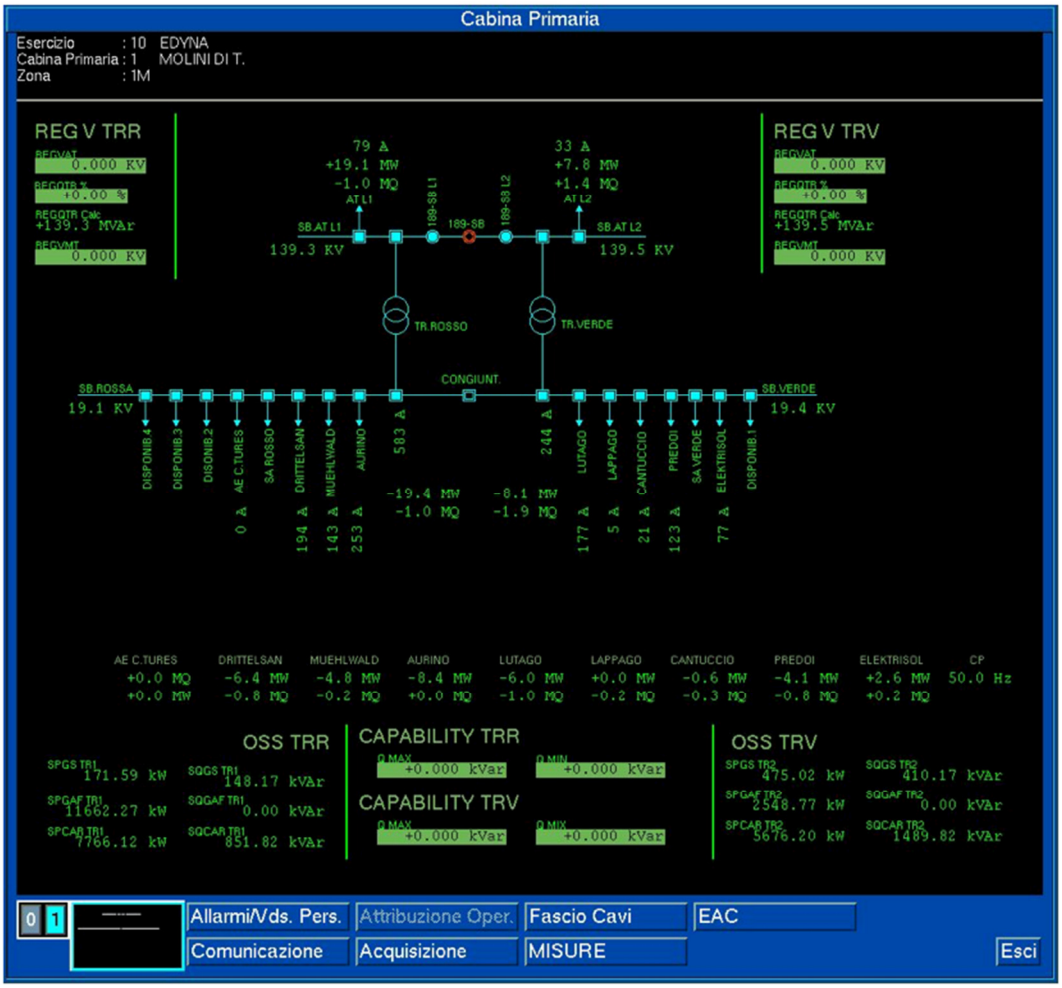

Figure 23: Human-Machine Interface of Siemens MVRS

4.3 f/P regulation

The last functionality implemented in the MVRS is the frequency/power regulation through DG. The main task of the MVRS is to receive a level command by the TSO and to perform an active power variation of the VPP in order to modulate active power fed into the grid complying with the TSO requirement.

This service (aFRR) consists of providing a modulation of the active power according to a signal level sent by Terna every 4 seconds to the control system. Figure 24 represents how the aFRR works in the Italian regulation.

The level is between 0-100 and represents the variation within the active power regulation band: 0 is the lower end of the band, 100 is the upper end of band and 50 represents the generation program.

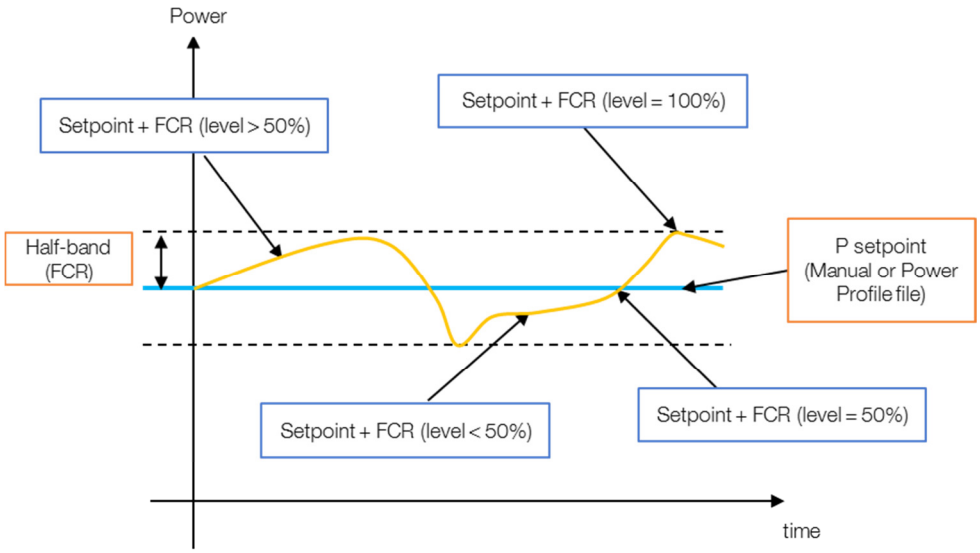

Figure 24: Representation of the aFRR regulation in Italy

In SmartNet application, the MVRS, considering all the available data (topology, measurements, etc.), calculates an aggregated dynamic active power capability (i.e. the active power range available for the TSO to provide the power/frequency regulation). The information sent to the TSO are the planned production (mid-value band) and the available modulation (half-band). In this case, due to the non-programmable nature of the power plants involved, each manufacturer has decided which could have been the more suitable value to be considered as mid-value of the band. Furthermore, the half-band available for the regulation is normally defined by the bids and the market outcomes but, in this application, it has been necessary to define an achievable band.

Once the command is received, the algorithm provides a smart splitting of active power command among the controlled plants according to single DERs capability in order to deliver the total necessary active power at the primary substation. The communication with DG is carried out via the PCRs installed at controllable power plants.

4.3.1 Selta solution for the f/P regulation

MVRS aFRR functionality pursues a specific algorithm to offer this ancillary service to the TSO. Its data centre considers the aggregation of the controllable MV generators, subtended at the HV/MV transformer, as an equivalent generator and it elaborates the information coming from the PCRs.

For each MV plant of the aggregation, the increasing and decreasing half-bands are elaborated in accordance with the actual dispatching and the physical constraints of the generators.

In particular for hydroelectric power plants, available just for the downward service, MVRS calculates the decreasing active power band as the difference between the available power and a minimum power generation, as shown in Figure 25: the upper limit represents the power output and corresponds to the

50% value of the band; the lower limit refers to a minimum value that can be the technical or contractual minimum power and corresponds to the 0% value of the regulation band.

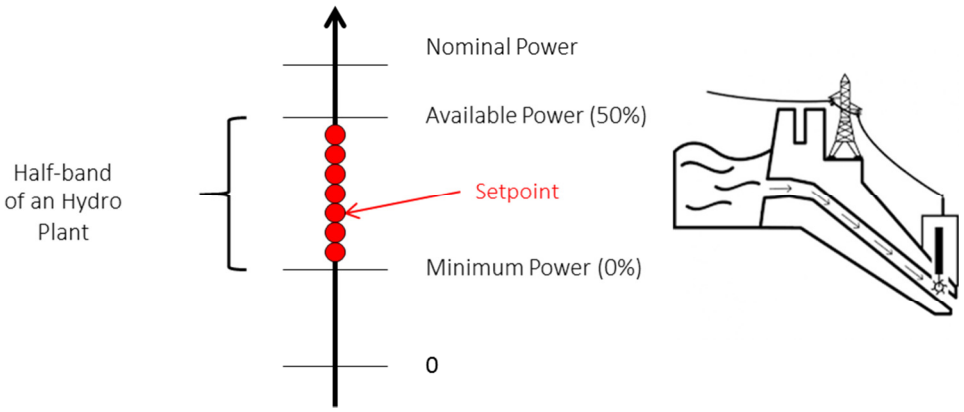

Figure 25: Representation of the band available for the f/P regulation

From the TSO point of view, the sum of the half-band values constitutes the entire half-band of the equivalent VPP at the HV/MV connection.

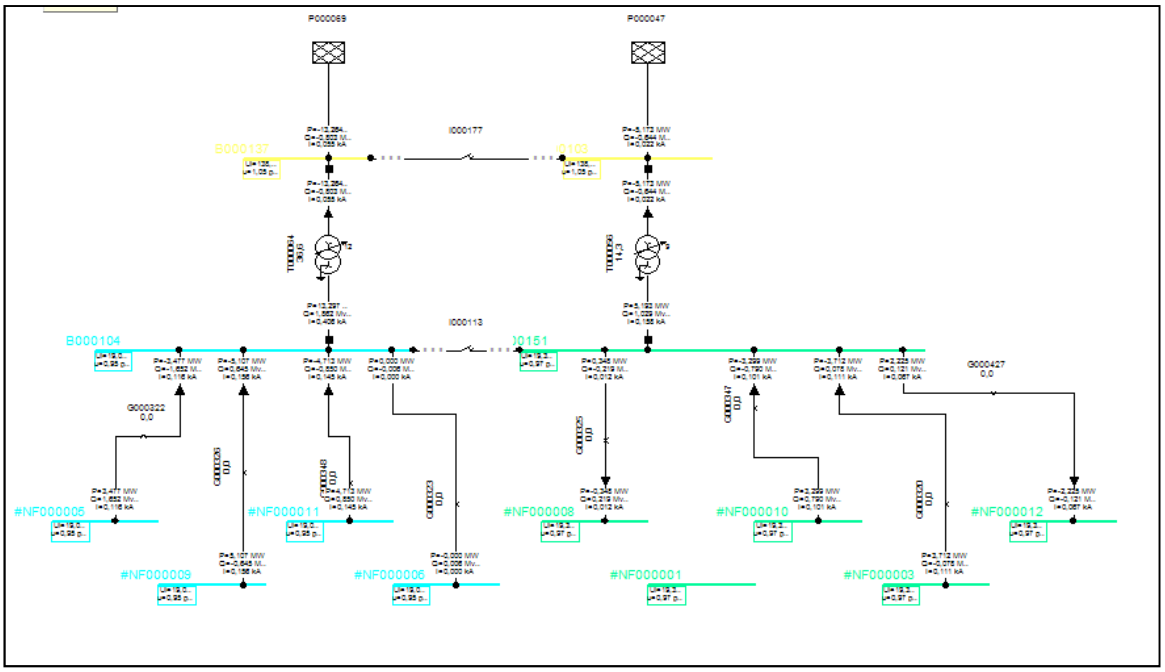

Figure 26: Primary Substation and MV feeder representation

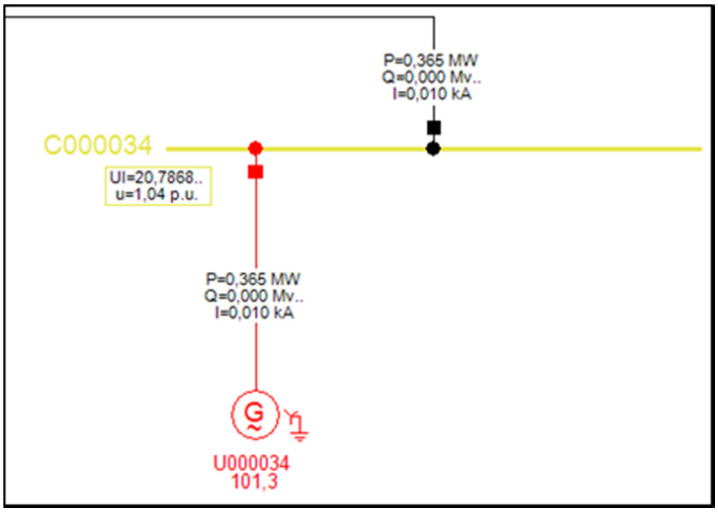

Figure 27: Detail about MV plant representation

The technical test has shown the operations performed by the MVRS every 6 seconds:

- Gathering of the availability for the regulation from the controllable plants;
- Evaluation of the mid-value and half-band of the single plants;
- Composition of the mid-value and half-band about the whole aggregate;
- Acquisition of the regulation level from the TSO OC (0-100 %);
- Homogeneous distribution of the level to the available generators, considering the single capabilities;
- Calculation of the % setpoint referred to the nominal power of the single power plant controlled by a PCR.
- Writing of the setpoint values on the variable of the SCADA, for every enabled PCR.

Finally, the controller of each power plant sends the feedback corresponding to the setpoint coming from the PCR, with a delay of about 10 seconds.

```
MacroFeeder ROSSO percentuale di banda richiesta: P = 50,00000
GD U013566 P pre  1,44546 MW | P post  2,03000 MW (P percentuale -100,00000 sulla S nominale  2,03000 MVA)
GD U013597 P pre  0,43970 MW | P post  0,79325 MW (P percentuale -95,00000 sulla S nominale  0,83500 MVA)
GD U000034 P pre  0,36541 MW | P post  0,36000 MW (P percentuale -100,00000 sulla S nominale  0,36000 MVA)
GD U013481 P pre  5,12486 MW | P post  5,60000 MW (P percentuale -80,00000 sulla S nominale  7,00000 MVA)
GD U013640 P pre  4,36696 MW | P post  7,90500 MW (P percentuale -85,00000 sulla S nominale  9,30000 MVA)
```

Figure 28: Calculation of final setpoints for DERs

4.3.2 Siemens solution for the f/P regulation

Each MV generator, which is available for regulation, is characterised by two active power regulation ranges: one to increase the power and one to decrease the power. The computation on these "regulation

bands" for a MV plant is performed considering the concept of equivalent generators (the individual physical generators are clustered considering homogenous primary energy source and nominal power).

When the TSO sends a f/P setpoint (0-100 % format), the MVRS calculates the necessary active power according to the available power of all the MV loads. Then, the MVRS system splits this amount according to the capacity of each MV plant. The final active power setpoints are sent to each PCR installed on field to actuate the power regulation.

The whole process described is represented in Figure 29.

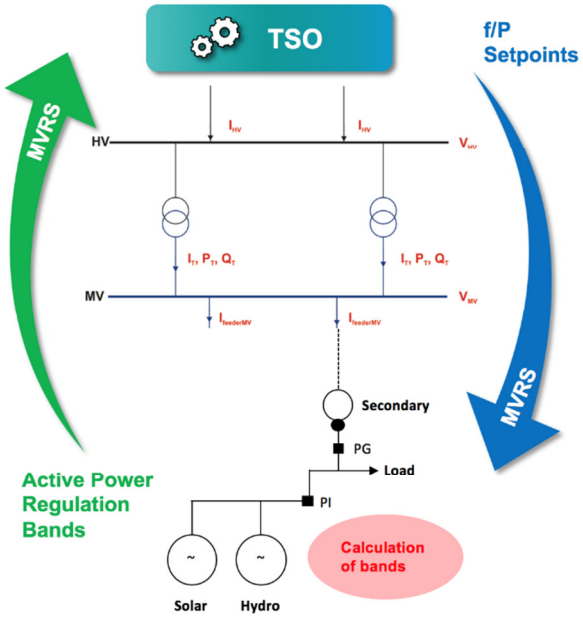

Figure 29: Elaboration flow for the aFRR functionality

In particular, the calculation of the regulation ranges for the TSO is based on the following steps:

- MVRS gathers the real and reactive power measurements from each MV controllable plant;
- MVRS gathers the switch states from each MV controllable plant; each power plant is graphically represented with its measurement in a specific HMI page as represented in Figure 30;
- The regulation bands, for each MV controllable plant, are calculated considering the difference between the reference power and the minimum dispatchable active power limits;
- The overall regulation bands, which are sent to the TSO, are the sum of the bands of each MV plant. The calculated data are reported in the MVRS HMI as illustrated in Figure 31.

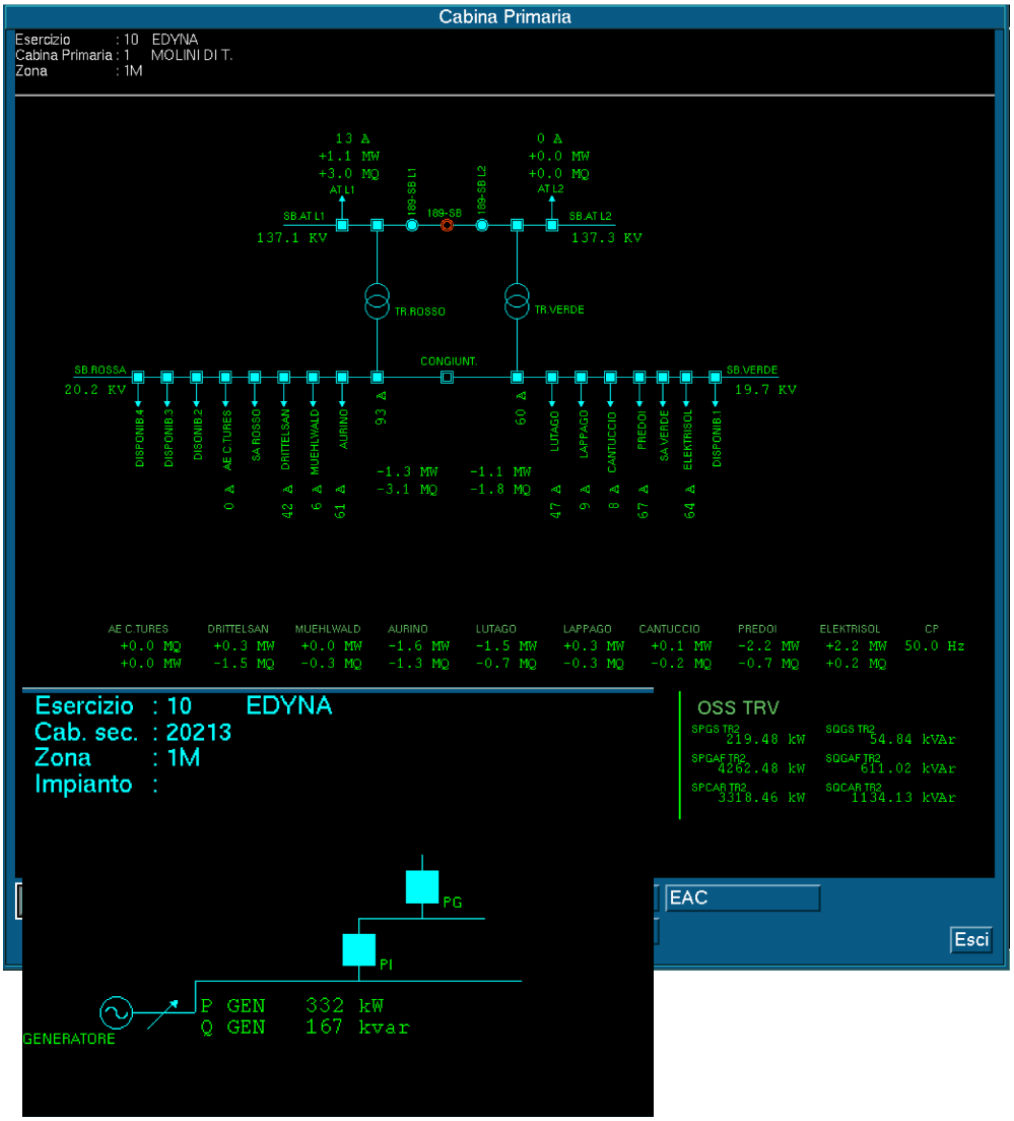

Figure 30: Screenshot of the MVRS interface (MV plant)

Figure 31: Screenshot of the MVRS interface (regulation bands)

5 Tests and Experimentation

The following section gives an overview of the testing procedure adopted to evaluate the operation in field of the devices implemented, functionality by functionality.

5.1 Voltage regulation by HVRS

The Factory Acceptance Tests were performed during 2017 at the premises of Siemens in order to simulate the various configurations of the grid during the regulation and the different types of regulation: voltage or reactive power regulation, busbar or single generator regulation, partial participation of some generator at the regulation, etc.

The Site Acceptance Tests (SATs), performed with the HVRS installed in the HV substation of Molini di Tures since March 2018, were aimed to verify:

- The information exchange between Terna, the HVRS and the regulators of the plants (DCS) involved in the project (Lappago and Molini di Tures)
- The proper functioning of the device developed concerning the voltage and reactive power regulation, as well as the calculation of the capability, the reactive power availability of the plants and the proper splitting of the requirement among the controlled generators.
- The response of the generators during both the local regulation and tele-controlled regulation of the busbar voltage or reactive power.

The tests were carried out using both the local control through the HVRS HMI and the telecontrol from TSO OC. The local tests, together with the data recorded locally during the experimentation, are necessary in order to evaluate the response of one generator at a time, whilst the remotely regulation permits only the busbar regulation, in order to consider all the generators connected to a busbar as a unique virtual plant.

The initial tests enabled to update the regulation system of the single generators in order to improve their response. In particular, the aim was to reduce the overshoot shown following the setpoint profile during the test and to minimize the response delay.

Furthermore, the tests in field allowed to improve the selection of the variable parameter of the HVRS, especially regarding the correlation curves between voltage and reactive power used by the device to convert a voltage optimal setpoint into a reactive power requirement. In fact, the cubic correlation developed by Siemens is a parametric function and it is possible to increase or reduce the contribution at the regulation on the basis of the needs by acting on the characteristics of the function.

The data recorded during the tests and the experimentation phase and stored in Terna SCADA are:

Data
HV busbar voltage
MV busbar voltage
Active and reactive power generation of each generator
Active and reactive power generation at the HV busbar
Switch status
Type of regulation: Reactive power/voltage
HV busbar theoretical reactive power capability (that takes into account all the generators)
HV busbar real reactive power capability (that takes into account only the running generators)
Reactive power/voltage setpoint for the HV busbar
Feedback of the setpoint received by HVRS
Anomaly at the regulation system alert
Limit value reached alert

Table 1: data recorded in Terna SCADA for the analysis of the voltage regulation tests

The data recorded during the tests and the experimentation phase and stored in HVRS are:

Data
HV busbar theoretical reactive power capability (that takes into account all the generators)
HV busbar real reactive power capability (that takes into account only the running generators)
Reactive power capability at the operational point of each generator of the controlled plants
Active and reactive power generation of each generator and at the HV busbar
Reactive power/voltage setpoint received by Terna
Reactive power requirement split among generators involved in the regulation
MV busbar voltage measurement for each generator
Feedback of the setpoint received by each plant regulator

Table 2: data recorded in HVRS for the analysis of the voltage regulation tests

During the experimental phase, the device has been continually used as voltage regulation resource by the remote control from the TSO OC. The interface of Terna SCADA designed to monitor and control in real time the plants is reported in Figure 32.

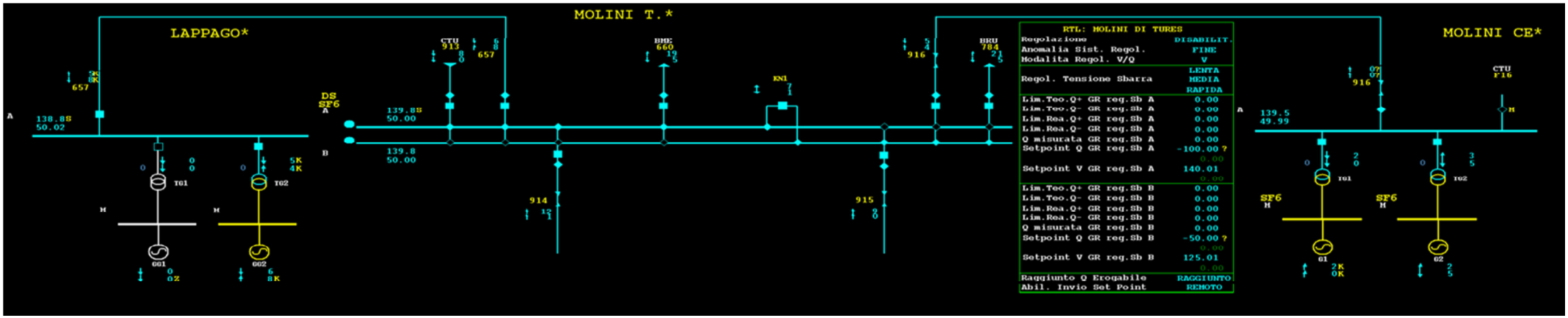

RTL: MOLINI DI TURES
Regolazione DISABILIT.
Anomalia Sist. Regol. FINE
Modalita Regol. V/Q V
Regol. Tensione Sbarra LENTA MEDIA RAPIDA
Lim.Teo.Q+ GR reg.Sb A 0.00
Lim.Teo.Q- GR reg.Sb A 0.00
Lim.Rea.Q+ GR reg.Sb A 0.00
Lim.Rea.Q- GR reg.Sb A 0.00
Q misurata GR reg.Sb A 0.00
Setpoint Q GR reg.Sb A -100.00 ?
Setpoint V GR reg.Sb A 140.01
Lim.Teo.Q+ GR reg.Sb B 0.00
Lim.Teo.Q- GR reg.Sb B 0.00
Lim.Rea.Q+ GR reg.Sb B 0.00
Lim.Rea.Q- GR reg.Sb B 0.00
Q misurata GR reg.Sb B 0.00
Setpoint Q GR reg.Sb B -50.00 ?
Setpoint V GR reg.Sb B 125.01
Raggiunto Q Erogabile RAGGIUNTO
Abil. Invio Set Point REMOTO

Figure 32: Representation of HVRS system in Terna SCADA HMI

5.2 Observability by MVRS

In order to evaluate the observability functionality of the MVRS developed, it is necessary to consider various aspects.

Firstly, the proper transmission of the aggregations sent to Terna SCADA by Edyna was analysed. For that purpose, Terna set up a specific page on the control system devoted to the representation of the MV-level as virtual plants connected at HV/MV Primary Substation, as reported in Figure 33.

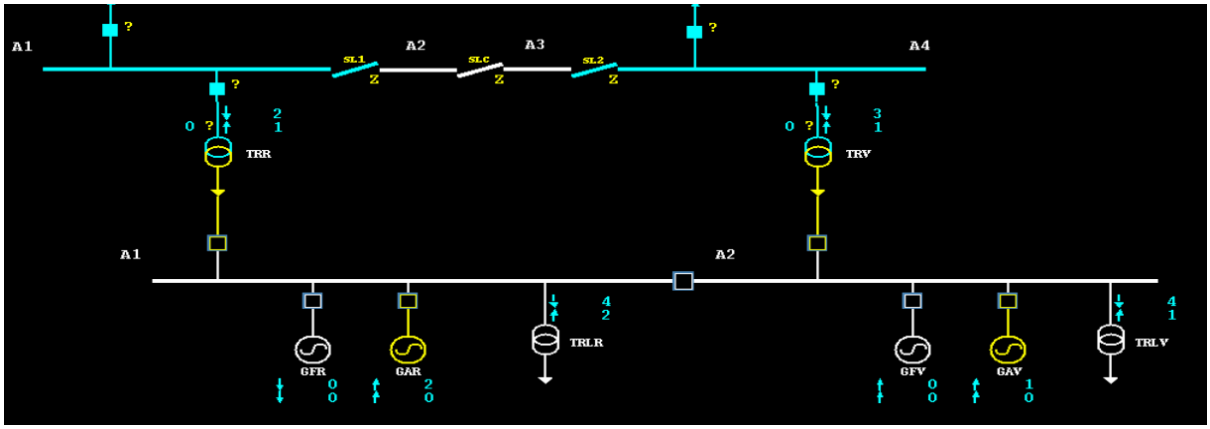

Figure 33: Representation of MV grid aggregations in Terna SCADA HMI

The MVRS updates the aggregations every 20 seconds, in accordance with the NRA resolution above-mentioned and sends the data to TSO OC every 4 seconds.

The estimation module needs the weather data too, in order to evaluate the correlated RES production. The weather data were made available thanks a specific software module able to reach out to the meteorological website of the valley.

Secondly, in order to evaluate the accuracy of estimation algorithms implemented by constructors, an ex-post analysis calculated the Estimation Accuracy Index (IPS), which relies on the comparison of monthly actual metering and the corresponding estimation. It is calculated as follows:

$$IPS_{aggr} = \frac{ASS\left(\sum_j E_{metering\_15'_j} - \frac{\sum_{ij} P_{ij} \cdot T_i\big|_{15'}}{3600}\right)}{\sum_j E_{\_nom\_15'_j}} \cdot 100$$

where:

IPSaggr: Estimation Precision Index of the aggregate

ASS: Absolute value

i = index of the i - th sample in the considered 15'

j = index of the j – th plant belonging to the considered aggregate

P_i: Power measurement [kW]

$\mathbf{T_i}$: Sample time [s]

$\mathbf{E_{metering\_15'j}}$: 15' energy elaborated considering the real measure of the j – th plant$\mathbf{E_{nom_15'j}}$: 15' energy elaborated considering the nominal power of the j – th plant

The accuracy required within the project by Terna is 10% of nominal power installed at the Primary Substation.

The approach of Selta's solution made it possible to include an offline analysis of the number of measurements necessary to have an adequate accuracy of the estimation, adopting a sentinel method. It consists of simulating various scenarios, characterized by a decreasing number of measurements, until the requirement is satisfied.

5.3 Voltage regulation by MVRS

The tests performed with MVRS, which were aimed at assessing the voltage regulation functionality of the device, are similar to those used for the HVRS. It was necessary to verify:

- The information exchange between Terna, the MVRS and the regulators of each plant involved in the regulation (PCRs).
- The proper functioning of the devices developed concerning the voltage and reactive power regulation, as the calculation of the capability, the reactive power availability of the plants and the proper splitting of the requirement among the controlled generators.
- The response of the generators at the remote regulation of the busbar voltage or reactive power.

Figure 34 is part of the HMI, where reactive power data of the aggregation of controllable plants at MV are gathered and from which the TSO OC can send voltage and reactive power setpoints.

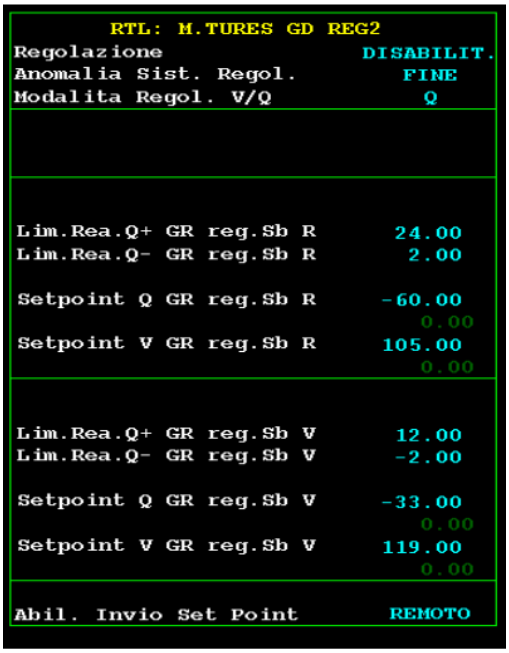

Figure 34: Representation of voltage regulation functionality in Terna SCADA HMI

The data recorded during the tests and the experimentation phase and stored in Terna SCADA are:

Data
HV busbar voltage
Active and reactive power generation of the aggregations connected at the primary substation
Switch status
Type of regulation: Reactive power/voltage
Reactive power capability of the virtual plant calculated by MVRS considering the plants involved in the regulation and taking into account the distribution grid constraints
Reactive power/voltage setpoint sent to the virtual plant
Feedback of the setpoint sent
Anomaly at the regulation system alert

Table 3: data recorded in Terna SCADA for the analysis of the voltage regulation tests

The data recorded during the tests and stored in MVRS are:

Data
Reactive power and voltage at the busbar prior to setpoint dispatch
Reactive power capability of the virtual plant calculated by MVRS
Reactive power capability of each MV plant involved in the service
Feedback of the setpoint received
Reactive power setpoint split and forward towards each plant
All data recorded by PCR (reactive power, active power, voltage at the generator terminals)

Table 4: data recorded in MVRS for the analysis of the voltage regulation tests

5.4 f/P regulation by MVRS

The performance tests were preceded by preliminary blank tests in order to evaluate the communication chain between the TSO OC and each plant involved in the frequency/power regulation test. In particular, it was verified:

- the proper transmission of the level signal by Terna to the MVRS installed in Edyna Control Room and the proper forwarding towards each PCR of the involved plants,
- the transmission of the feedback from the field to Terna, and
- the correct receipt of active power availability of the virtual plant composed by MV plants involved in the tests and calculated by MVRS (mid-value band and half-band).

The tests have been arranged adapting the standard secondary regulation tests to project needs. In particular, the test takes into account only the downward reserve, because the run-of-river hydro power plants are not remunerated to maintain a power margin to provide upward reserve. For this reason, the setpoint varies between 50 % and 0 %, i.e. the programmed mid-value and the minimum band provided, where 50 % represents the mid-value and 0 % represents the lower half-band.

The frequency regulation tests were performed sending a level signal with the profile reported in Figure 35, composed of:

- 80 seconds constant at 50 % (mid-value band declared by the VPP).
- Ramp-down from 50 % to 0 % in 100 seconds (from the mid-value to the minimum value declared by the VPP).
- 180 seconds constant at 0% (minimum value available for the regulation).
- Ramp-up from 0 % to 50 % in 100 seconds (from the minimum value to the mid-value declared by the VPP).
- 180 seconds constant at 50 % (mid-value declared by the VPP).

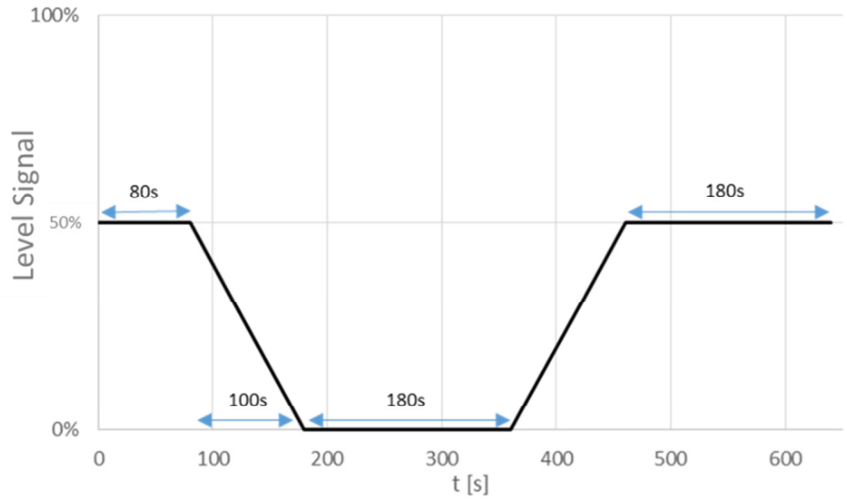

Figure 35: Ramp of the level signal used for the f/P regulation tests

During the tests, all the interesting data have been monitored and recorded by each device of the chain (MVRS, PCR, Edyna SCADA and Terna SCADA). In particular, the electrical variables examined are:

Data
Active power measured at the HV busbar
Active power of each plant measured by Edyna involved in the regulation tests
Electrical data recorded by PCR for each plant (active power, reactive power, voltage)
Mid-value band of the VPP calculated by MVRS and received by Terna
Half-band of the VPP calculated by MVRS and received by Terna
Mid-value band of each plant involved in the regulation tests
Half-band of each plant involved in the regulation tests
Level signal sent by Terna
Setpoint forwarding towards each plant
Feedback of the level signal sent to Terna
Feedback of the setpoint received by each plant and sent to MVRS

Table 5: electrical variables recorded for the analysis of the aFRR regulation tests

To analyse different scenarios about the active power involved in the f/P regulation, the tests were carried out setting different half-band values. Moreover, in order to test the calculation of the mid-value and half-band based on the number of the DGs available, the single power plants were enabled and disabled in different times.

The purpose of these tests is firstly to verify the response of the plants in terms of accuracy and timing, to evaluate the compliance with the current prescriptions required for the aFRR service. Another important aspect is to analyse the variation measured at the HV-side of the substation in order to quantify the possible contribution of the DG in the management of the transmission grid.

6 Results

The following section describes the outcomes reached in the testing of the devices and the functionalities developed within the project.

6.1 Voltage regulation by HVRS

Several tests have been performed in order to check the functioning of the HVRS. The purpose was to check the reliability of control loop as described in chapter 3 and the performance of the regulation. The first step in field was to verify the correctness of the data flow, communications and response of each generator at a time considering both the reactive power control and the regulation of the busbar voltage. The telecommunication configurations needed to obtain the data exchange among the devices involved in the communication chain initially encountered connectivity and compatibility issues; the problems have been overcome with the intervention of experienced technicians for each device.

Once proved the proper controllability of the power plants, preliminary tests have been carried out to verify the response of each generator, as reported in Figure 36.

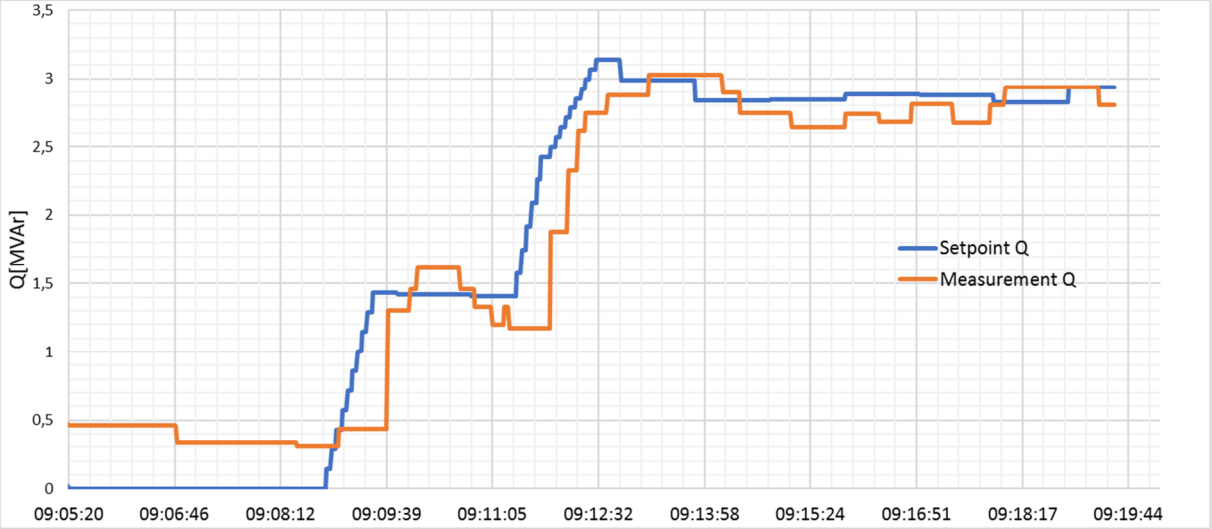

Figure 36: Example of preliminary tests carried out considering each generator in reactive power regulation

Then, test sessions have been carried out to verify the coordination of the 4 generators in the regulation by acting both on the reactive power setpoint and on the voltage setpoint referred to the 132-kV busbar.

The following examples analyze the results of the tests.

6.1.1 Voltage regulation through generators connected at the sub-transmission grid

This example shows how the HVRS allows the TSO to regulate the HV busbar by the control of the reactive power production/consumption of 3 generators connected at the same HV substation.

A unique setpoint expressed in per unit (p.u.) of the nominal voltage of the busbar is sent by the TSO considering the generators involved in the regulation as a single power plant.

In this application the setpoint series, as represented in Figure 37 is composed as follow:

- 10:27:30: 1 p.u. (132 kV)
- 10:29:48: 0.99 p.u. (130.68 kV)
- 10:36:24: 1.03 p.u. (135.96 kV)
- 10:44:47: 1 p.u. (132 kV)

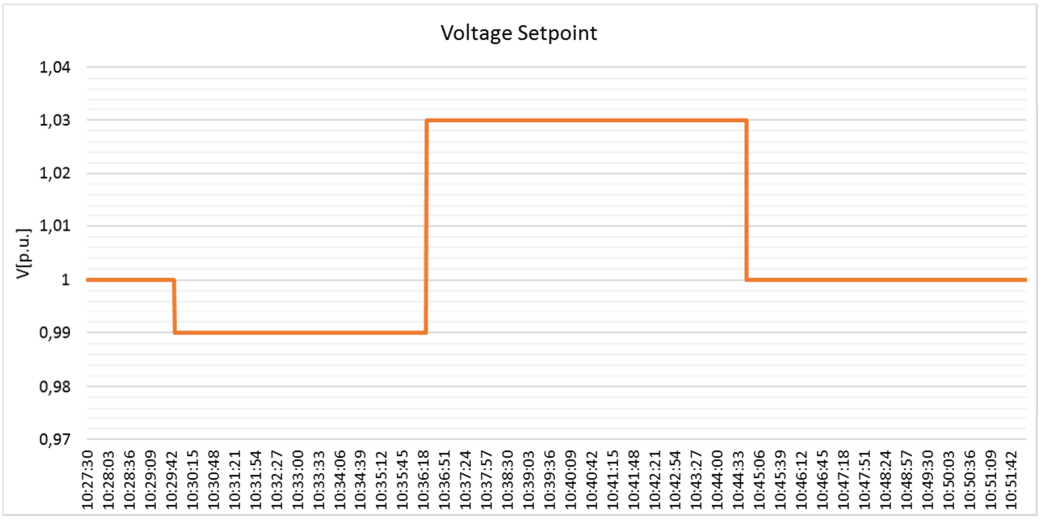

Figure 37: Voltage setpoint sent by TSO

As described in 3, the device converts the setpoint in a reactive power command in order to obtain the voltage variation required, considering the correlations of the control law. The trend of the corresponding amount of reactive power is shown in Figure 38.

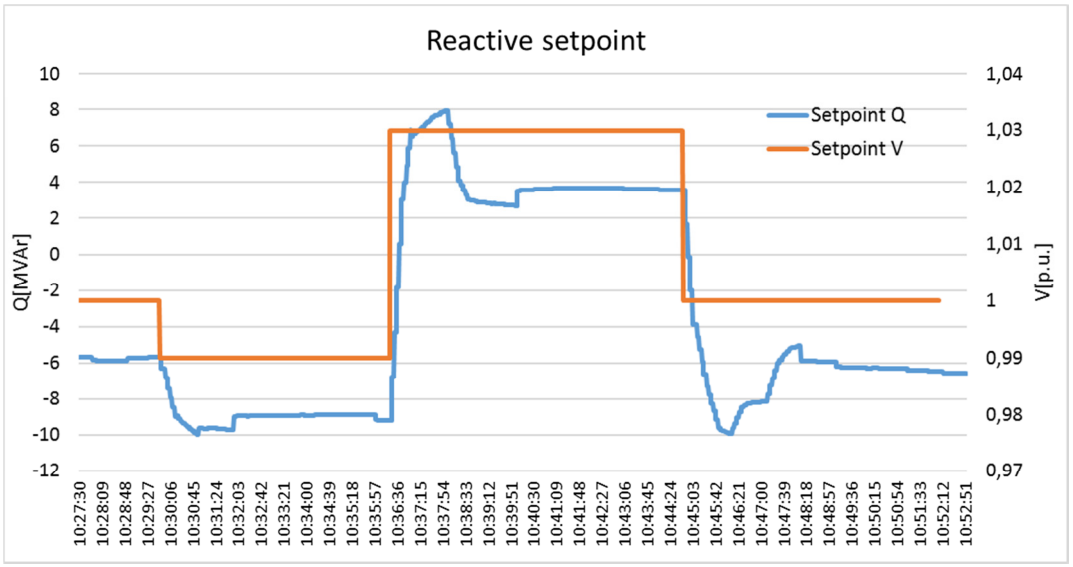

Figure 38: Trend of reactive power requirement calculated by HVRS

The HVRS split the provision among the controlled generators: in this way the system avoids overloading a single group and coordinates the reactive power flow to avoid wasting reactive power within loop. Figure 39 shows the setpoints: the request from G1 and G2 is very similar because working point of two identical groups which compose the power plant is the same and have the same capability and so also the distribution of the provision.

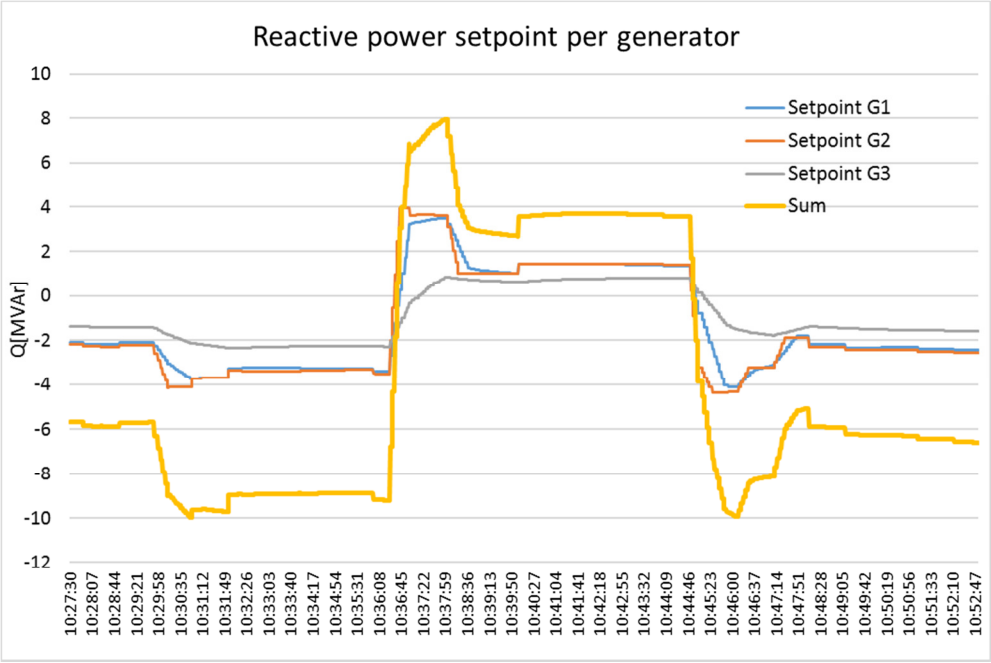

Figure 39: Distribution of the request among the generators

Figure 40 reports the consequent variation of the voltage at the terminals of each generator.

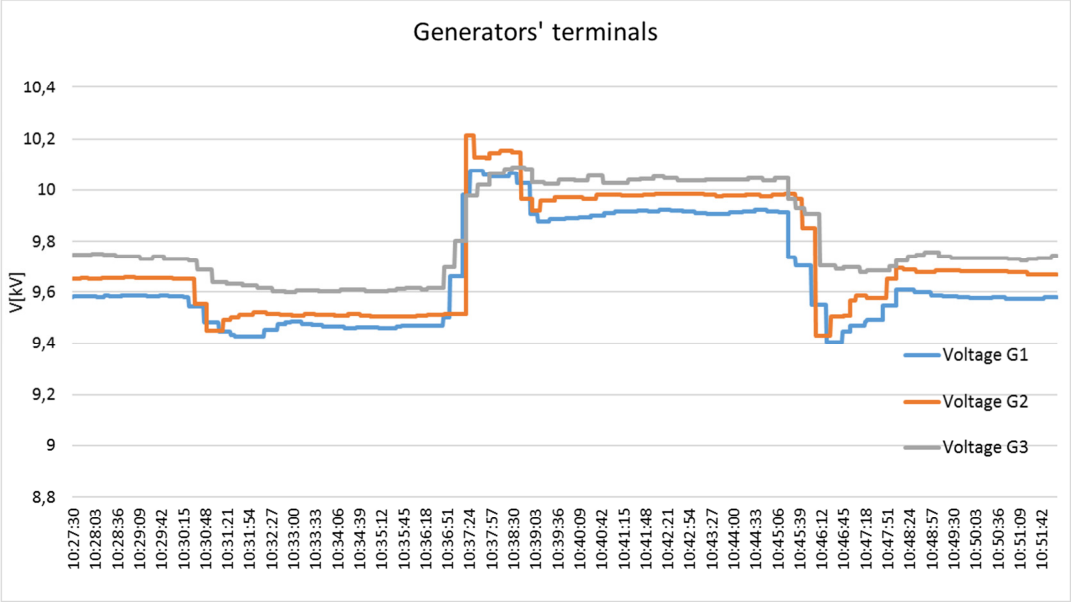

Figure 40: Voltages at generators terminals

The sum of the setpoints and of the measurements of the three generators constitutes the overall response of the coordinated regulation (Figure 41).

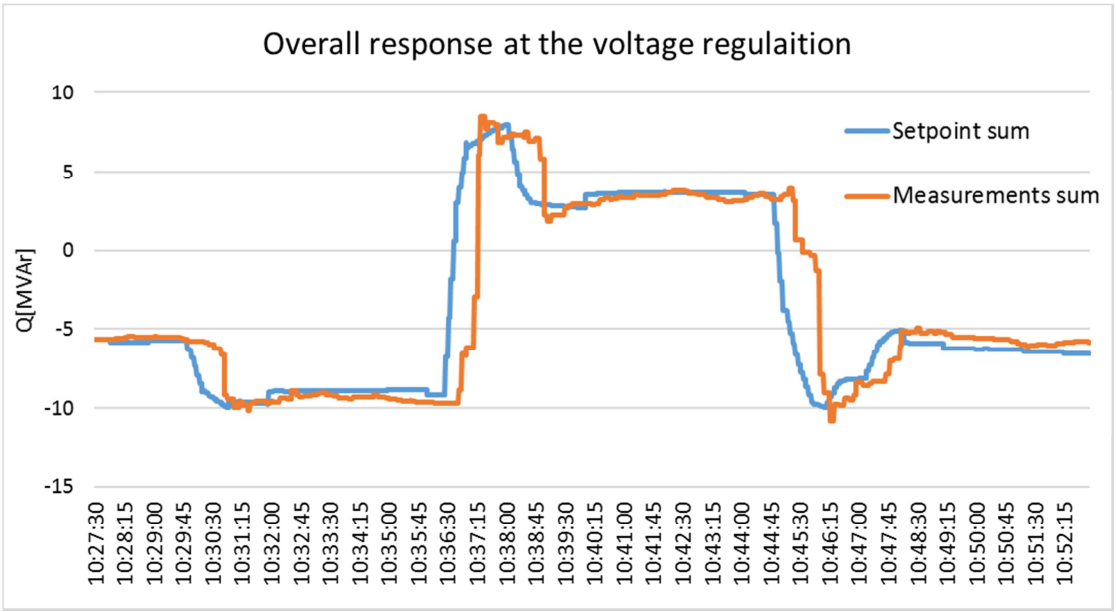

Figure 41: Reactive power response of the coordinated regulation

The response of each generator is reported in Figure 42: the dynamic transient is characterized generally by an overshoot in case of step command and the controller shows some oscillation around the required value. Regarding the delay of the response the behaviour is different for each system with values of the order of the minute. Successive improvements in configuration of the control system of the power plants aimed to reduce the delay and the overshoot of the response.

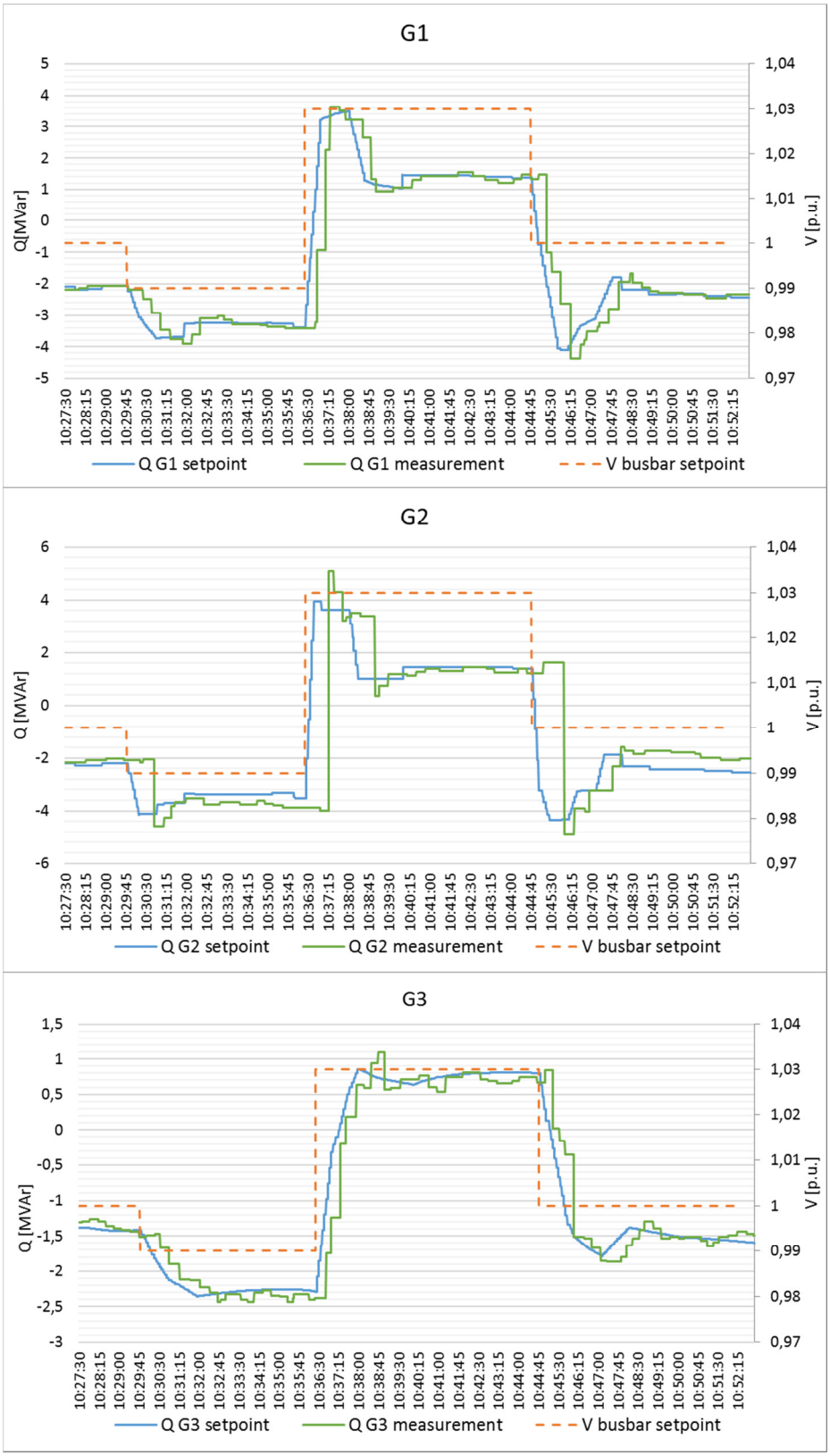

Figure 42: Dynamic response of each generator

As illustrated in Figure 43, it has to be pointed out that the controlled voltage depends on several grid parameters (load, short circuit power, etc.) and even the modulation of reactive power exchange by the power plants is interesting, the regulation of voltage at the HV busbar is not comparable with the contribution of a programmable power plant connected at the transmission grid. The voltage trend shows a consequent delay and overshoot due to the inaccurate response of each Automatic Voltage Regulator (AVR) controlled. Anyway, the coordination of the reactive trend of this kind of generators can help to support the voltage management avoiding waste of reactive power in internal loops, especially in future scenarios characterized by a reduction of available HV sources.

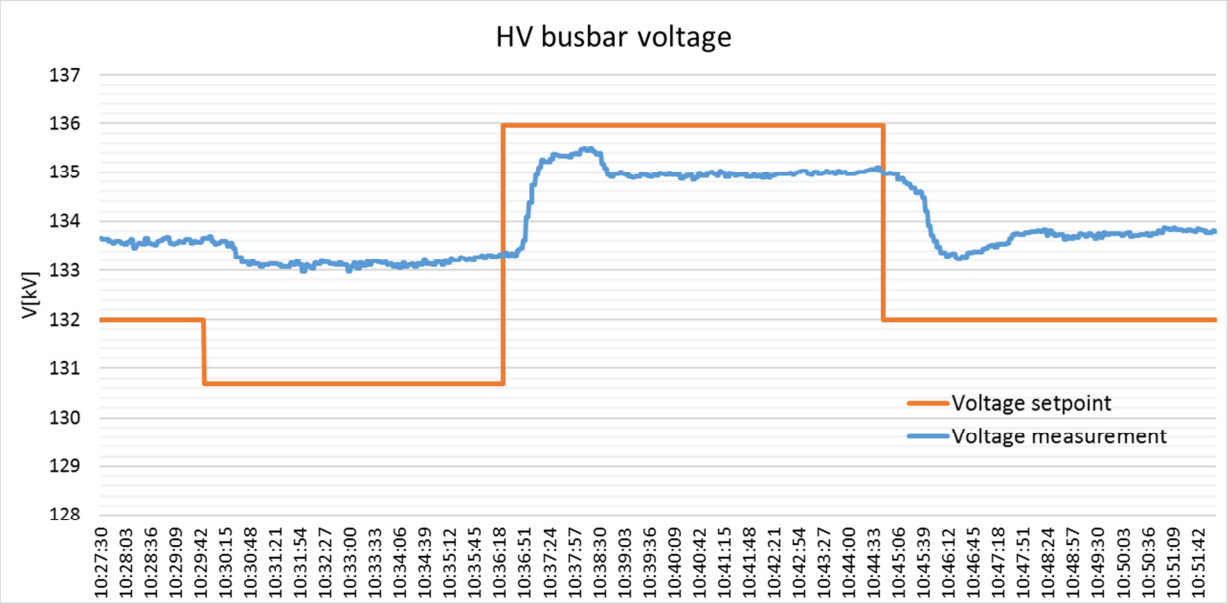

Figure 43: Effect of the regulation at the HV busbar

6.1.2 Test on parameters of the correlation ΔQ=f(ΔV)

The experimentation has also included rehearsals regarding the impact of parameters of the correlation between voltage setpoint and reactive power requirement on HVRS operation. These tests involved changing the parameter of the cubic correlation described in chapter 3.

The events of the example of Figure 44 are:

- 09:56:13 t1 Voltage Setpoint from 1.02 to 1 p.u.
- 10:05:30 t2 Increase of the proportional parameter to increase the contribution in the regulation
- 10:12:25 t3 G2 stops following the setpoint
- 10:18:09 t4 G2 re-starts following the setpoint again
- 10:21:39 t5 Change from slow to fast gradient of Figure 11
- 10:23:39 t6 Further increase of the proportional parameter to increase the contribution

in the regulation

- 10:29:51 t7 Voltage Setpoint from 1 to 0.99 p.u.

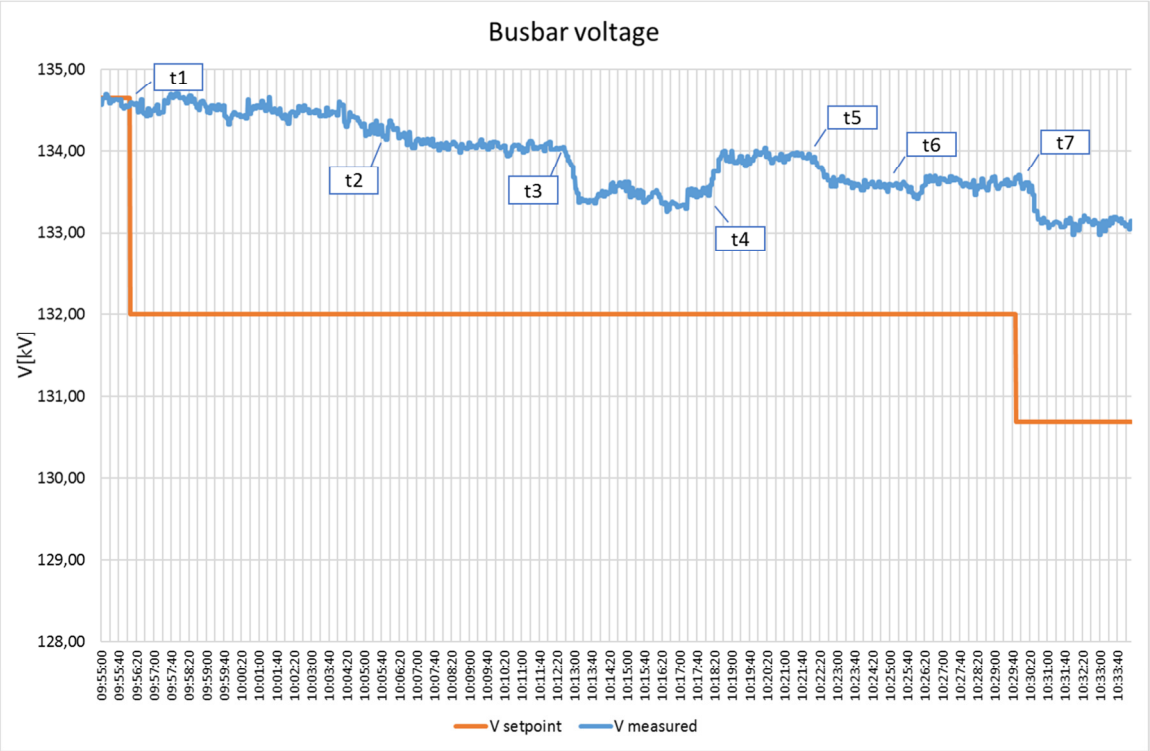

Figure 44: Voltage trend at the busbar as the parameters change

It is evident that the adjustable control law allows to vary the contribution of the generators in the reactive power management acting on the parameters. The gap between t3 and t4 due to the lack of regulation of G2.

The response of the system in terms of reactive power contribution is shown in Figure 45, while the trend in Figure 46 is not considered G2.

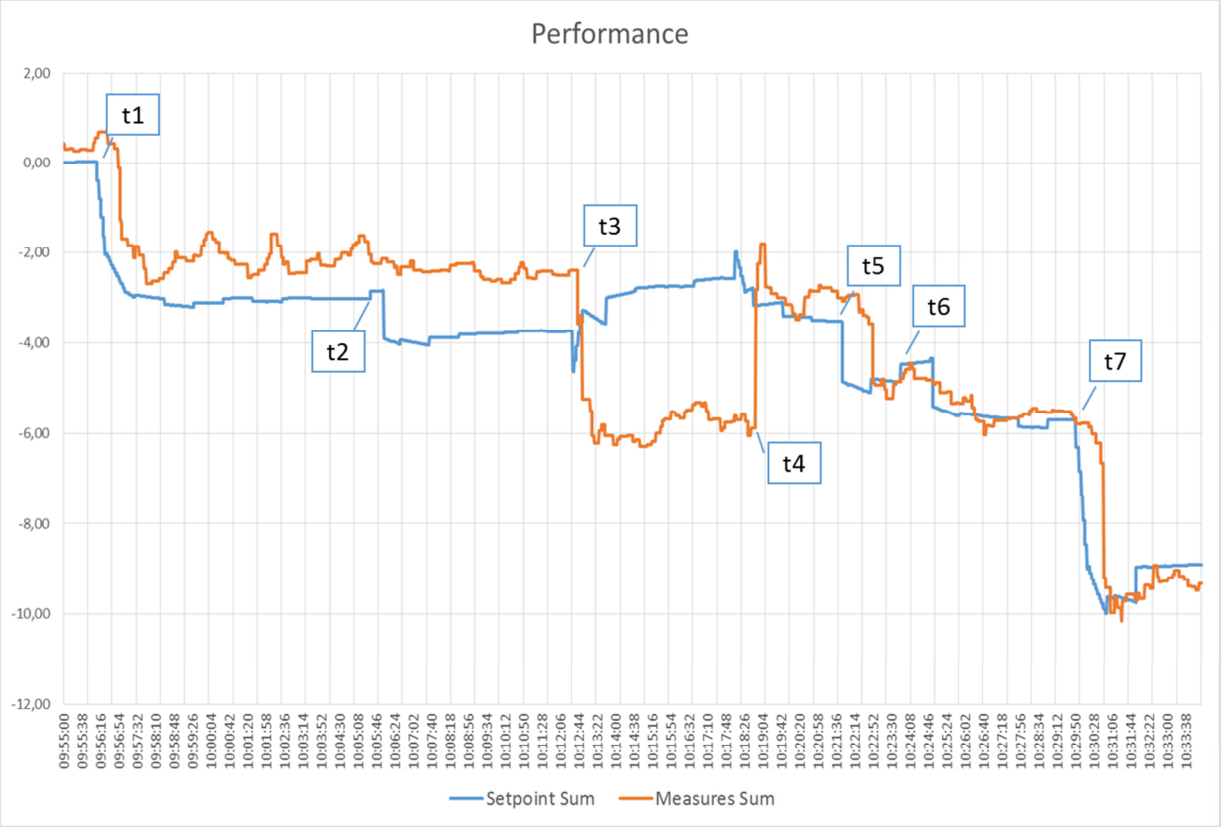

Figure 45: Performance in voltage regulation of the whole coordinated system

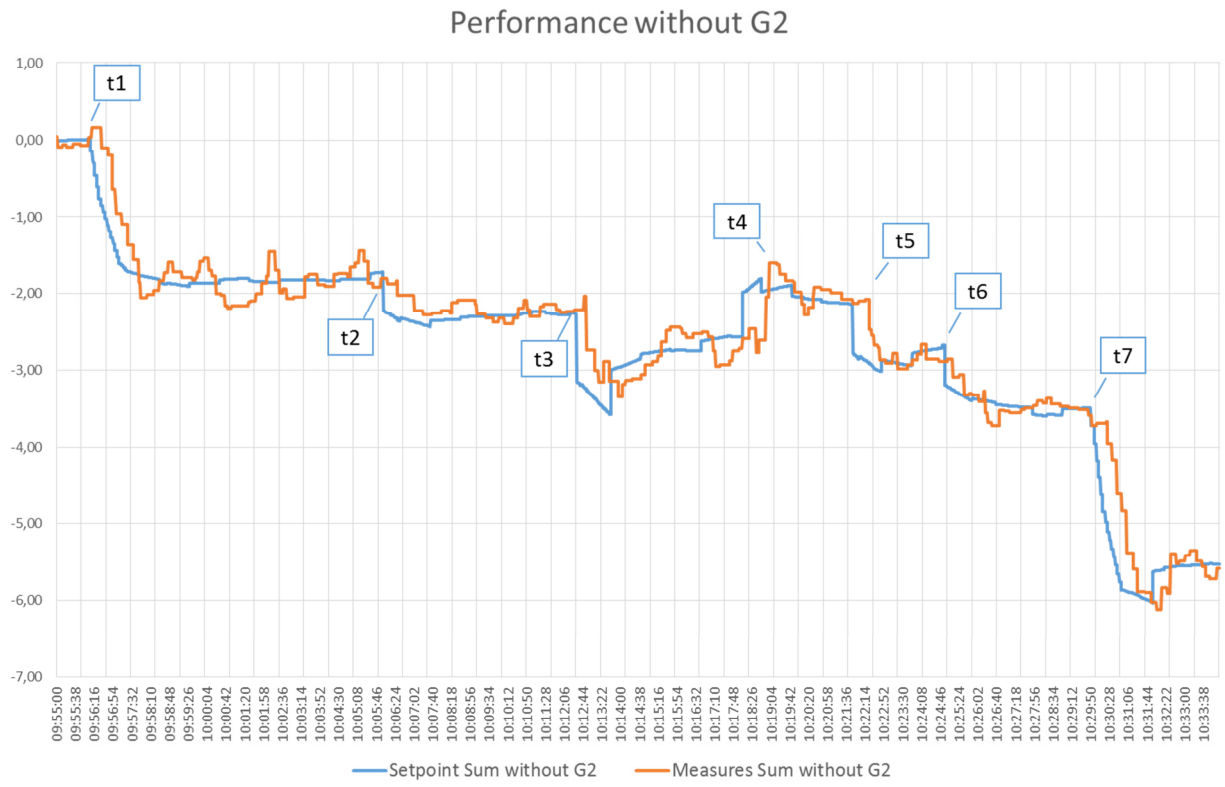

Figure 46: Performance in voltage regulation of G1 and G3

6.2 Observability by MVRS

6.2.1 Selta estimation algorithm

As described in paragraph 4.1.1, the estimation algorithm is based on the correlation between unmonitored plants and Sentinel Measurement that is calculated from historical data. An example of the off-line comparison between active power metering and the corresponding estimation about a hydroelectric plant is shown in Figure 47. The blue line represents the power estimation and it tries to follow the meter, characterized by the red line. The green curve represents the Estimation Accuracy Index (IPS in Italian wording and described in section 5.2), which is calculated every 15 minutes. Through this analysis it is possible to evaluate the correlation between data.

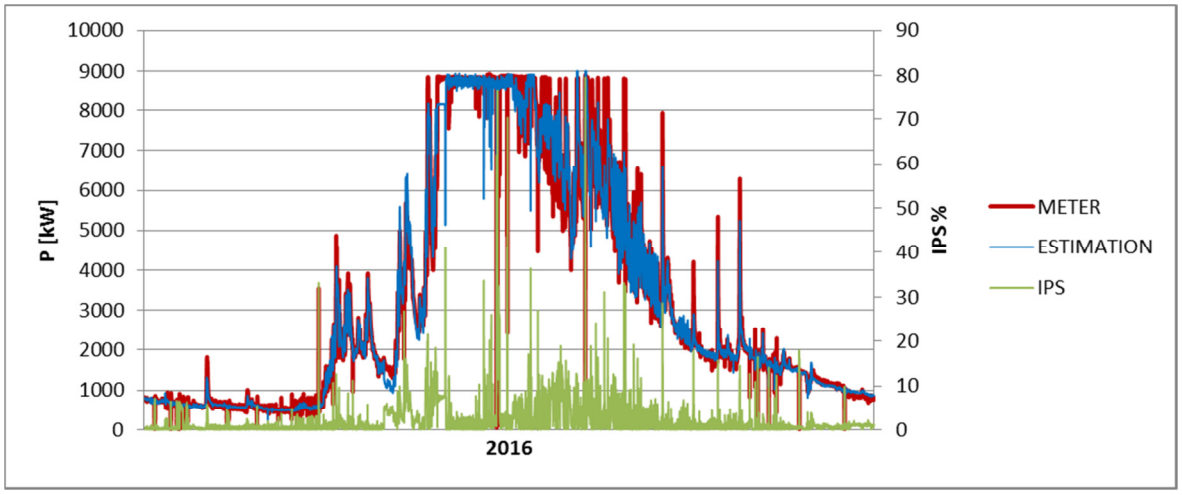

Figure 47: Off-line comparison about a hydroelectric plant, from January to December 2016

From the graphics, it is evident that the trend depends on the seasonality of hydro power production: high generation in summer and low generation in winter. In order to follow the seasonality of the power generation, for each month the set of SMs is updated and the correlation coefficients are evaluated. One of the most important issues is the necessity that the historical data are synchronized and that they are available for many years. Considering the coefficients calculated, it is possible to represents the correlation among productions of the plants involved in the project; an example is shown in Figure 48.

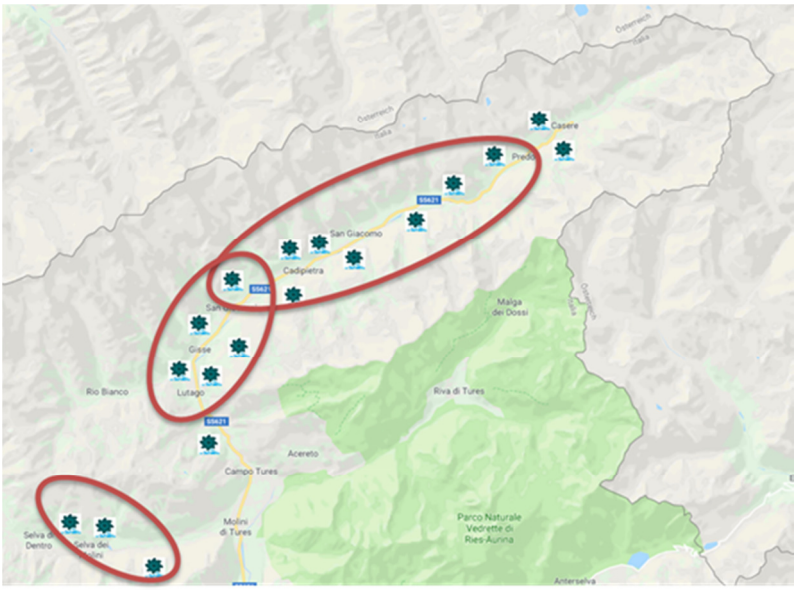

Figure 48: Correlated neighbouring hydroelectric plants

Once the best SM are defined for each unmeasured plant, the real time estimation of DER power amount is based on the weighted average of the selected SMs, correlated by the respective coefficient:

$$P_i^{DER} = \frac{\sum_{m=1}^{M}\left(k_{m,i}^{DER} \cdot \frac{P_i^{DER,nom}}{P_m^{SM,nom}} \cdot P_m^{SM} \cdot \frac{1}{\sigma_{m,i}^{DER}}\right)}{\sum_{m=1}^{M}\frac{1}{\sigma_{m,i}^{DER}}}$$

where:

- P_i^{DER} is the estimated power referred to the i-th DER
- P_m^{SM} is the value referred to the m-th Sentinel Measurement
- $P_i^{DER,nom}$ is the nominal power related to the i-th DER
- $P_m^{SM,nom}$ is the nominal value related to the m-th Sentinel Measurement
- $k_{m,i}^{DER}$ is the correlation coefficient between the power of the i-th DER and the m-th Sentinel Measurement, obtained by historical data pre-elaboration.
- $\sigma_{m,i}^{DER}$is the weight due to the error in the previous estimations related to the couple i-th DER and m-th Sentinel Measurement.
- M is the number of the Sentinel Measurements (3 in the practical application)

In order to assess the estimation algorithm implemented by Selta, measurements about 2016 and 2017 have been analysed. The computation regarded mostly hydroelectric plants power but also a PV plant connected at LV grid. For this purpose, the generation has been estimated and the results have been compared with the corresponding meters.

In Figure 49, few summer days of monitored power about a PV plant are reported. The graphic allows to make a comparison between the estimation and the real profile of the active power production. In this case, the Sentinel Measurements used in the nowcast estimation of the PV plant are weather variables, in particular solar radiation values.

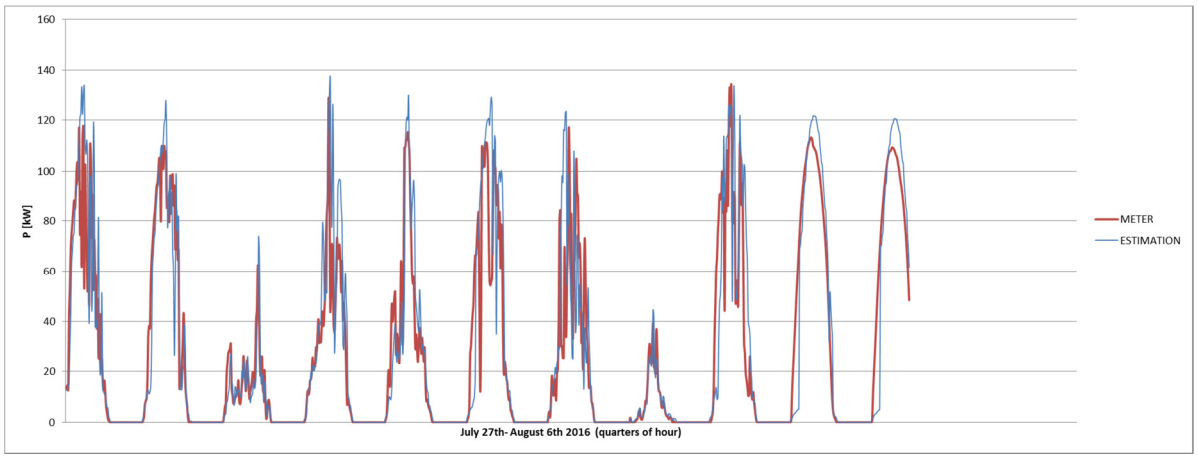

Figure 49: Comparison between estimation and corresponding metering (11 days)

On the other side, regarding MV hydro plants, once the off-line considerations and adjustments described above have been completed, the real time module runs every 10s and elaborates the estimation of the active power for each MV plant.

Figure 50 shows the trend of the real time estimation algorithm from April to June (2018). The considered aggregate includes 13 MV plants and its nominal power is around 16.7 MW as summarized in Table 6. The estimation achieves a good performance for all the time period taken in consideration, when the hydroelectric power is close to the maximum (summer season, when snow melts) and when the power is very low (winter season). Looking at the graphic, it is possible to note that estimation algorithm adapts itself during the year with the season effects.

AGGREGATE DETAILS	
Total Nominal Power	**16.675 kW**
Number of MV Plants	**13 plants**

Table 6: Details of the aggregation considered

In April, when the power production is very low, the estimation module recognises the situation and provides an accurate performance. In the weeks since May, hydroelectric power increases its amount and the estimation follows the variations in a very prompt way.

The weekly IPS is based on the formulation reported in section 5.2 and allows to verify the acceptability of the estimation results. In order to eliminate spikes in the graphics, IPS considers the 95%ile value. From the same graphic is possible to see that only a week involves the IPS over 10%.

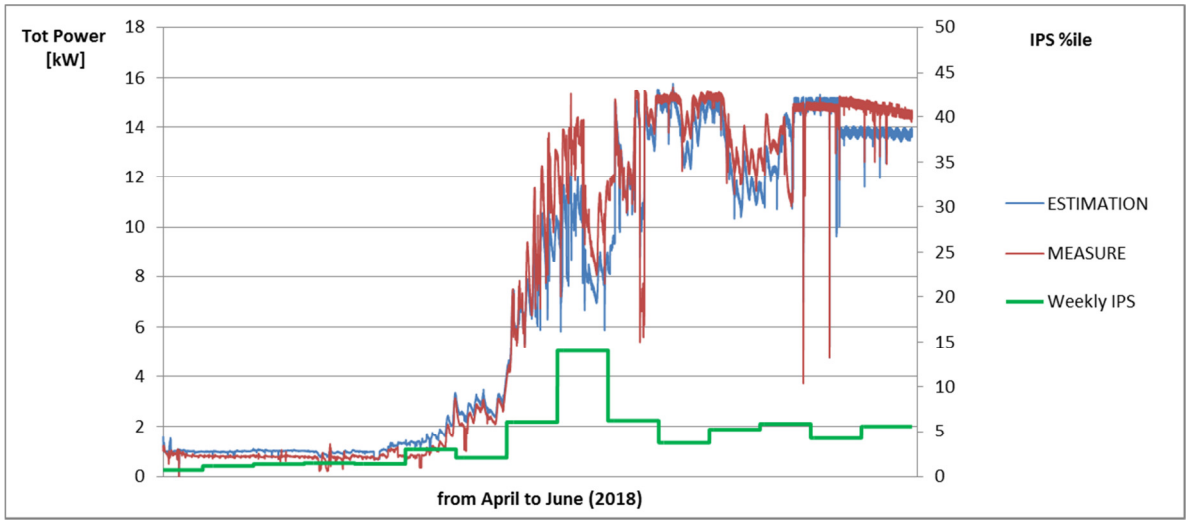

Figure 50: Comparison between estimation and metering and the resulting IPS

The aggregation sent to TSO collects both measurements, where a PCR has been installed, and estimations, supported by the algorithm.

Considering the IPS formulation, Selta has conducted also another type of investigation in order to quantify the needed number of PCR installed in the distribution grid to obtain an estimation of the production with an Estimation Accuracy Index below 10%, as requested by the TSO.

In this reverse problem too, the cumulate plot is elaborated and the IPS value corresponds to its 95°ile to eliminate possible spike values, due to incorrect measurements or "out of service",

The results obtained, represented in Figure 51, show that the IPS value reaches the target of the 10% if the system measures, through the PCR, the power generated by the plants corresponding to the 60% of the aggregate nominal power and estimates the power of the remaining unmonitored 40%.

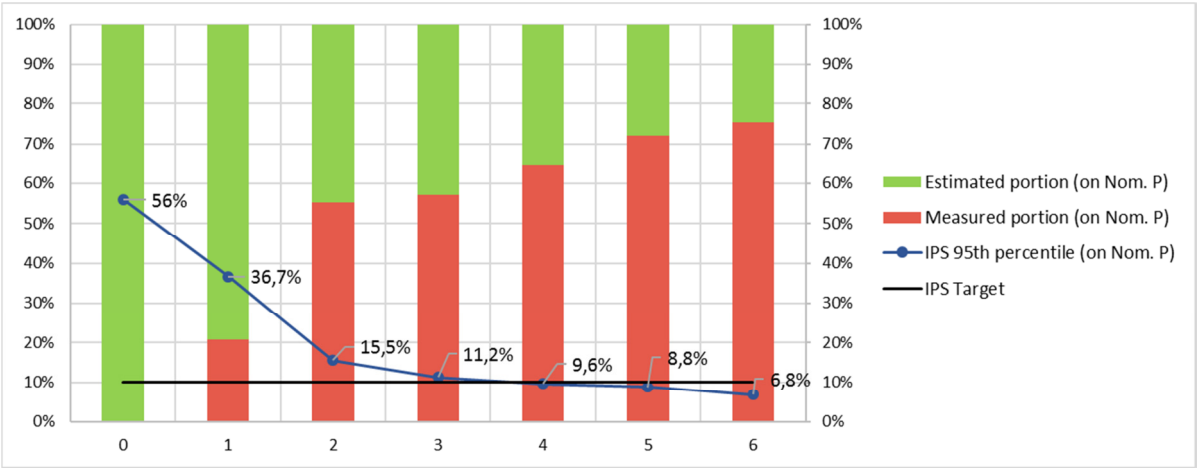

Figure 51: Graphic of the necessary measurements to satisfy the IPS target

For this analysis, the choice and the location of the PCRs and therefore of the monitored plants has been computed using an optimization algorithm to minimize the number of measurements. This approach highlights the influence of this choice on the estimation accuracy: for instance, as shown in Figure 51, the difference between bar 2 and bar 3 is a small increase of the amount of measured power but it reduces the index by more than 4%. This means that the monitoring of a small plant that is a good sentinel for the estimation of many hydro plants has major effect than the monitoring of another plant.

6.2.2 Siemens estimation algorithm

This paragraph illustrates the results of Siemens approach for the estimation simulations. In particular, the outcomes for the period 9th-12th of August 2018 are described considering the different hierarchical levels of the network; the main focus was to test the integration between the systems involved and the processing of information coming from different data sources.

In Figure 52 the processed Nowcast data and the "near real-time" data flow are shown considering the hydro component of the whole DSO network. The "near real-time" data flow was simulated processing on the SIEMENS Energy Management System the yearly data provided by the DSO.

Figure 52: Nowcast data for the entire Distribution Network

In Figure 53 the processed Nowcast data and the "near real-time" data flow are shown considering the HV/MV transformer level.

Figure 53: Nowcast data for the green HV/MV transformer

Figure 54 considers a single MV feeder connected to one of the two HV/MV transformers of the primary substation; compering the figures, it is evident how the data trend changes reducing the area observed and going closer to the single power plants. The trend shows a shape that differs from the profile at the level of primary substation and the values are generally more variable because the data are more affected by the behavior of single power plants.

Figure 54: Nowcast data for a MV feeder

Figure 55 shows the Nowcast data for a single MV hydro plant; this example shows a plant that has a very regular production during the considered period; this means that, although some plants may have a fairly constant production measured at their terminals, the power trend is more fluctuating considering larger portions of the network.

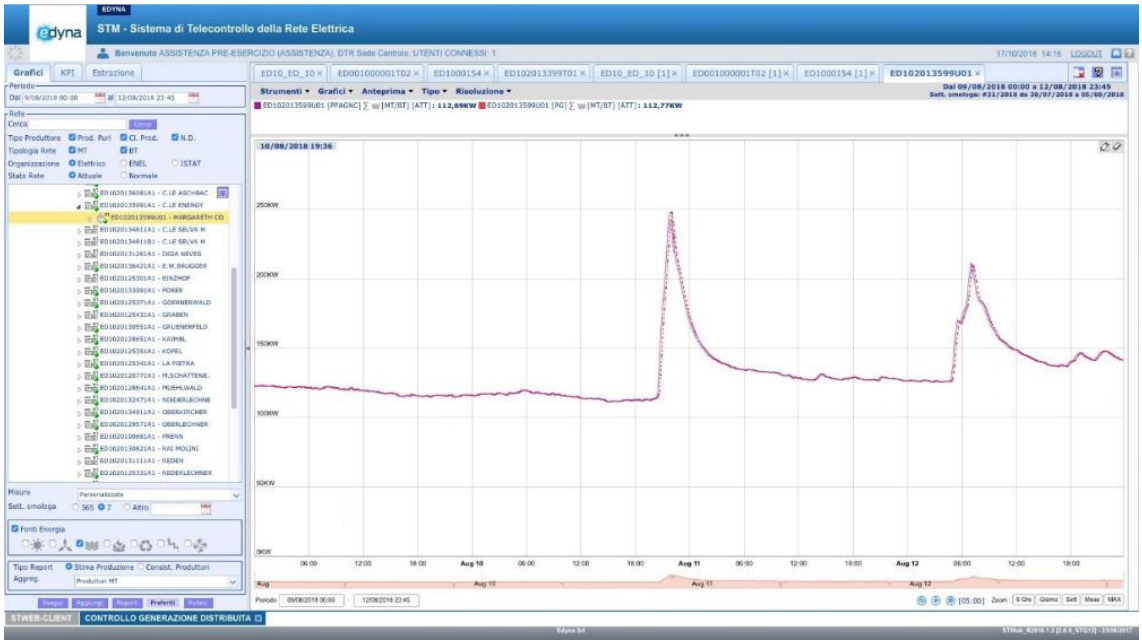

Figure 55: Nowcast data for a single MV plant

In Figure 56 the difference between the processed Nowcast data and the forecast data are shown considering the PV component of the production connected at the MV/LV transformer. The "real-time" weather data (solar radiation and temperature) was acquired and pre-processed by the Siemens Energy Management System gathering the data via Webservice from the public Bolzano Region weather Website. The red line represents the estimated trend of the delivered active power whereas the pink line is the real measure of the production.

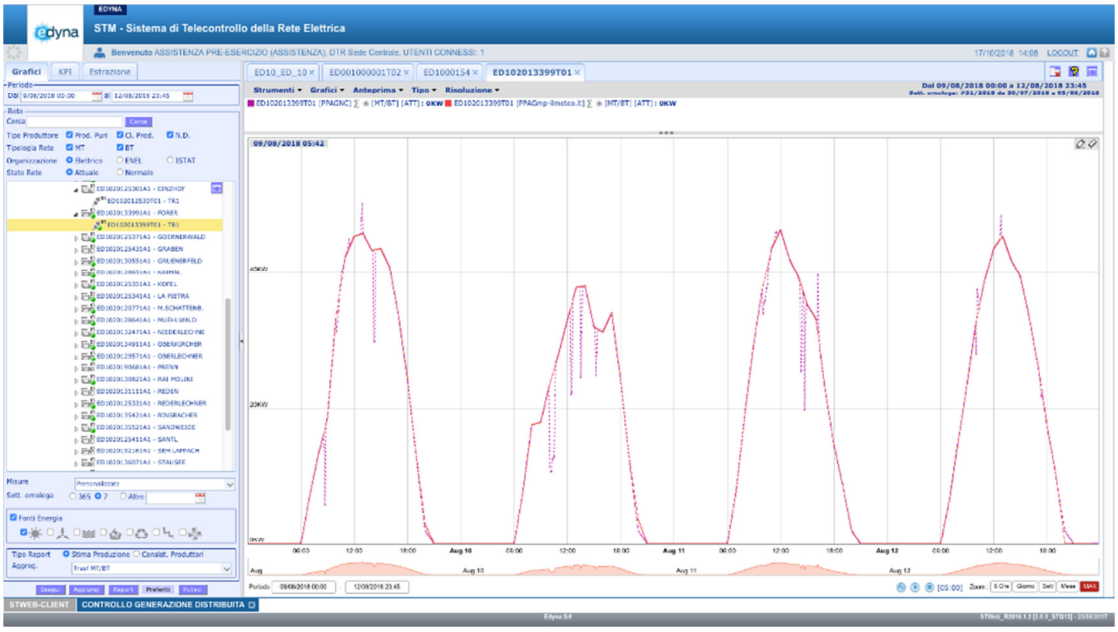

Figure 56: Nowcast data for a single MV/LV transformer

Figure 57 shows the aggregated results for the period 16th-17th of June 2018 considering the three relevant categories (PV, "other" DG meanly hydro and load) required by the TSO to represent the sources underlying primary substation as aggregations.

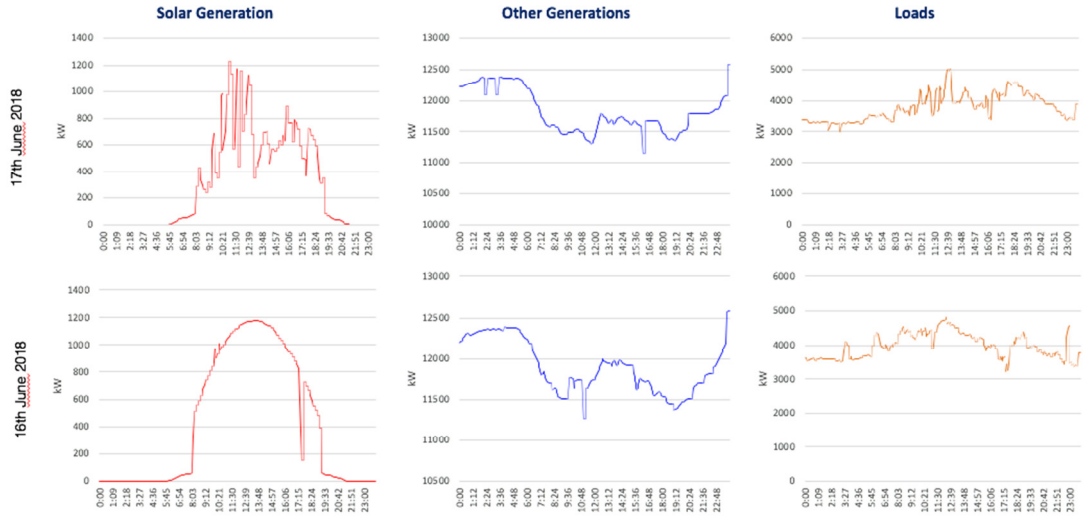

Figure 57: Aggregated data for the whole Distribution Network

In this part of the paragraph, some more results are described focusing on the measurement/nowcast trends comparison and on the IPS evaluation.

To evaluate in a consistent way the quality of the estimation with the solution adopted for the hydroelectric plants, types of indices were calculated:

- for each 15 minutes sample, an indicator referred to an energy comparison as defined in paragraph 5.2:
- for each minute sample, an indicator referred to the instantaneous active power comparison:

$$Accuracy = \frac{\left(\sum_j P_{metering\_j} - \sum_k P_{nowcast\_k}\right)}{\sum_j P_{\_metering\ j}} \cdot 100$$

$\mathbf{P}_{metering\_j}$: active power considering the real measure of the j – th plant

$\mathbf{P}_{nowcast\_k}$: active power considering the nowcast data of the k – th plant

Figure 58 shows the results for the aggregated hydroelectric component on the 2nd of December 2018. It is possible to see that basically the nowcast has a 15 minutes shift compared to the real measurement and also that the nowcast trend is more regular than the real measure; this last difference is connected to the nowcast processing that applies a linear interpolation between the available "near real-time" energy meters data (simulated for each MV plants).

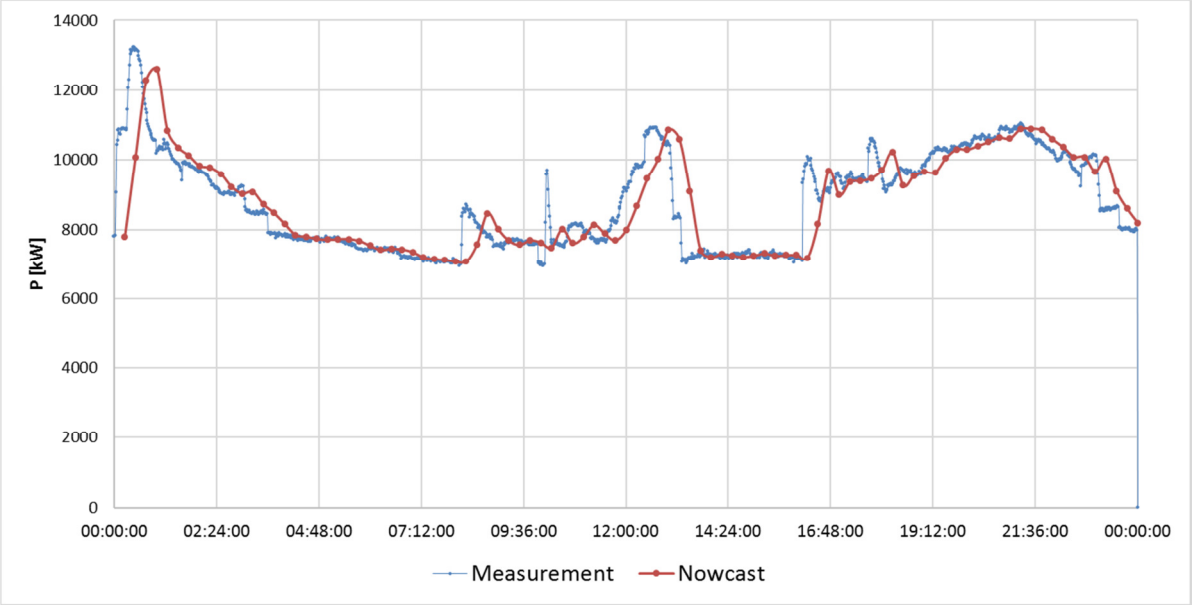

Figure 58: Aggregated hydro Nowcast vs Measure (2nd December 2018)

Figure 59 shows the trend for the IPS_{15min} on the 2nd of December; below some more data about the calculated index:

- average value: 0.736 %
- min value: 0.003 %
- max value: 4.850 %

IPS is an energy index of the accuracy and then related to the area under the power vs time graph; it means that it is not meaningful for this approach that provides to translate the same line of the measurement: the IPS only depends on the difference between the first and last values of the period considered.

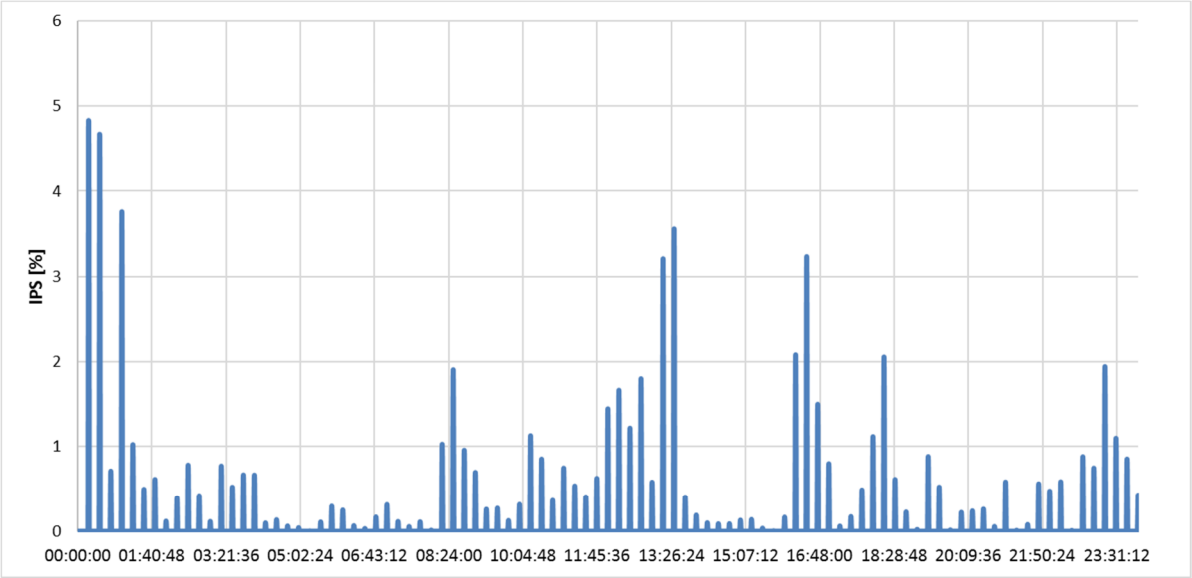

Figure 59: IPS_{15min} (aggregated hydro 2nd December 2018)

Considering the instantaneous accuracy of the power, Figure 60 shows the normal distribution obtained with the following calculated data:

- average value: 0.631 %
- standard dev: 8.123 %

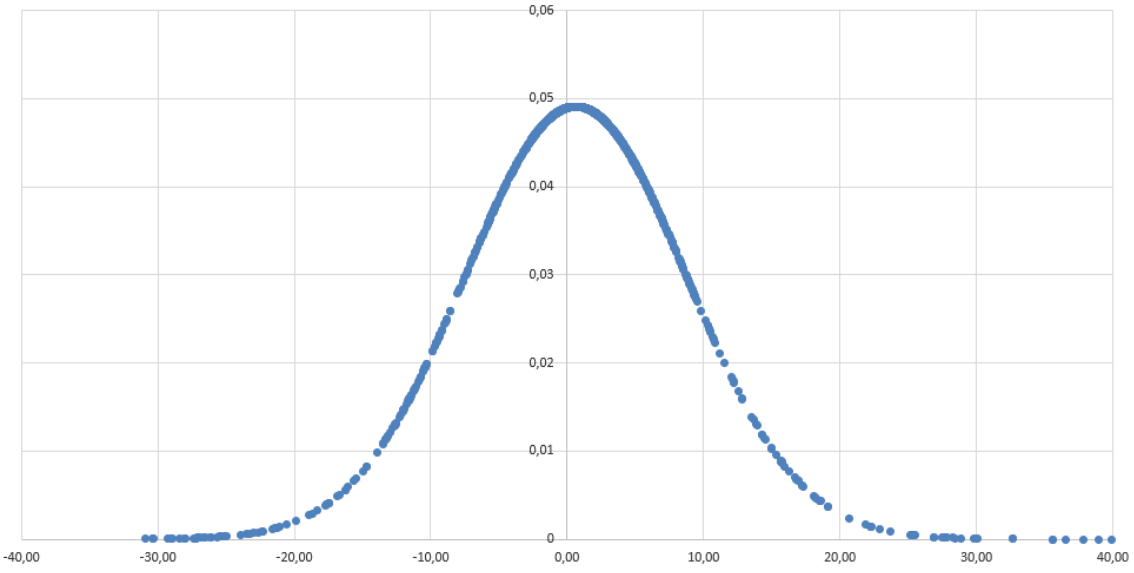

Figure 60: Normal distribution for the Accuracy index (aggregated hydro 2nd December 2018)

Same evaluations have been performed considering the data recorded 5th of March 2019. In Figure 61 the active power trends for the aggregated hydroelectric component are reported.

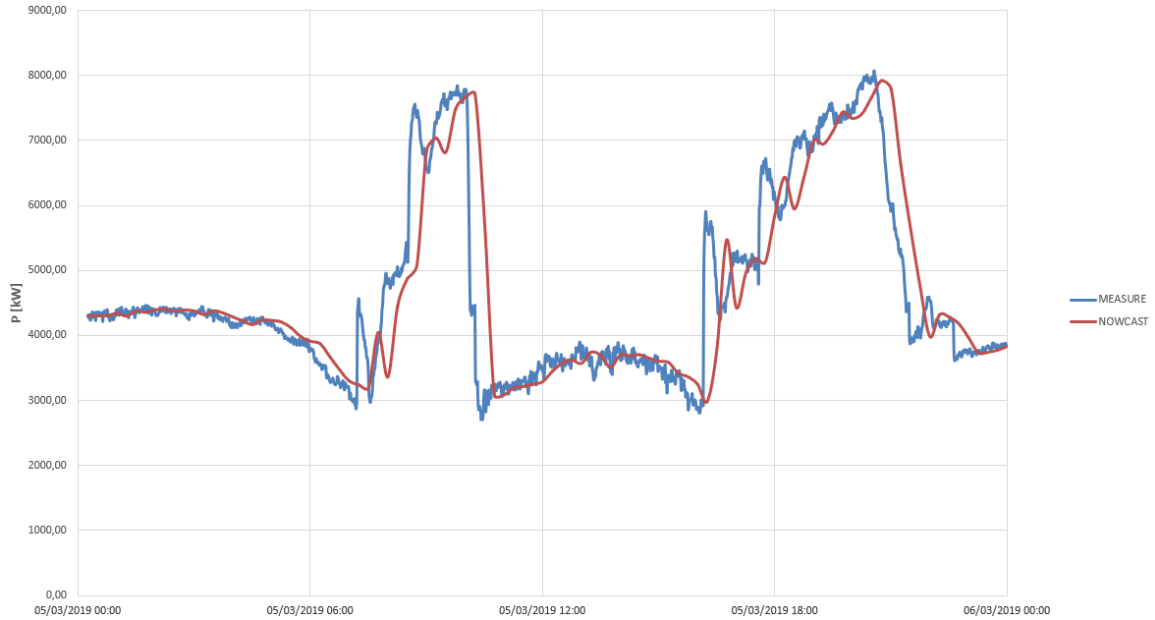

Figure 61: Aggregated hydro Nowcast vs Measurement (5th March 2019)

Figure 62 shows the trend for the IPS_{15min} on the 5th of March; below some more data about the calculated index:

- average value: 0.626 %
- min value: 0.008 %
- max value: 5.611 %

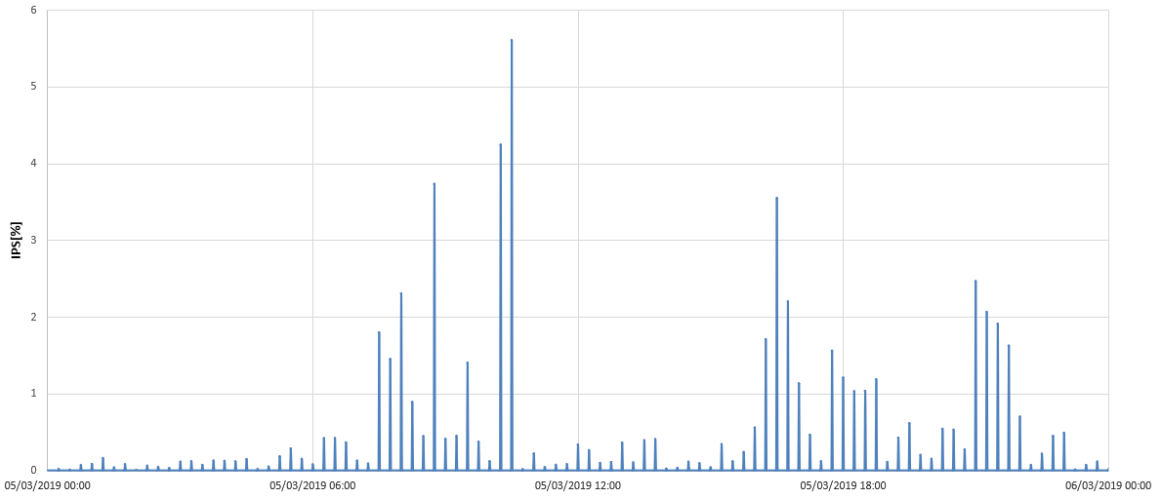

Figure 62: IPS_{15min} (aggregated hydro 5th March 2019)

Figure 63 shows the normal distribution for the Accuracy index obtained with the following calculated data:

- average value: 1.734 %
- standard dev: 18.238 %

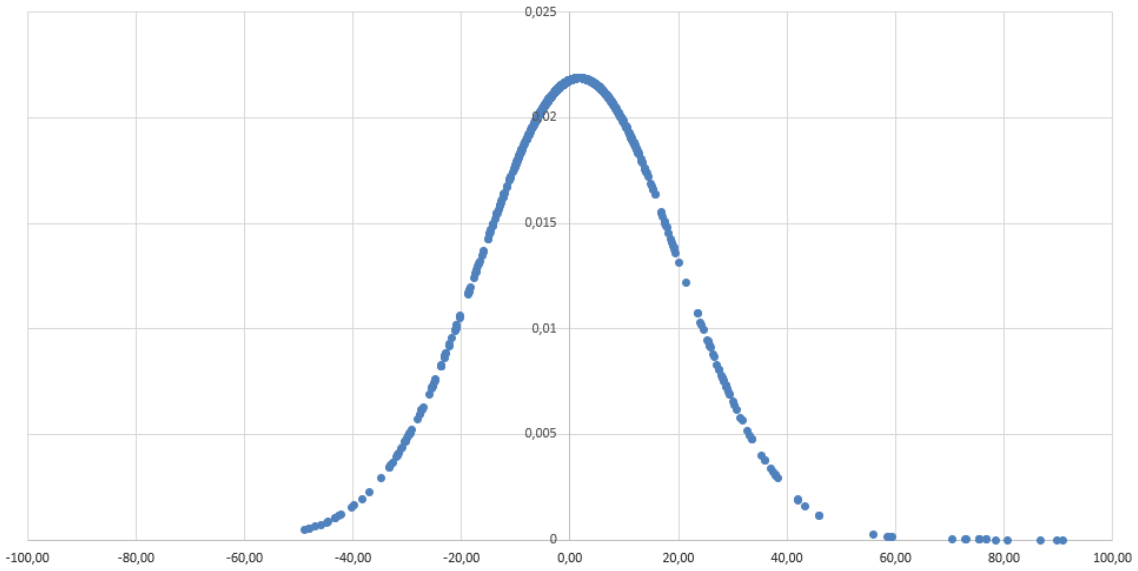

Figure 63: Normal distribution for the Accuracy index (aggregated hydro 5th March 2019)

Comparing the different test cases, it is possible to observe that the average value for the IPS_{15min} is slightly lower for the day in March. The most significant conclusions can be found considering the Accuracy index where it is clear how the lower and more irregular hydro generation registered in March brings to a higher (and more dispersed) instantaneous error.

Regarding the PV component of the DG, the evaluation has been carried out calculating the IPS already described in section 5.2 on a daily and weekly basis to evaluate the quality of the estimation.

Figure 64 shows the comparison between the real measurement and the nowcast estimated data (for the only MV PV plant of the network) considering one week from 13th to the 19th of March 2019. It is possible to see how the "classical" solar forecast is replaced by the nowcast trend obtained using he "real-time" solar radiation and temperature data acquired from the public Bolzano Region weather Website.

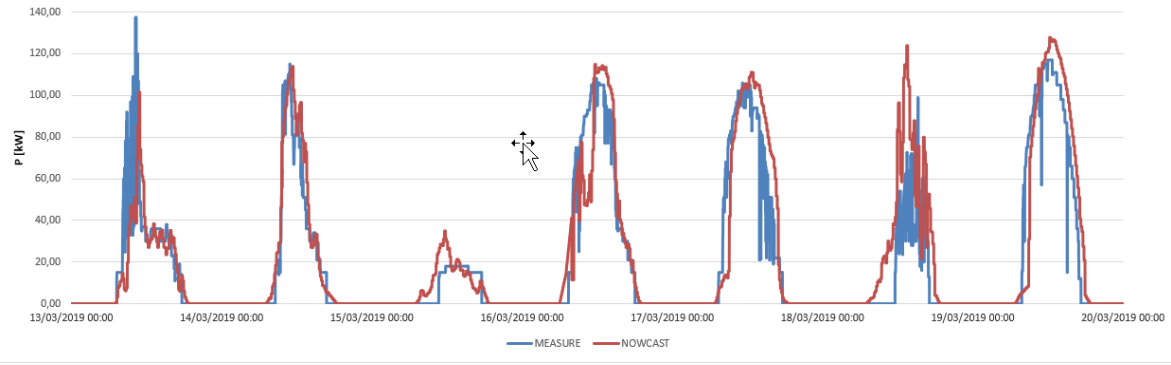

Figure 64: Aggregated solar Nowcast vs Measurement (13-19th March 2019)

The more significant residual offsets between the two curves can be explained considering disturbance factors like the possible "out-of-order" status of the plant/measure errors that can be seen on the 18th of March or, generally, the periodicity and exact geographical position considered for the acquired weather data (i.e. the available data had a periodical refresh every 10 minutes).

The figure below (Figure 65) shows the trend for calculated daily IPS for the whole week:

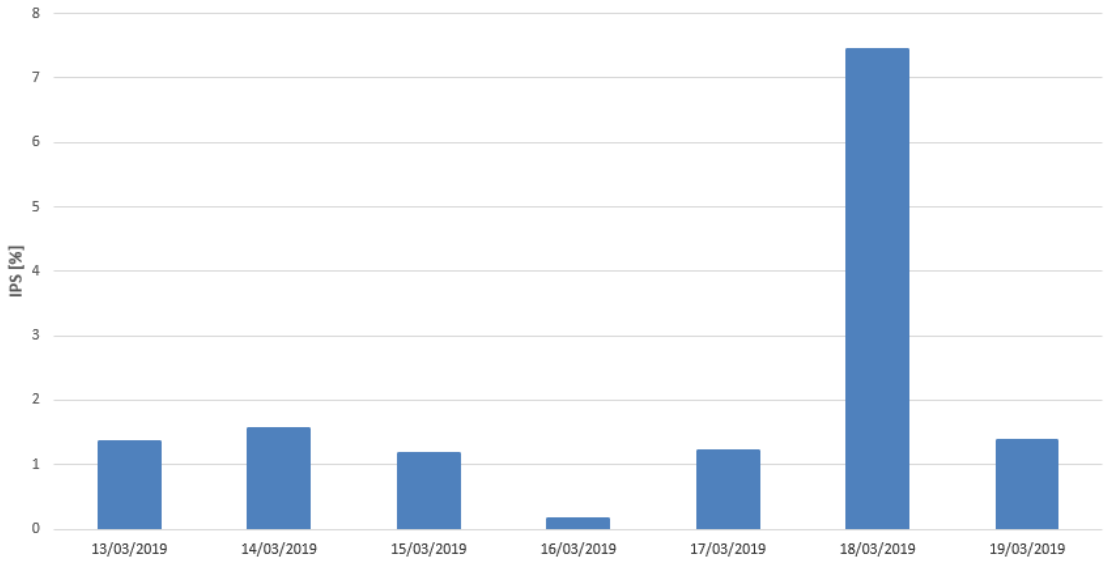

Figure 65: Solar plant IPS (13-19th March 2019)

As already highlighted before, the 18th of March offered some specific issues for the nowcast estimation and this is confirmed also by the IPS value that is quite high compared to the other days of the week. Another reason that explains this high value of the IPS is that there was a predominant over estimation and almost no under estimation (generally speaking, since the IPS is calculated according to the overall energy balance on the considered period, over and under estimations compensate each other lowering the IPS).

6.3 Voltage regulation by MVRS

6.3.1 Selta voltage regulation

As described in paragraph 4.2.1, in order to provide the voltage regulation, it is necessary to have an accurate estimation of the considered network. Selta MVRS allows to monitor in real time the state of the MV distribution grid, along the feeders subtended the Primary Substation. With these details, every cycle of load flow calculation provides the evaluation of the nodal voltage profiles and the power transfer.

This information allows to represent the MV grid as shown in Figure 66.

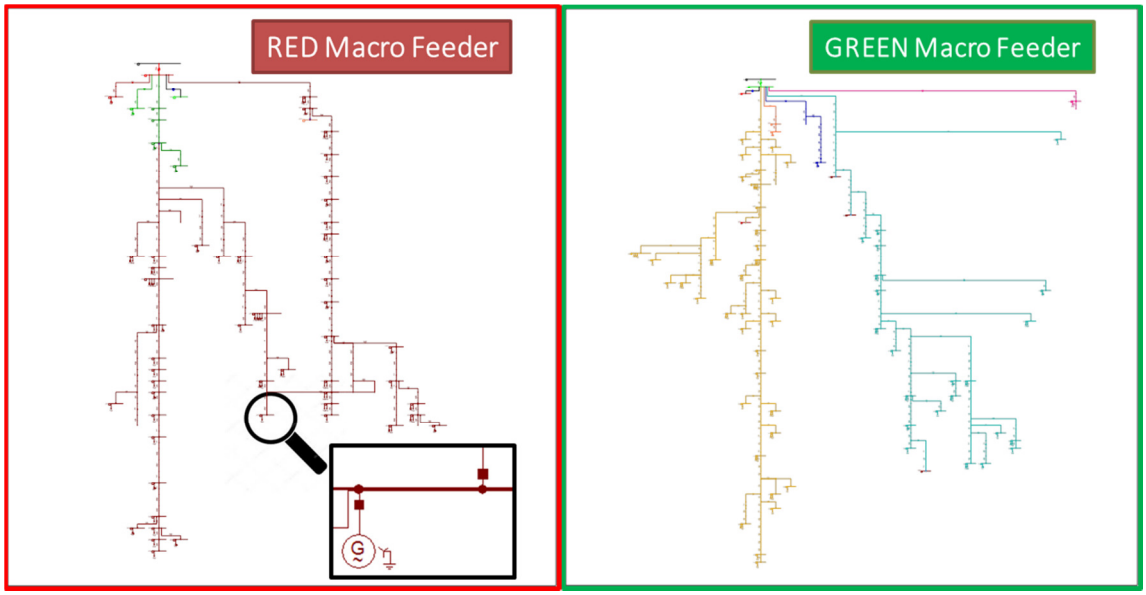

Figure 66: Representation of the feeders below the two transformers of the Primary Substation

An important functionality of the MVRS is the possibility to get the voltages of the portion related to the distribution grid under control: from the MV side of the transformer at the primary substation until the farthest secondary substation. Keeping the feeder voltage profile within the range recommended (±5% of the nominal voltage) is a priority for the system. This functionality allows the DSO to comply also with the new requirements regarding the maintenance of the reactive power exchange with the transmission grid, established by the new European regulations (DCC – Demand Connection Code).

In fact, if some violations occur, MVRS advises the TSO about the impossibility to satisfy the ancillary services requested and chooses as a priority the best action in order to solve the voltage violations, as illustrated in Figure 67:

- Reactive Power of DGs is modified if it is sufficient to solve violations;
- Control of OLTC is selected if the maximum violation is higher than a single tap value.

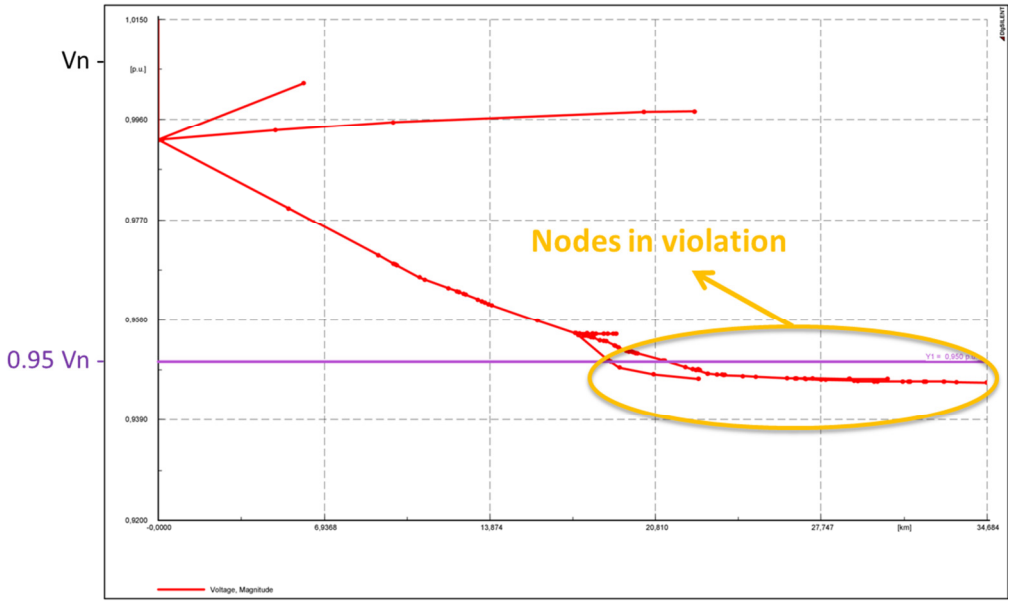

Figure 67: Feeder voltage profile

For this reason, the MVRS is employed by the DSO for the local voltage regulation. In fact, due to the spread of DG, the MV grid involved in the project is characterized by high voltage profiles at the MV busbars of the primary substation and at the MV lines connected to them. The voltage along some lines tends to reach values close to 22kV and it gets hard to maintain voltage values within the limit required in accordance with standard CEI EN 50160.

For example, the graph in Figure 68 shows the average voltage values of the MV busbars of the Primary Substation in the period April-October 2017.

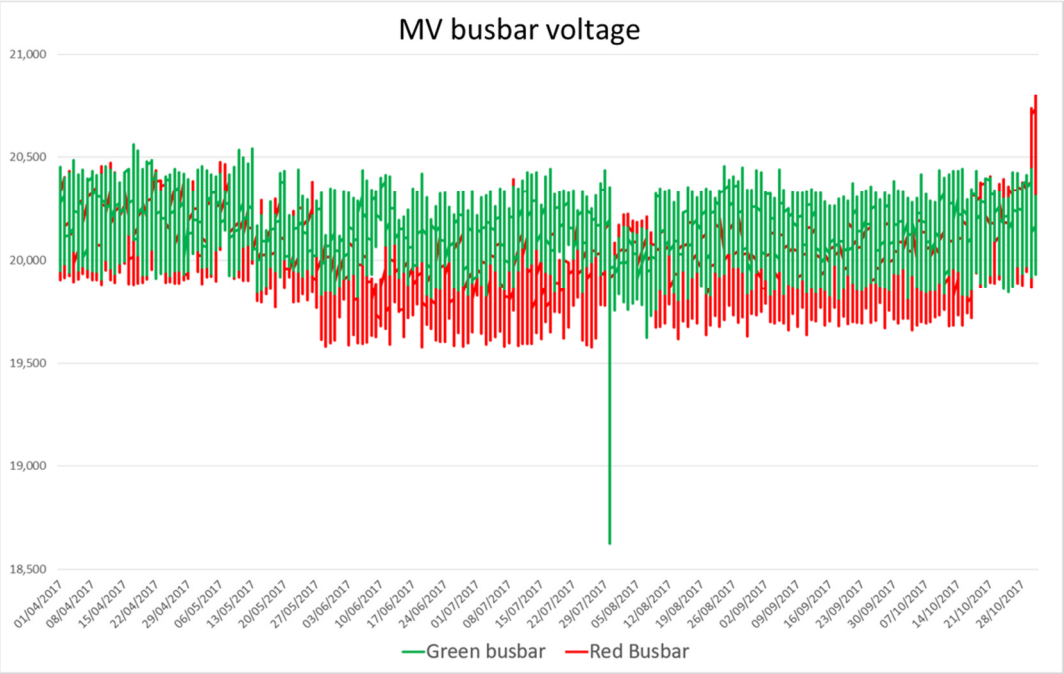

Figure 68: Voltage trend at the MV/HV transformers during 2017

Figure 69 represents the typical trend of the voltage along the MV feeders, that increases by moving from the primary substation towards the end of the feeders.

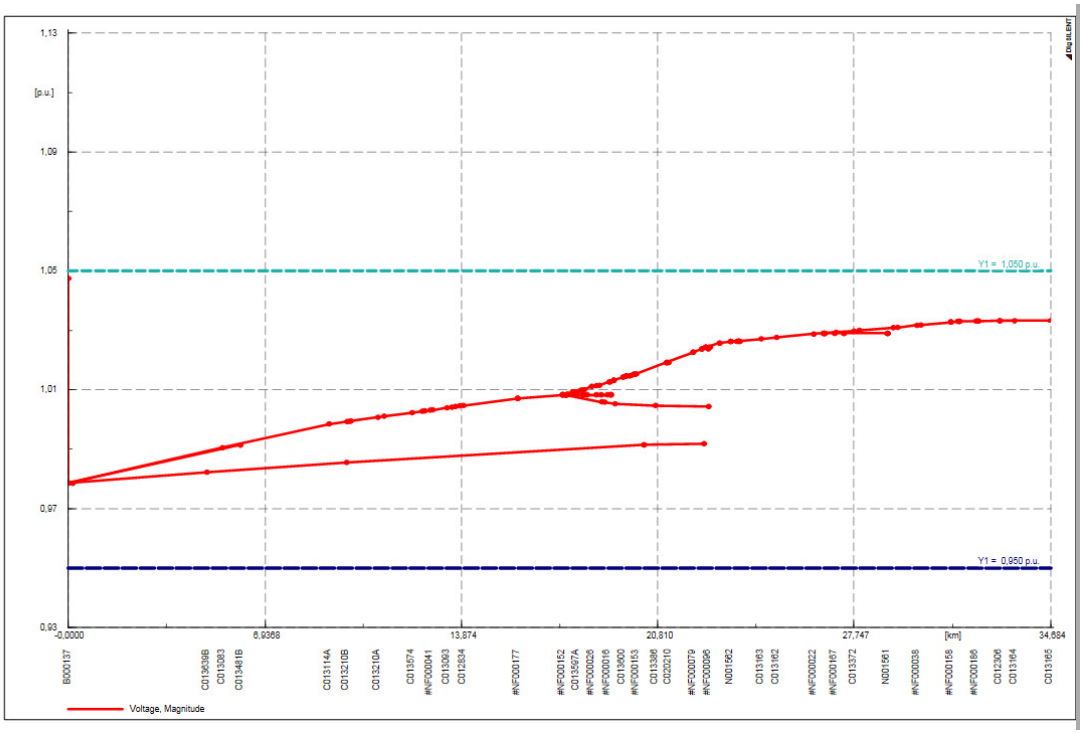

Figure 69: Voltage trend along the MV feeders connected to the primary substation

The DSO Edyna is currently using the device to regulate the reactive power of the hydro power plants involved in the project to improve the voltage levels.

The system calculates regularly the load-flow of the whole MV grid considered taking into account the available measurements to obtain real time capability at the substation and report any violation of voltage limits in the MV grid. If the MVRS detects a violation, it dispatches commands to the OLTC of the substation transformer and to each power plant to regulate the reactive production, to ensure that the voltage remain within the permissible limits, in the current configuration set to ± 7% of the nominal values. The DSO uses a passive sign convention, so that an inductive reactive power is negative and lead to an increase of the voltage, while a capacitive reactive power is positive and lead to a decrease of the voltage.

Figure 70 and Figure 71 have been introduced to explain the functioning of the voltage regulation. Each graph illustrates the electrical measurements of two power plant connected to the same busbar between 16:00 on 12th September and 24:00 on 13th September. Around 21:30 on 12th September, the MVRS recognized a violation in the grid and sent a setpoint to the plants to increase the reactive power. The plants started to absorb reactive power and the effect is a reduction of the voltage at their terminals. Instead, around 10:00 on 13th September, the command was to reduce the reactive power: the plants reverted to inject reactive power in the grid and the voltage tended to increase.

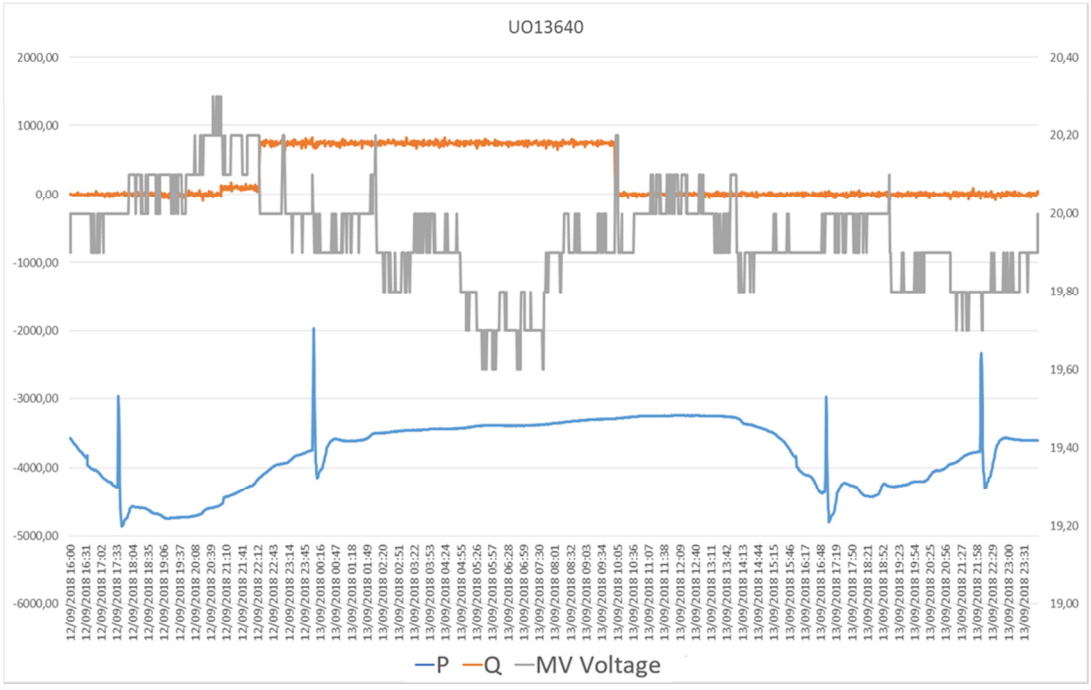

Figure 70: Power and voltage measurements at the terminal of a power plant - 12th -13th September 2018

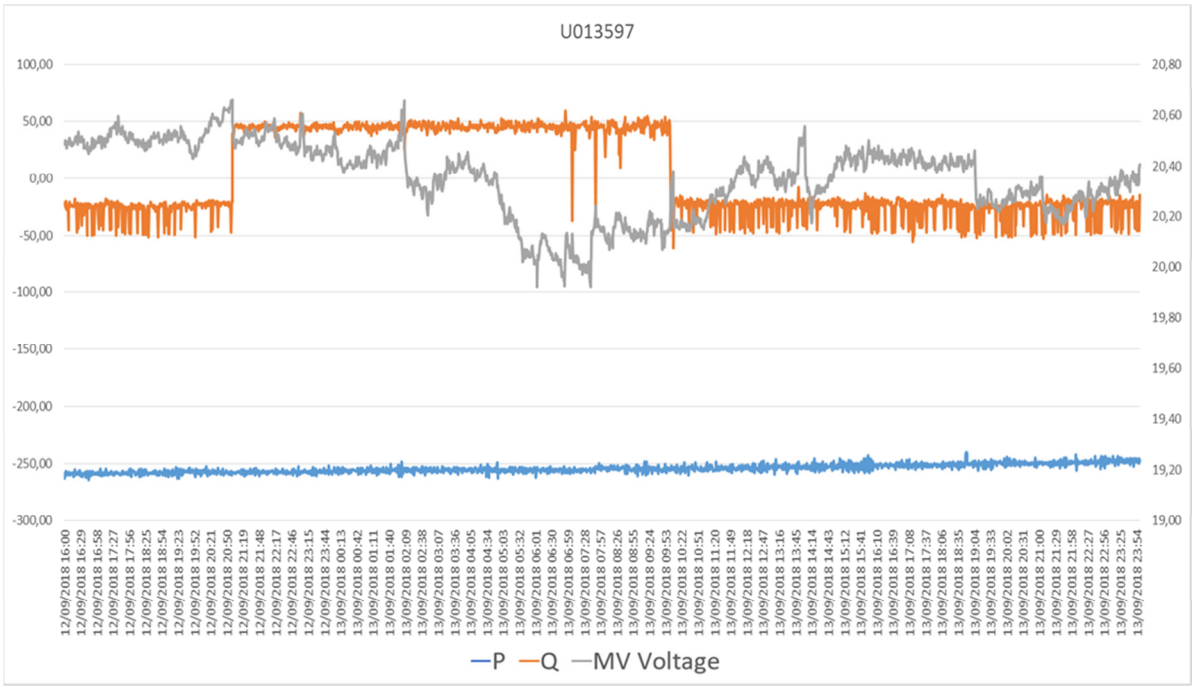

Figure 71: Power and voltage measurements at the terminal of a power plant - 12th -13th September 2018

The effect at the MV busbar of the substation in clearly less evident in terms of voltage, as reported in Figure 72, due to the contribution of the other part of the grid connected.

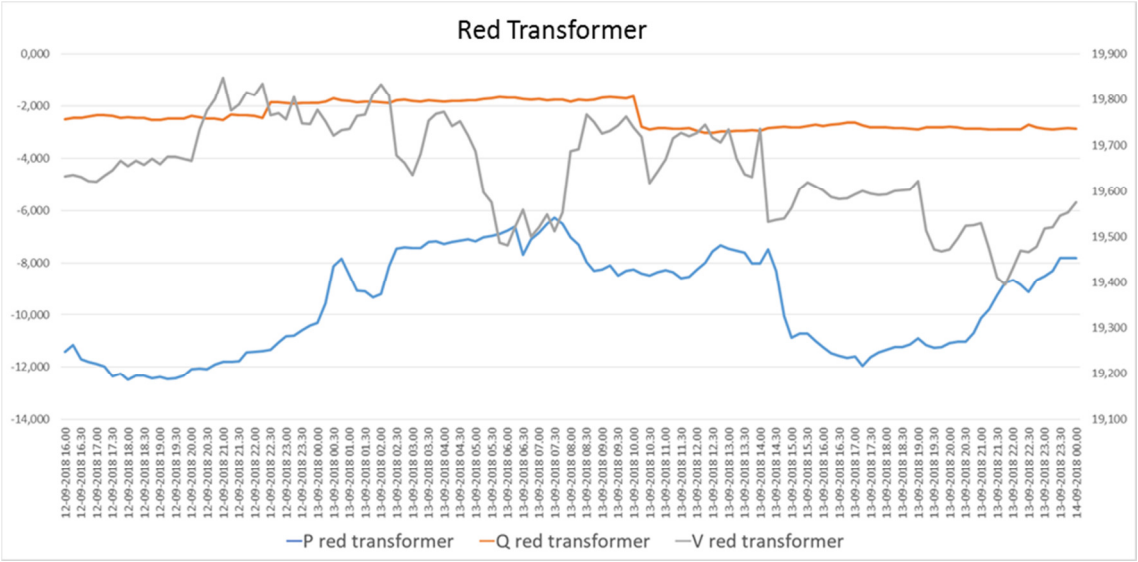

Figure 72: Power and voltage measurements at the substation transformer 12th -13th September 2018

The functionality is continuously operational from July 2018 and the benefits will be shown here below through comparisons between the voltage measurements in 2017 and 2018. Figure 73 compares the voltage profiles at HV/MV transformers, while Figure 74 shows the voltage at the terminals of a hydro power plant, that historically has had main voltage problems.

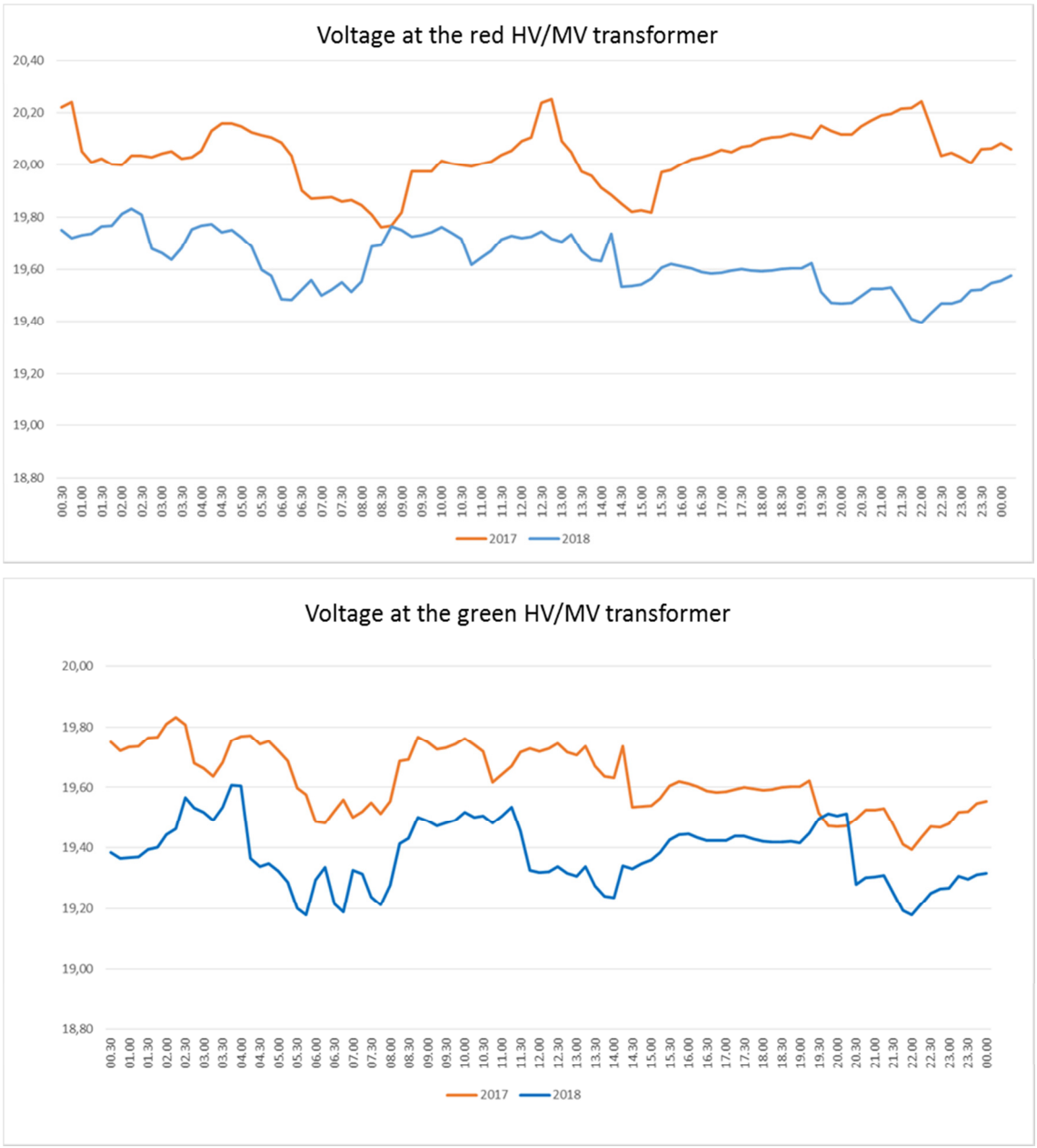

Figure 73: Comparison between the voltage trends during 13th September 2017 and 2018 at the substation transformers

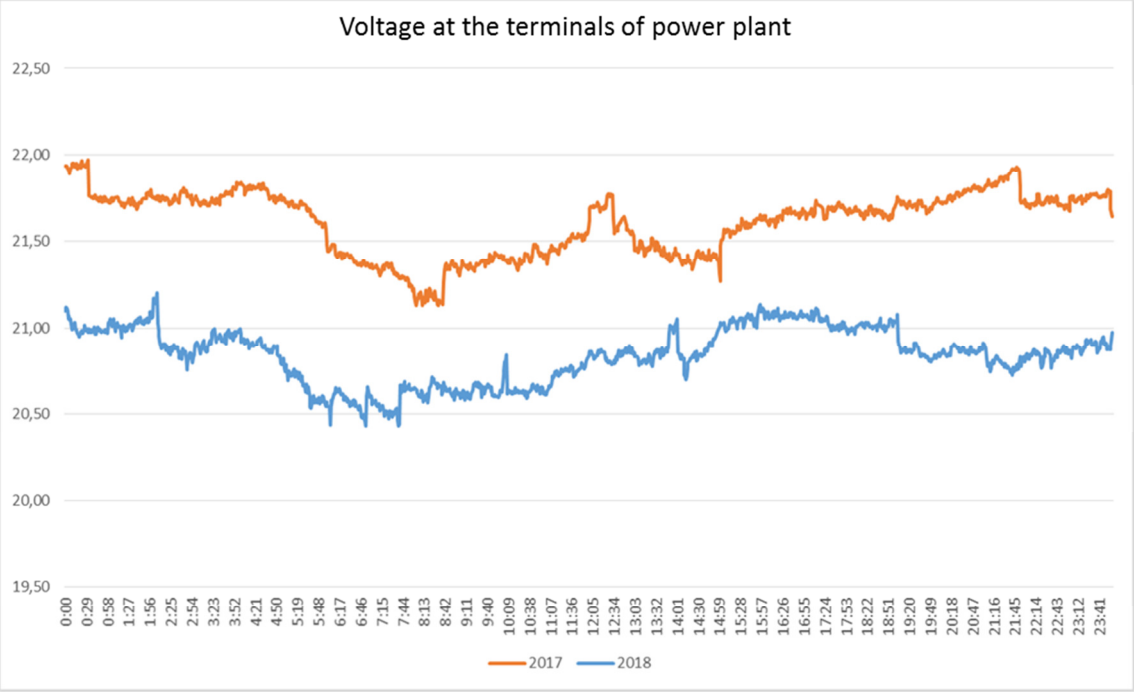

Figure 74: Comparison between the voltage trends during 13th September 2017 and 2018 at the terminal of a power plant

It is evident the benefit obtained in the management of the voltage in the distribution grid: the voltage of the plant has been reduced by about 1 kV, remaining in a deviation range of 7% of the nominal voltage.

If no violations are detected, MVRS recognizes the controlled power plants as available for the centralized voltage regulation and the voltage regulation modules run as described in paragraph 4.2.1 to calculate the VPP reactive power capability and to allow the remote control of the involved power plants.

In order to test the operation of the voltage regulation functionality of MVRS, a study case has been carried out and significant results have been collected. With the participation of every partner and included power plants owners, physical devices have been tested and real time effects have been recorded. The experimentation has been carried out with the participation of 5 hydroelectric power plants.

The regulation was provided separately at the two transformers involving the power plants connected at the corresponding transformer. Once the dynamic capability of the controlled MV system is elaborated and transmitted to the TSO for each transformer, the regional control centre of the TSO sends reactive power setpoint to MVRS in order to regulate HV busbar voltage. Then MVRS elaborates the level received and spread the single setpoint to the controlled DERs connected at the corresponding transformer.

The following part of the document describes the tests and results of the experimentation.

In Figure 75 the three different reactive power measurements available at Red Transformer during the tests are reported. The yellow line represents the reactive power generated by the controlled and

aggregated DERs (corresponding to the aggregation as define in the observability functionality). The same diagram reports the reactive powers exchanged at the interconnection point: blue line indicates the reactive flow at the MV side instead red line states HV side measure at the transformer.

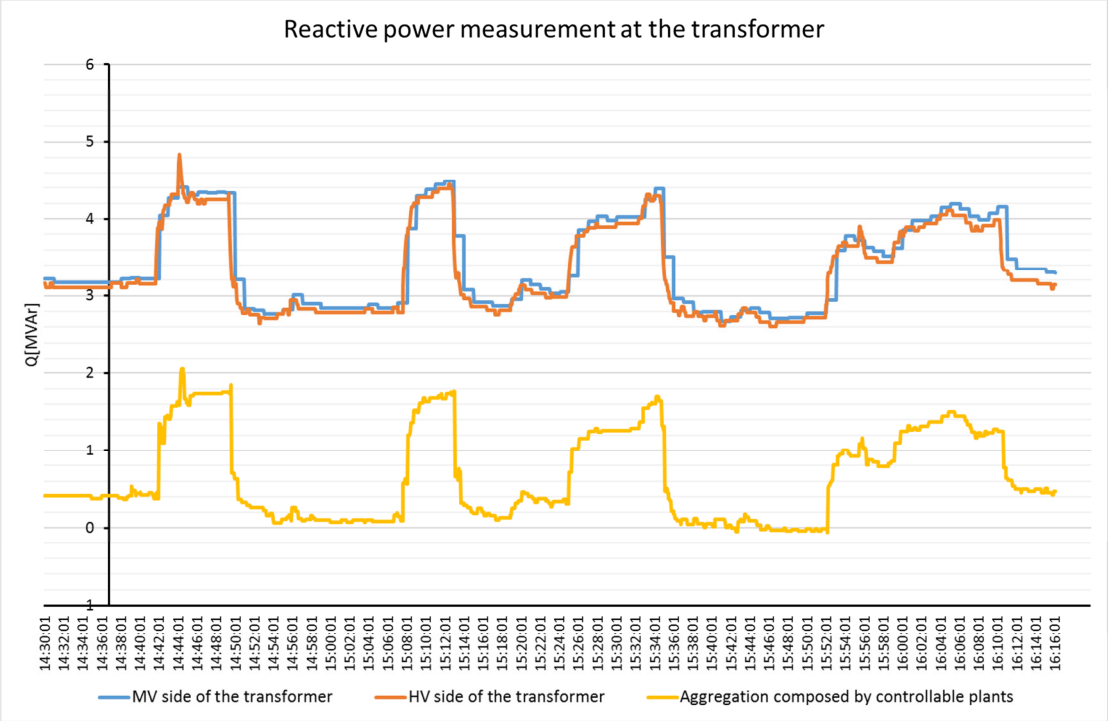

Figure 75: Trends of the three different measurements of reactive power recorded during the tests

Figure 76 illustrates the three different physical points where the control system takes the three measurements mentioned above. HV/MV sides of the transformer and the controlled DERs aggregate are monitored in real time.

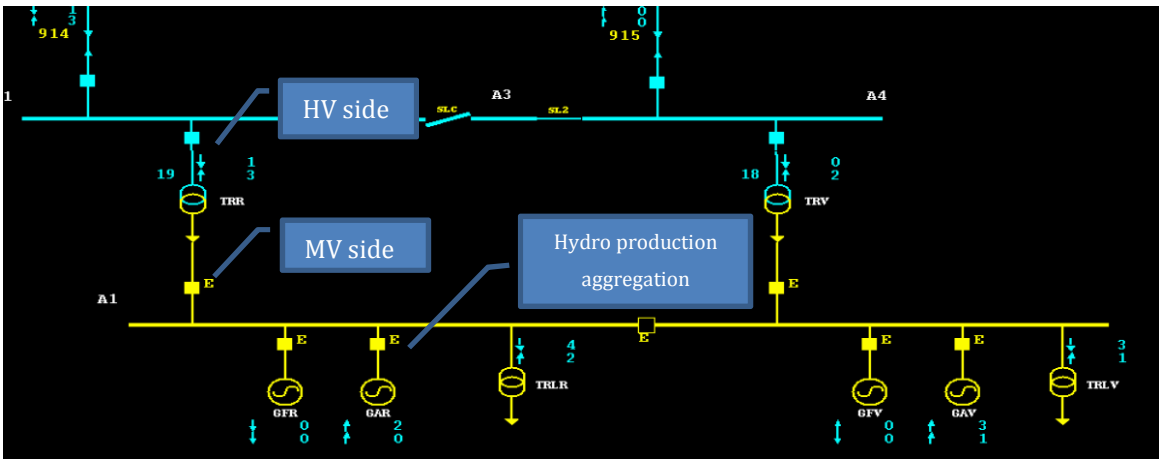

Figure 76: Indication of the measurement points

Collecting information from the PCRs and considering the nodal voltages of the grid, MVRS calculates the available reactive contribution of the controlled group of hydroelectric generators considered as a

Virtual Power Plant. Figure 77 illustrates the trend of the capability of the aggregate subtended at the Red Transformer calculated by MVRS during the tests in question: blue line represents the inductive reactive power (positive reactive power to increase the voltage) and grey line represents the reactive power (negative reactive power to reduce the voltage). The reactive power capability is here expressed in terms of maximum reactive variation (in over- and under-excitation) compared with respect to the operational point of the VPP and then referred at the interconnection point. Graphically it means that the x-axis can be considered as the reactive value of working point. The two instantaneous values are sent to TSO control system in order to allow the TSO to exploit the whole capability being sure not to cause voltage violation in MV grid.

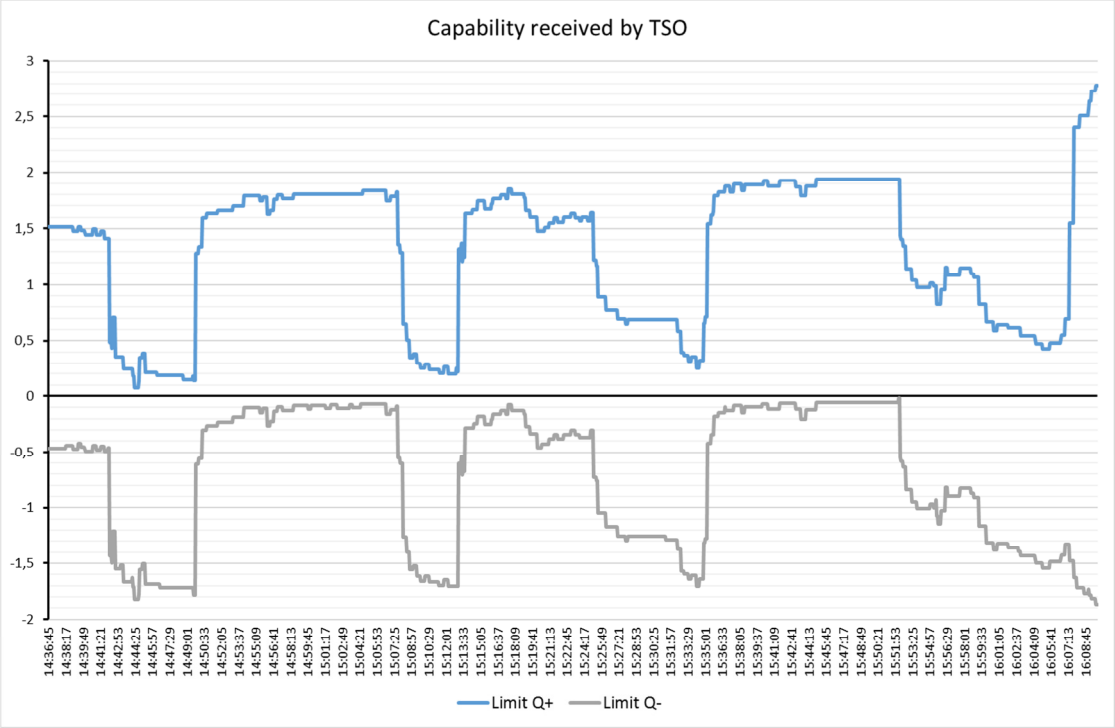

Figure 77: Reactive capability subtended to the Red Transformer transmitted to the TSO control system

Figure 78 shows from another viewpoint the time trend the capability (red and blue lines) and the working point (green line) in terms of the reactive power exchange at the Red Transformer. Green line (QLAV) indicates the reactive power flow at the interconnection point as absolute value. The limits of the reactive power, calculated as working point plus instantaneous capability values, are reported in the same diagram and, specifically, the red line represents the positive limit and blue line the negative limit: the area between the limits is the available band and the area between the working line and each limit can be used by TSO to manage the regulation.

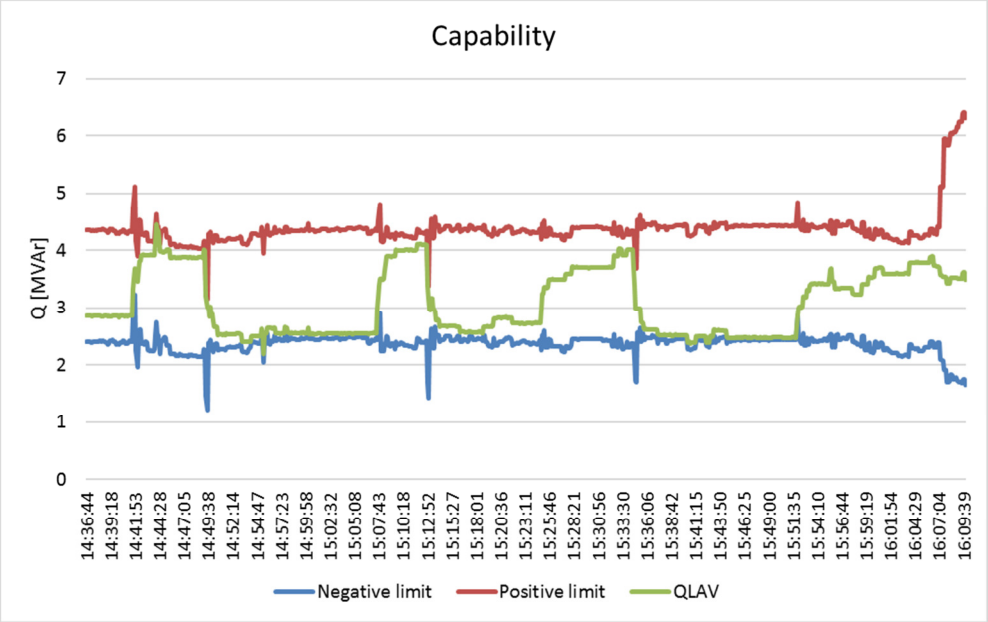

Figure 78: Capability of the VPP as reactive power flow at the Red Transformer

Figure 79 shows the trend of reactive power generated by the DERs aggregate (blue line) during the reactive power regulation. The reactive power setpoint expressed as a percentage is sent by the TSO (grey line) and it is followed by its feedback sent by MVRS (orange line) once received the command. Moreover, it is evident that the reactive power contribution of the aggregation changes its measured value according to the modification of the requested target. When the setpoint is positive (between 0 and 100%) reactive power rises and if it is negative (between 0 and -100%) reactive power decrease. When the setpoint is null, the MVRS maintains the static situation.

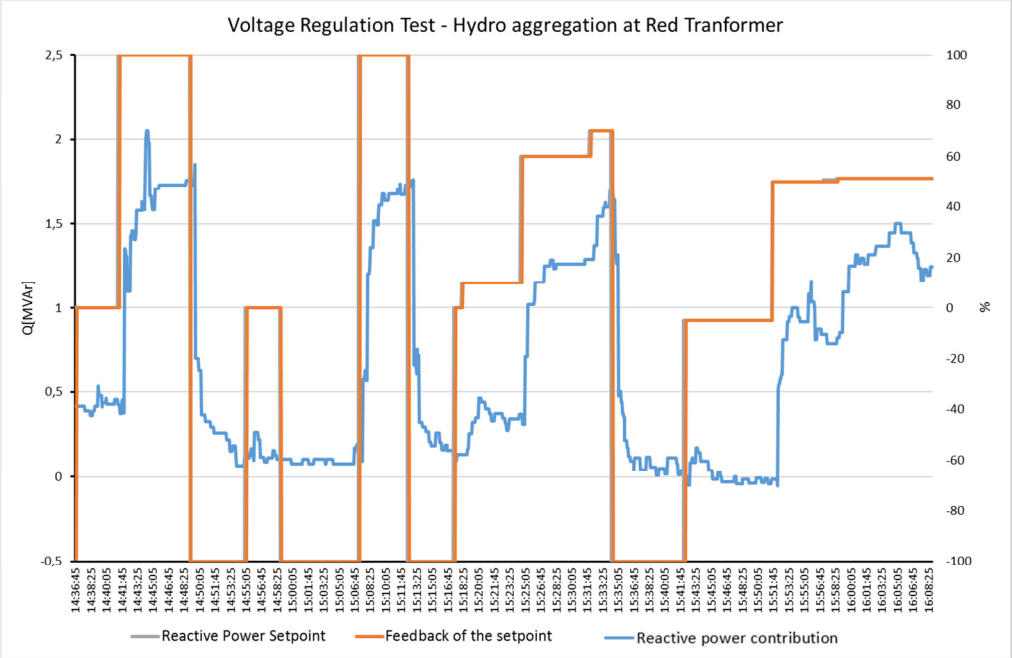

Figure 79: Comparison between the setpoint and the real contribution of the VPP

In order to interpret the signal from the TSO in a correct way and to forward the command to the single plants, MVRS calculates the absolute value of the reactive power requested at the interconnection point. Figure 80 shows that when the TSO level changes its value the system calculates a new reactive power setpoint, taking into account the total dynamic capability. When the level sent by the TSO is constant or null, the MVRS does not modify its command and maintains the previous level.

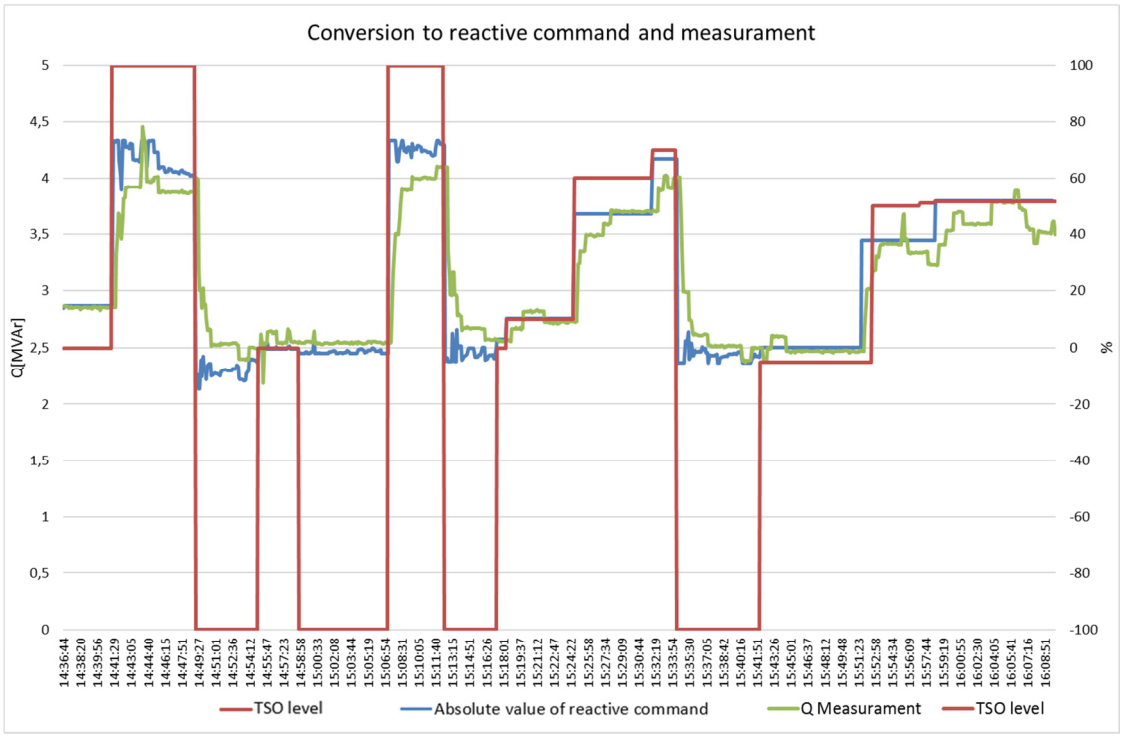

Figure 80: Percentage setpoint, reactive power command and reactive power measurement at the Red Transformer

Figure 81 shows how the power plants through the control of the MVRS applied the setpoint and the effect at the interconnection point between TSO and DSO. Blue line indicates the target of the regulation requested by the TSO in terms of reactive power and calculated by MVRS. Red line represents the measurement of the reactive power at the MV side of the transformer. The measurement of the reactive power at the HV side is expressed with the green line. The difference between MV and HV value depends on accuracy of measurement equipment and power losses of the transformer.

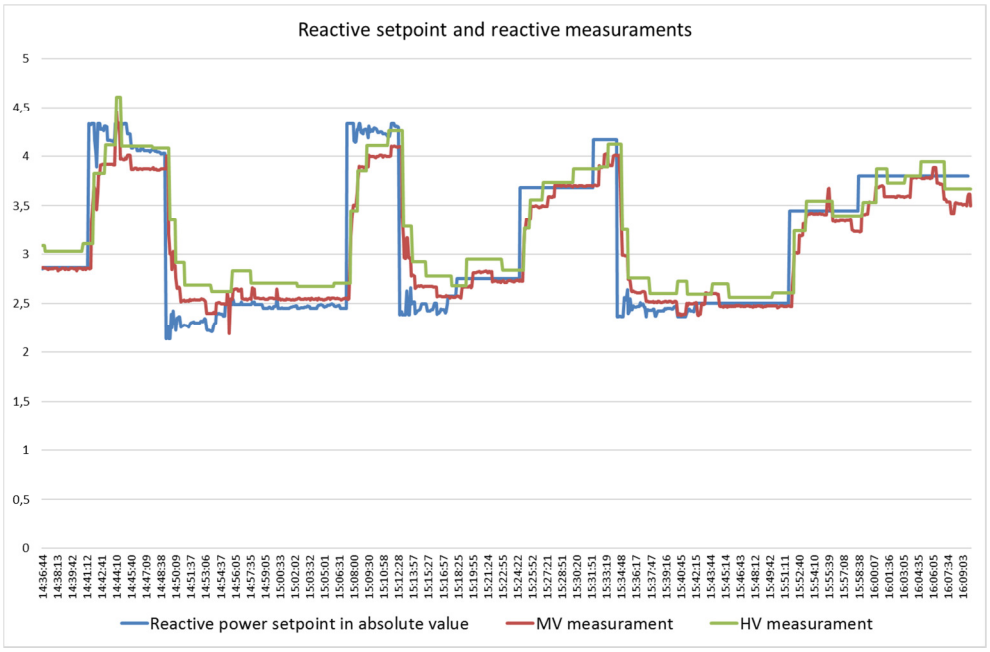

Figure 81: Reactive setpoint and measurements

The total setpoint calculated by the MVRS is then split in specific commands for the single DER. In Figure 82 the blue line is the total setpoint and the other lines represent the command forwarded to each of the three power plants regulated by the MVRS.

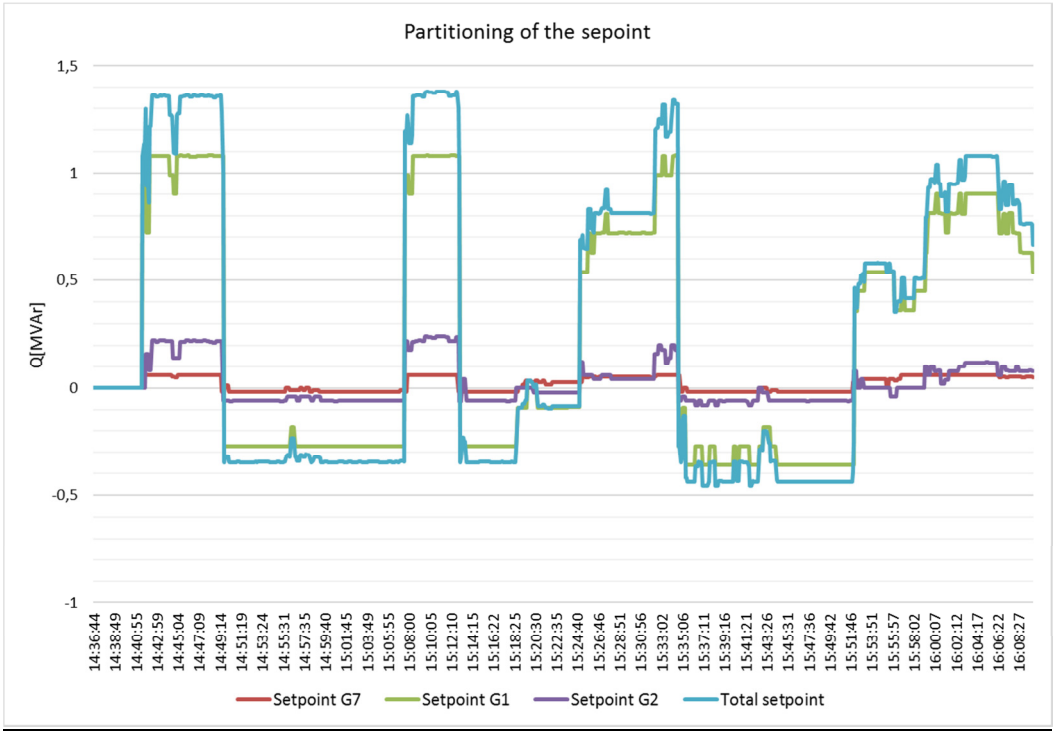

Figure 82: Splitting of the setpoint to the single controlled plants

The diagrams below describe the behaviours of each power plant involved in the reactive power regulation through setpoints calculated and provided by the MVRS. The blue broken line represents the level requested by the TSO, expressed as a percentage. The green line is the command sent to the single DER, expressed in MVAr. The measurement of the reactive power at the terminal of each plant, measure through the PCRs, is represented by the red line and is expressed in MVAr.

As detailed below, each power plant had different response that depends on the single characteristics of the generator and of their control system.

Figure 83 shows the response of the hydro power plant 1, that provide the best response among the plants involved in the regulation. In fact, the trend of reactive power measurement follows properly the reactive power command sent by the MVRS to the plant. The group reached the limits both in over- and under-excitation and the time response is acceptable (maximum 1 minute).

As illustrated in Figure 84, the hydro power plant 7 achieves good results in terms of regulation. The behavior is clearly not symmetric: in over-excitation, the reactive power generated is close to the requested values while in under-excitation, the regulation is less accurate and the measurement did not reach the reactive setpoint received. This behavior is due to technical constraints of the generator that are not taken into account by the MVRS.

Considering Figure 85, the tests about the the hydro power plant 2 show a slower dynamic response to the commands. The regulator system reverses correctly the trend of reactive power in accordance with the setpoint, but the delay of the response is not compliant with this kind of service, especially in reducing the reactive power production; the delay to reach the reactive power target, as represented in the figure, is in the order of minutes upward and till 20 minutes downward. Furthermore, as described for the power plant 7 the controller cannot reach the limit imposed.

An important aspect highlighted by the experimentation is that each regulation is characterized by an asymmetrical mode, due to technical limits of the hydroelectric generators. In fact, it is evident the greatest contribution in case of over-excitation, while no power plant shows the capability to absorb reactive power to further reduce the voltage following the TSO command. The technical limits are intrinsic in the static capability curve adopted for the controlled power plants.

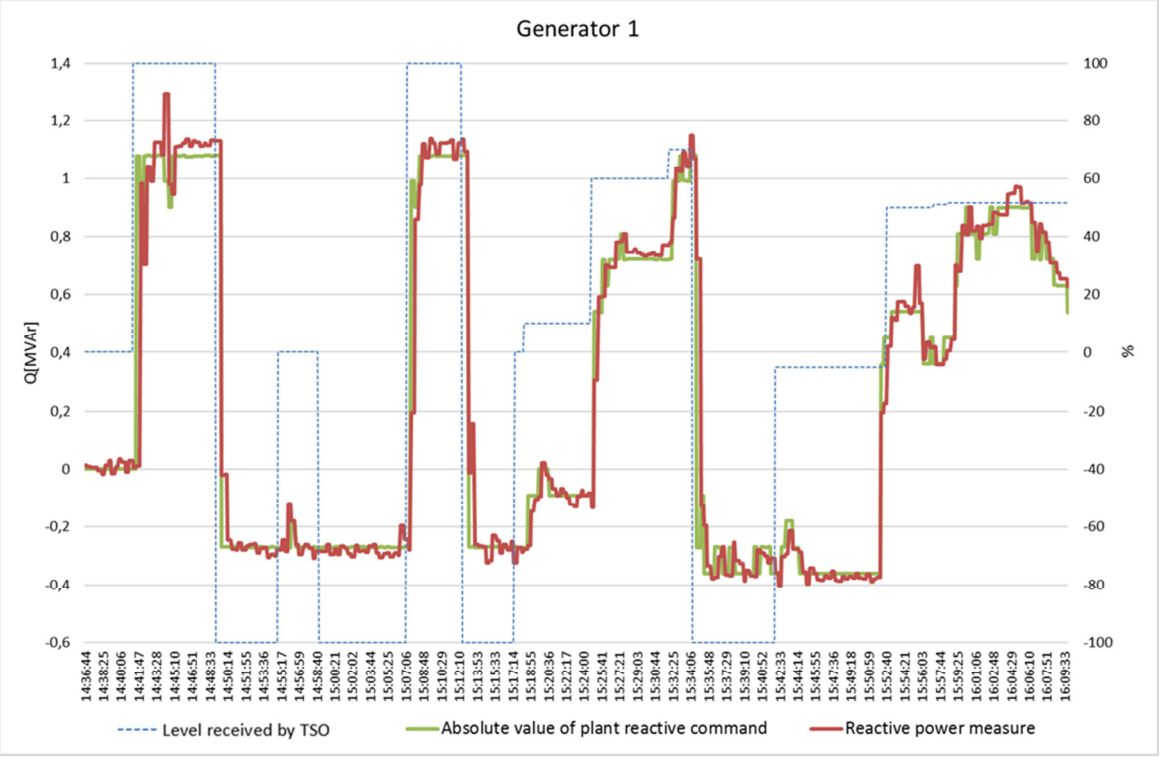

Figure 83: Response of Generator 1 in reactive power regulation

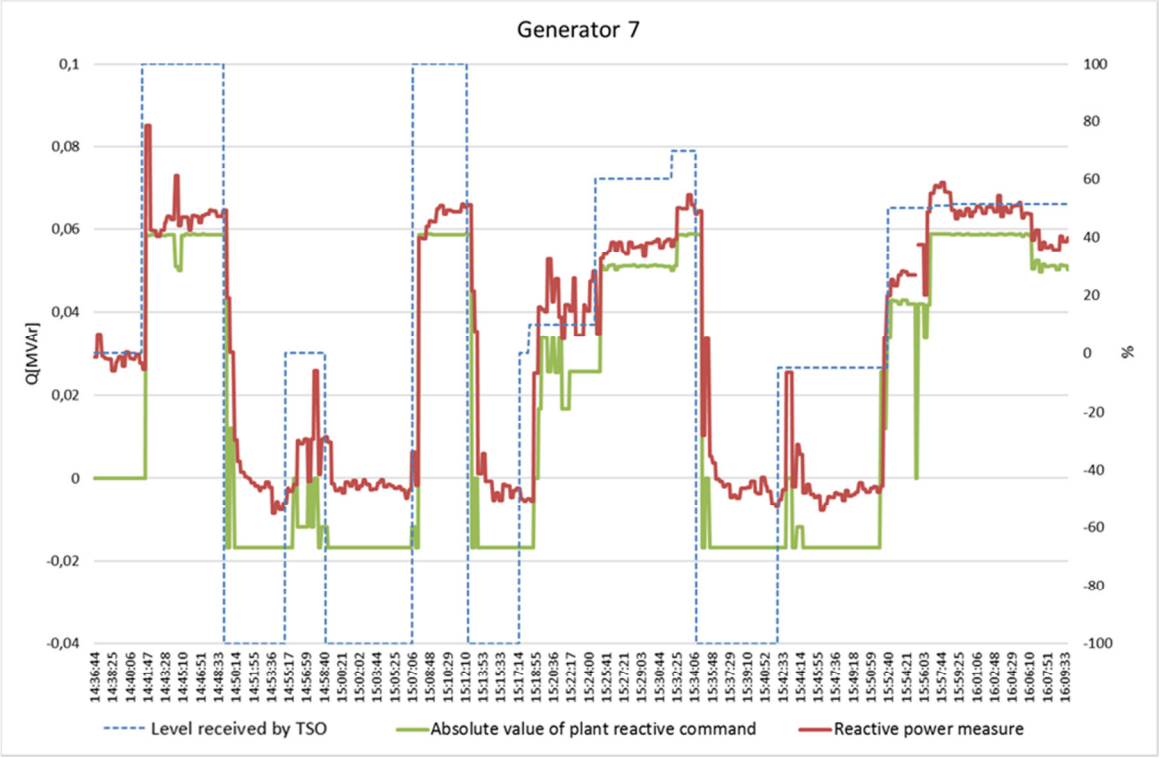

Figure 84: Response of Generator 7 in reactive power regulation

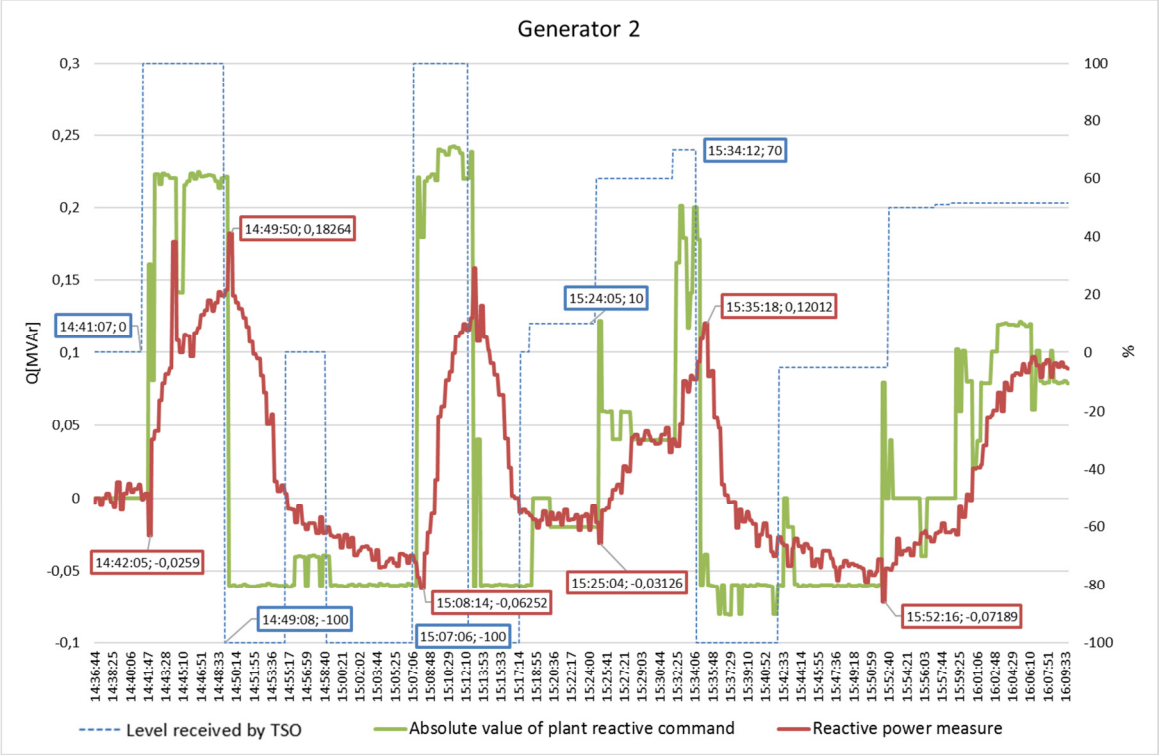

Figure 85: Response of Generator 2 in reactive power regulation

Similar analysis has been carried out considering the Green Transformer involving two hydroelectric power plants connected at it. The process of the regulation was the same described for the Red Transformer and following paragraphs reports the results.

In Figure 86 the measurements of reactive power are illustrated: yellow line indicates the sum of the aggregated power plants measurements defined in accordance with the composition of the aggregation in observability functionality, while the red and blue lines show respectively reactive power at the HV and MV side of the primary substation.

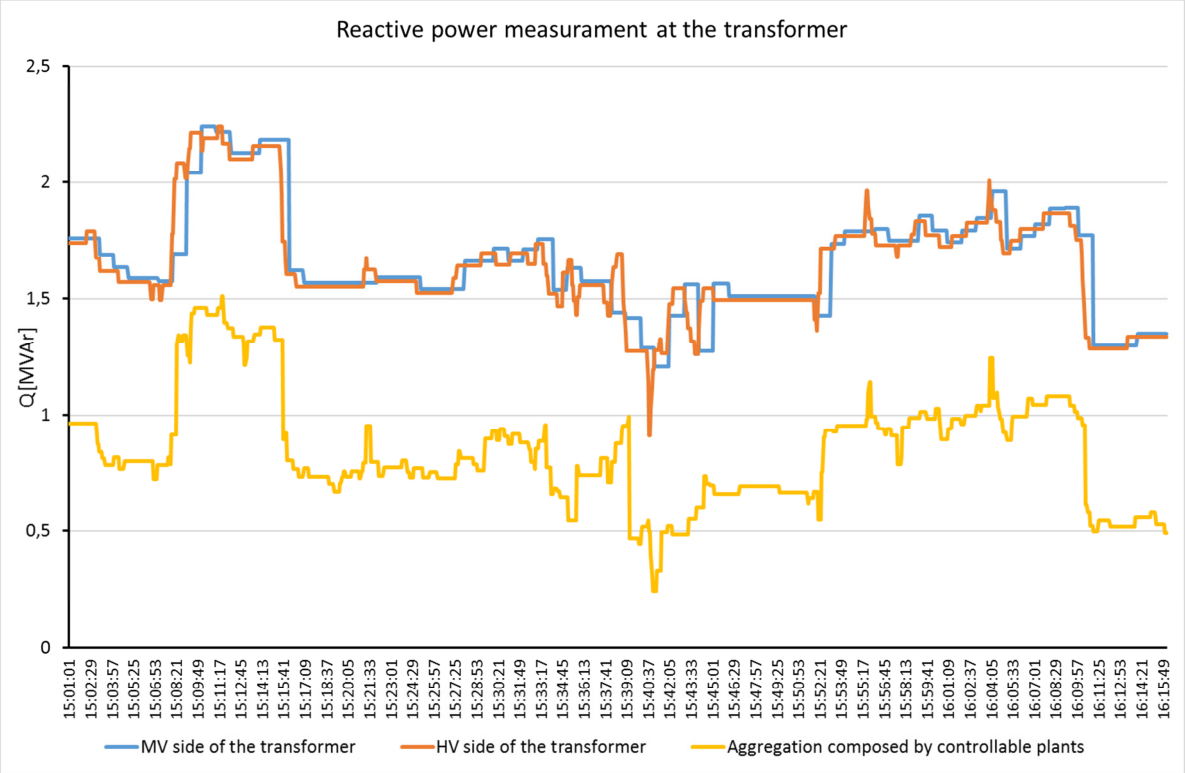

Figure 86: Trends of the three different measurements of reactive power recorded during the tests

The capability that the TSO can use for HV voltage regulation is presented in Figure 87. Grey line (QLAV) indicates the operational point in terms of reactive power exchanged at the interconnection point between DSO and TSO. Orange line is the positive limit and blue line is the negative limit of the reactive power availability.

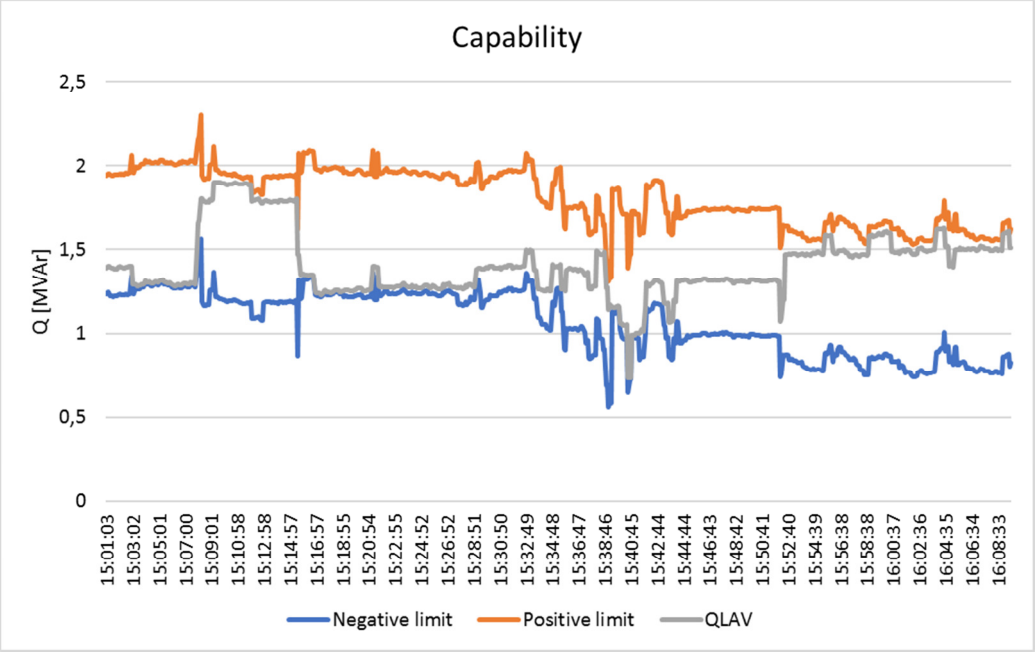

Figure 87: Capability of the VPP as reactive power flow at the Green Transformer

The percentage level sent by Terna (dashed line) is converted in a reactive power setpoint required from the aggregation and then the setpoint is split into two commands for each DER involved. In Figure 88, blue line represents the total setpoint and the other lines indicates the commands received by each power plants for the reactive power regulation.

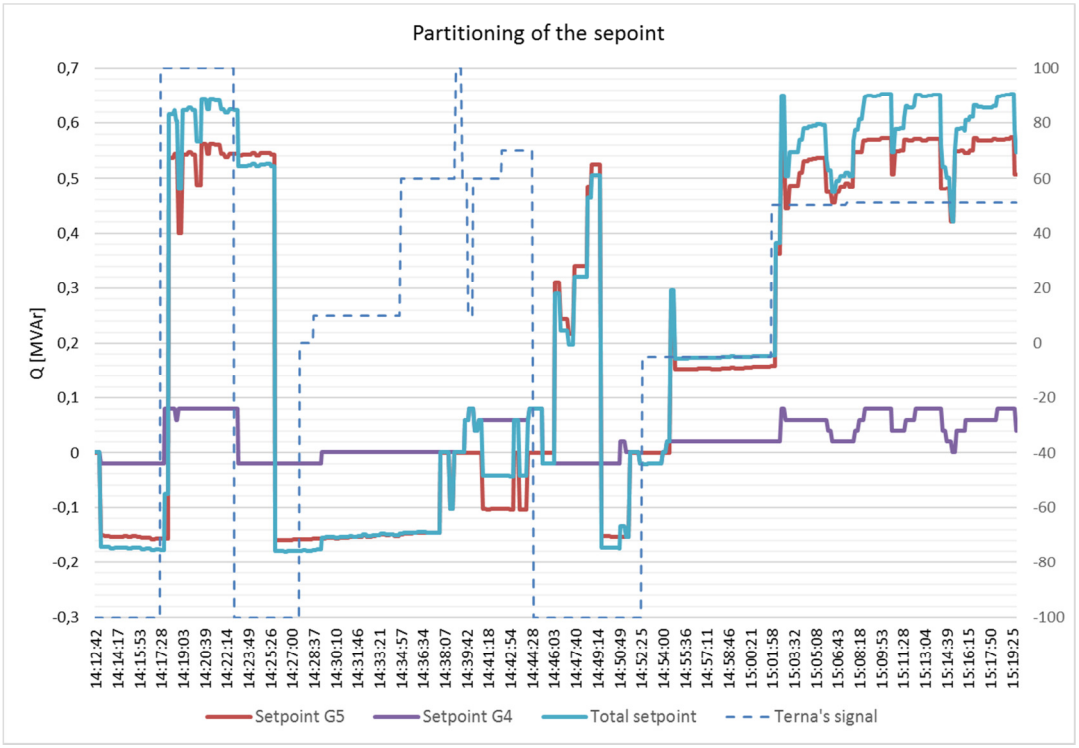

Figure 88: Splitting of the setpoint to the single controlled plants

The global contribution of the VPP connected at the Green Transformer is shown in Figure 89; the reactive power value varied between 0.3 and 1.5 MVAr.

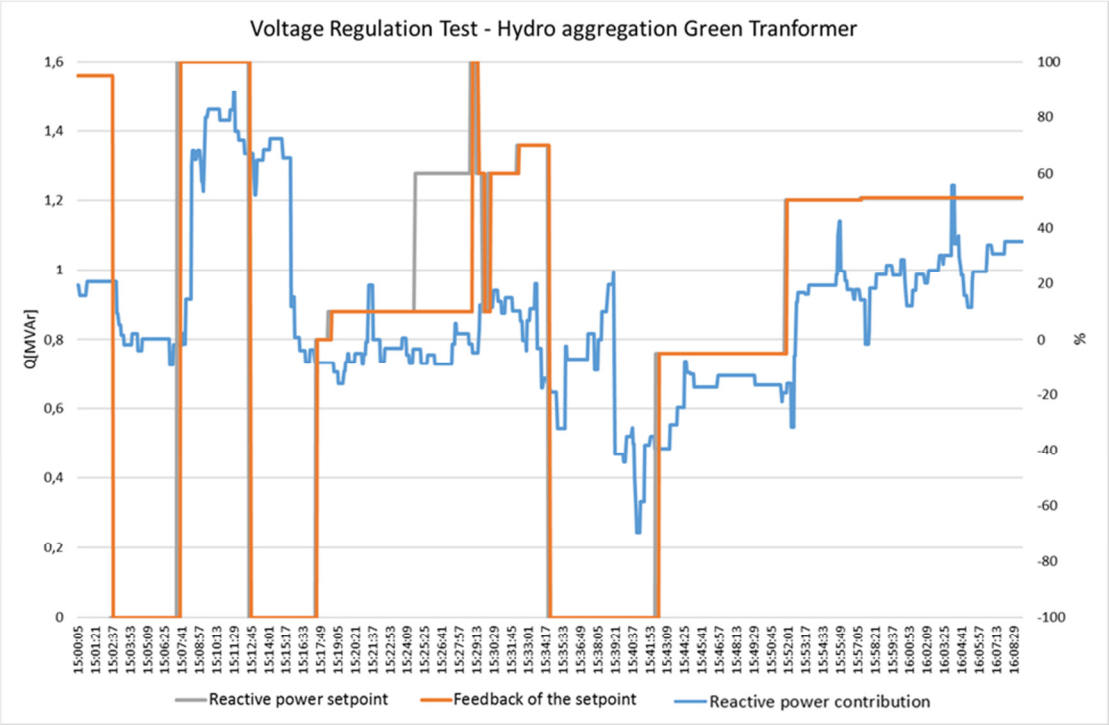

Figure 89: Comparison between the setpoint and the real contribution of the VPP

The following graphs represent the response of each power plant involved in the tests.

In Figure 90, the response of power plant 5 shows that the command calculated by MVRS is not in line with the level sent by Terna: the conversion of the command was not accurate. It is evident the delay between the sending of the signal and the forwarding of the signal to the field. In any case the plant tried to module its reactive power production to follow the command received by MVRS. As happened for generator 7, over-excitation the controller is not capable to reach the target requested and it can be due to technical limits imposed to the generator, not properly represented by the static capability employed.

In terms of utilization of the full band, power plant 4, as reported in Figure 91, showed a better response in both the direction of the regulation.

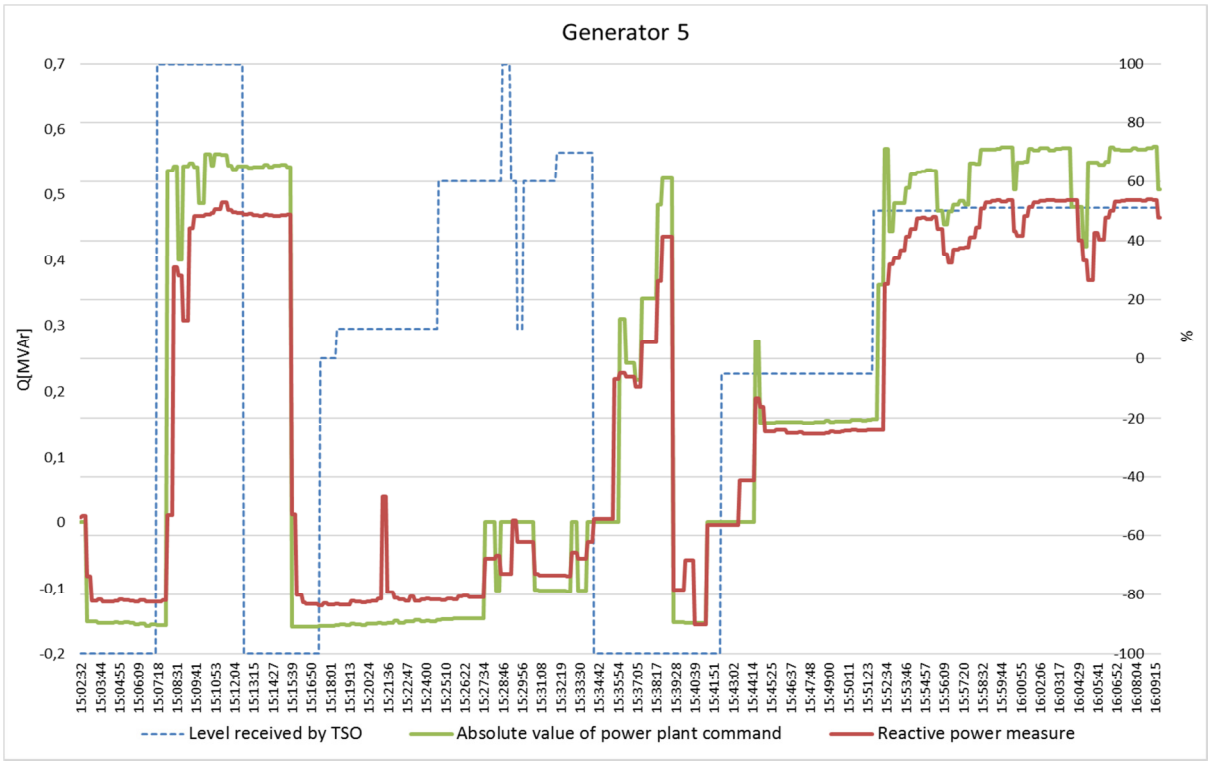

Figure 90: Response of Generator 5 in reactive power regulation

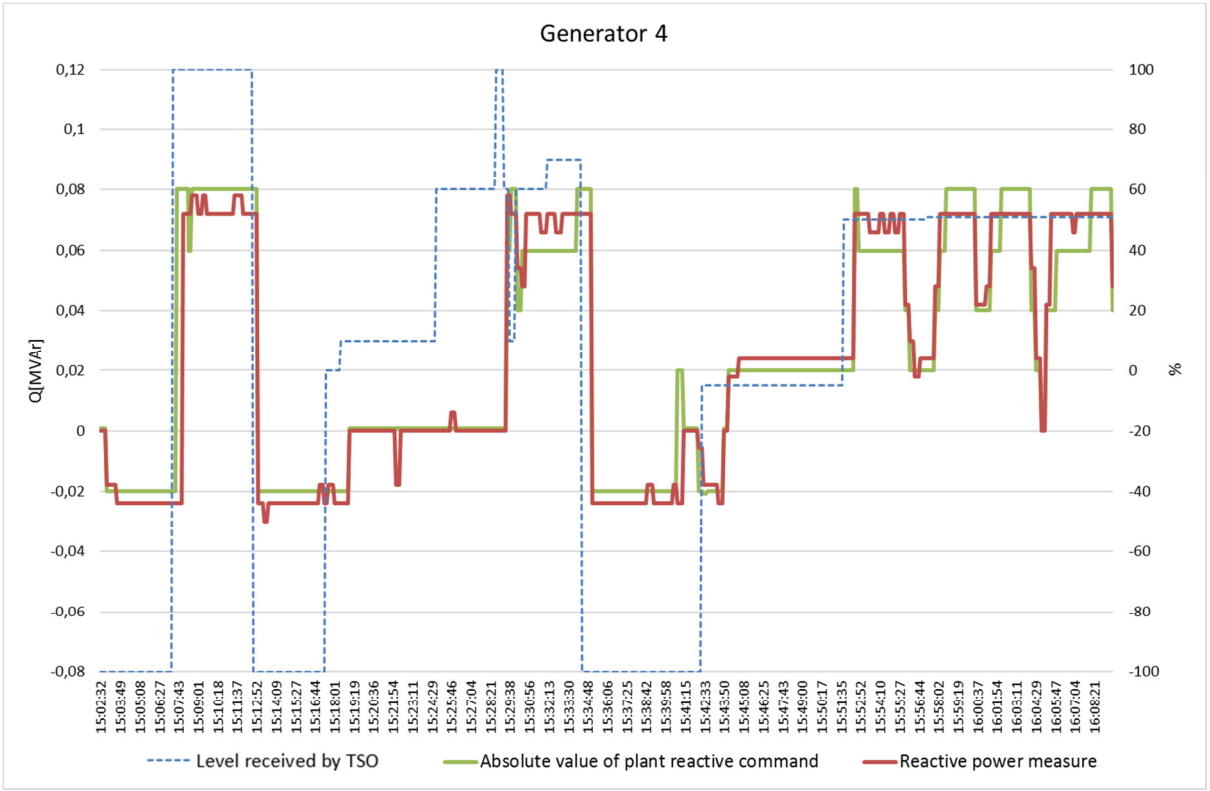

Figure 91: Response of Generator 4 in reactive power regulation

The final effect of the reactive power regulation is the control of the HV side nodal voltage at the interconnection point. The outcomes reported in Figure 92 show how the system is able to move the nodal voltage using the reactive power modulation of DG. In particular when the reactive power setpoint requested is about 100% of the capability (orange line), MVRS spreads the commands to each controlled power plants and the voltage increase the value.

In detail, the handling of about 1.5 MVAR increases the voltage of 500 V at the HV side. This happened at 14:40 when an increasing of voltage was requested.

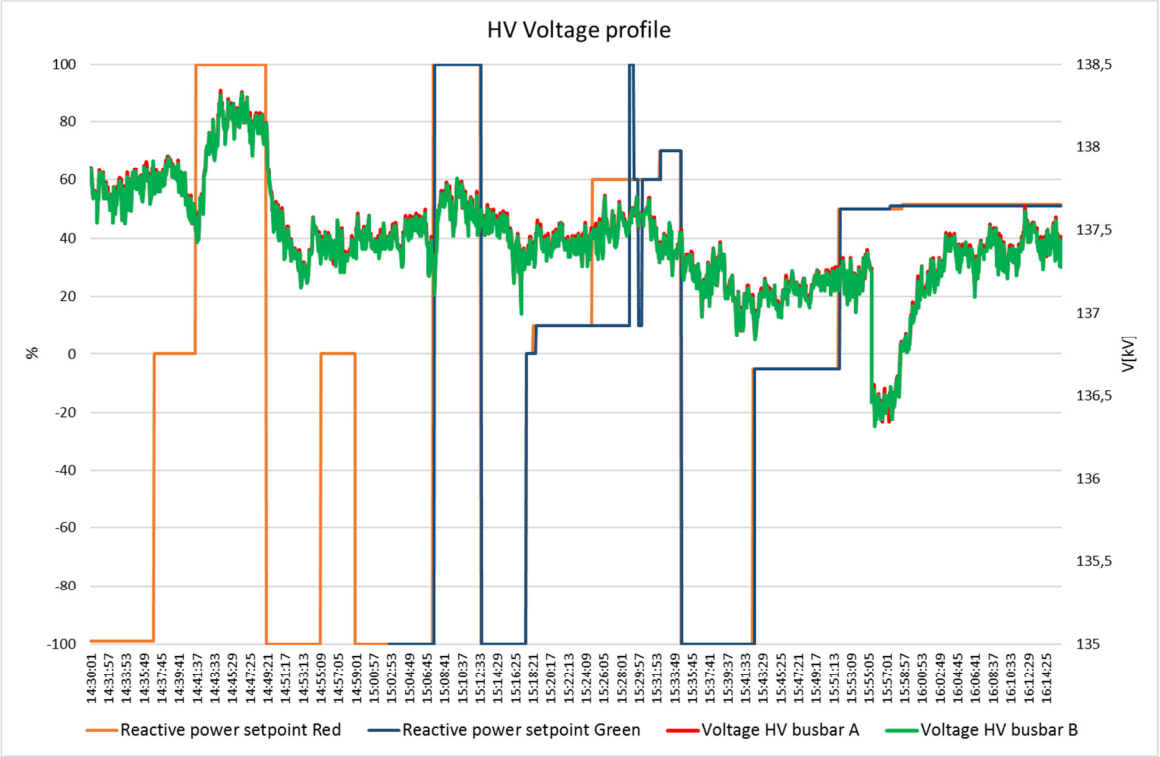

Figure 92: Trend of the voltage at the HV side of the primary substation during tests

However, it is also important to highlight that HV voltage is affected by other events in the grid, in particular due to the operation on neighboring HV power plants. For example, at 15:55 in the diagram it is possible to see that a decreasing of voltage was independent of any MV regulation.

In conclusion, the tests on regulation Q/V performed in the Italian Pilot has confirmed the possibility to control the reactive power exchanges of DG by the MVRS to support the TSO in the management of the voltage of the grid. Of course, the number of involved power plants and the amount of available reactive power remain a crucial issue in order to increase the effect on the grid for future practical application.

6.3.2 Siemens voltage regulation

This section describes the outcomes of the steps described in paragraph 4.2.2 to obtain the voltage regulation through DG.

6.3.2.1 State Estimation

The Voltage Regulation functionality need an accurate estimation of the MV network to ensure a reliable adjustment of the network. For this reason, all the network topology (both the Primary Substation and its connected MV network) is replicated inside the MVRS. Represented the network, all the electrical data, provided by the DSO, has been loaded inside the system to characterize each network element (i.e. length of branches or nominal power of MV/LV transformers).

Moreover, to initialize the state estimation problem, the typical load profile was generated processing historical data, provided by the DSO.

Figure 93 and Figure 94 show some examples of the topology and data loaded in the MVRS.

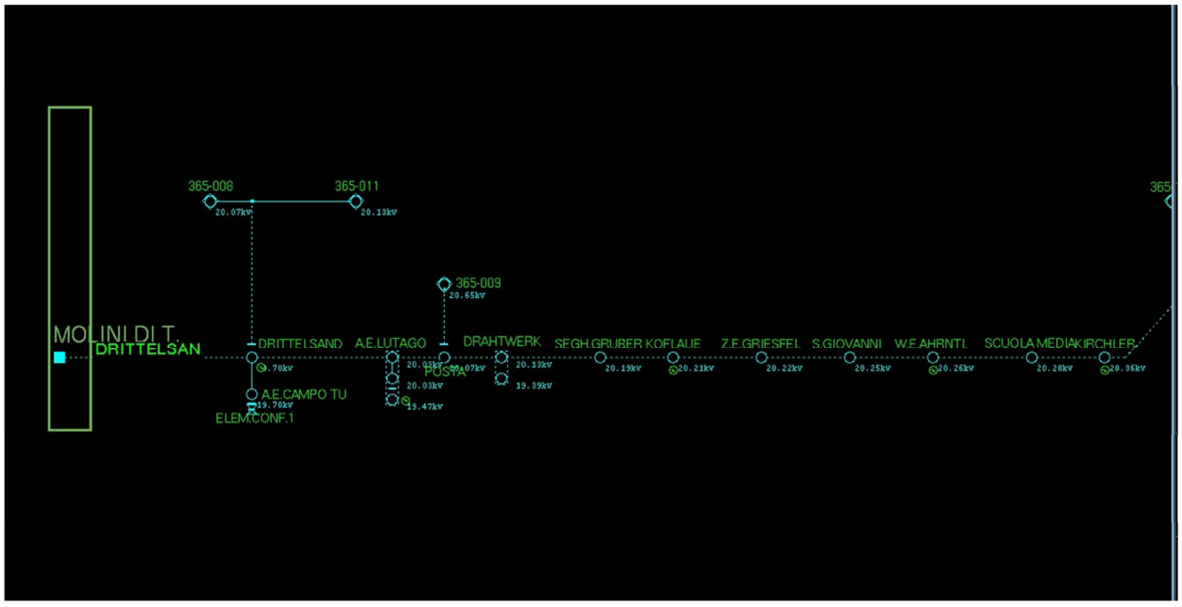

Figure 93: Example of a MV feeder on the MVRS real time operation

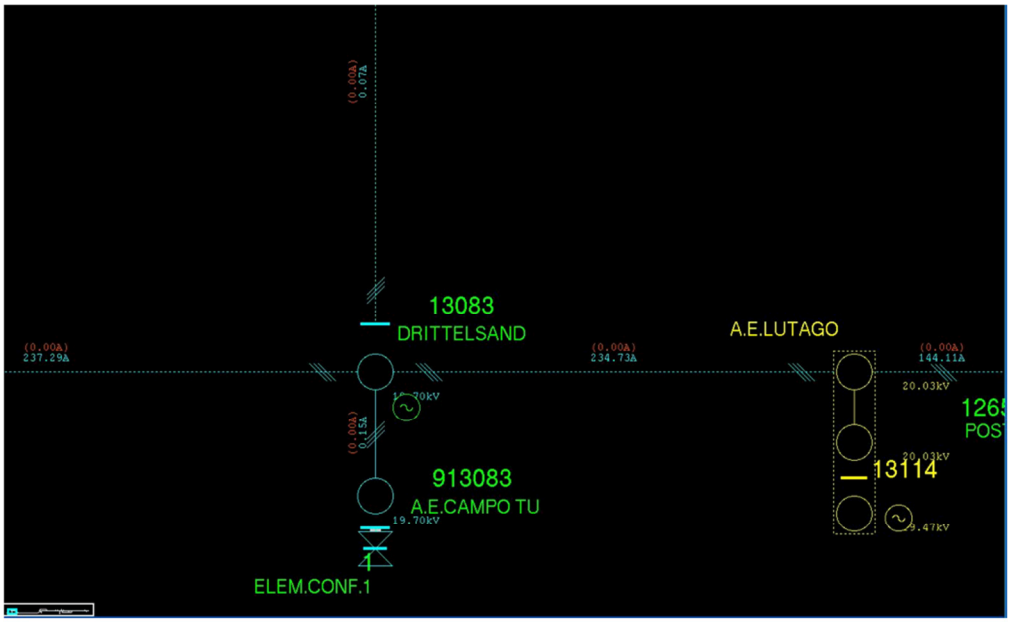

Figure 94: Detail of a MV feeder on the MVRS real time operation

The State Estimation algorithm uses:

- Primary Substation measurements:
  - V_{HV} (HV busbar voltage)
  - I_T, P_T, Q_T (current, real and reactive power on HV/MV transformers)
  - V_{MV} (MV busbar voltage)
  - $I_{feederMV}$ (current on each MV feeder)
- MV network measurements:
  - I_{MVn}, V_{MVn}, P_{MVn}, Q_{MVn}
- Load and generation data (P_G, Q_G, P_L, Q_L)

I_{MVn}, V_{MVn}, P_{MVn}, Q_{MVn} are real-time measurements provided by PCRs installed in the MV grid and by the Observability nowcast data. In Figure 95 there is a scheme describing the position of each input on the network.

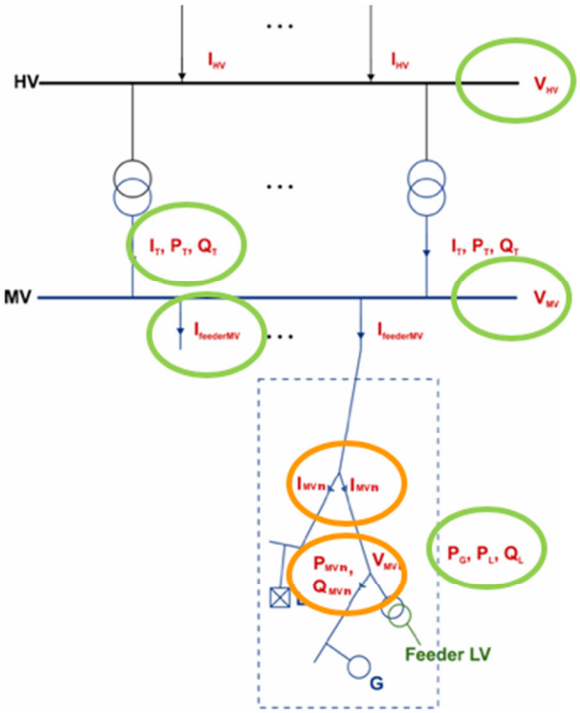

Figure 95: Input data for the State Estimation algorithm

In the next paragraphs, the State Estimation results regarding the Red Medium Voltage busbar for 30th June 2018 are described.

6.3.2.2 HV/MV TR

In Figure 96 the measurement of active power of the HV/MV TR is compared with the estimation calculated by the State Estimation algorithm. Figure 97 shows the same comparison for the reactive power.

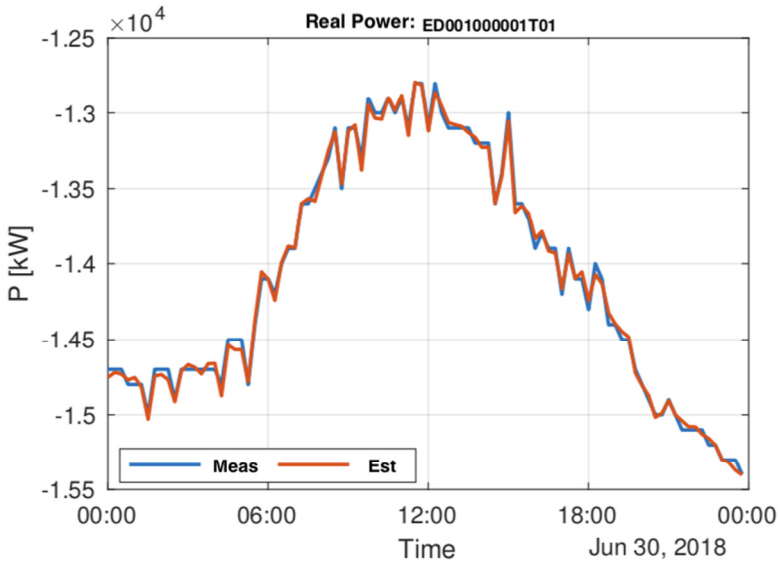

Figure 96: Comparison of the measurement and estimation of HV/MV TR active power

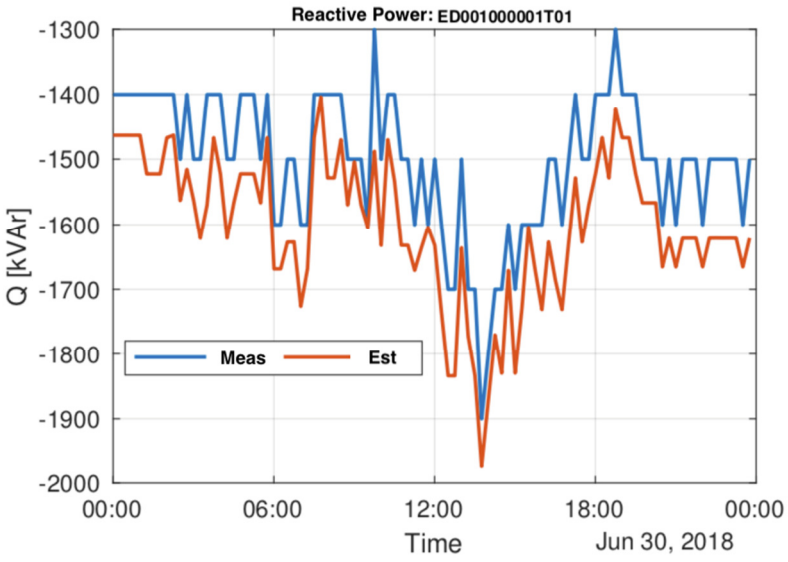

Figure 97: Comparison of the measurement and estimation of HV/MV TR Reactive Power

In Figure 98 the measured current of the HV/MV TR is compared with the estimation calculated by the State Estimation algorithm: it is possible to see that there is an almost constant little over-estimation; generally speaking, this kind of behavior is connected to the not perfect coherence of all the field measurements.

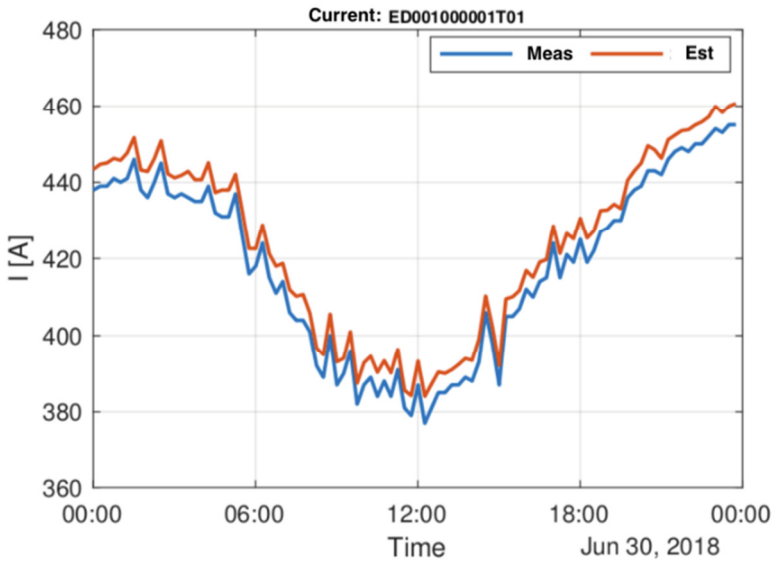

Figure 98: Comparison of the measurement and estimation of HV/MV TR Current

6.3.2.3 Medium Voltage feeders

Figure 99 and Figure 100 show how the State Estimation algorithm is able to identify the direction of currents of MV feeders (active power flow). This correct estimation is possible although the input measurements are given only in magnitude.

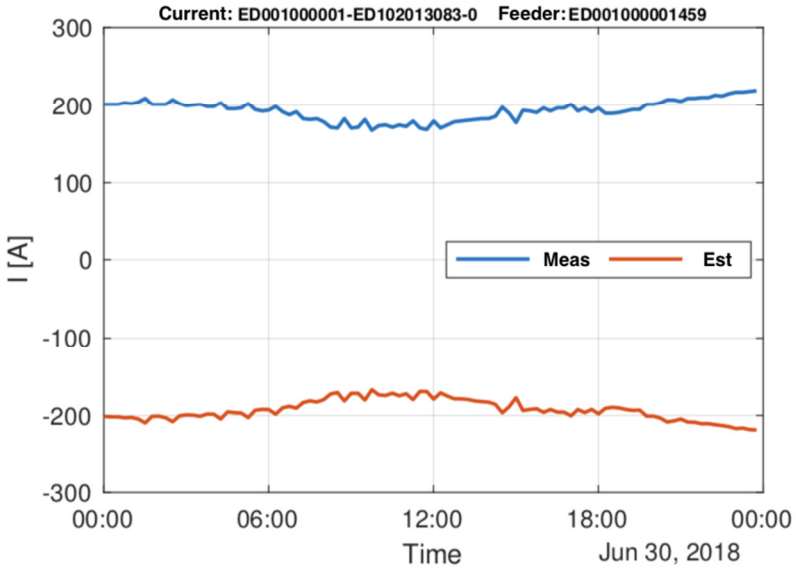

Figure 99: Comparison of the measurement and estimation of a MV feeder

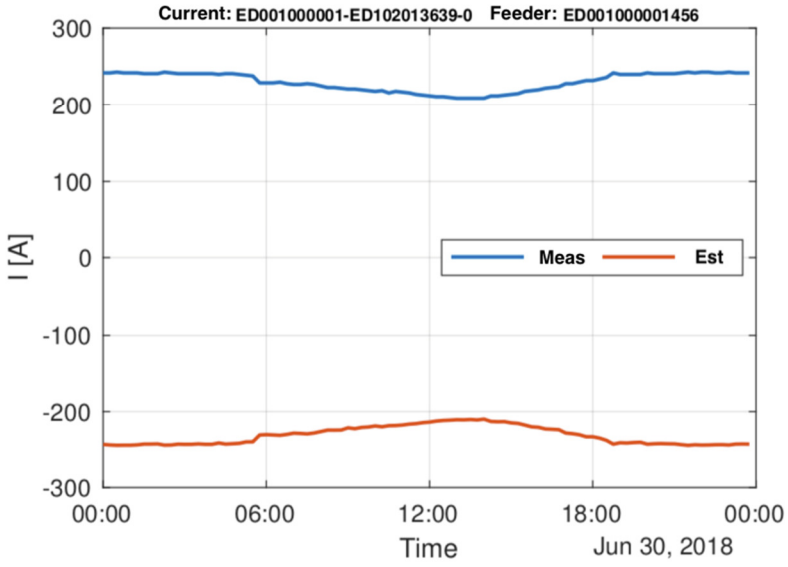

Figure 100: Comparison of the measurement and estimation of a MV feeder

6.3.2.4 MV busbar

Generally, an accurate estimation of the MV busbar voltage (error lower than 1-2%) is an indicator of the goodness of the entire State Estimation. Figure 101 shows how, after the State Estimation process, the voltage calculated for the MV busbar of the Primary Substation fits to the real field measurements.

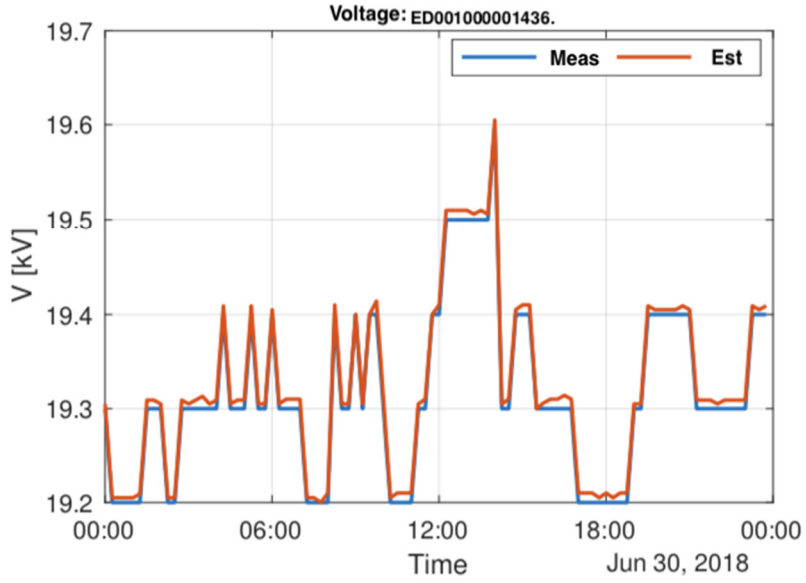

Figure 101: Comparison of the measurement and estimation of the Medium Voltage busbar

6.3.2.5 Other results

Figure 102 shows, for each MV feeder connected to the Red MV busbar, the trend of the maximum voltage estimated during the day; it is possible to see that in this case the maximum voltage is always

located on one feeder (blue line). The voltage behavior on this feeder represents during the whole day the maximum limit that influences the execution of the Voltage Regulation function.

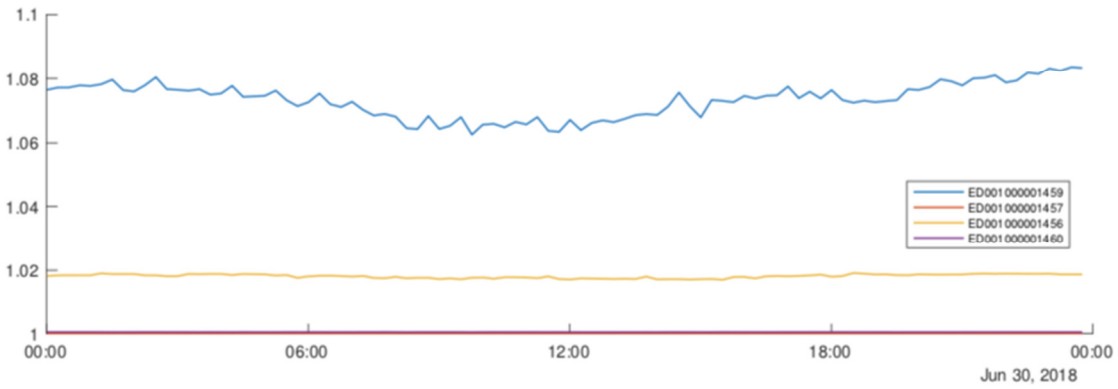

Figure 102: Maximum Voltage daily trends in p.u. for each MV feeder

Figure 103 shows, from a geographical point of view, the distribution of voltages along a MV feeder evaluate with a state estimation calculation. The starting point on the left shows the voltage at the MV Primary Substation busbar; moving to the right part of the graph, the voltage of locations further from the Primary Substation is shown. The voltage values are higher towards the end of power lines.

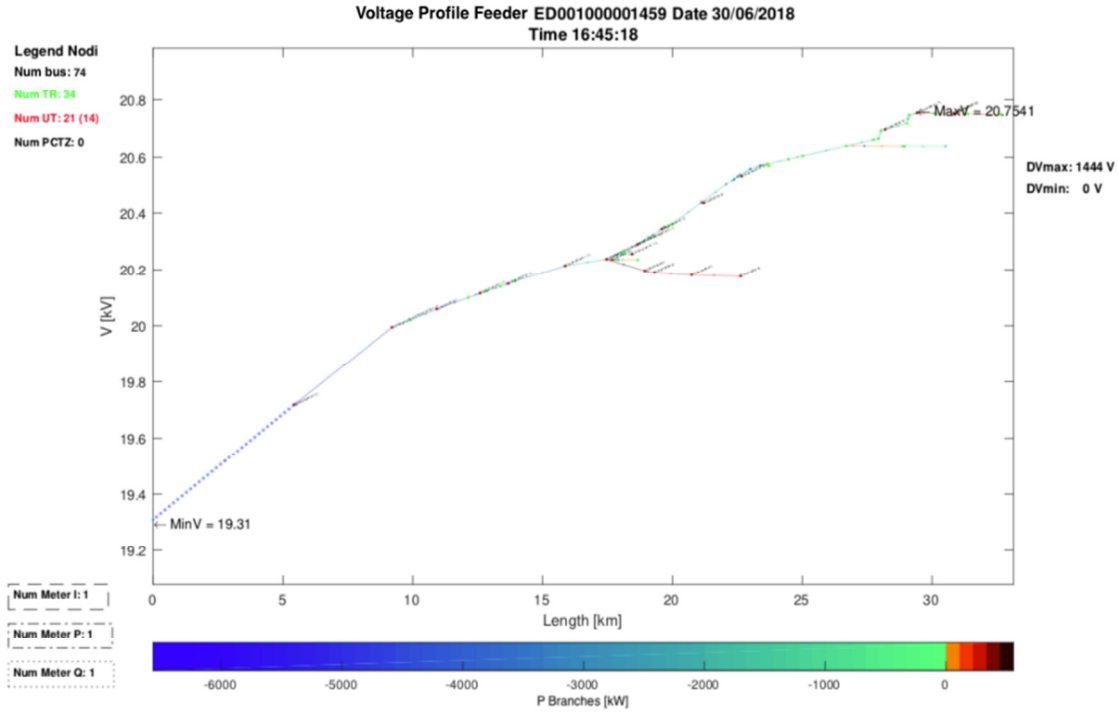

Figure 103: Voltage profile along a MV feeder

Figure 104 shows how the State Estimation process modifies the data of the single grid elements; the graphs show the starting daily aggregated profile (MV users and MV/LV transformers) and how the algorithm, according to the field measurements, acts during the computation.

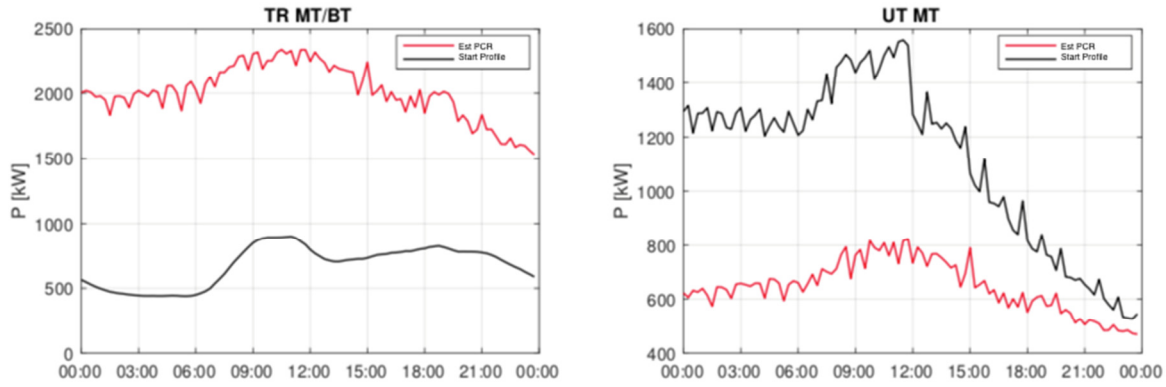

Figure 104: Comparison of the initial and estimated load profile for MV/LV TR and MV user

6.3.2.6 Virtual Capability

Figure 105 shows the Virtual Capability related to the red HV/MV TR considering five dispatchable MV plants. These data are defined following the load convection: a positive value indicates an absorption of reactive power toward the Medium Voltage Network and a negative value means a production from the Medium Voltage Network.

From the graph, it is clear that the Virtual Capability is asymmetric in relation to the reactive power estimation. This finding is coherent with the network state because of the reactive power of MV generators; generally, the MV generators work with a non-unitary power factor. Anyway, the capability would be completely symmetric only if the generators operate with a unitary power factor and the computation does not lead to any violations of technical constraints.

In the example here reported, the MV Network can inject more reactive power than it can absorb; this means that the estimated behavior of generators, within the network, is overall inductive.

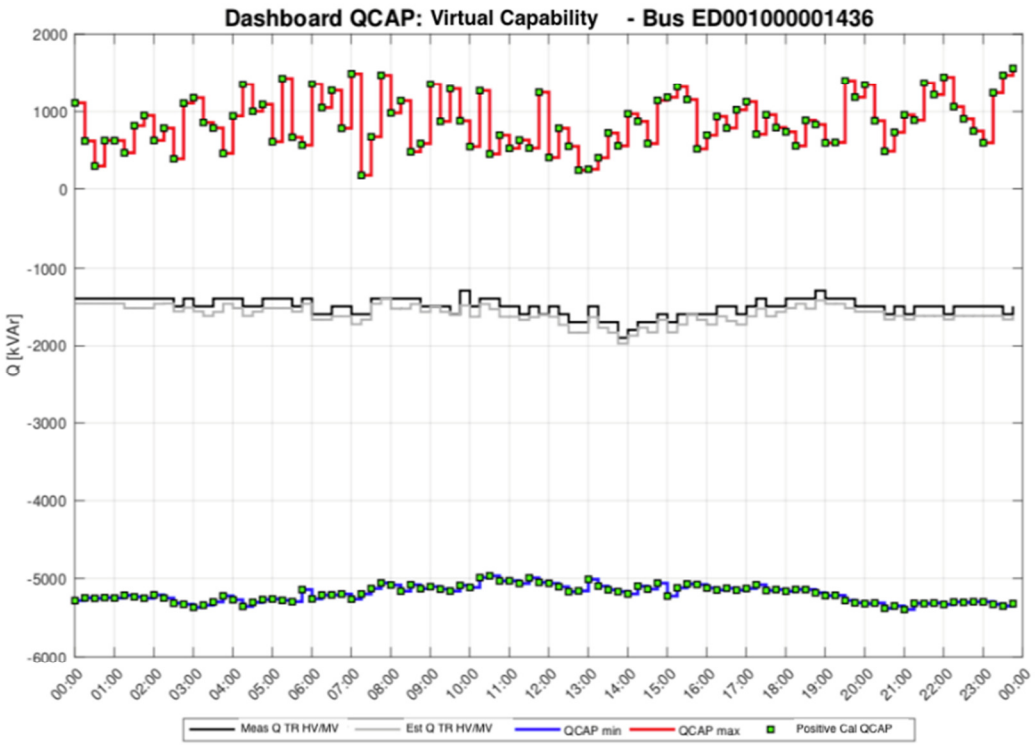

Figure 105: Virtual Capability of the HV/MV TR

6.3.2.7 Voltage Regulation

Figure 106 and Figure 107 show how the Voltage Regulation algorithm controls the MV busbar voltage. During the analyzed day, the negative values of the active power indicate a continuous reverse power flow at the HV/MV transformer. This situation forces the Voltage Regulation algorithm to maintain a setpoint lower than the maximum available voltage in the MV network.

Between the 06.00 am and 17.00 pm, reverse power flow is weakened and consequently the Voltage Regulation algorithm increases the voltage setpoint at the busbar until it reaches the technical constraints. This behavior is clearly represented in Figure 107.

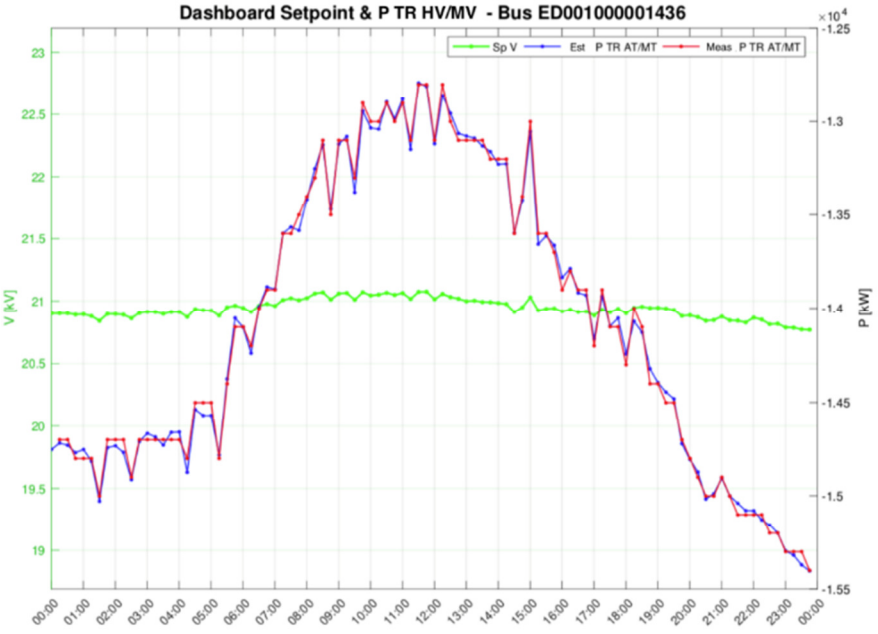

Figure 106: Comparison of the MV busbar setpoint and HV/MV TR active power (measurement and estimation)

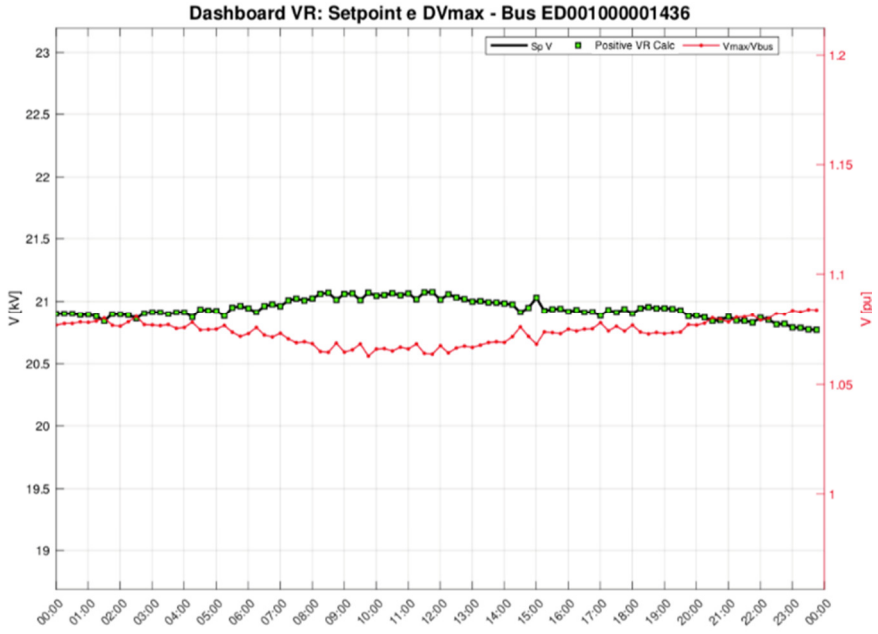

Figure 107: Comparison of the MV busbar setpoint and the ratio V_{max}/V_{busbar}

Figure 108 shows two different treatments on a controllable generator. On the left, the generator is strongly adjusted by the Voltage Regulation algorithm in order to respect the technical constraints and to optimize the network losses. On the right, the generator is constantly adjusted but with a smooth trend. The graphs labelled "Quantity" show the trend of the difference between the setpoint and the

measurement. The strategy adopted by the algorithm for each single generator is not univocal, but it is connected on one side to the specific local network behavior and on the other side to the overall optimization target.

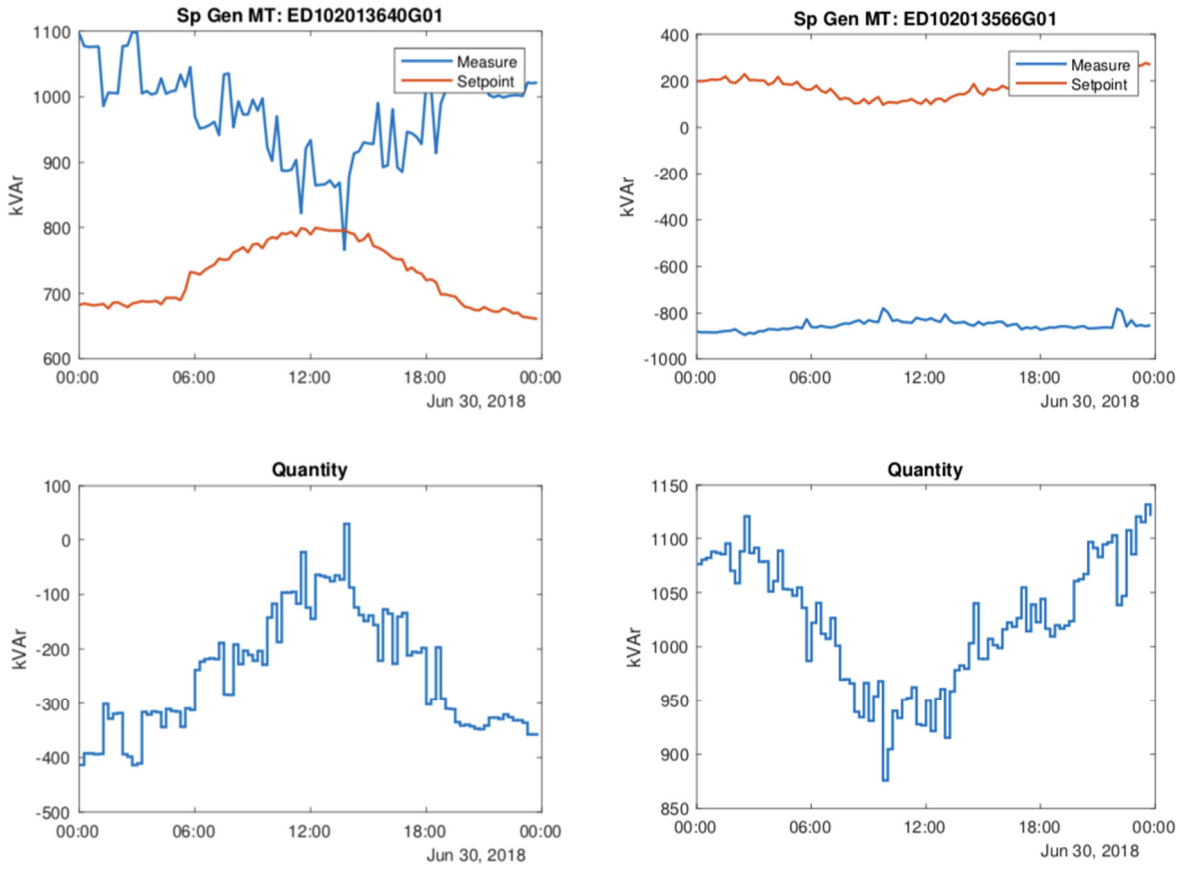

Figure 108: Example of reactive power setpoint for controllable generators

6.4 f/P regulation by MVRS

6.4.1 Selta f/P regulation

As detailed in section 5.4, the f/P tests carried out required Terna to send a ramp setpoint of active power modulation to evaluate the performance of the response of the DG at the interconnection point between DSO e TSO grids. During the tests each involved partner has been committed to record the measurements and the signals for which they are responsible.

The first test session, carried out on 07/06/2018, involved 3 hydroelectric power plants, with an initial operating power of approximately 12 MW. In this case, the reference program value is defined as the nominal power and the half-band (HB) as a percentage of the nominal power. The results of the tests are shown below.

6.4.1.1 Test 1

In the first application, the power plants made available for the regulation the 20% of the nominal power amounting to 2.3MW of which approximately 2 MW allocated at the red transformer by 2 power plants (G1 and G2) and approximately 0.3MW at the green transformer by G3.

The analysis which follow were carried out considering separately the trend of the measurements of the hydroelectric power plants, that are represented in Terna's Control System HMI as an equivalent aggregation connected at the MV side of the transformers, as shown in Figure 33, in order to evaluate the contribution of the VPP. At the transformer level, both at the MV and at HV sides are actually affected by other productions and by the load.

As an example, Figure 109 shows the measurements of active power at three different monitored points the grid: at the terminals of the equivalent aggregation (orange line), at the MV side of the transformer (blue line) and at HV side of the transformer (grey line). It is evident that the active power profile is translated mainly due to the consumption of the load connected at the same transformer.

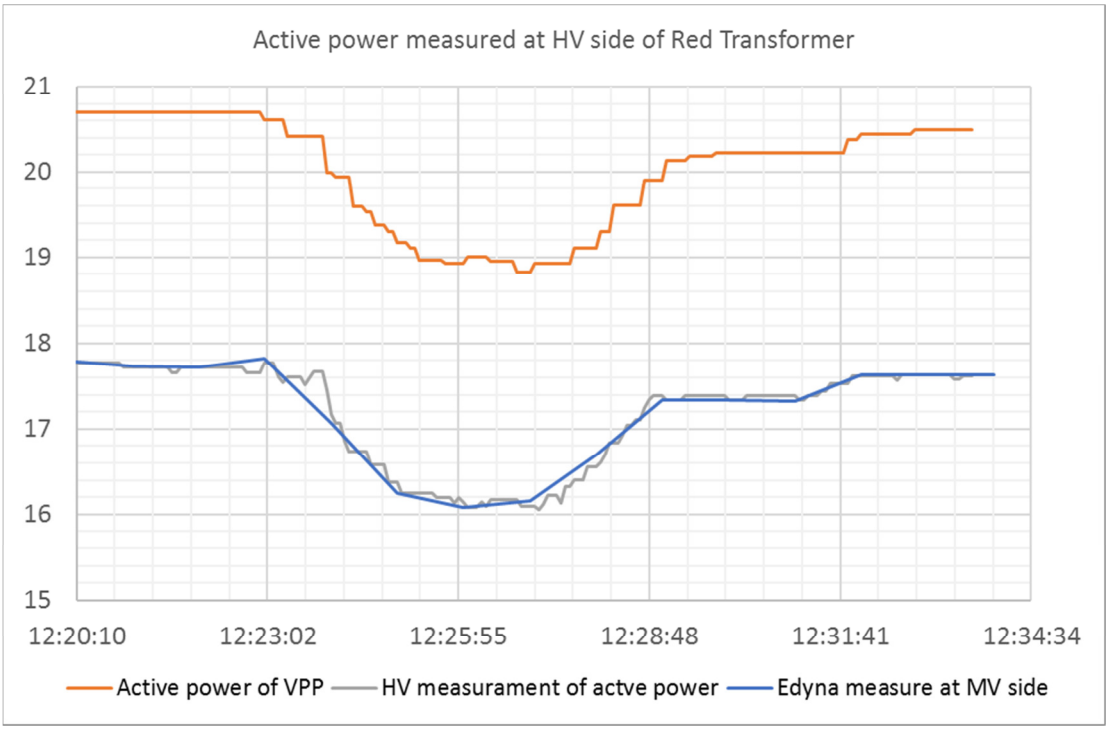

Figure 109: Trends of the three different measurements of reactive power recorded during the tests

In Figure 110 and Figure 111, the profile of the power exchanged at the transformers of the primary substation and measured by the TSO is reported: the blue line is the expected contribution calculated from the percentage setpoint sent by Terna and the orange line is the real contribution of DG calculated by subtracting an offset value to better appreciate the trend. In the lower part of the graph the trend of the dynamic error has been reported compared with the limit value used for acceptance to the secondary frequency control service (10%). The error increases with increasing response inaccuracy and delay. Exploiting DG, the error of the aggregation contribute is affected by the dynamic errors of each power plant involved in the test as will be better illustrated in the following figures.

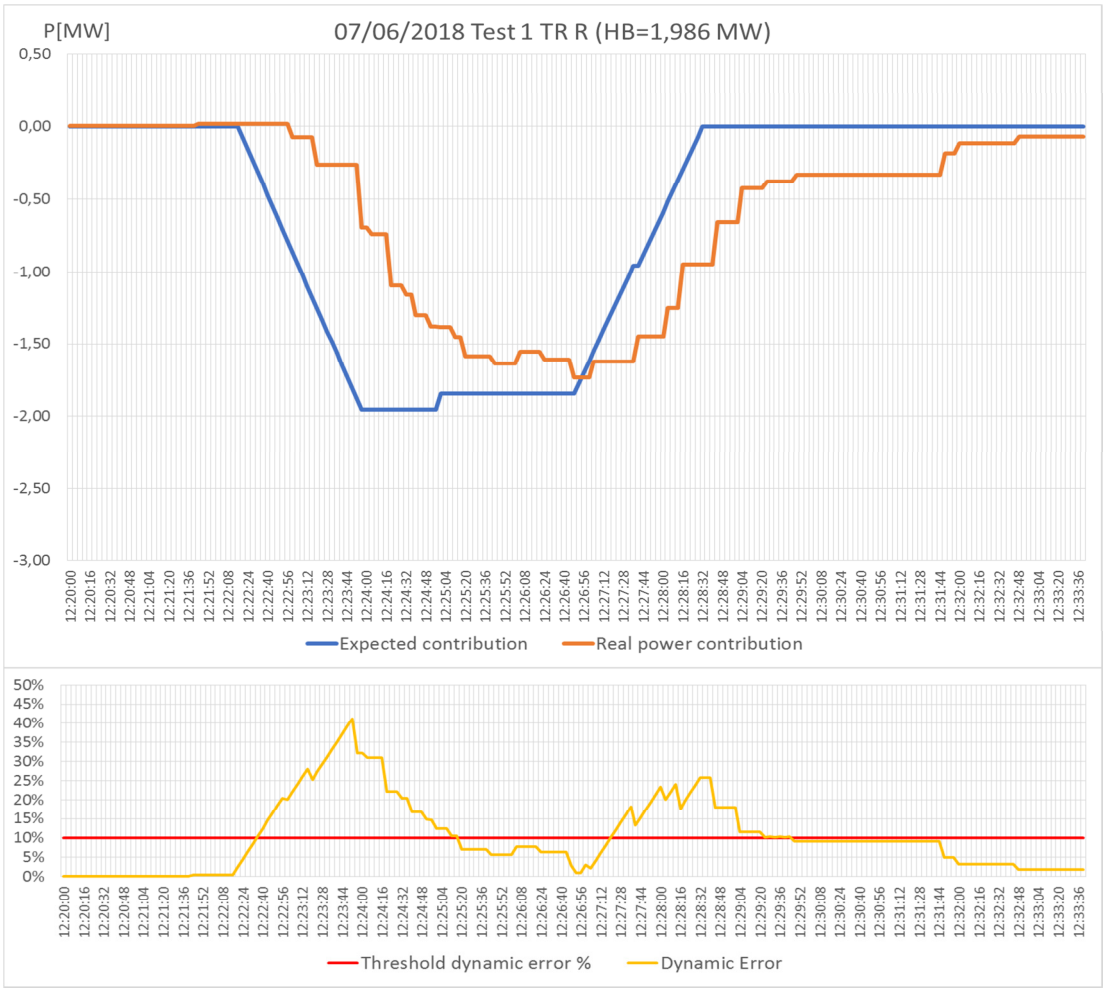

Figure 110: Analysis of the HV contribution at the red transformer - Test 1 07/06/2018

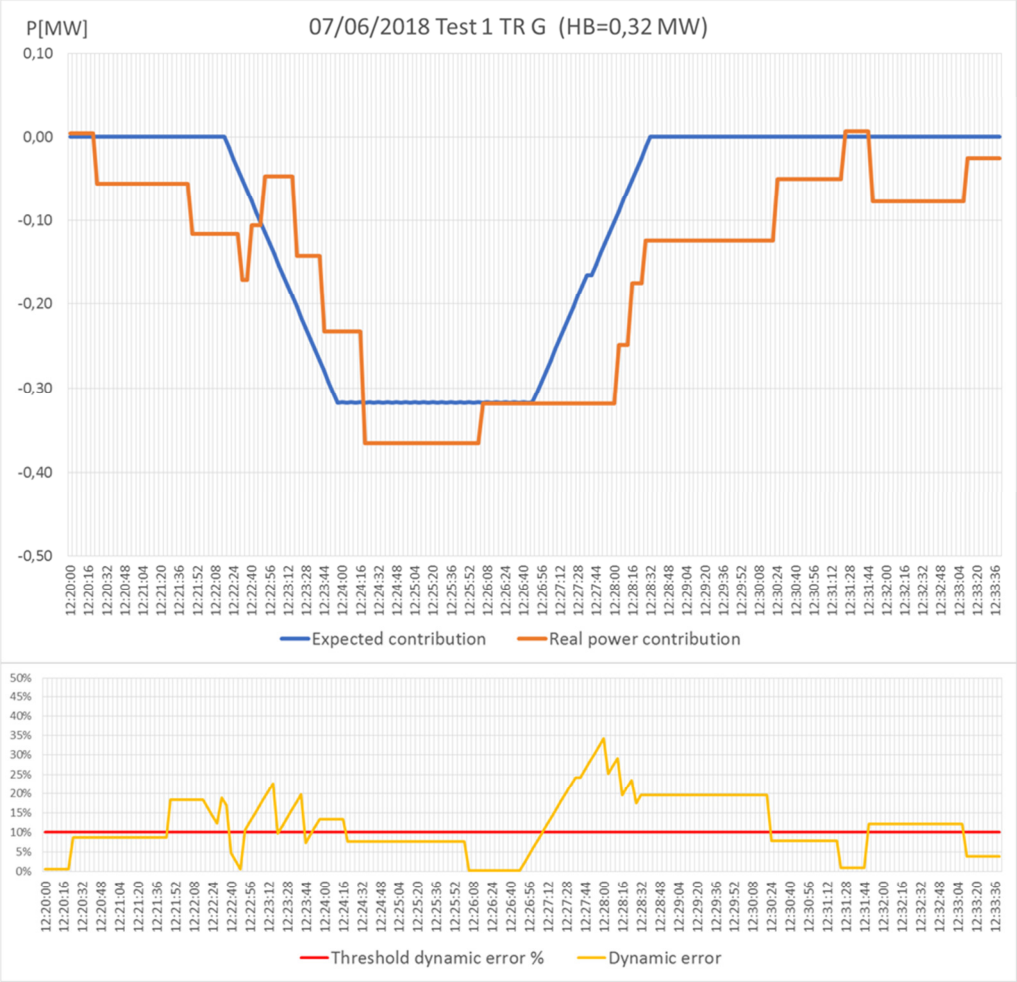

Figure 111: Analysis of the HV contribution at the green transformer - Test 1 07/06/2018

Figure 112, Figure 113 and Figure 114 show the performance of each generator involved in the f/P regulation; in particular:

- the light blue line represents Terna setpoint expressed as a percentage between 50% and 0% because only the downward service has been tested (as detailed in section 5.4);
- the blue line represents the setpoint calculated by MVRS and sent to the power plant
- the yellow lines are the upper and lower limits of the available band
- the orange line is the active power production measured at the power plant terminals by the meter called PCR.

In the lower part of the graph the trend of the dynamic error calculated for each power plant. It is evident that the error increase at ramps. In particular, the decreasing segment of ramp is followed by the MV system better than the rising one, despite a delay due to the communication and command actuation. The rising ramp instead highlights technical problems of the MV system in terms of delay and accuracy

probably due to unsuitable regulator performance. Generally, each power plant regulator shows a different behaviour in the provision of active power modulation.

An interesting aspect highlighted by this test is the management of the distribution grid constraints. In fact, the null setpoint calculated by MVRS for the power plants connected at the red transformer between 12:22:53 and 12:23:28 was due to a voltage violation in the grid connected at the red transformer (Figure 112 and Figure 113). In this case, the MVRS indicated the aggregation as unavailable for the f/P regulation and solved the violation. Moreover, the setpoint for G2 after 12:27:20 shows a profile that was not proportional to the level sent by Terna because affected by the consideration of other limiting elements in the calculation of the capability.

In this regard, the graphs show that the controls of the power plants connected at two transformers are independent and the regulation through G3 connected at green transformer continued, as represented in Figure 114.

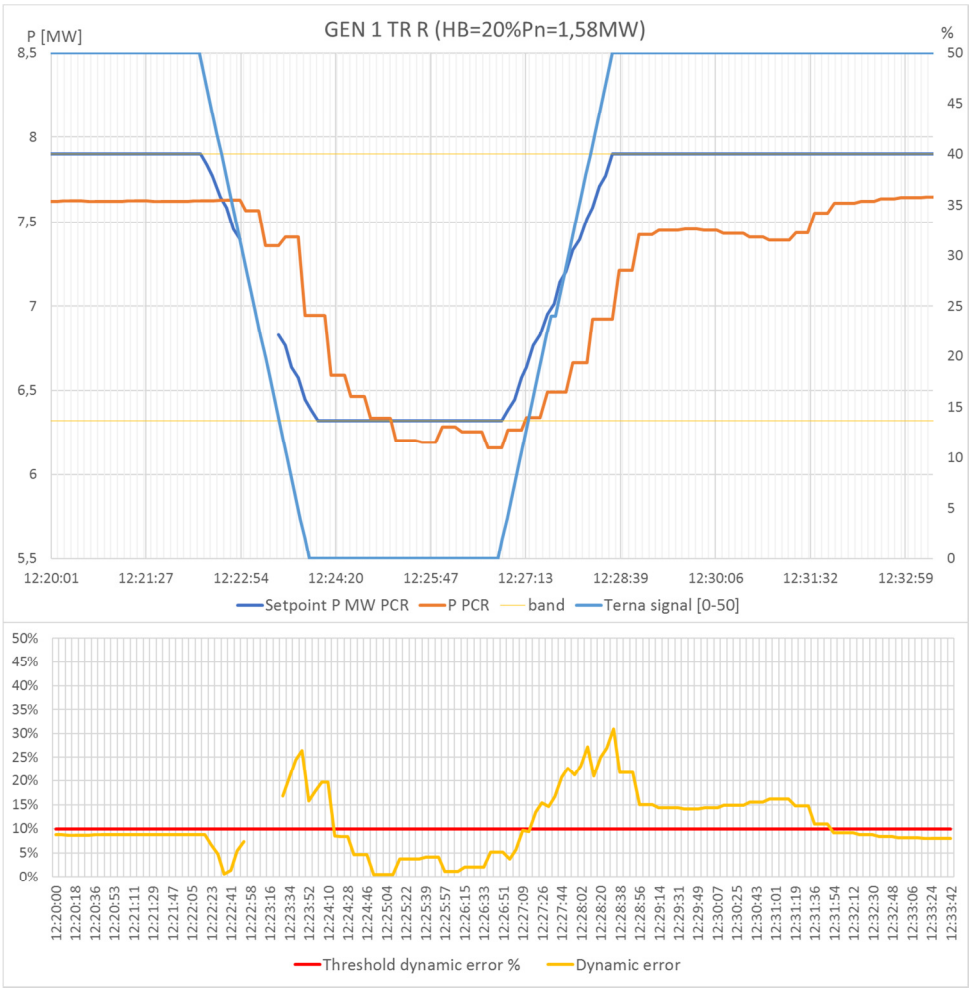

Figure 112: Performance of G1 connected at red transformer – Test 1 07/06/2018

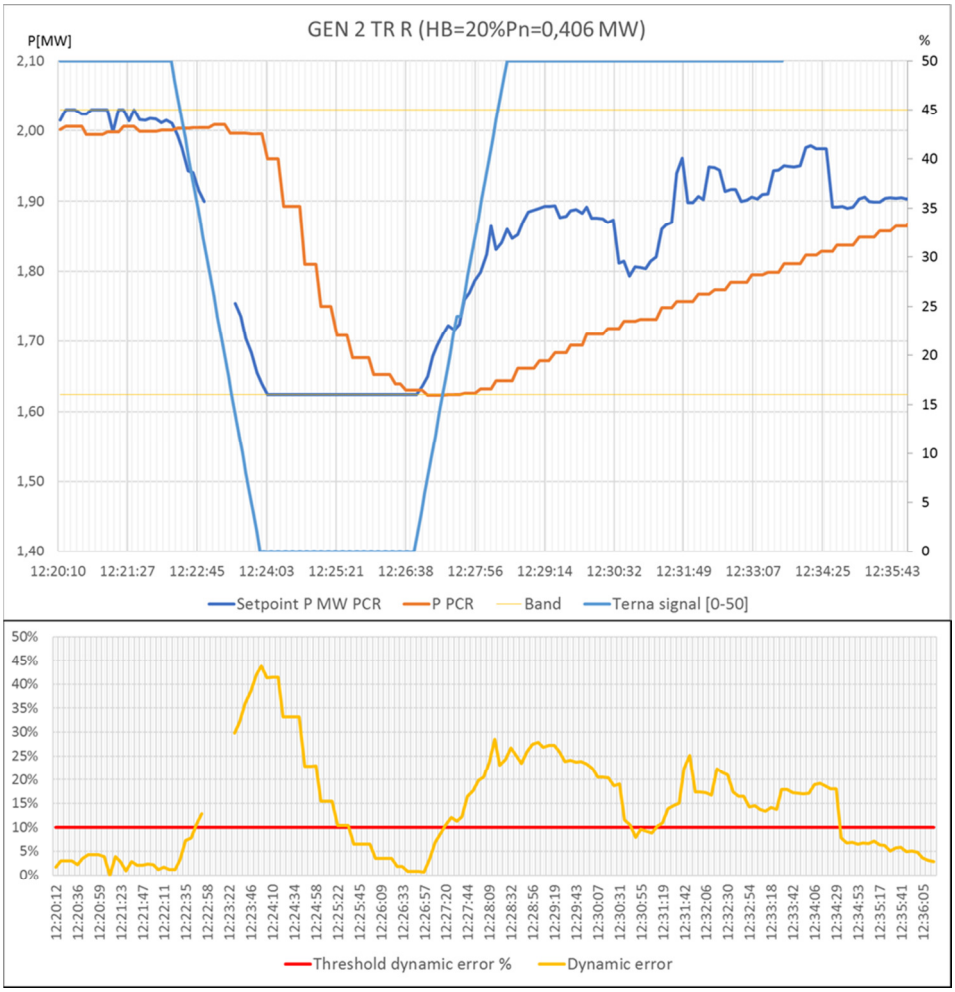

Figure 113: Performance of G2 connected at red transformer – Test 1 07/06/2018

Figure 114 shows a continuous offset error due to the fact that the nominal power of the generator has been considered as the starting value of the ramp, while the power plant has never produced that amount of active power during the test. As will be seen below, to reduce this error in the second test session, the last measurement was considered as the programmed mid-band value.

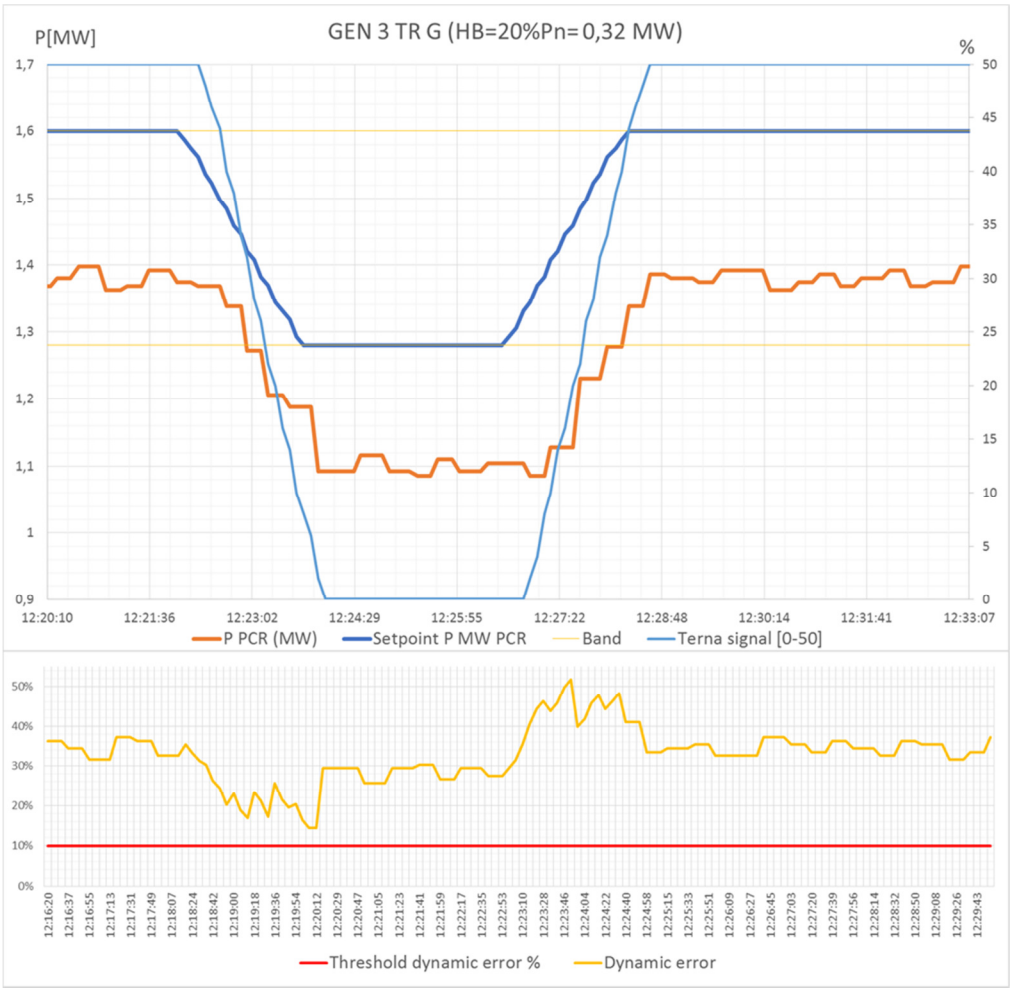

Figure 114: Performance of G3 connected at green transformer – Test 1 07/06/2018

6.4.1.2 Test 2

In the second test, the power plants made available for the regulation the 60% of the nominal power amounting to 6.92 MW.

The two power plants connected at the red transformer made available 5.9 MW to be modulated for the regulation. In Figure 115, the behaviour of the power exchanged at the red transformer is reported: the blue line is the expected contribution of the VPP for the f/P regulation and the orange line is the actuation of the provision of the power plants The positive result is the complete activation of the required amount of active power, despite the performance highlighted technical problems of the MV system in terms of delay, mainly in the rising ramp, where the dynamic error reaches 40%

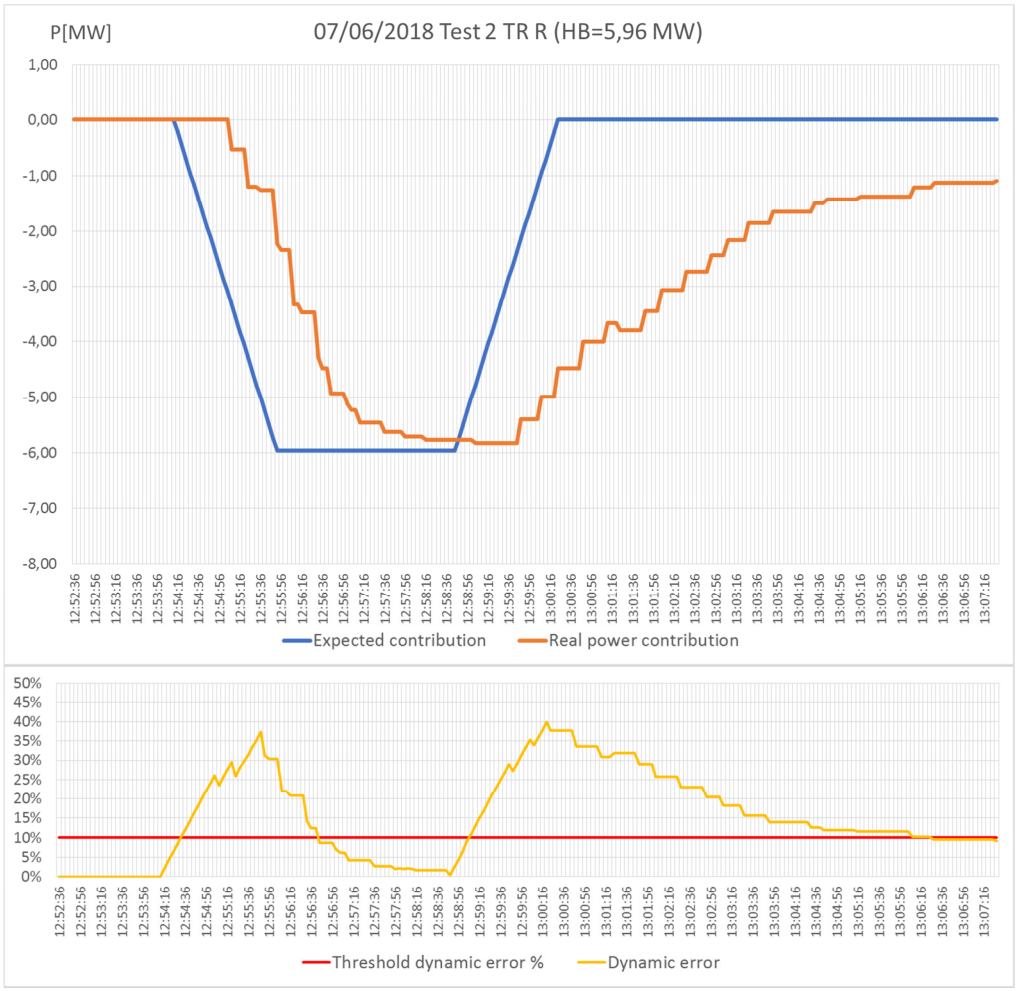

Figure 115: Analysis of the HV contribution at the red transformer – Test 2 07/06/2018

In detail, Figure 116 and Figure 117 show the performance of each generator. TSO's signal (light blue line) is converted by MVRS in the specific setpoint for each PCR that allow the control of the generator (blue line). The orange line indicates how the plants move their production trying to achieve the target.

It is important to note that both the power plants have greater technical difficulties in increasing dynamic to return to the initial production value. In particular, G2 the group seems not to react to the reception of the ramp to rise of the setpoint, increasing its production by only 200 kW in 6 minutes instead of the entire half-band available of 1.2 MW. This technical limitation is due to the low performance of the power plant regulator which does not have adequate characteristics for this application.

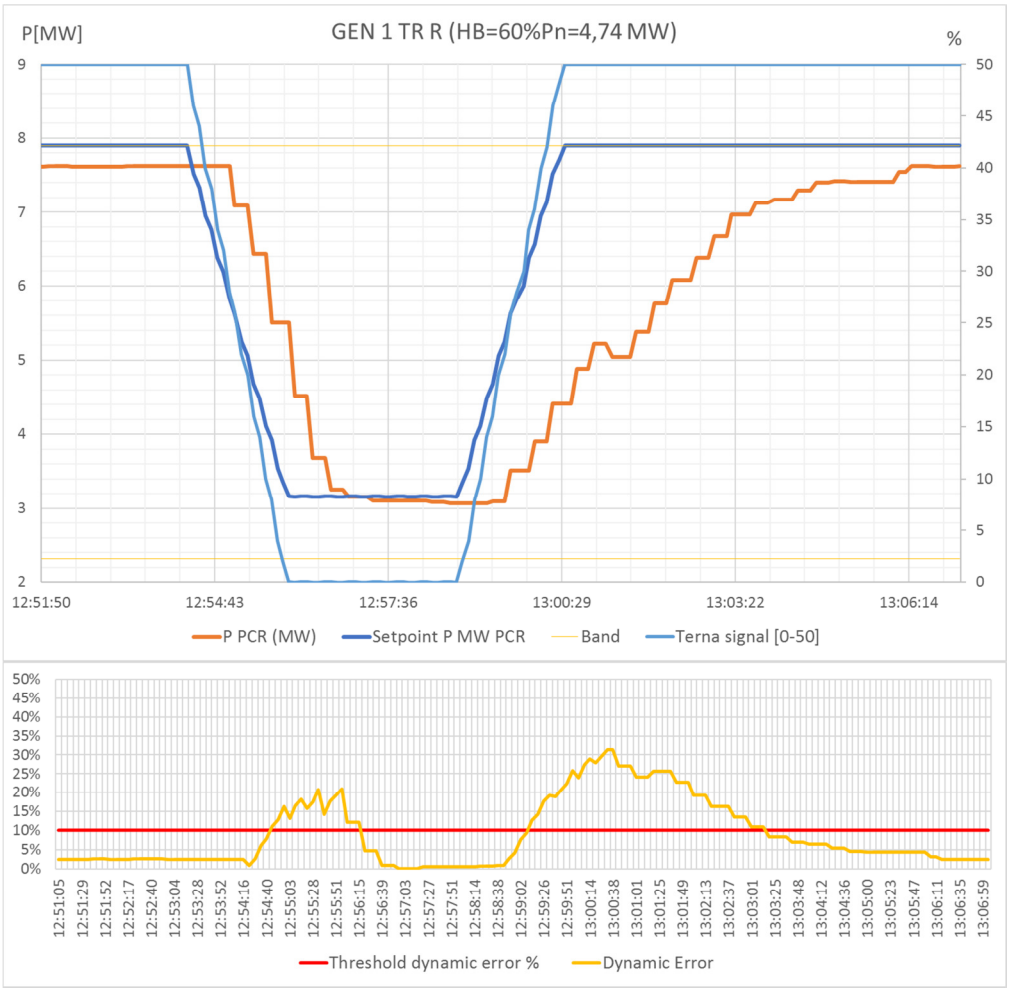

Figure 116: Performance of G1 connected at red transformer – Test 2 07/06/2018

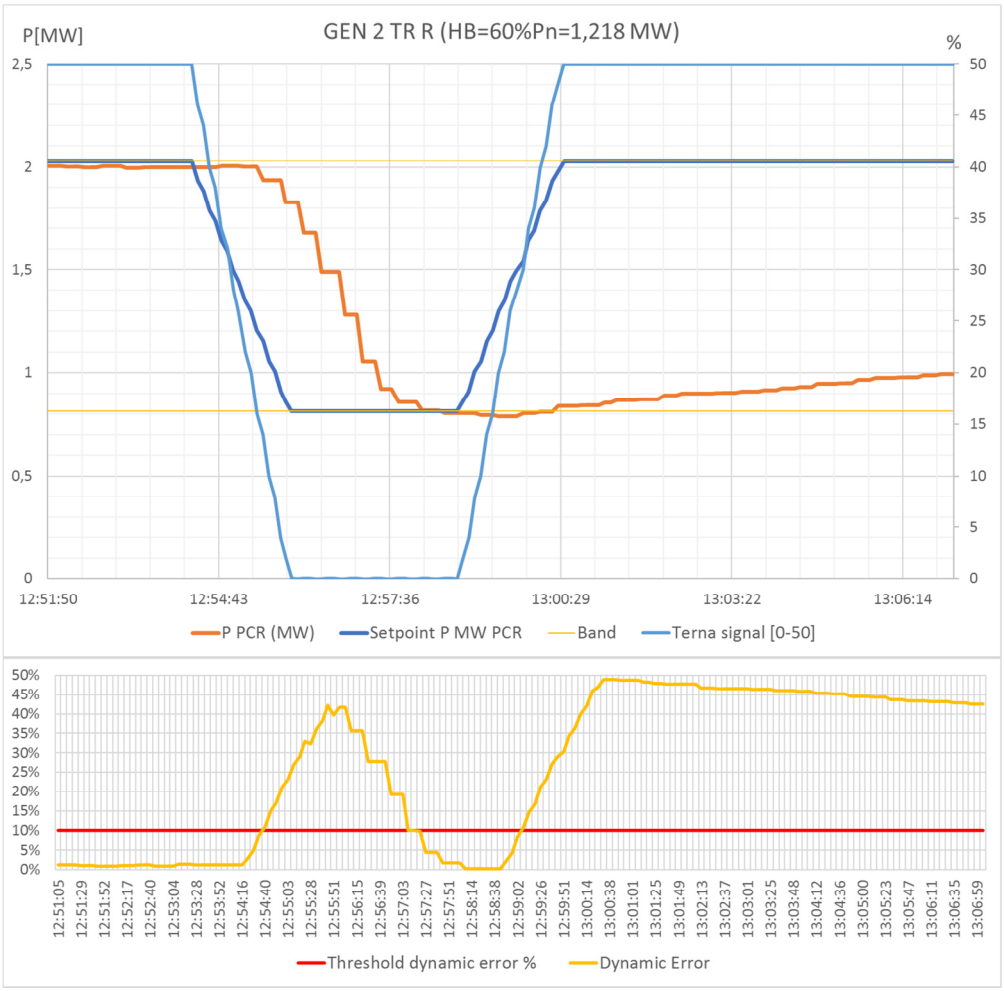

Figure 117: Performance of G2 connected at red transformer – Test 2 07/06/2018

Regarding the green transformer, the active power band made available by the power plant G3 is 0.96 MW. In Figure 118, the comparison between expected contribution and supplied provision at the green transformer is reported. The trend of the active power production at the interconnection point has a better quality than the one recorded for the red transformer.

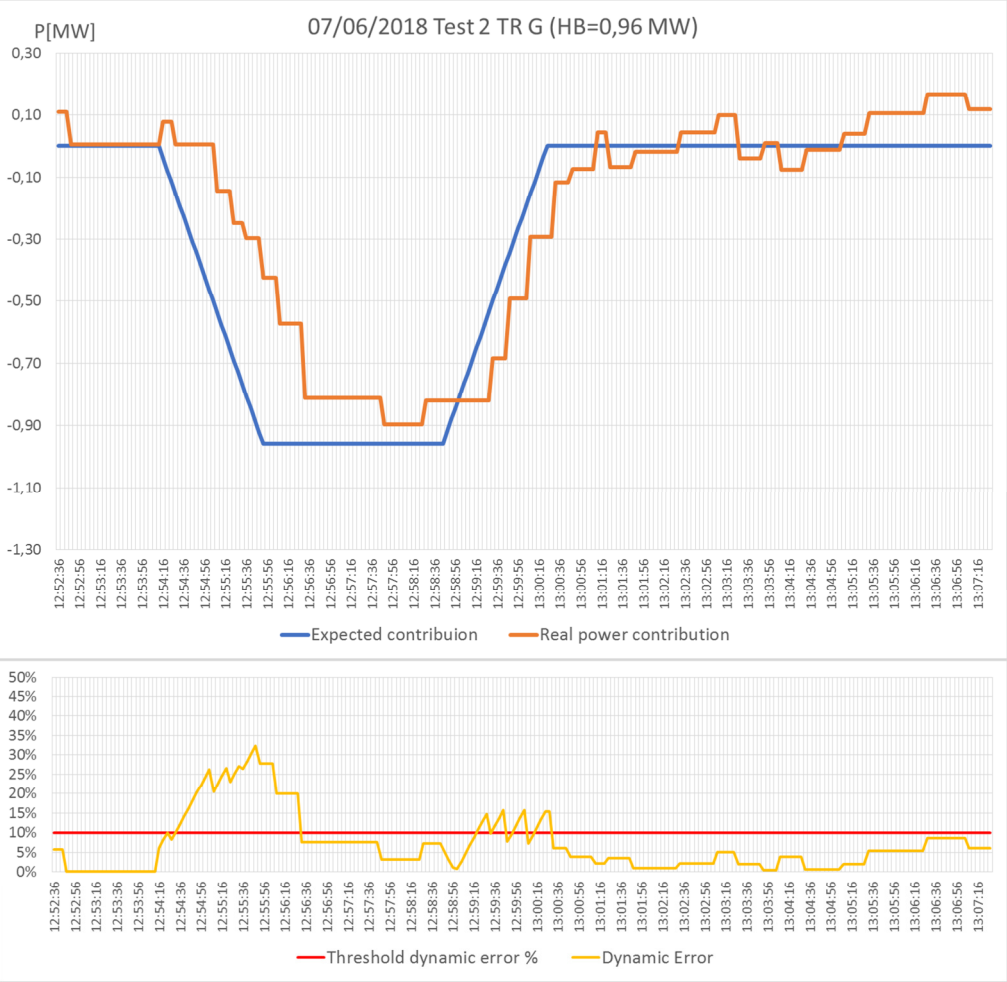

Figure 118: Analysis of the HV contribution at the green transformer – Test 2 07/06/2018

The generator G3 involved in the P/f regulation test made available the 60% of its nominal power. The performance of the power plant is reported in Figure 119. The light blue line is the trend of the TSO's signal and the blue one is the command calculated by MVRS for the PCR of the generator. The orange line is the measurement of the active power generation of the generator in regulation.

It is evident that, among the three power plants, this generator has the most accurate response both in increasing and in decreasing ramps, despite an offset error between the setpoint signal and the measurement record. The maximum dynamic error is 30%.

Considering now the dynamic error detected at the interconnection point with HV grid (Figure 118) and at the power plant terminals (Figure 119), it is evident the difference between the trends and the peaks of the error are reached at different times: for the transformer at the ramp-down while for the power plant at the ramp-down. The measurement at the interconnection point can be affected by consumption or generation variations relative to the rest of the MV grid. It means that it is not possible consider an exact correlation between the errors and therefore not even between the accuracy of the provision of the service.

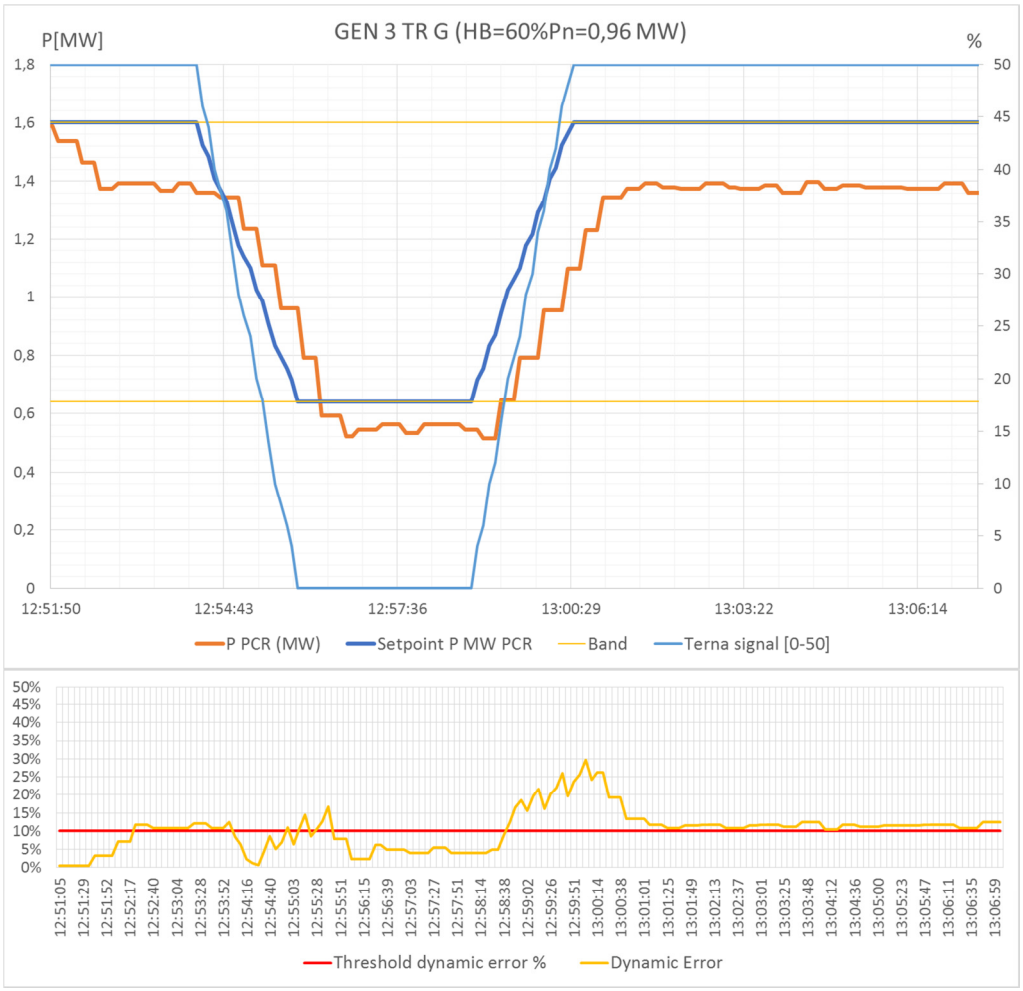

Figure 119: Performance of G3 connected at green transformer – Test 2 07/06/2018

6.4.1.3 Test 3

The second test session, carried out on 12/09/2018, involved 5 hydroelectric power plants: 3 controlled generators connected at red transformer and 2 controlled generators connected at green transformer.

Unlike the previous tests, in this application, the half-band available for f/P regulation for each power plant has been defined as a percentage of the last measurement of active power at the machine terminals. This adjustment was introduced in the MVRS to reduce the offset error due to the fact that considering the plant nominal power the value considered as maximum limit of the regulation band could never be reached during operation.

During the session test different configurations was tested considering a different number of power plants involved in the regulation so as to assess the performance of the device in calculating the available band and in splitting the command among the operated power plants. Moreover, it is useful to analyze the

impact of the configuration on the provision of the service at transformer level. The results of some tests are shown below.

Figure 120 and Figure 121 show the analysis of the f/P regulation at the interconnection point between TSO and DSO grid of the first test of the session: respectively Figure 120 reports the performance of 3 power plants that made available 843 kW at the red transformer while Figure 121 the contribution at the green transformer of 2 power plants with 217 kW. The real provision (orange line) is compared with the expected contribution (blue line) and the dynamic error is reported at the bottom of the graph. Regarding the VPP connected at the red transformer, it is evident a response delay of up to 40 s which leads to an error of 40% during the ramp-down, while the modulation at the green transformer reveals an error of more than 80% and sharp fluctuations.

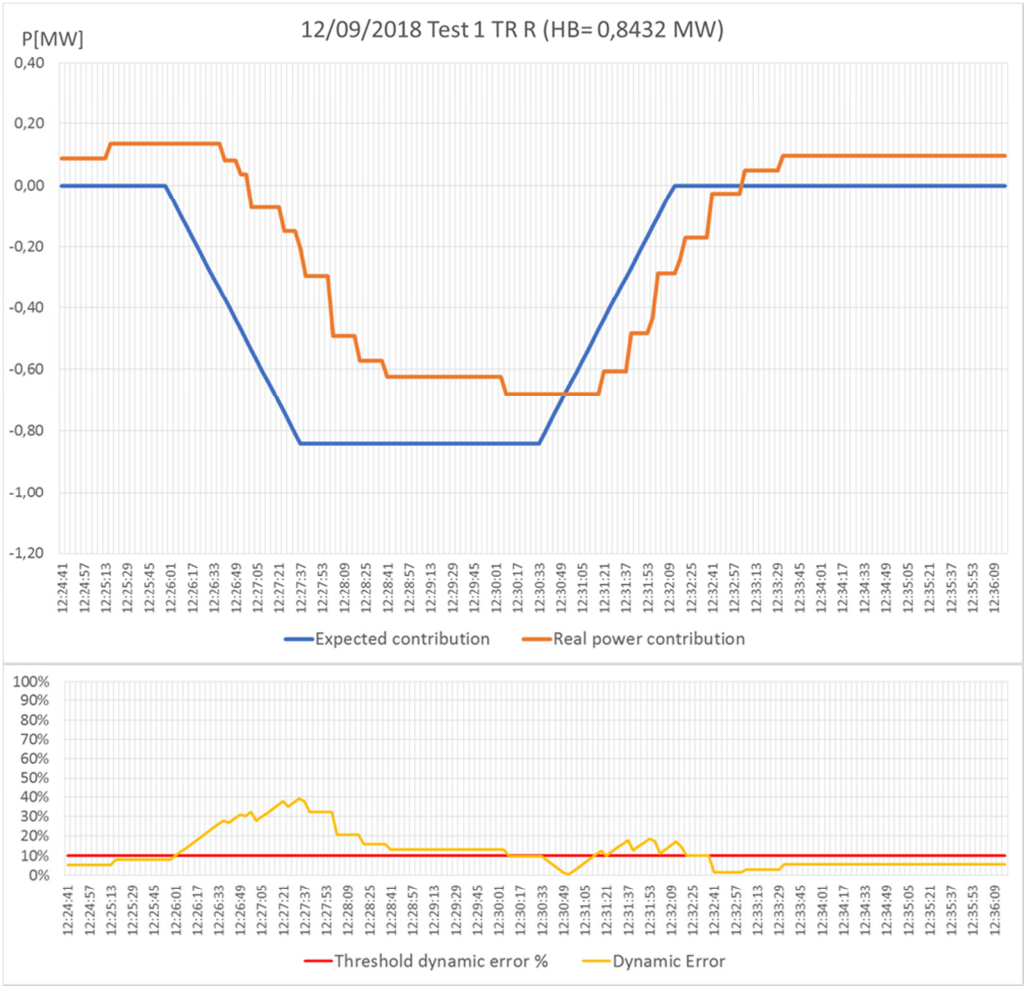

Figure 120: Analysis of the HV contribution at the red transformer – Test 1 12/09/2018

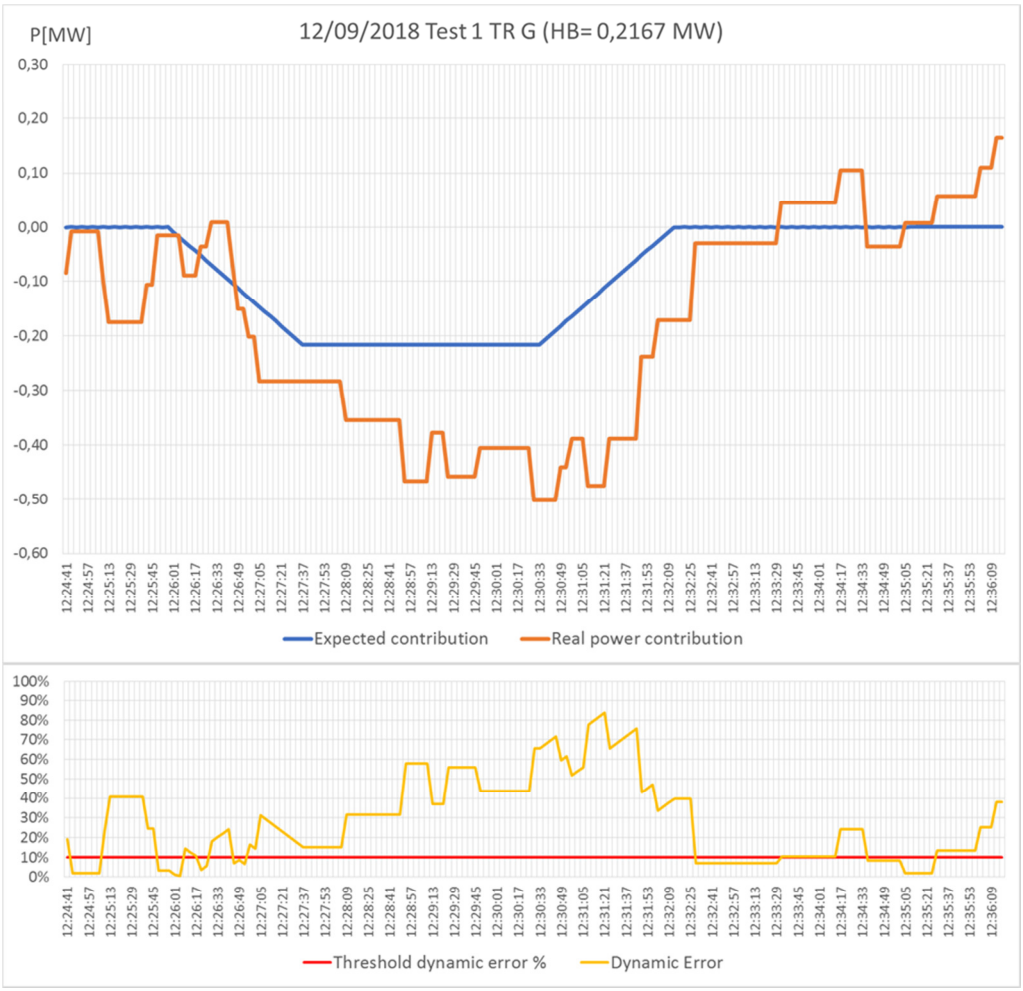

Figure 121: Analysis of the HV contribution at the green transformer – Test 1 12/09/2018

In Figure 122, Figure 123 and Figure 124 the behavior of each power plant involved in the f/P regulation test is represented. The dynamic error calculated at the terminal of the power plants varies between 25, 30 and 30% of the band declared leading to the 40% of error at the transformer.

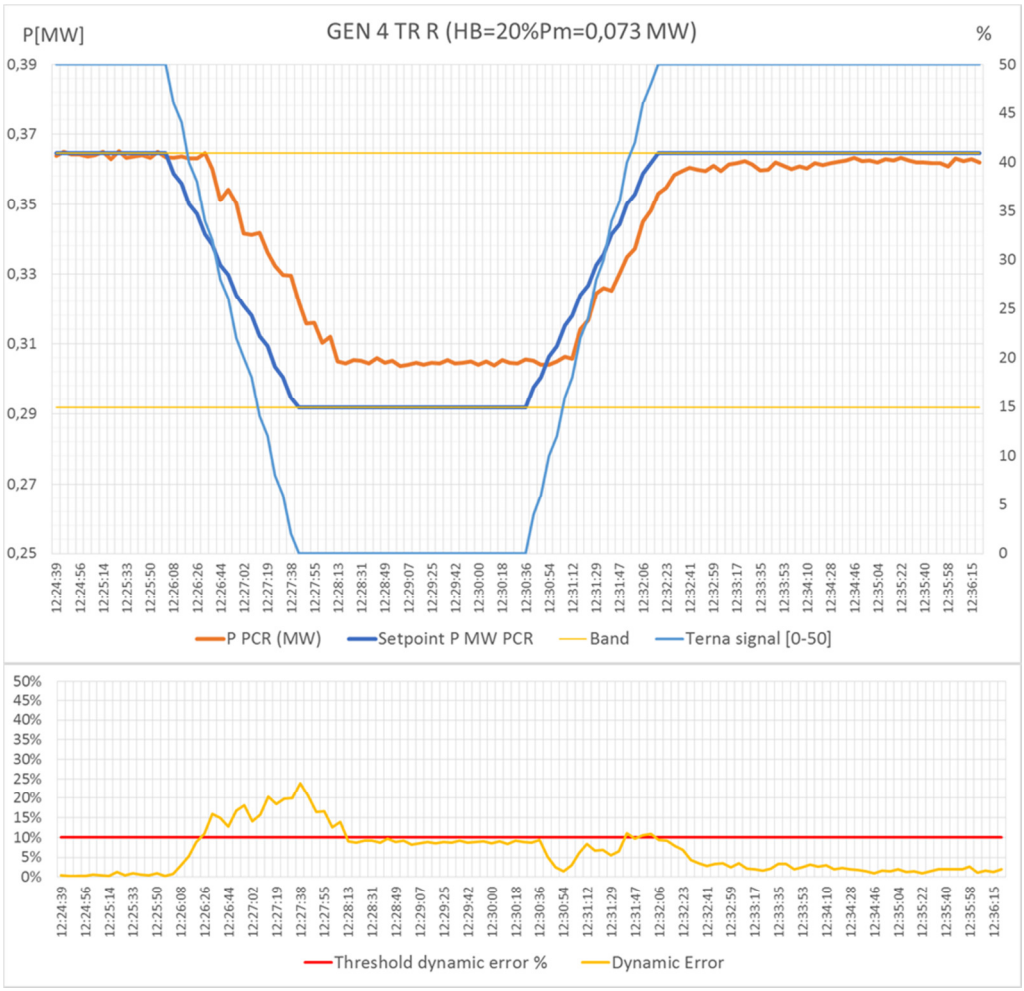

Figure 122: Performance of G4 connected at red transformer – Test 1 12/09/2018

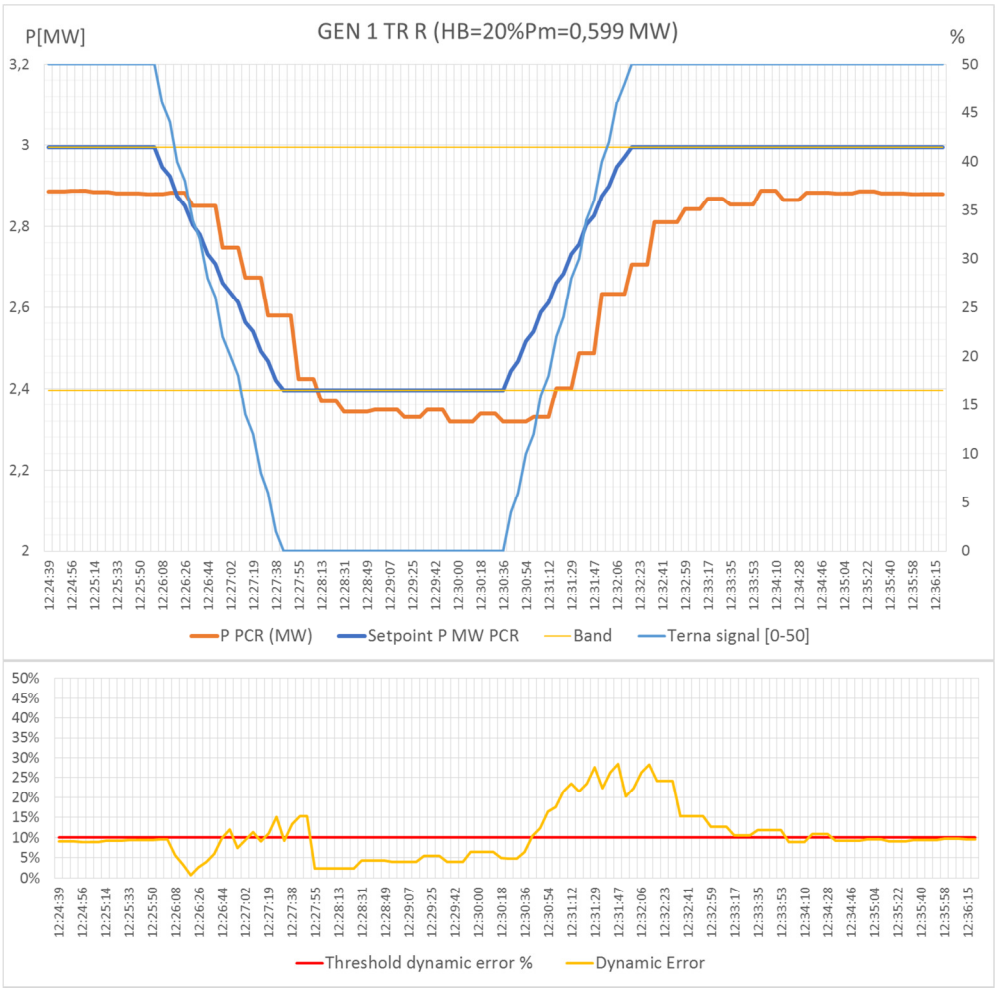

Figure 123: Performance of G1 connected at red transformer – Test 1 12/09/2018

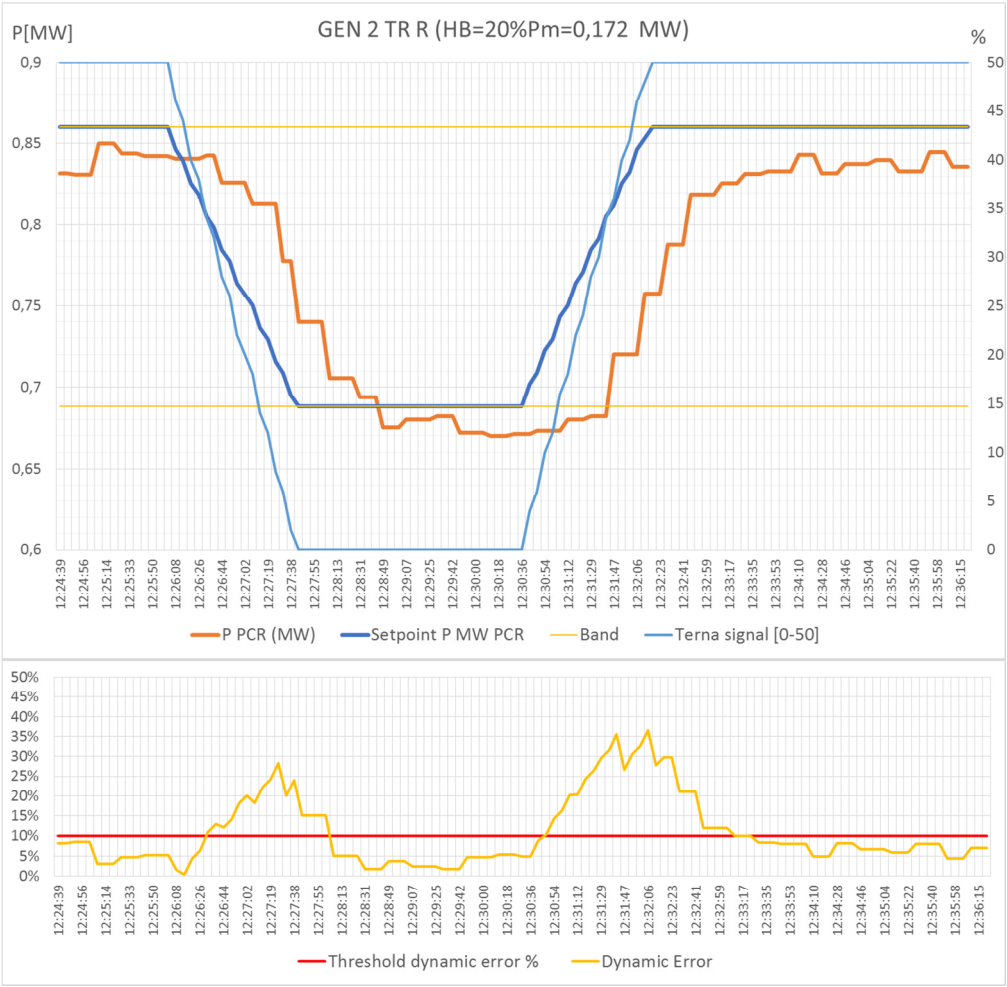

Figure 124: Performance of G2 connected at red transformer – Test 1 12/09/2018

Figure 125 and Figure 126 show the comparison between setpoint and production measurement of the power plant connected at the green transformer. The trend of the errors compared with the dynamic error calculated at transformer level is not always correlated. In fact, considering the ramp-down the response of the single governors show maximum errors of 10-15 %, while the error of the VPP connected at the transformer reaches 40%: this means that the reliability of the regulation at the interconnection point does not depend solely on the performance of the controller, but it is influences by other uncontrolled and unforeseeable elements of the network. Moreover, the fluctuation and the inaccuracy of the ramp is clearly not compliant with a sufficiently reliable service.

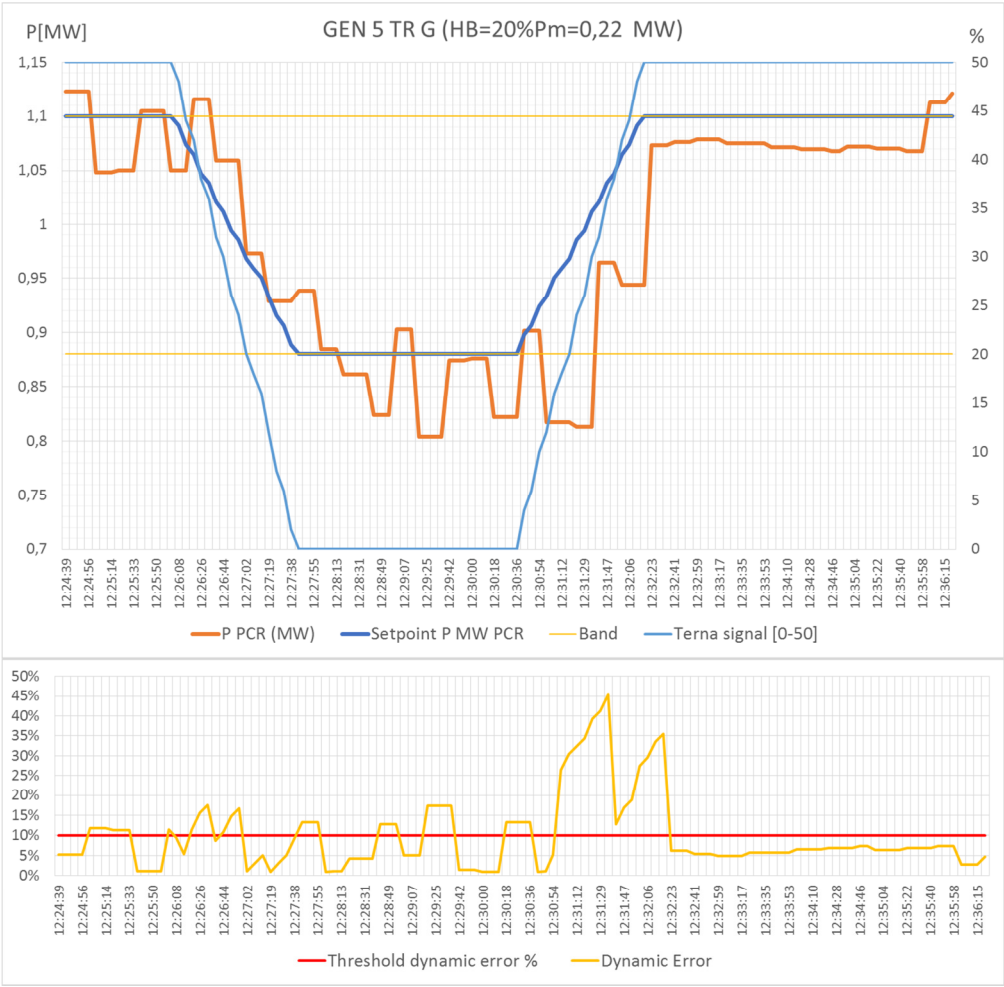

Figure 125: Performance of G5 connected at green transformer – Test 1 12/09/2018

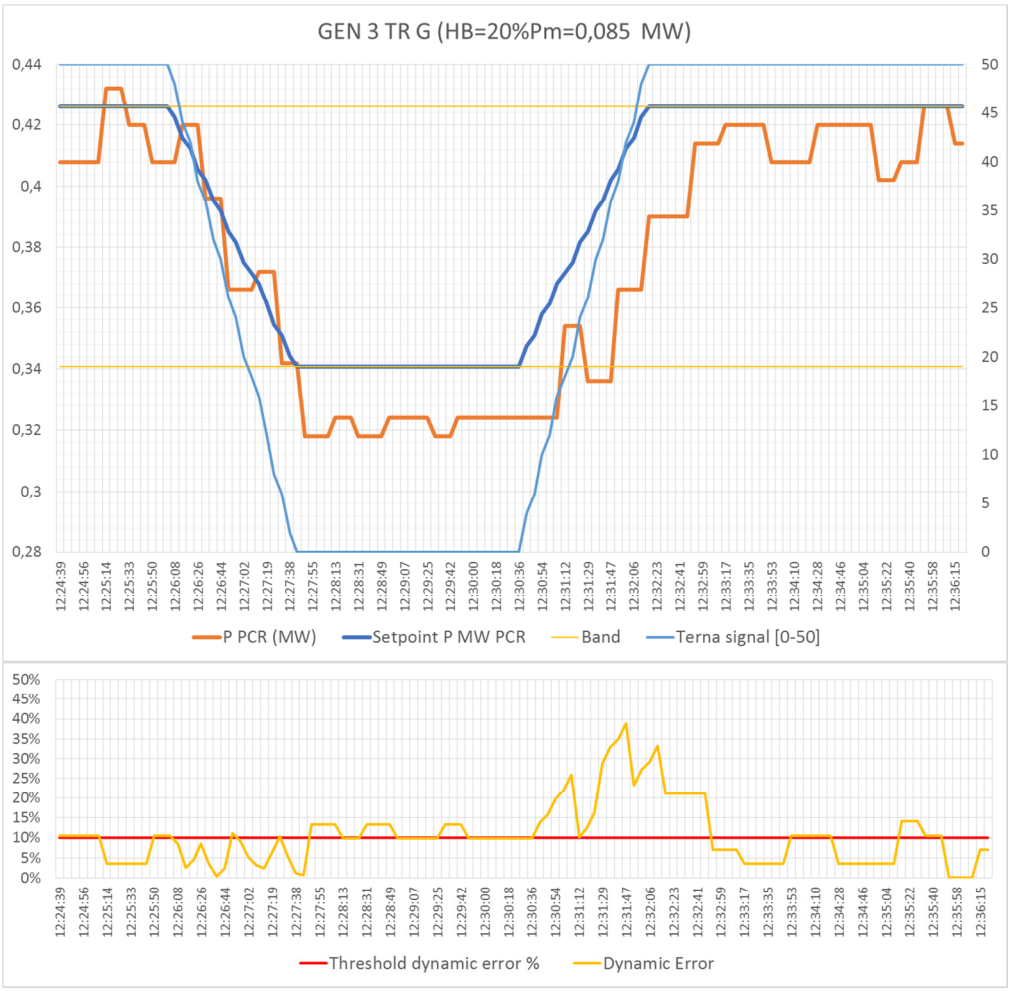

Figure 126: Performance of G3 connected at green transformer – Test 1 12/09/2018

The same test described above was carried out by enabling only three distributed generators (G4 and G1 connected at the red transformer and G5 connected at the green transformer) in order to evaluate the calculation of the band for the regulation and the difference in the response performance. During this test, the reduction in power made available by each power plant was maintained at 20% of production.

In Figure 127 the performance of the aggregation of G4 and G1 at the transformer level, while Figure 128 and Figure 129 show the response of each power plant involved in the regulation.

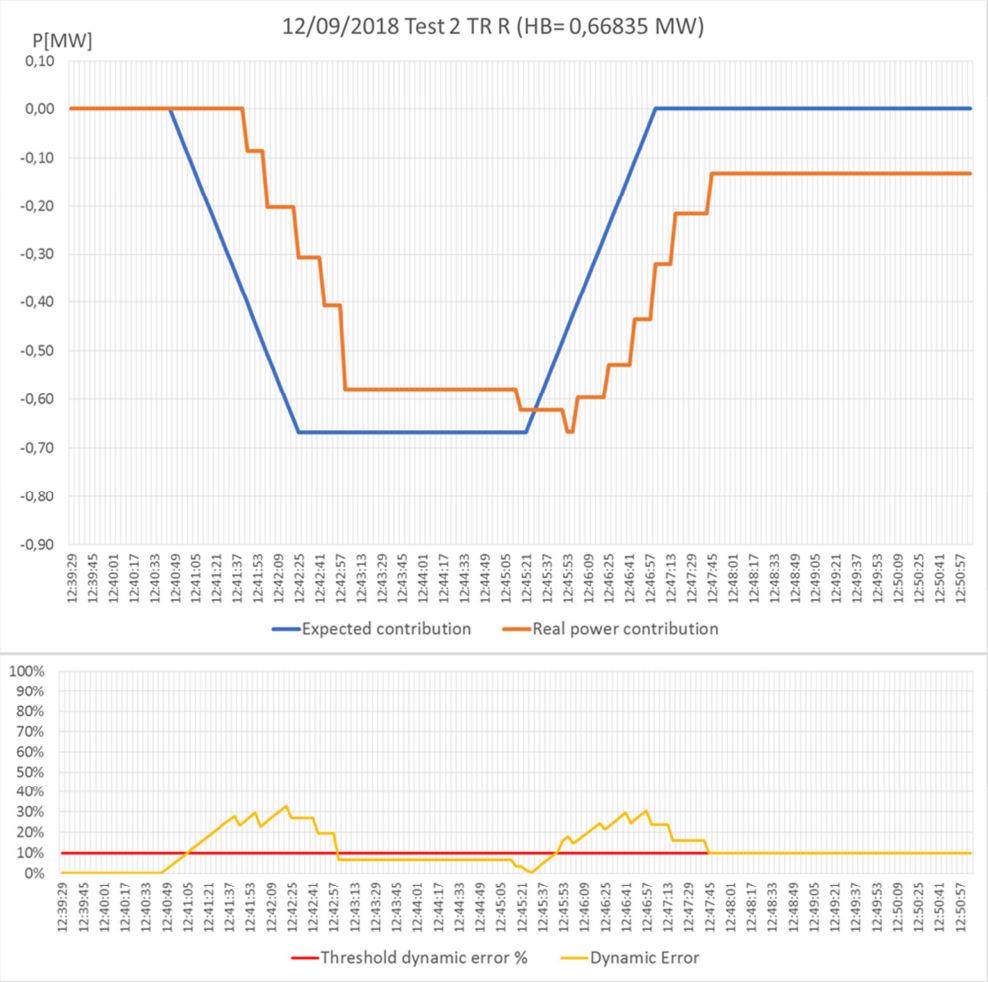

Figure 127: Analysis of the HV contribution at the red transformer – Test 2 12/09/2018

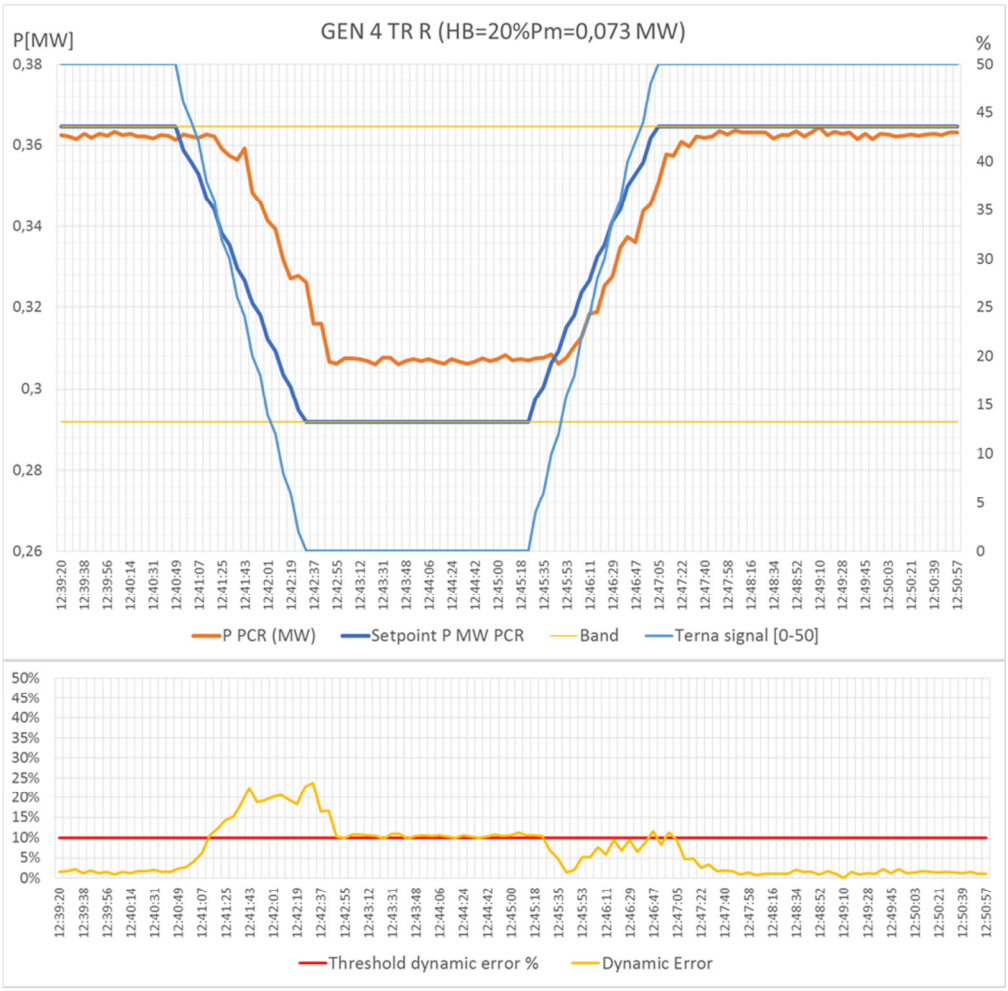

Figure 128: Performance of G4 connected at red transformer – Test 2 12/09/2018

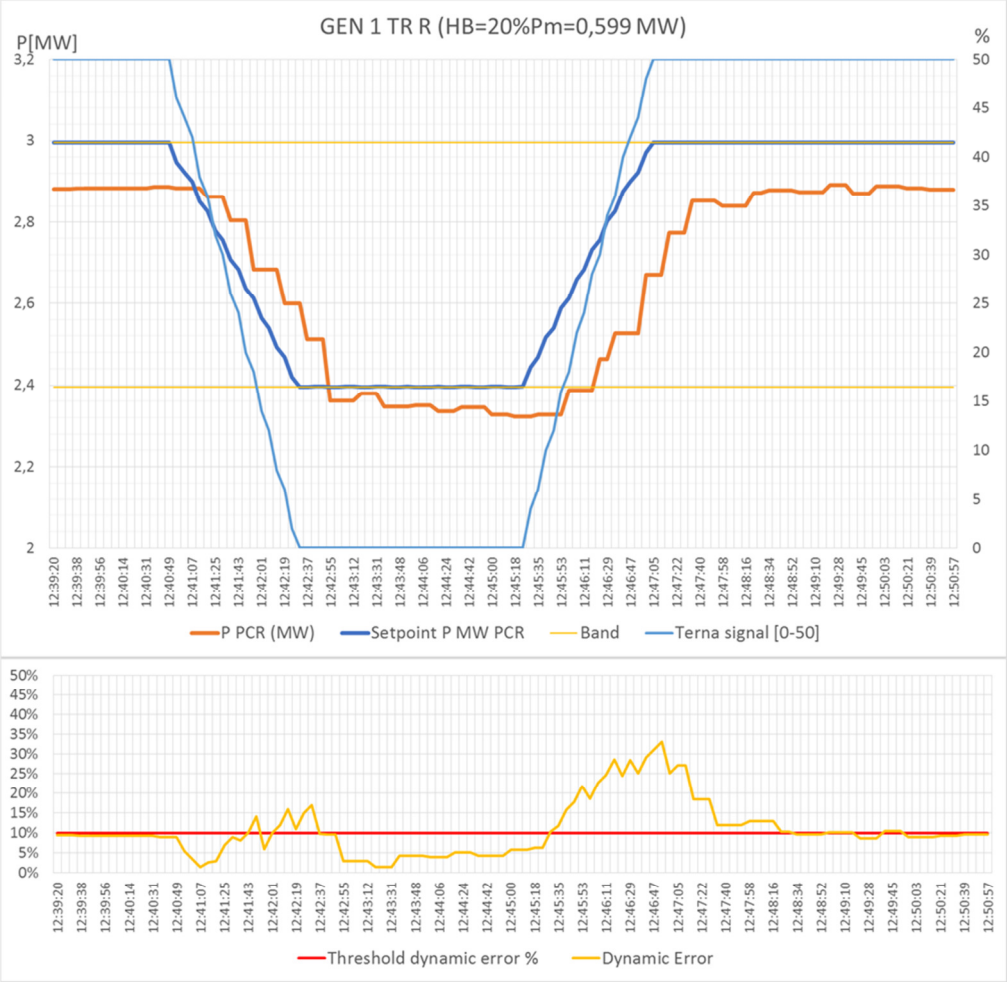

Figure 129: Performance of G1 connected at red transformer – Test 2 12/09/2018

In this example, it can be seen that the maximum error at the transformer decreases from 40% to 30% due to the unavailability of G2 for the regulation that introduced additional error in the previous test. The two regulating power plants shows a response similar to the previous test (Figure 122 and Figure 128).

Finally comparing the trend of the two power plants is evident the different performance of the governors: G4 show a better response in the ramp-up while G1 has better performance during ramp-down.

6.4.1.4 Test 4

The subsequent tests of this session were carried out by increasing the amount of active power made available for the f/P regulation. In particular, the following part of the report shows the results of the test, in which all five power plants under regulation were declared to have a half-band equal to 60% of the measured production.

Regarding the red transformer, the test involved 3 power plants with an adjustable power of about 3 MW for the regulation. In Figure 130, the behaviour of the power exchanged at the red transformer is

reported. The comparison between expected contribution (blue line) and real provision (orange line) proves that the MV system follows better the ramp-down despite a delay due to the communication and actuation timings. The up-word regulation shows technical problems of the hydroelectric generators to follow the setpoint and the VPP returns to the production initial value after 5 minutes. The slow dynamic causes a large deviation between expected contribution and real modulation that lead to a dynamic error of 40 %.

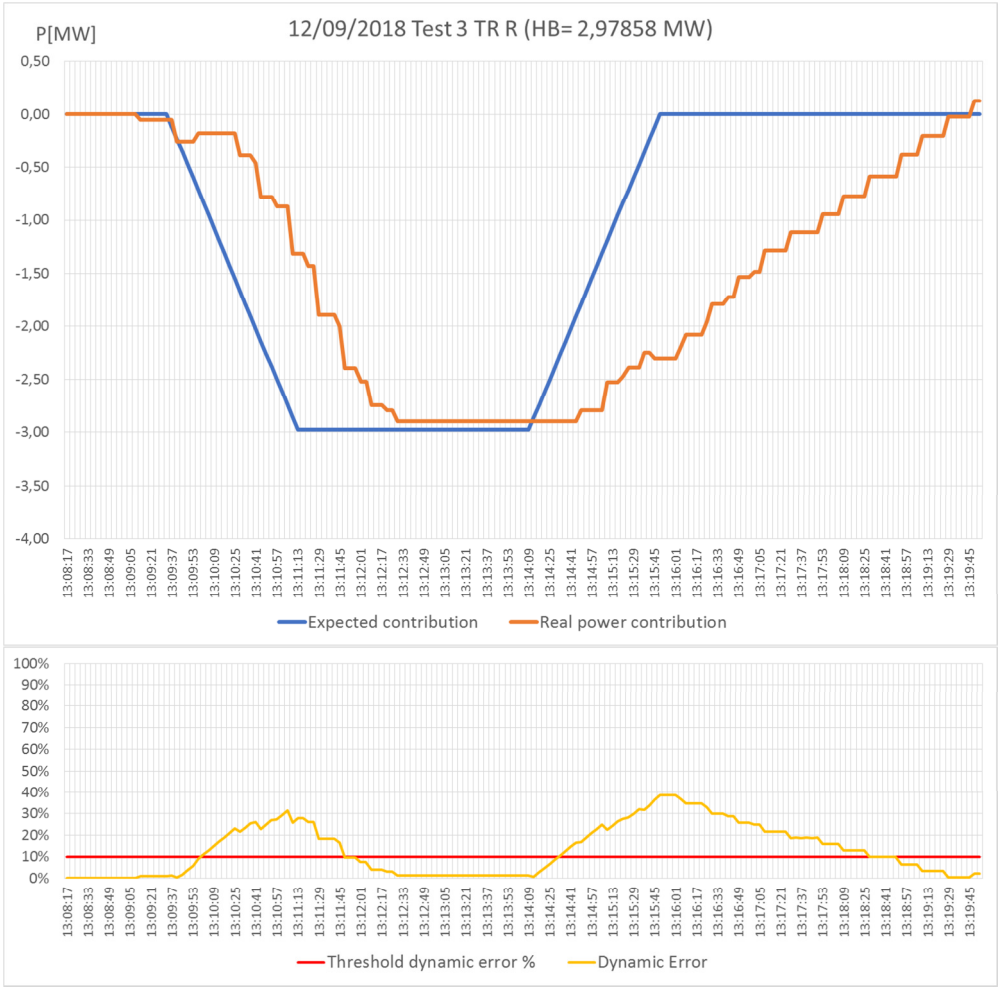

Figure 130: Analysis of the HV contribution at the red transformer – Test 3 12/09/2018

The MV system controlled by TSO is composed by 3 controlled hydroelectric power plants that made available the 60% of their own initial operating point.

In detail, Figure 131, Figure 132 and Figure 133 show the behaviour of the each generator. In particular, the blue line represents the setpoint that the power plant receives through the PCR installed at the generator terminals and that is calculated from the TSO's signal (light blue line) by MVRS. On the graph the trend of the production measurement is represented by the orange line.

Comparing the three figures, it is evident the difference among the response of the three power plants. The first power plant (G4) showed the best performance in terms of shape of the ramp and, despite the delay that causes a translation of the trend, the maximum error was keeping below 25 %. G1 instead encountered technical problems, especially during the ramp-up. The graphic related to the dynamic error shows that the maximum value achieved the 50 % and it seems that the response of this plant strongly influenced the trend of the power exchange at the interconnection point with the transmission grid. The response of the third hydro power plant (G2) indicates also fluctuation problems following the ramp-down setpoint.

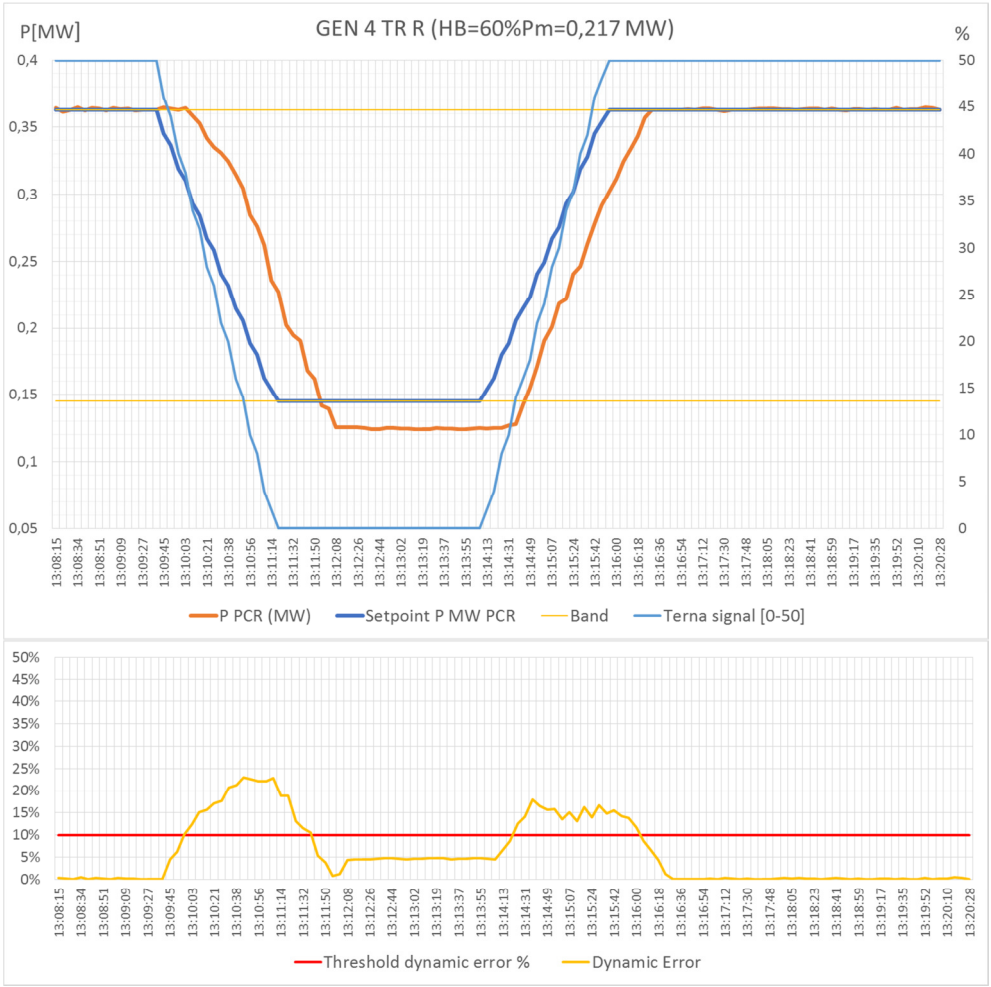

Figure 131: Performance of G4 connected at red transformer – Test 3 12/09/2018

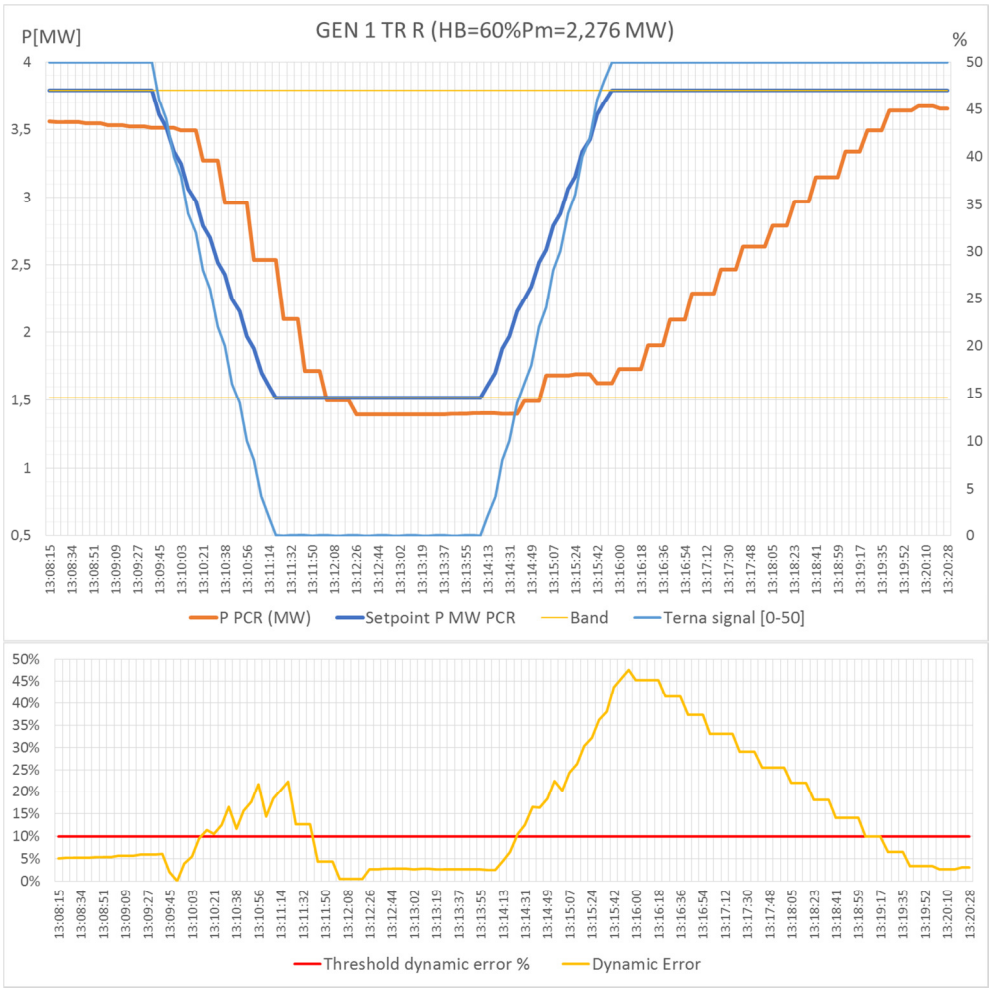

Figure 132: Performance of G1 connected at red transformer – Test 3 12/09/2018

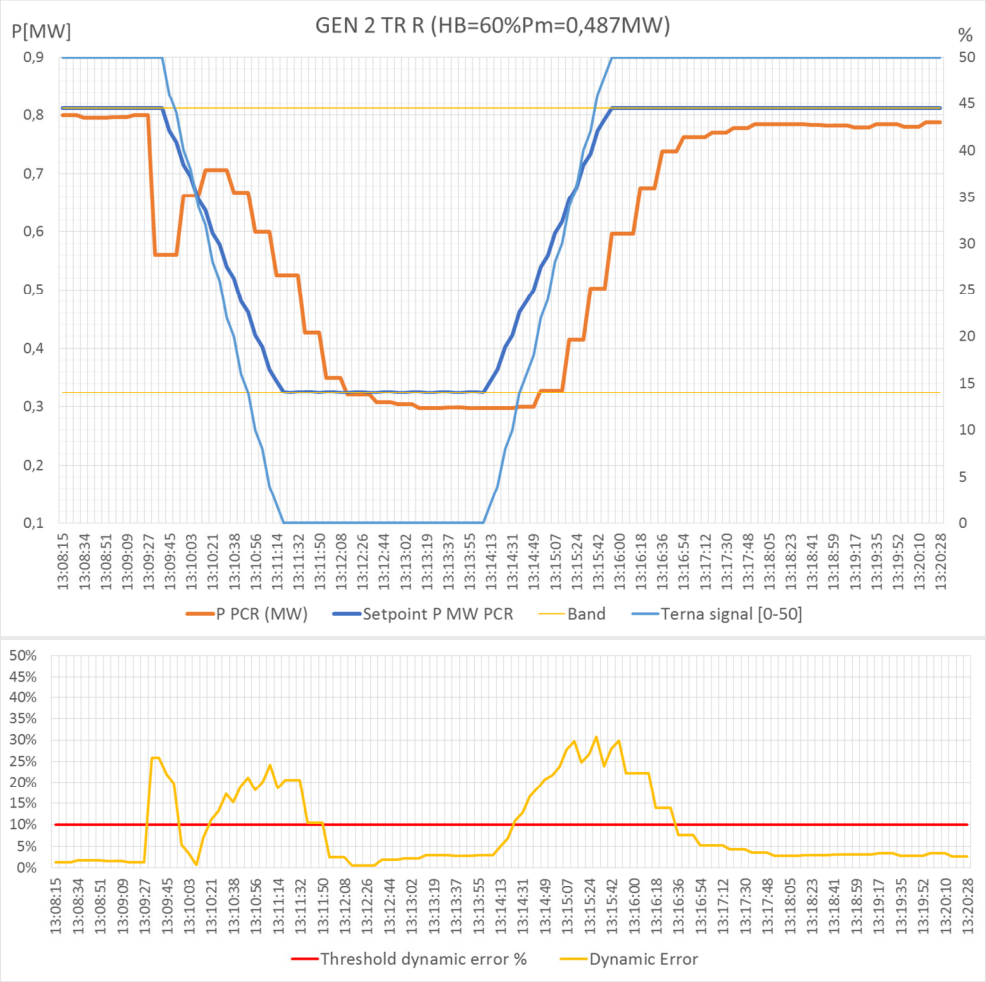

Figure 133: Performance of G2 connected at red transformer – Test 3 12/09/2018

Regarding the green transformer, the test involved 2 plants that made available 1,022 MW for the downward regulation. Figure 134 shows the performance of the MV system connected at the green transformer considering the contribution at the service at the HV side of the primary substation.

The reference signal (blue line) is achieved by the MV system (orange line) with an evident delay due to the technical constraint and the communication chain that involves many devices. The active power fluctuation measured at the interconnection point may be caused by load or generation variations relative to the rest of the MV grid.

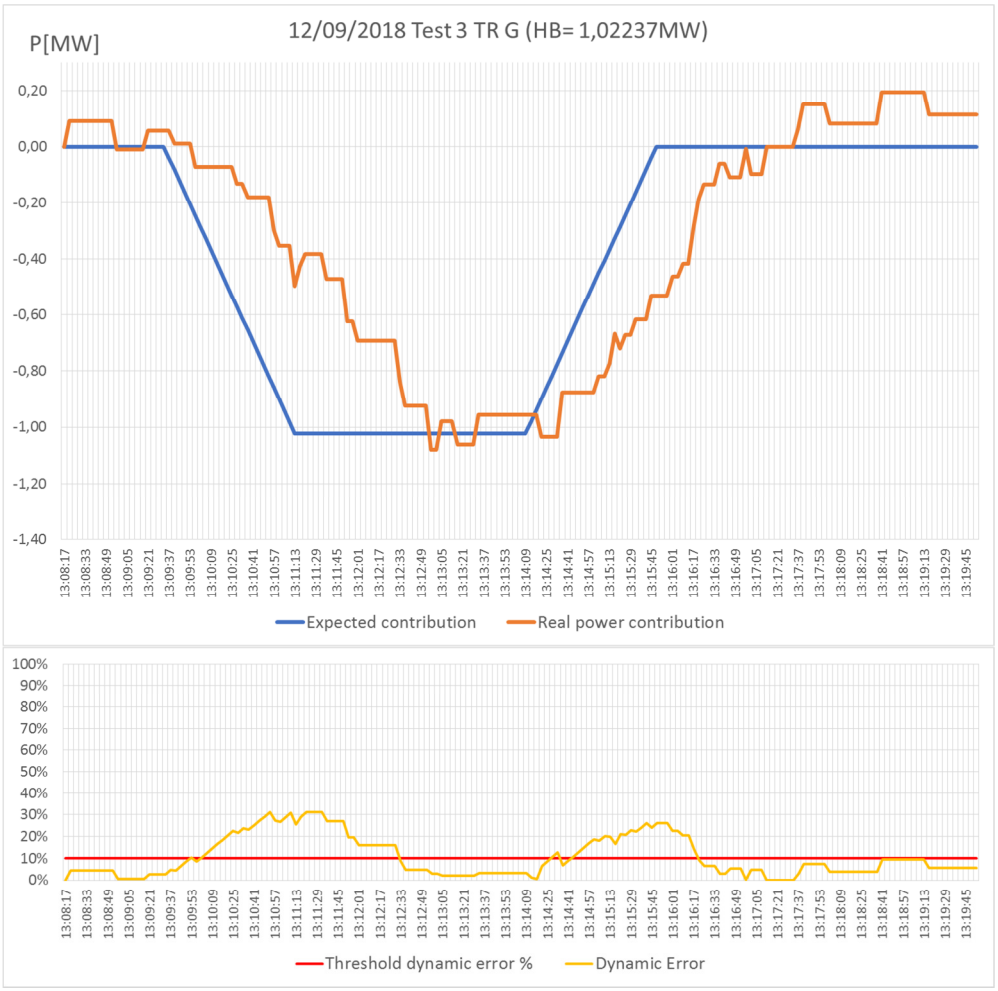

Figure 134: Analysis of the HV contribution at the green transformer – Test 3 12/09/2018

To evaluate the response of the individual power plant, the following are the graphs of each plant involved. Figure 135 shows the response of the G5 with 0.8 MW half-band. It is important to note that in terms of amount of modulation this power plant shows a good performance both ramp-down and in ramp-up and the production reached the target value both in the minimum direction and in the maximum direction: the offset between the setpoint signal and the measurement record is reduced but the dynamic error is increased by the evident delay due to the communication chain remains evident. In this case, the distance from the primary substation, the devices interposed in the communication and the size of the power plant play a key role.

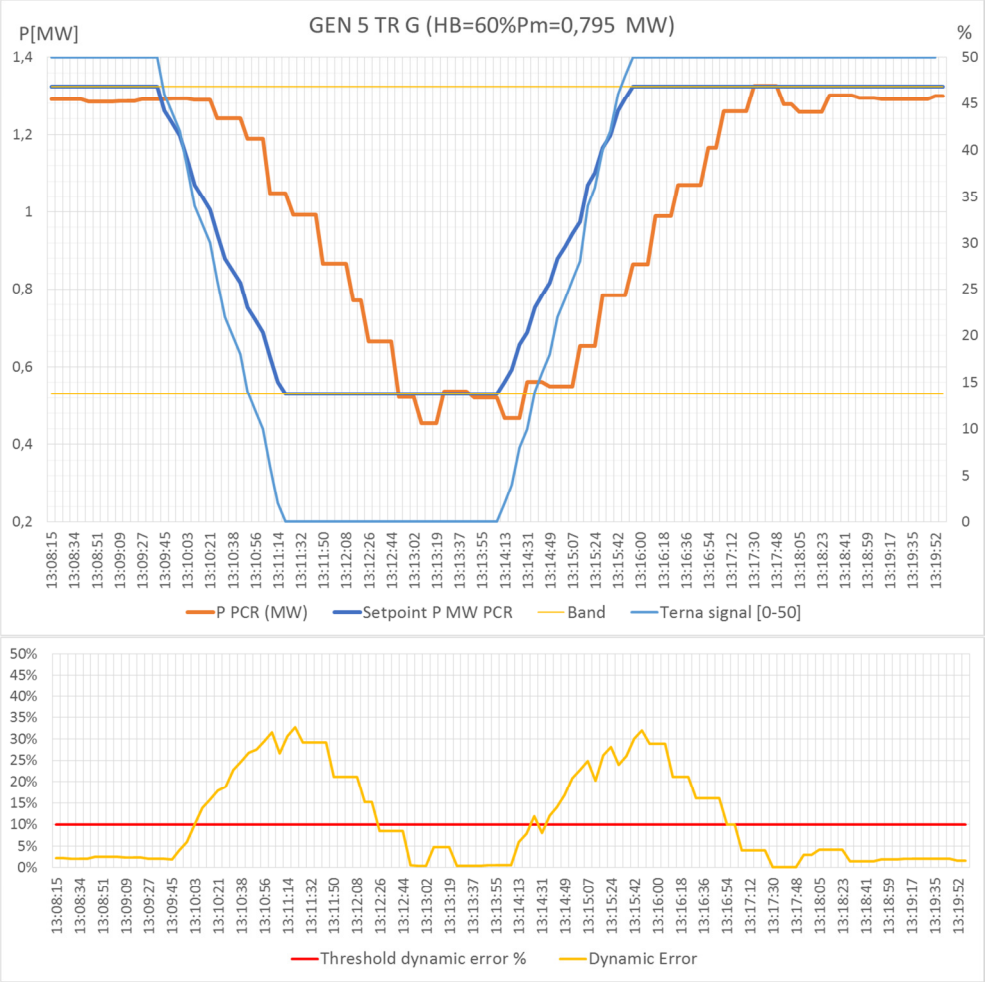

Figure 135: Performance of G5 connected at green transformer – Test 3 12/09/2018

As reported in Figure 136, G3 is the power plant that provide the regulation in the better way in terms of offset, delay and accuracy. The quality of the response is indicated by the dynamic error graph, in which the value was usually kept under the 10 % and the maximum value reached 25 % only during the ramp-up. This evaluation can be confirmed by considering also the G3 response during the other tests reported in the document and the, in particular, the correlated error trends in Figure 119, Figure 126, Figure 136 and Figure 145.

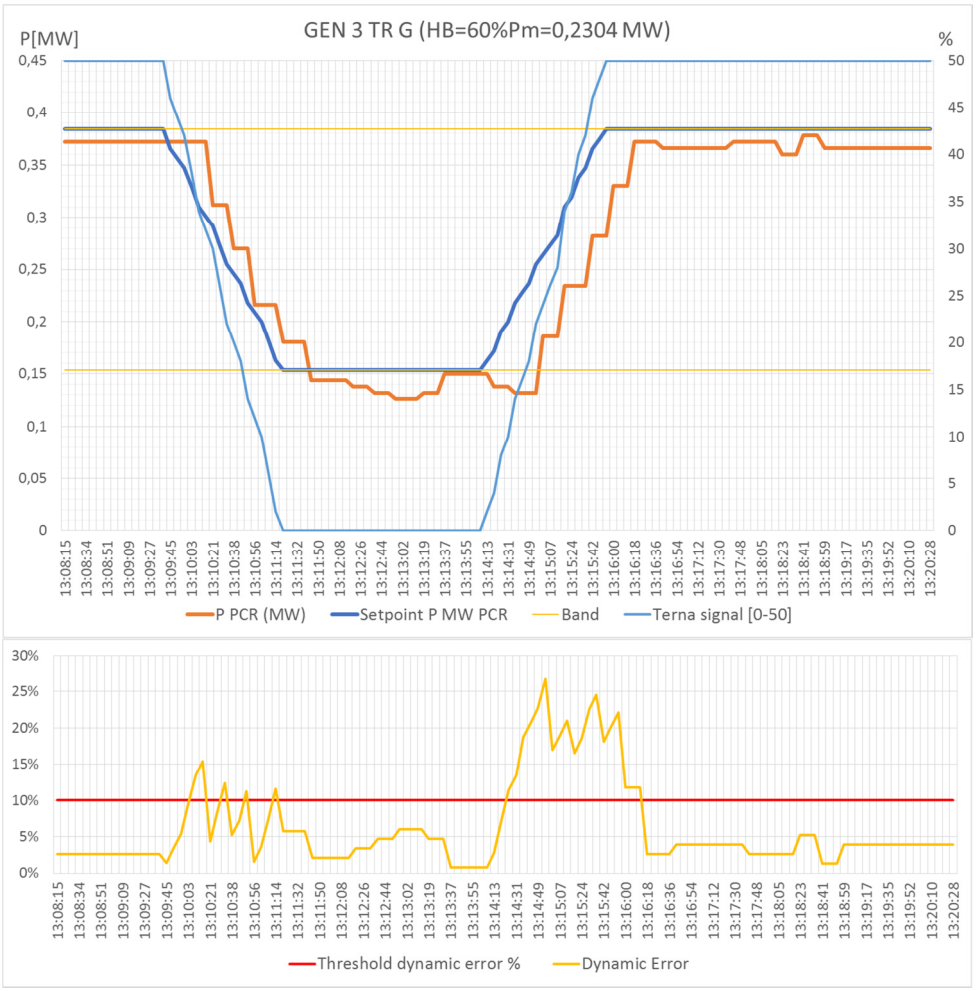

Figure 136: Performance of G3 connected at green transformer – Test 3 12/09/2018

As in the previous case, this test was repeated considering 3 power plants available for the f/P regulation with the same 60 % half-band: in this case G1 and G2 connected to the red transformer and G3 connected to the green transformer. The result achieved is a change in the availability of active power adjustable at the transformer level due to the participation of fewer distributed generators: regarding the red transformer the declared half-band was reduced from almost 3 MW to 2.7 MW, while the green transformer half-band was reduced from 1 MW to 0.2 MW.

Figure 137 and Figure 138 show the performance of the service provision at the interconnection point with the transmission grid. Regarding the red transformer the result is in line with previous results (Figure 130), while the measurements at the green transformer show unexpected fluctuations. In fact, the response of each power plant is similar to the behavior of the previous test and, in particular, Figure 139 shows the production trend of G3, which is the only controlled power plant connected to the green transformer, and it is noted that the trend does not explain the performance recorded at the transformer (Figure 138); the error trend is therefore affected by the operation of other uncontrollable and unpredictable elements of the grid that can modify and reduce the performance of the VPP. There is a

clear need in the experimentation of integration of DG in the management of the electricity grid to verify how to guarantee the quality, reliability and effectiveness of ancillary services and to figure out how to avoid this indeterminateness.

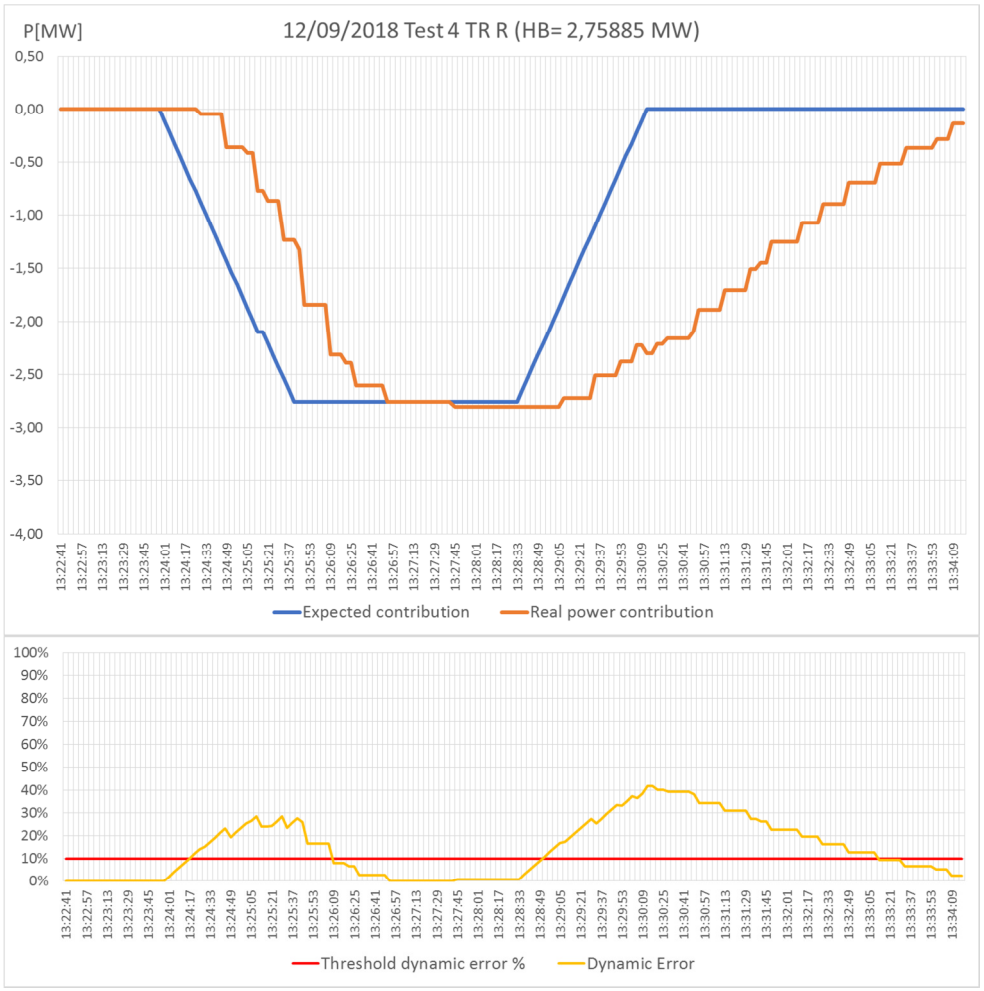

Figure 137: Analysis of the HV contribution at the red transformer – Test 4 12/09/2018

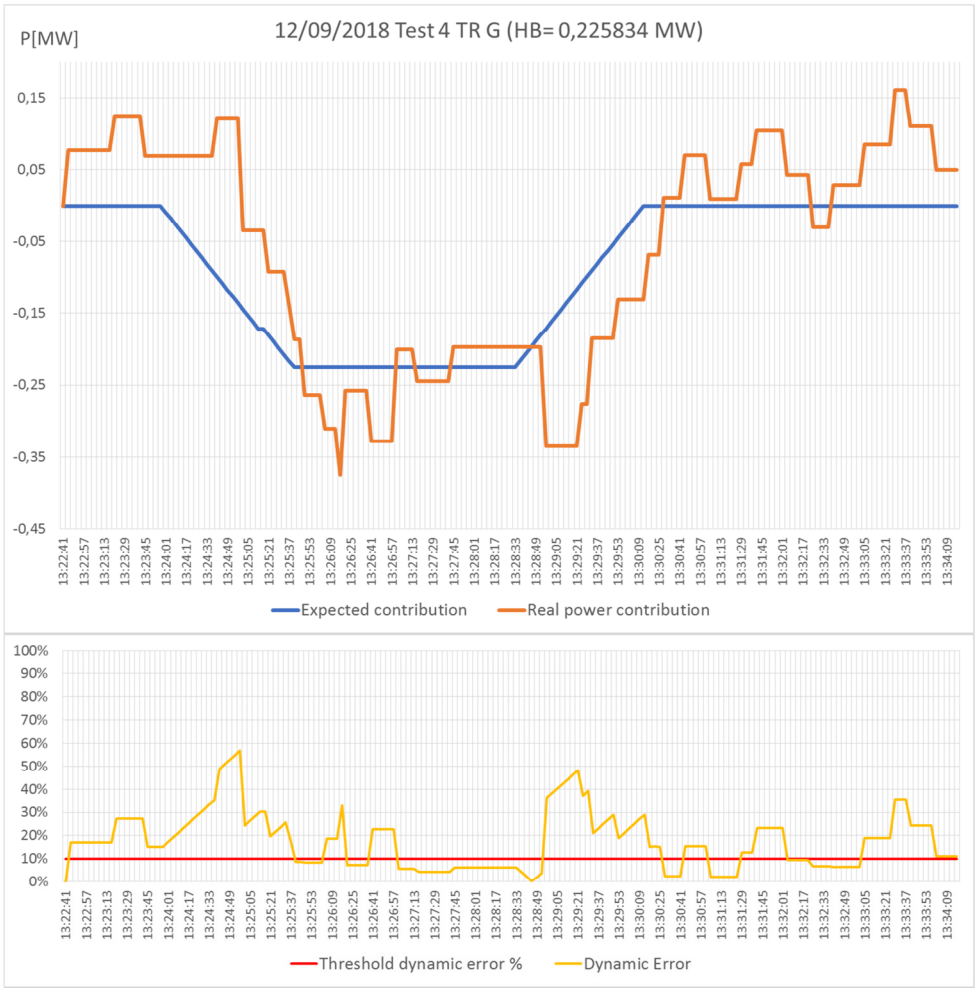

Figure 138: Analysis of the HV contribution at the green transformer – Test 4 12/09/2018

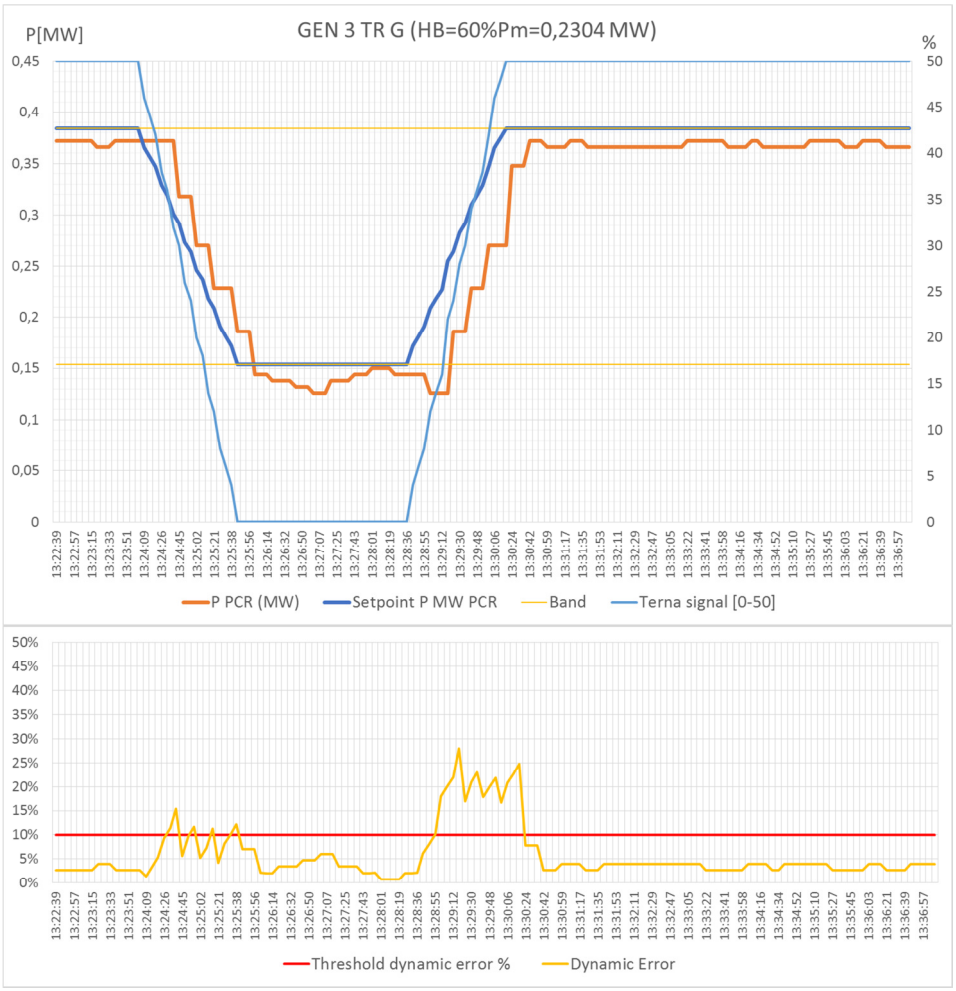

Figure 139: Performance of G3 connected at green transformer – Test 4 12/09/2018

6.4.1.5 Test 5

The last test of the session of 12/09 here reported was carried out by further increasing the power supplied to the f/P regulation: the half-band made available by each of the 4 power plants available for the regulation has been defined as 80 % of the measured production. The half-band calculated by the MVRS as the sum of the available half-bands and transmitted to Terna control system was equal to 6.1 MW distributed as follows: 4.5 MW available at the red transformer (G1 and G2) and 1.6 MW at the green transformer (G5 and G3).

Figure 140 shows the performance of the VPP composed by G1 and G2 and connected at the red transformer: the expected contribution calculated from the declared half-band and the setpoint ramp (blue line) is compared with the actual provision (orange line). In line with the results of previous tests, the performance deteriorates on the ramp to rise, i.e. when production should return to the program value, corresponding to the level signal of 50 %. In addition, comparing the graph with the trends drawn in previous tests (in Figure 120 half-band of 0.8 MW, in Figure 130 half-band of 3 MW and Figure 140 half-band of 4.5 MW), it can be seen that the delay and inaccuracy of the response increases with the

growth of the half-band made available for the f/P regulation. This aspect is also evident considering the dynamic error calculated in the three cases: in Figure 120 (half-band = 20 %) the maximum error during ramp-down was 20% and the error returns below the 10% limit 30 seconds after the end of the ramp; in Figure 130 (half-band = 60 %) the maximum error is 40% and with a delay of 225 seconds after the end of the ramp the power exchange reaches the program value and the error returns below the 10 %; finally, in Figure 140 (half-band = 80 %) the maximum error is again 40 % but at the end of the testing ramp the actual power exchange does not reach the target value.

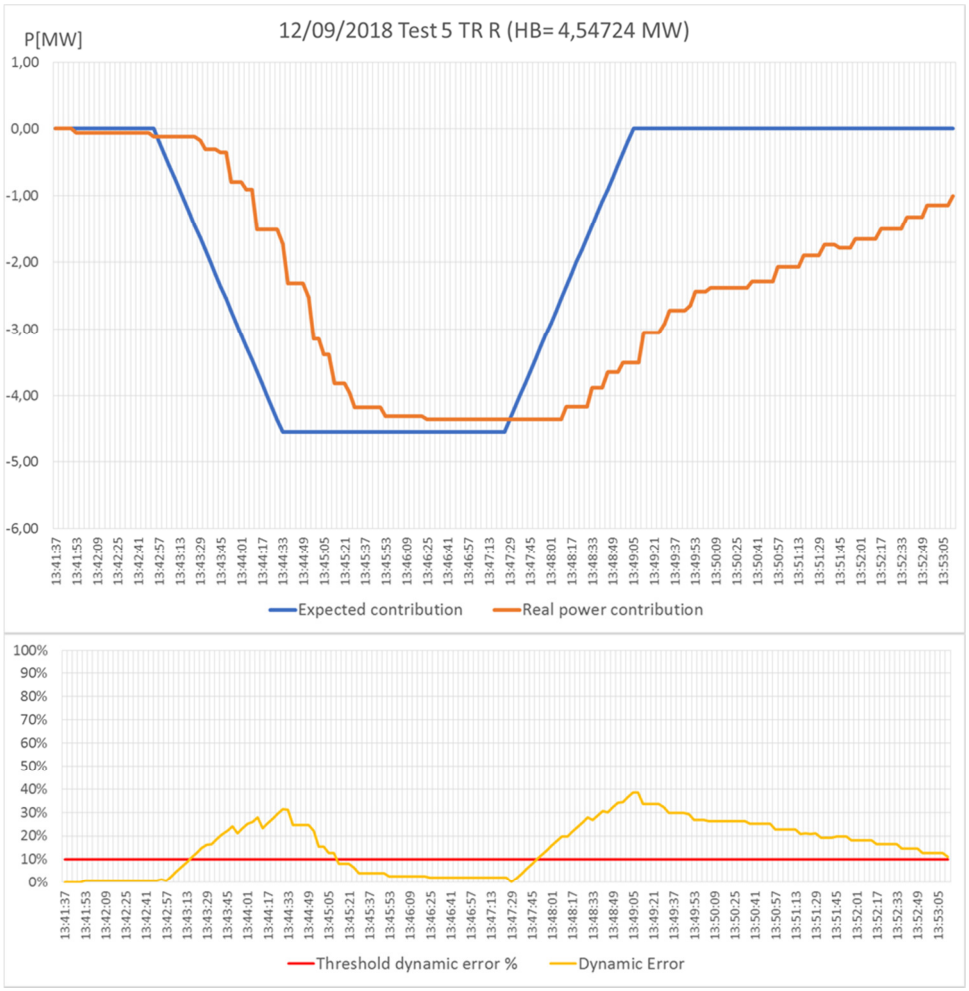

Figure 140: Analysis of the HV contribution at the red transformer – Test 5 12/09/2018

The following reports the performance of each power plant activated in the feeders connected at the red transformer. Figure 141 and Figure 142 show the trend of G1 and G2 respectively comparing their own setpoint calculated by MVRS (blue line) with the production measured at the power plant terminals. Regarding G1, the response and the corresponding dynamic error is in line with the results of the tests described above and represented in Figure 123 and Figure 132. The increase in inaccuracy with the increase of the power amount provided in the test leads to evaluations similar to those explained for the VPP connected to the red transformer.

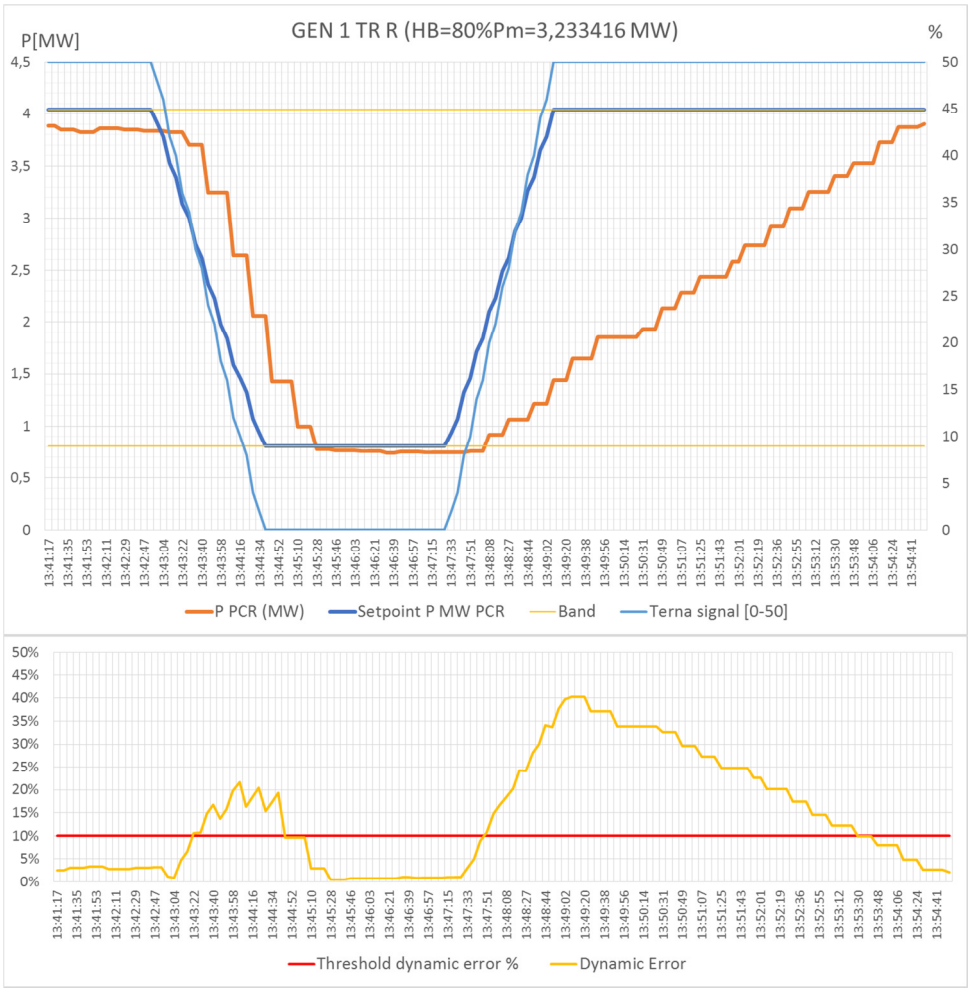

Figure 141: Performance of G1 connected at red transformer – Test 5 12/09/2018

The results are different for G2, which had better performance during test 3 where it provided 0.5 MW, while in this application the response has a drift during the ramp-up. The production did not reach the target value at the end of the ramp, but the measurement shows a decrease of the active power.

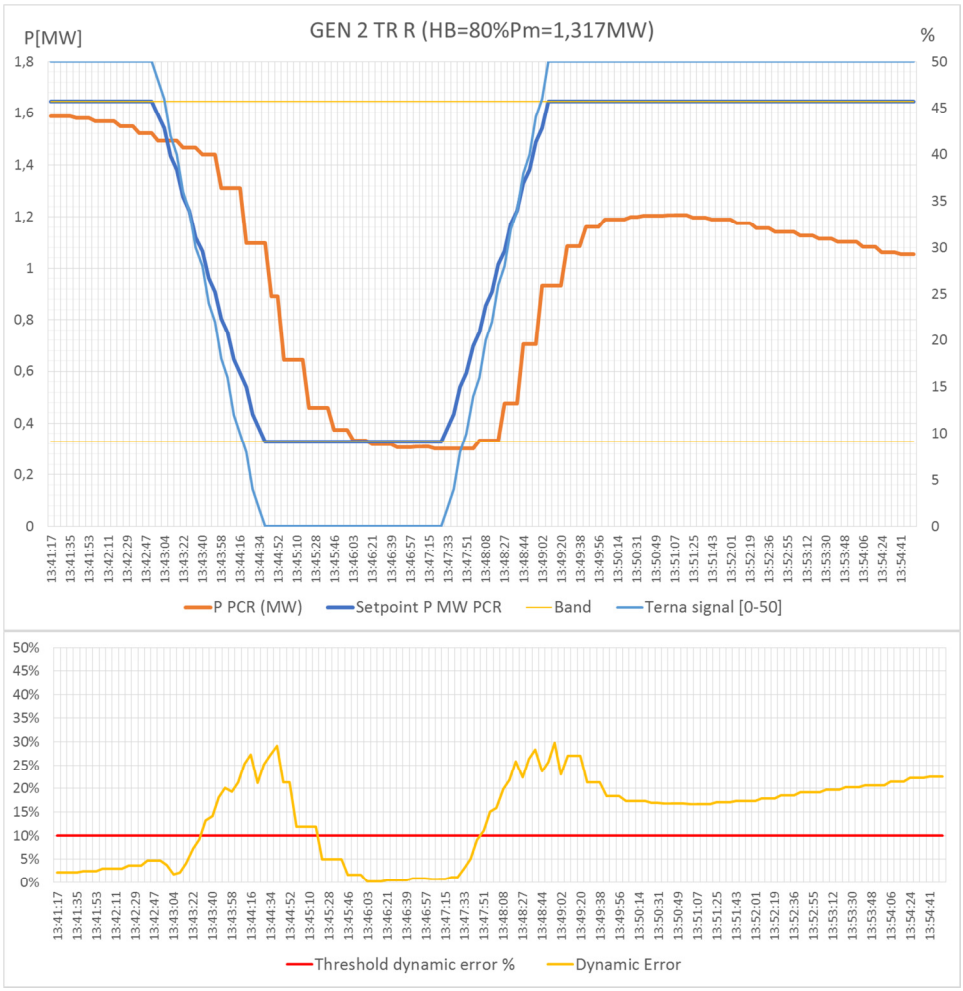

Figure 142: Performance of G2 connected at red transformer – Test 5 12/09/2018

Worse performances were achieved at the green transformer (Figure 143): the contribution at the transformer level (orange line) was not able to increase to return to the initial program value (blue line).

The most incisive factor is the lack of control of G5 during the ascending ramp, as showed in Figure 144.

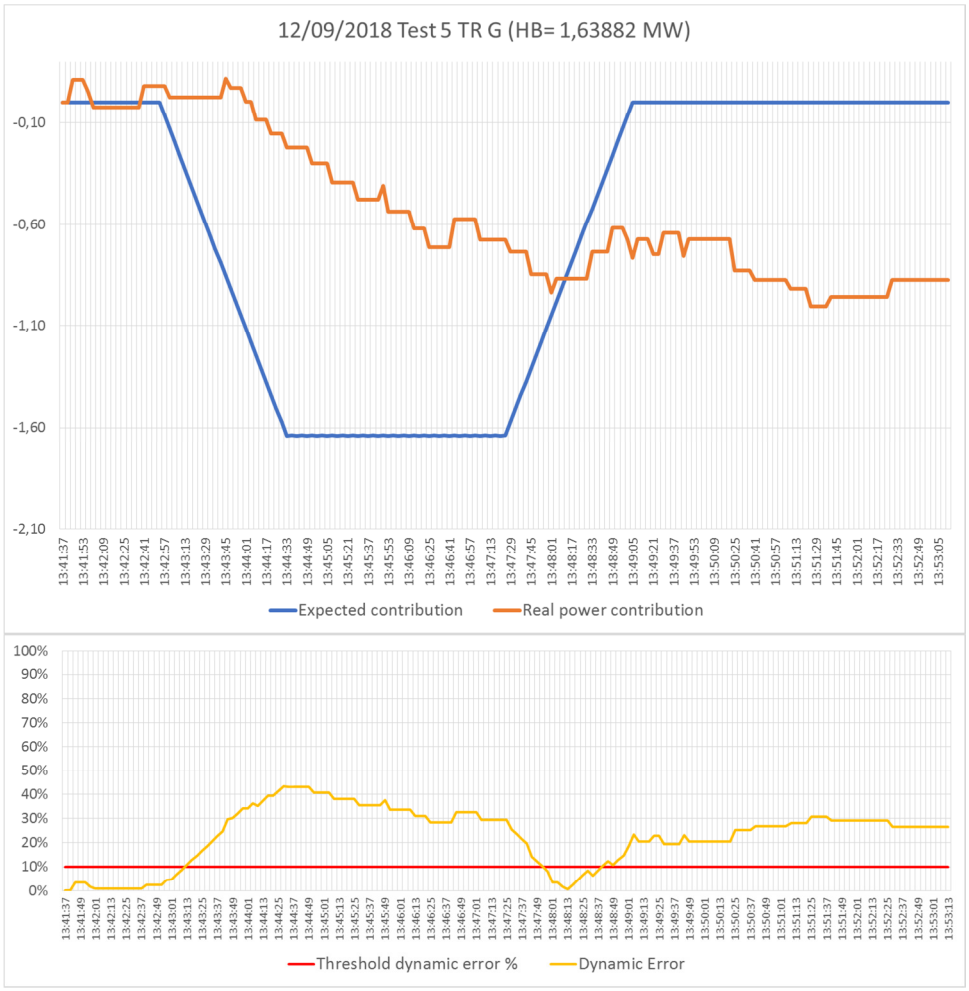

Figure 143: Analysis of the HV contribution at the green transformer – Test 5 12/09/2018

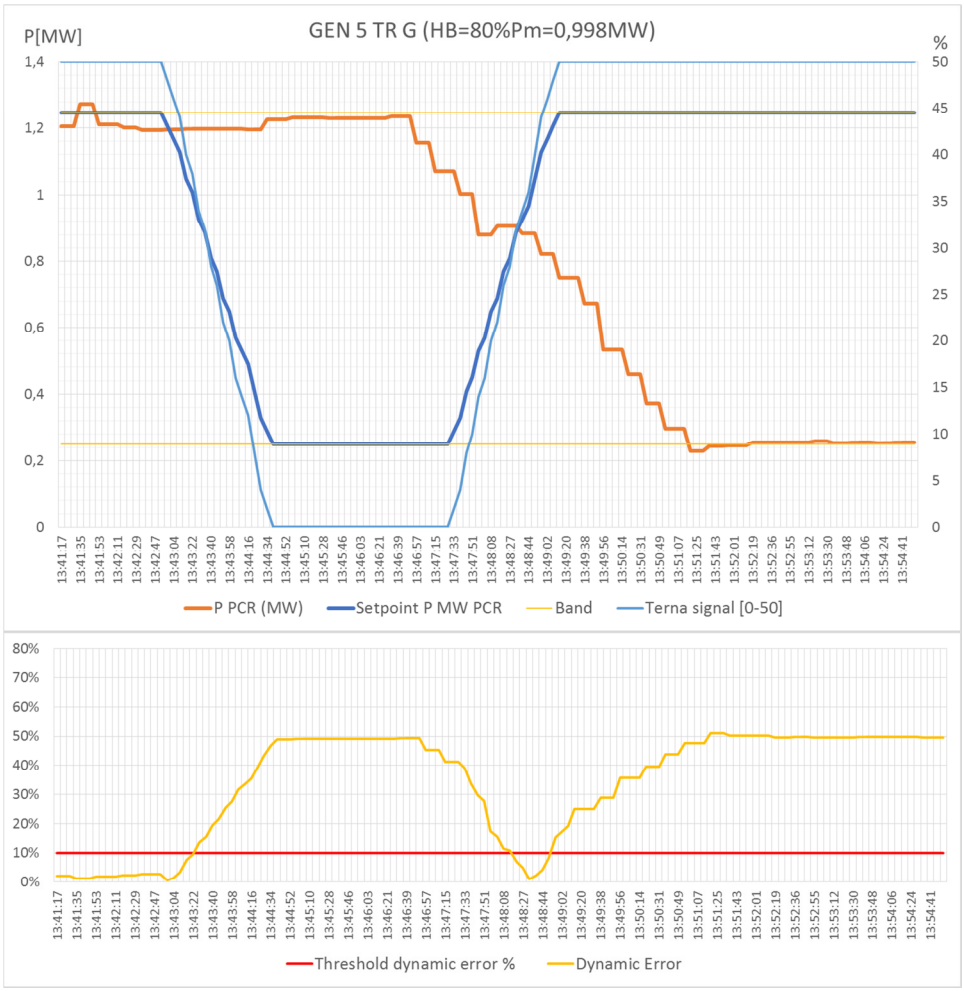

Figure 144: Performance of G5 connected at green transformer – Test 5 12/09/2018

On the other hand, the behavior of power plant G3 has completely different characteristics: the upward modulation has a delay that is reflected in a maximum error of 22 % of the expected contribution. This result is unexpected because it is not coherent with what was highlighted in previous tests, in which the local controller had never presented better performance in ramp-up than in ramp-down.

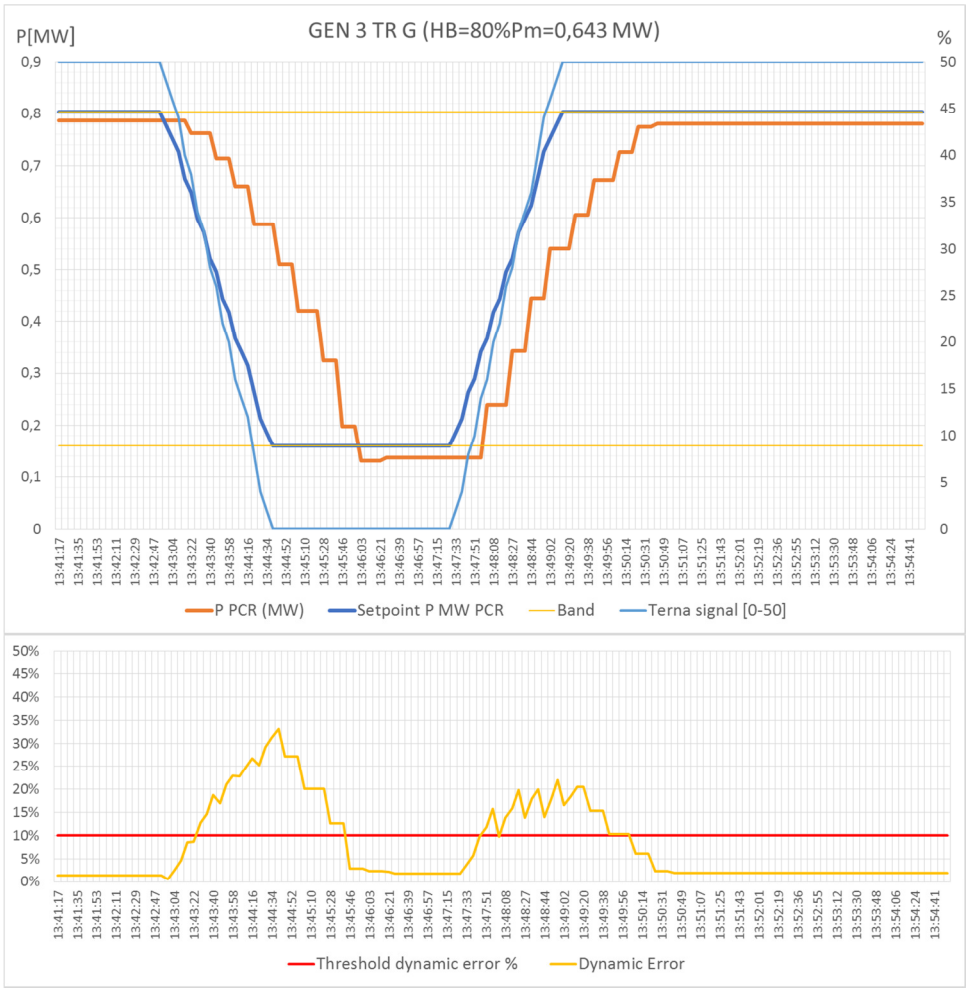

Figure 145: Performance of G3 connected at green transformer – Test 5 12/09/2018

6.4.2 Siemens f/P regulation

The first part of this paragraph presents some screenshots that show the real-time operation of Siemens MVRS during "open-loop" tests performed on the 23rd of October of 2018 through simulations. The focus of these tests was to verify all the steps described in paragraph 4.3.2, considering two MV plants and different test cases: TSO level varying from 50 %, 25 % and 0 %.

For example, Figure 146 shows the MVRS HMI where it is possible to see the active ("P GEN" in the figure) and reactive power ("Q GEN" in the figure) measurements acquired from one of the MV controllable plants.

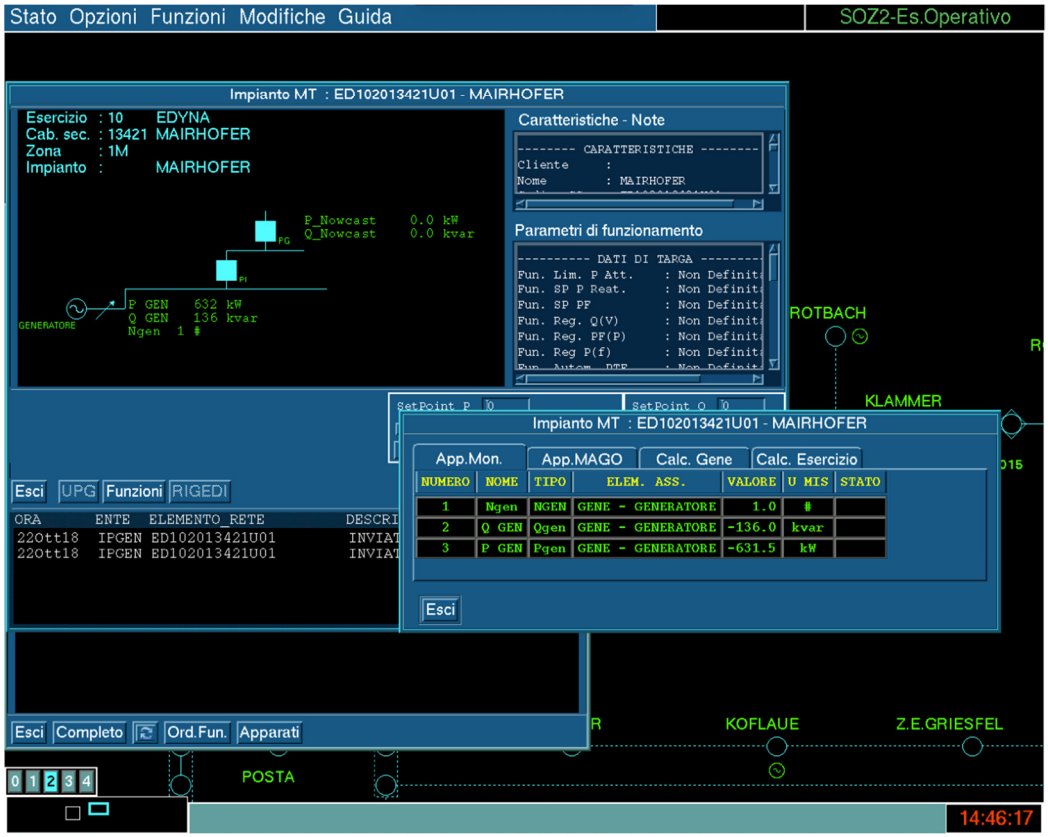

Figure 146: MV plant - power measurements and switch state acquisition

Figure 147 shows the data exchanged between the MVRS and the TSO: input "f/P regulation" setpoint ("SPP" in the figure), the overall reference power ("Punto Lavoro Tot" in the figure) and the overall step-down regulation band ("BRSC Tot" in the figure) calculated for the whole network.

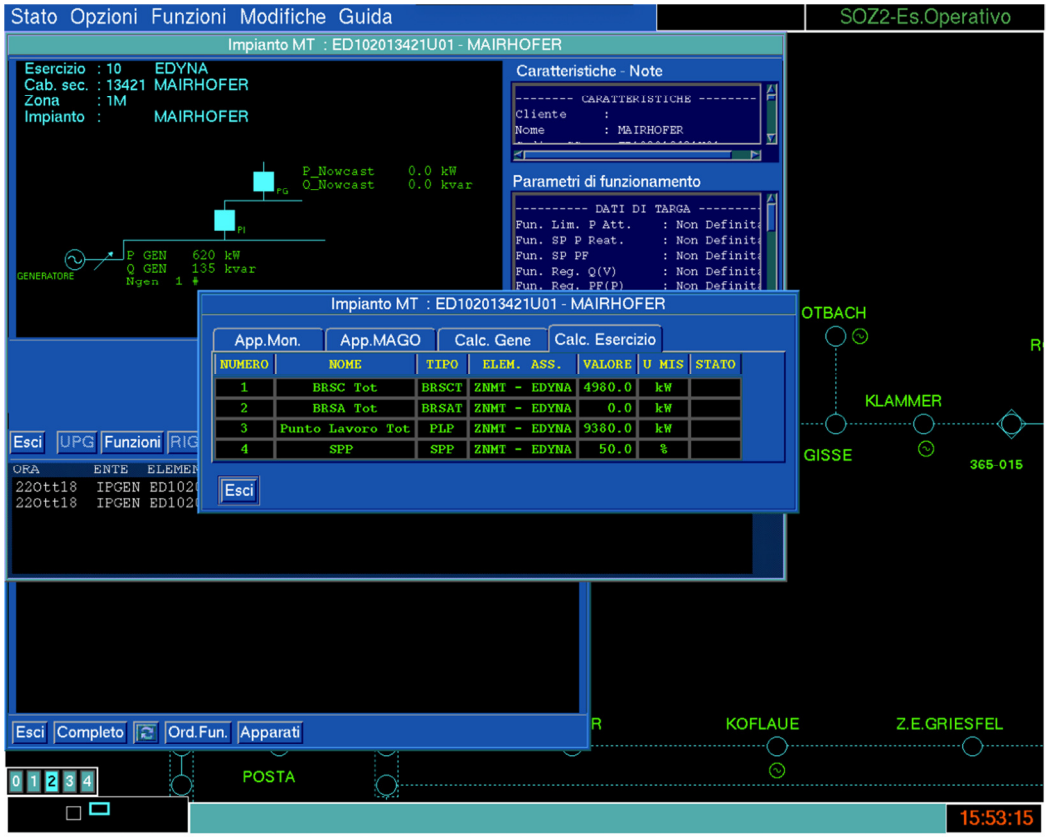

Figure 147: MV Network - Calculated regulation bands & simulated TSO setpoint (test 1)

On Figure 148, the section about the processing of the regulation bands for the single MV controllable plant is shown: reference power ("Punto di lavoro" in the figure) and step-down regulation band ("Banda a scendere" in the figure) can be found.

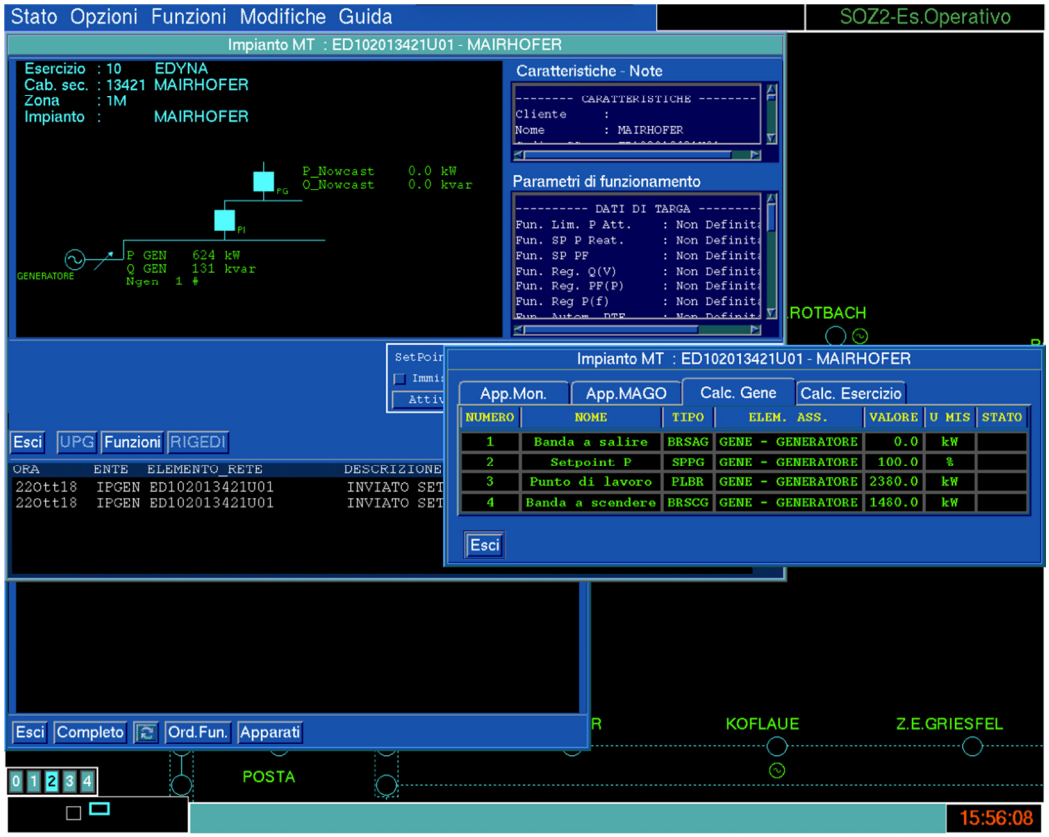

Figure 148: MV plant 1 - Calculated regulation bands & plant setpoint

The second part of this paragraph shows the real-time operation of Siemens MVRS during "closed-loop" tests performed on the 13th of March of 2019. According to the real-time hydro generators operating point, the different tests involved a variable number of MV plants (reaching a maximum of six); from the topological point of view, the bus coupler is open and the operational configuration is described in Table 7.

RED HV/MV TR	GEN 1
RED HV/MV TR	GEN 2
RED HV/MV TR	GEN 6
RED HV/MV TR	GEN 4
GREEN HV/MV TR	GEN 3
GREEN HV/MV TR	GEN 5

Table 7: Power plants involved in the tests and topology

During the f/P tests Terna sent a ramp setpoint of active power modulation as described in section 5.4. The objective was to evaluate the performance of the response of the DG involved in the regulation considering the contribution of each generator and at the interconnection point between DSO e TSO grids. With the approach proposed by Siemens the regulation provided by the DG is carried out considering the plants connected to both transformers as a unique VPP.

6.4.2.1 Test 1

During this test all the MV plants were involved in the regulation: 4 generators connected at the red transformer and 2 at the green one. The program reference value was calculated considering the production measured before each test and in this first application the minimum power value made available for the f/P regulation was configured considering the 80 % of the reference power (i.e. the half-band available for downward service is equal to the 20 % of its reference power for each power plant).

The total real power made available for the downward f/P regulation by DG is 460 kW and it correspond to the null setpoint sent by the TSO. Figure 149 shows the comparison between the expected contribution for the regulation (blue line) and the response of the network (orange line) up to a constant offset that has to be considered to take into account that the available active power measurement is not only related to the units in regulation but to all the equivalent non-solar production connected at the transformer. In the lower part of the figure, the related dynamic error is shown compared with the maximum error accepted for the aFRR service (10 % of the band). In both figures it is possible to see how the biggest errors (30 %) were obtained during the step-down regulation corresponding to reduction of the power and generally, with a lower peak but for a longer period, during the whole phase of restoring of the reference power of the MV plants.

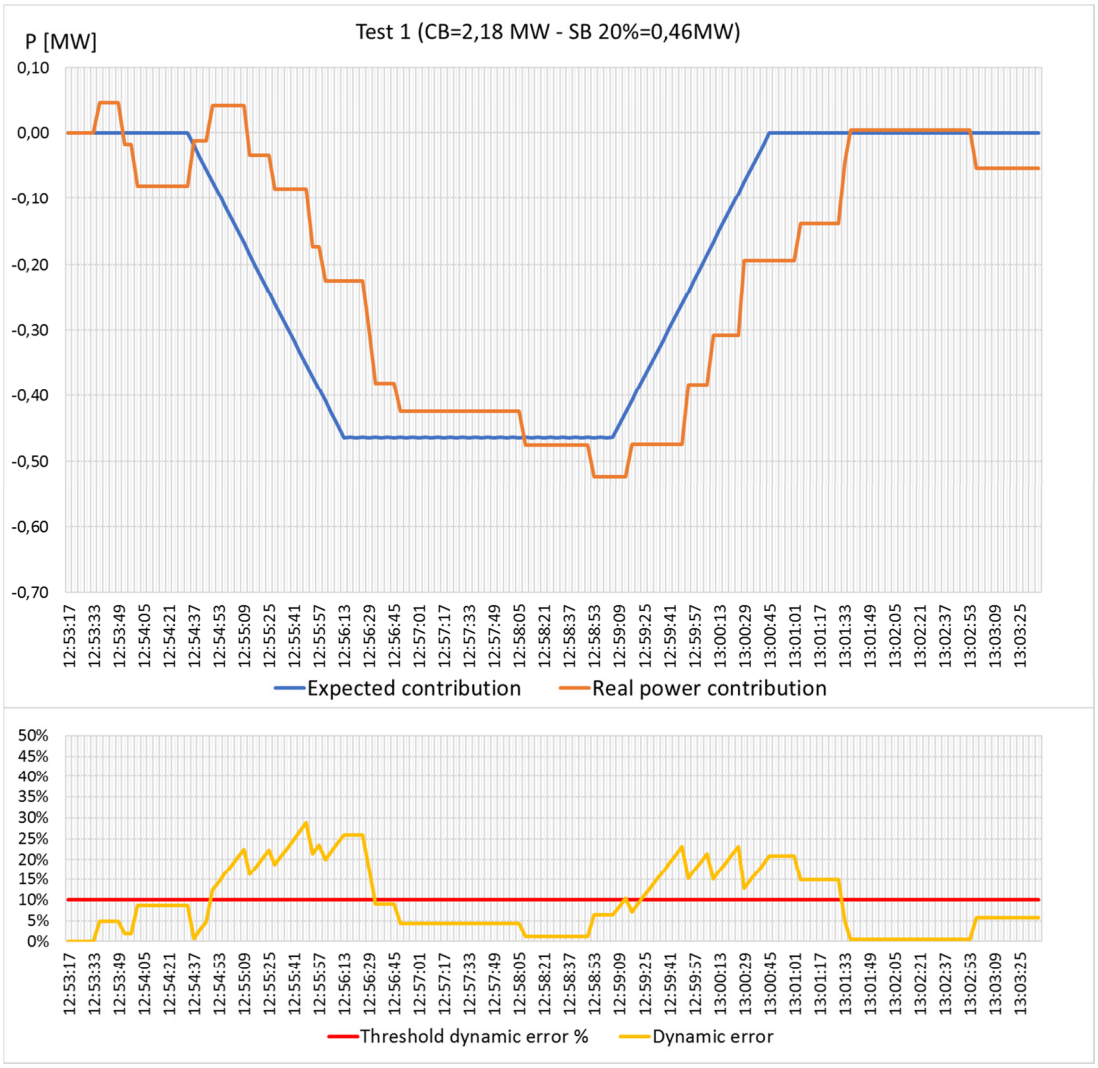

Figure 149: Analysis of the HV contribution of the VPP - Test 1 13/03/2019

The following figures show the data recorded at the power plants terminals to analyze the response of each MV power plant: in detail, the yellow lines represent the available regulation band (the upper value is the reference power considered as the program value in the service and the lower limit is the minimum power declared available for the f/P regulation), the light blue line is the level (between 0 and 50 %) received from the TSO, the blue line is the setpoint calculated by MVRS for the single power plant and the orange line is the real power response of the plant expressed by the active power measurement at the terminals of the power plant.

Figure 150 shows the response of G1 connected at the red transformer and the trends highlight that the setpoint calculated by MVRS (blue line) appears lower than the minimum value declared power (lower limit of the band represented in yellow): this difference is connected to the quite complex architecture and to the data flow that allows the transmission of only integer values. The setpoint value is transmitted as a percentage of the nominal power that is very big for this plant (about 9.3 MW) so a little

approximation on the integer value in percentage appears as a quite significant difference on the absolute values of active power (about 70 kW) but actually it is only because the calculated value is compared with a very low band and measurement (during the session test the hydro production was actually quite low). Moreover, the real contribution (orange line) shows an even lower trend in graph and reaches a minimum value of 380 kW instead of 534 kW of the half-band and 465 kW of the setpoint calculated for G1.

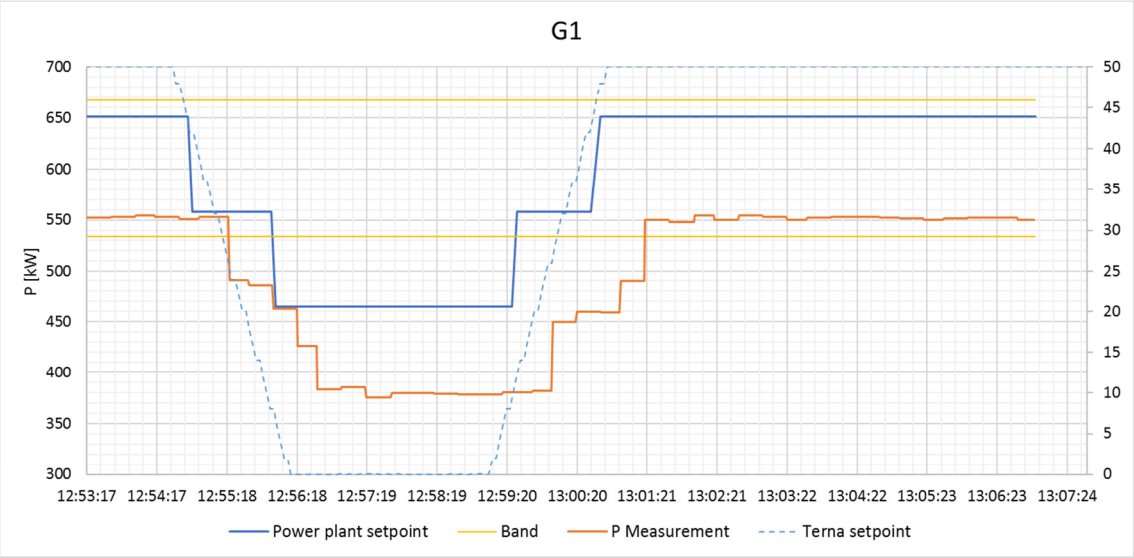

Figure 150: Performance of G1 connected at red transformer - Test 1 13/03/2019

In Figure 151 it is possible to see that, during the regime phase before and after the ramp regulation, there is an apparent significant fluctuation of the setpoint sent by the MVRS between two values; the explanation for this trend is that the input used for the calculation is received through a long communication chain composed by different systems that introduce noise, approximations and delays in the data flow.

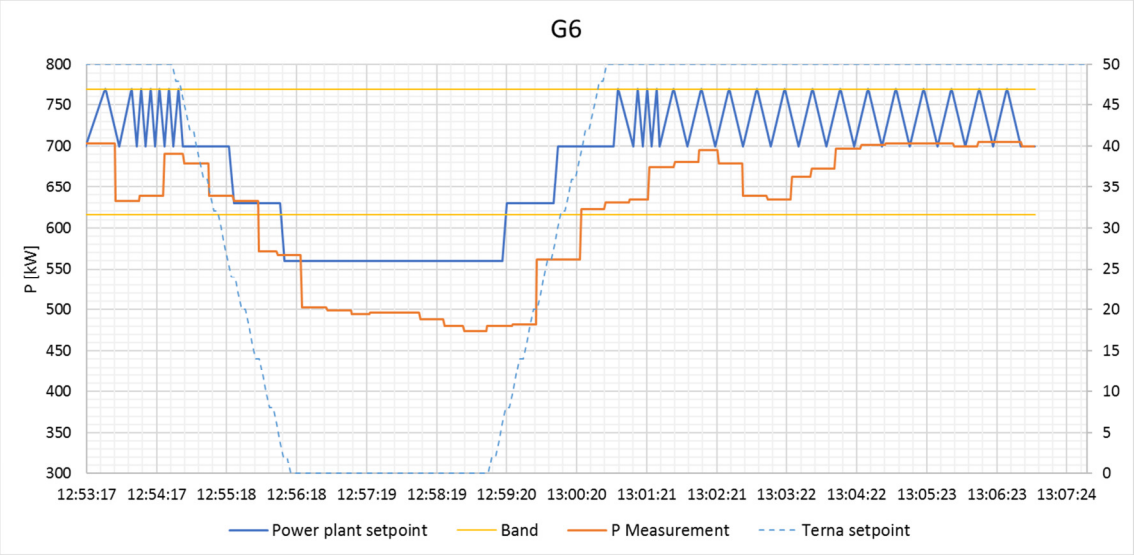

Figure 151: Performance of G6 connected at red transformer - Test 1 13/03/2019

Figure 152 regards the performance of G4 and shows that in this case the difference between the minimum setpoint received by MVRS and the minimum active power level declared available (lower limit of the yellow band) is less than the previous examples because the magnitude of the nominal power of the plant (360 kW) is comparable with the production measurement and with the half-band. The real contribution (orange line) is however lower than the request sent by the MVRS.

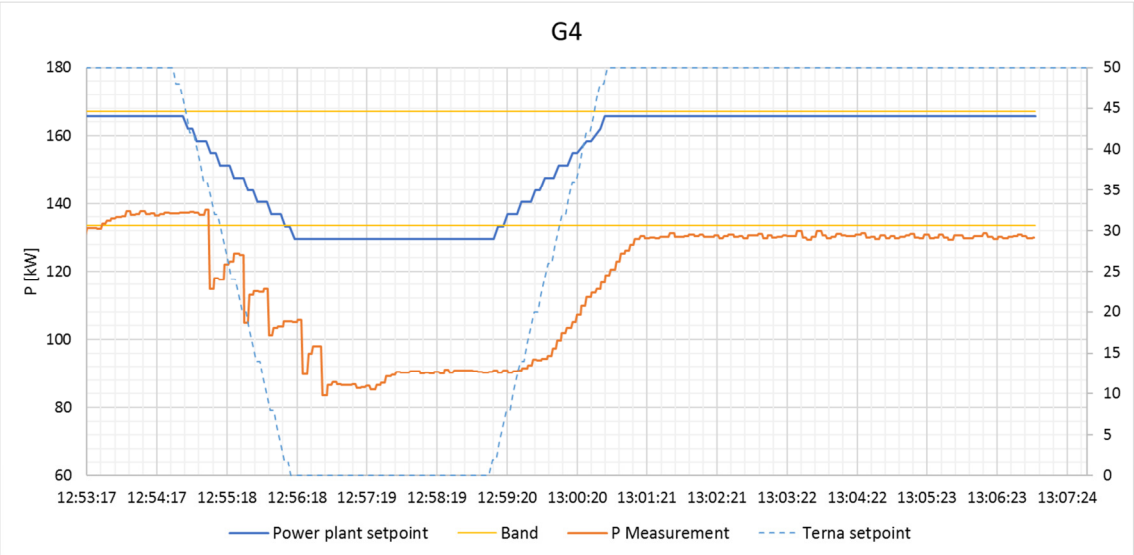

Figure 152: Performance of G4 connected at red transformer - Test 1 13/03/2019

A peculiar behavior was recorded at the terminals of Generator 2 (Figure 153) which decreased the active power until the complete switch-off probably due to the technical minimum of the power plant while Generator 5 (Figure 154) and Generator 3 (Figure 155) did not follow the setpoint sent by the

MVRS at all; the behavior of G3 and G5 can be connected to specific technical limits of the local control logics.

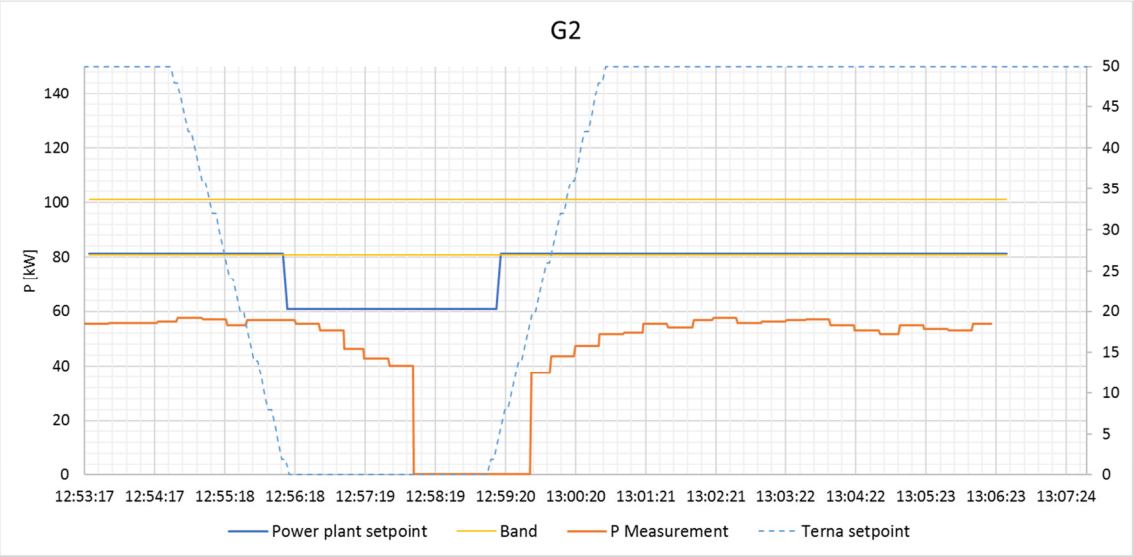

Figure 153: Performance of G2 connected at red transformer – Test 1 13/03/2019

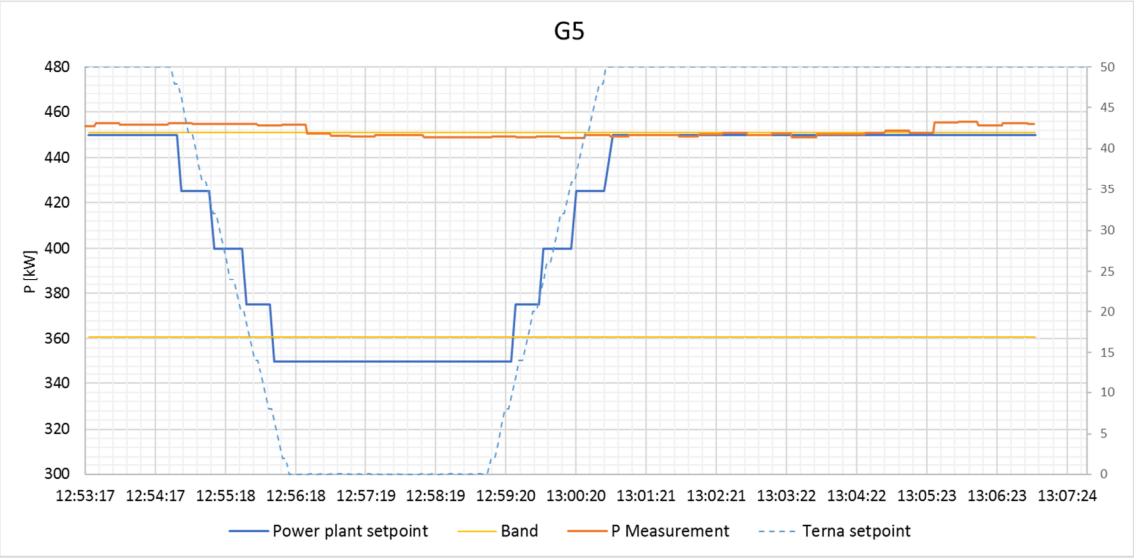

Figure 154: Performance of G5 connected at green transformer – Test 1 13/03/2019

Figure 155: Performance of G3 connected at green transformer – Test 1 13/03/2019

As explained above, the reference power and the minimum available power of the MV power plants were configured on the MVRS before the test considering the current operation points; since these values are not acquired dynamically in real time from the field, test graphs show an offset error between the setpoint trend and the real measurement due to changes in the operating state, such as hydro availability, which no longer allow the level of production declared at the beginning of the test; the non-programmability of production makes the planned contribution unreliable.

Because this offset is quite constant because it depends mainly on the variability of the production during the MVRS configuration phase that is less variable during the 10-minutes test, the following figures consider a constant shift of the active power measurement to evaluate the dynamic response of each generator. Figure 156 and Figure 157 show the dynamic response respectively of Generator 1 and Generator 6: both the figures shows delay in the response (about 1 minute for G1 and a delay of the order of tens of seconds for G6). G1 followed the setpoint trend quite well in the constant phase after the ramp-up. In the regime phase instead G6 production measurement shows little oscillations due to the fluctuation of the setpoint that does not allow a stable operating as explained above.

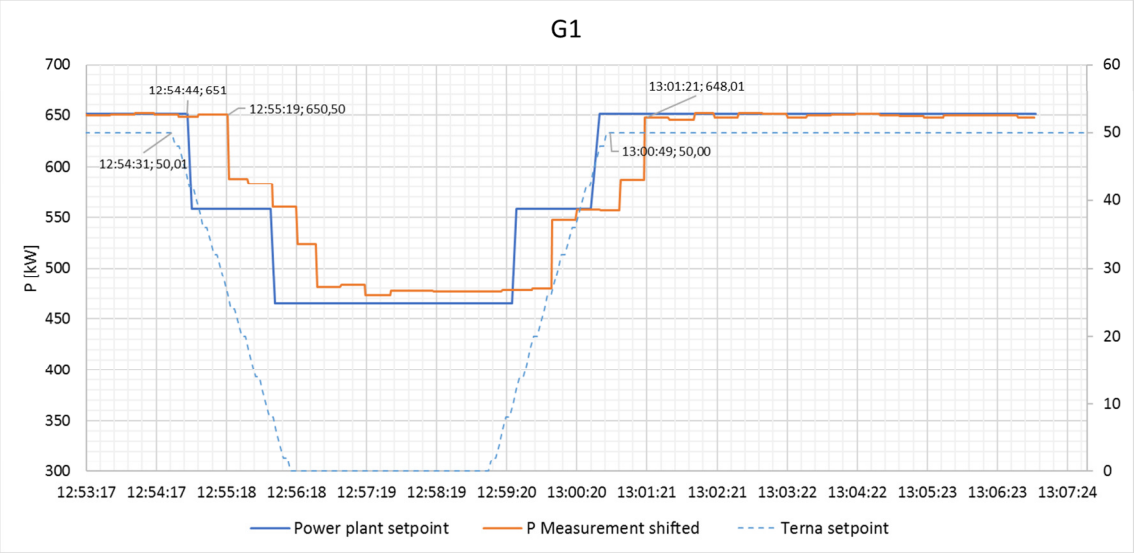

Figure 156: Trend of G1 contribution shifted to evaluate the dynamic response - Test 1 13/03/2019

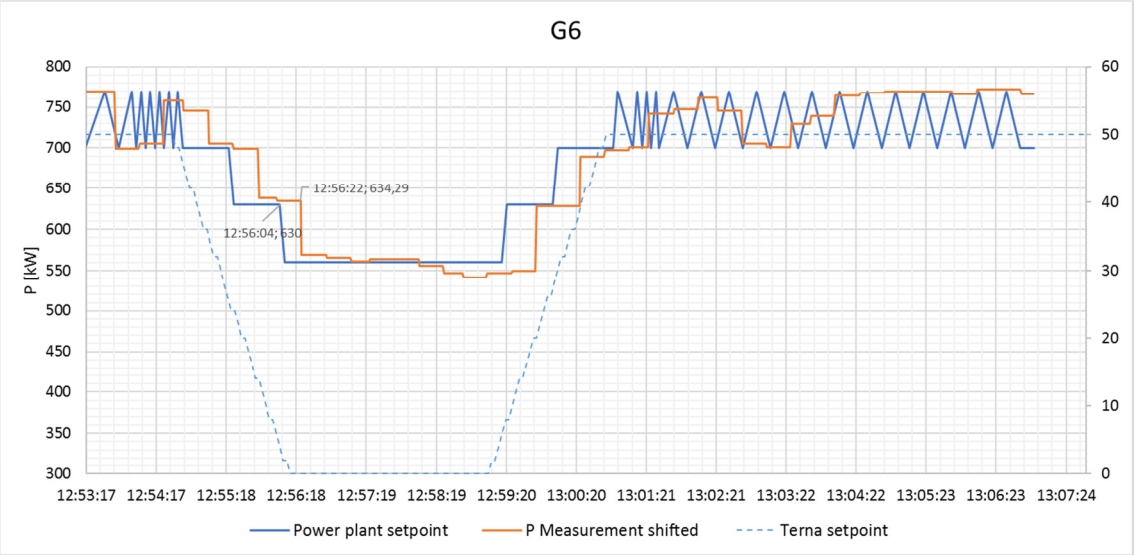

Figure 157: Trend of G6 contribution shifted to evaluate the dynamic response - Test 1 13/03/2019

As shown in (Figure 158), Generator 4 response shows a delay of about thirty seconds and a peculiar trend of the production during the ramp-down, which shows important oscillations having a similar shape while the operation during the ramp-up and the regime phase is more smooth. The sampling of the recorded measurement is more frequent and acceptable than in the previous graphs, where the variations were represented by high and long steps.

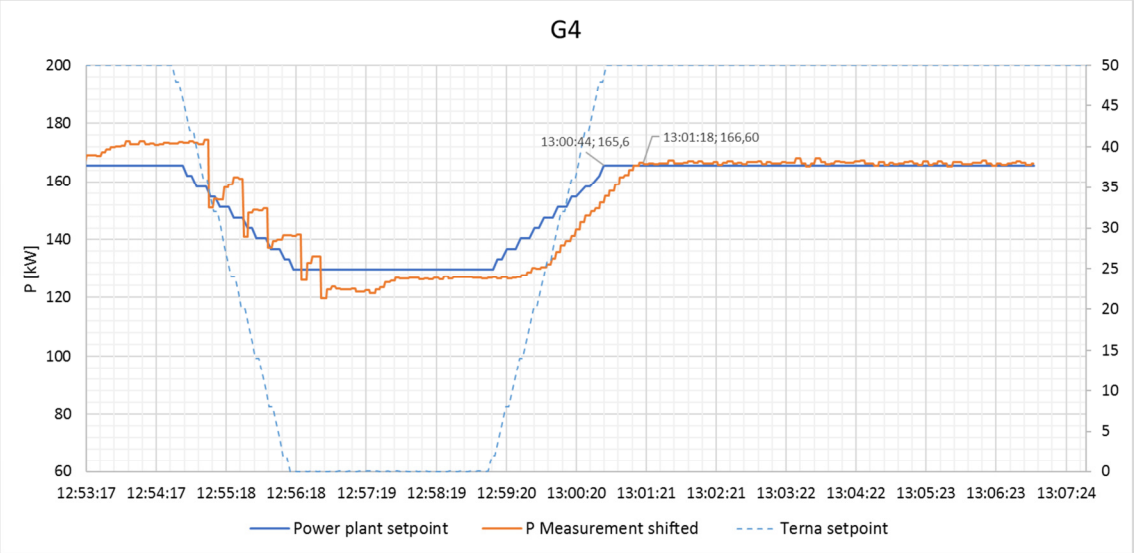

Figure 158: Trend of G4 contribution shifted to evaluate the dynamic response - Test 1 13/03/2019

As previously introduced, the measurements of the active power of the regulating aggregation alone are not available; to analyze the global response of the six power plants, Figure 159 reports the comparison between the sum of the power plants active powers (orange line) and the sum of the setpoints calculated by the MVRS for each of the six power plants (blue line). In face of a declared half-band of 464 kW transmitted to Terna, the MVRS requires the aggregation to reduce the production of 575 kW and the calculated (not measured) resulting reduction of the production is 575 kW.

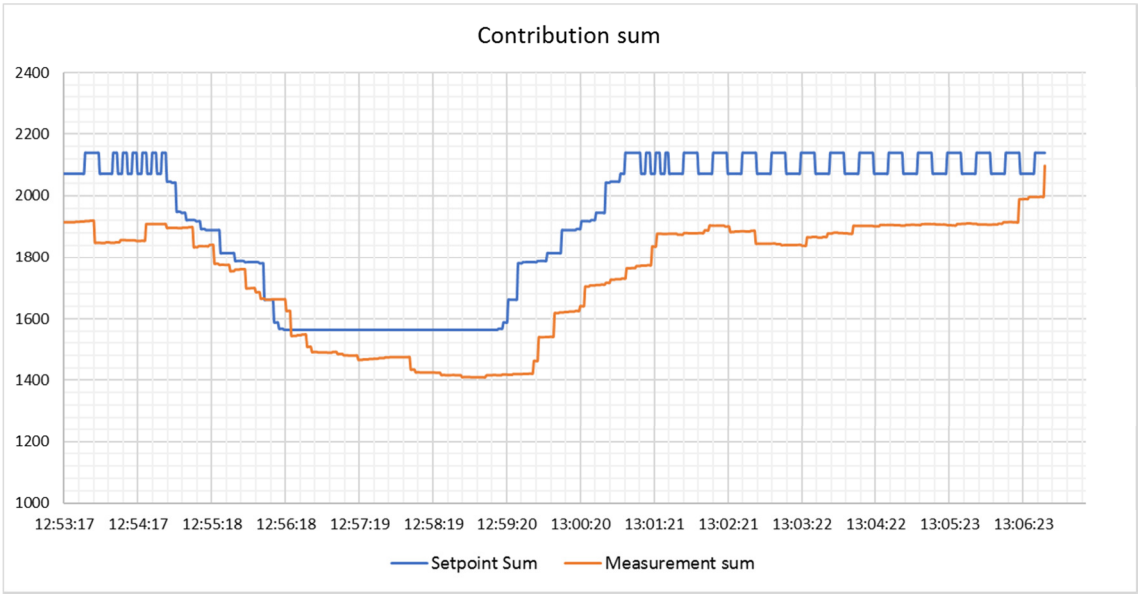

Figure 159: Calculated response of the aggregation with respect to the sum of the setpoints – Test 1

6.4.2.2 Test 2

During this test four MV power plants were involved in the regulation: generator 2 and 3 were deactivated due to the response provided in the previous test. The minimum active power available for the f/P regulation was maintained at the 80 % of the reference power for each generator and then the declared half-band was equal to the 20 % of the reference power.

The total real power made available for downward regulation controlled by the TSO became 420 kW, reduced value compared to the previous test due to the participation of less power plants. Figure 160 shows the comparison between the expected contribution calculated from the declared center-band and half-band values and the real behavior of the network and, at the bottom of the figure, the related dynamic error. The trends highlight most significant errors of up to 40 % during the ramp-up phase of the test where the MV plants were brought back to the reference power. Comparing these results with those obtained in the previous test, it is observed that the performance detected at the transformer level does not have a good correlation with the performance of each power plant because the error increased even though two power plants with anomalous performances that led to an incontrollable shutdown and therefore to the production zeroing have been excluded from the regulation.

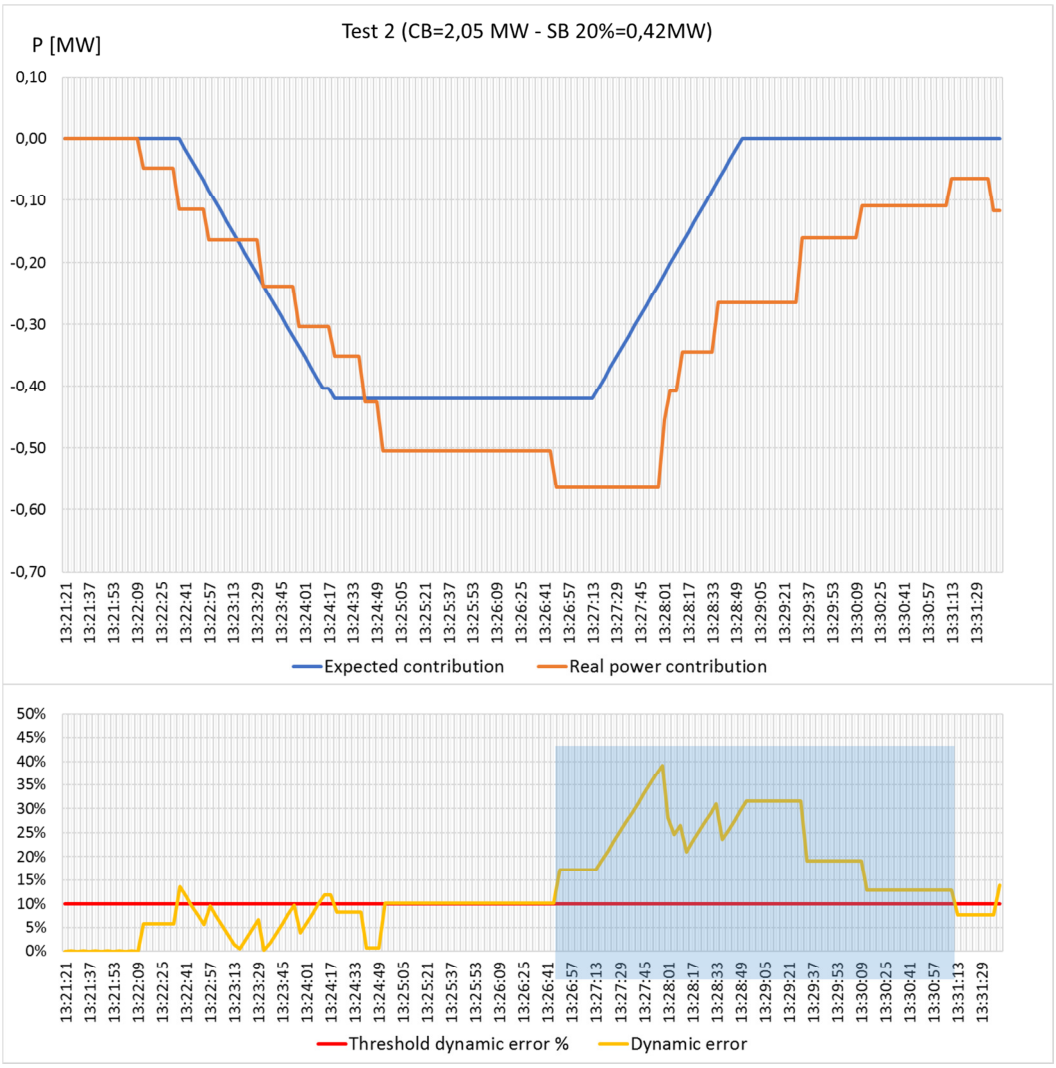

Figure 160: Analysis of the HV contribution of the VPP - Test 2 13/03/2019

The next graphs (Figure 161 to Figure 167) show the data recorded for the single MV plants to investigate the behavior of each regulating element. The responses of the Generator 1 (Figure 161 and Figure 162) and Generator 6 (Figure 163 and Figure 164) have similar trends of previous test and it means that the response depends on the performance of the governor of the power plant.

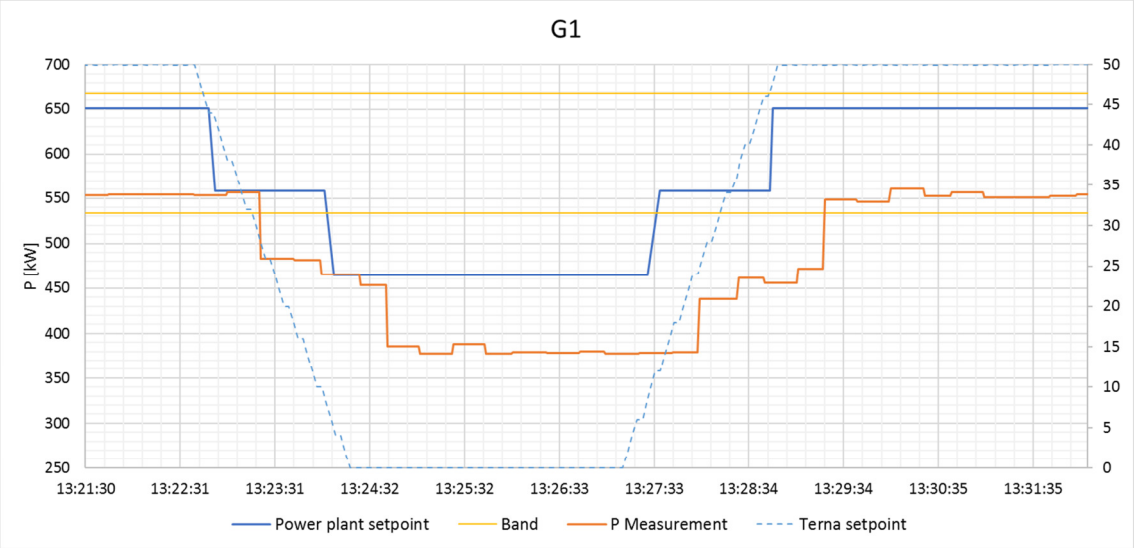

Figure 161: Performance of G1 connected at red transformer - Test 2 13/03/2019

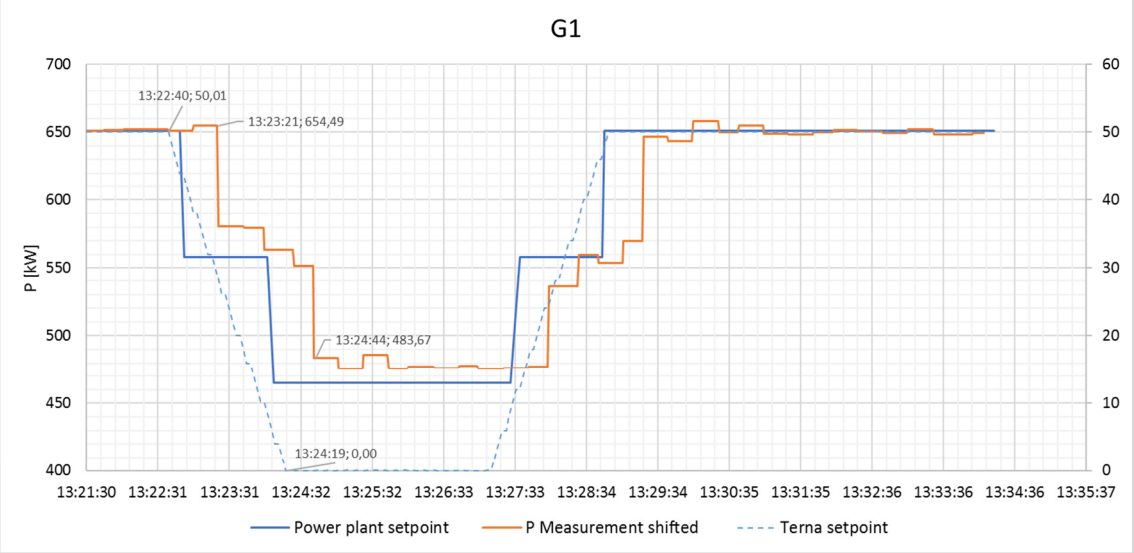

Figure 162: Trend of G1 contribution shifted to evaluate the dynamic response - Test 2 13/03/2019

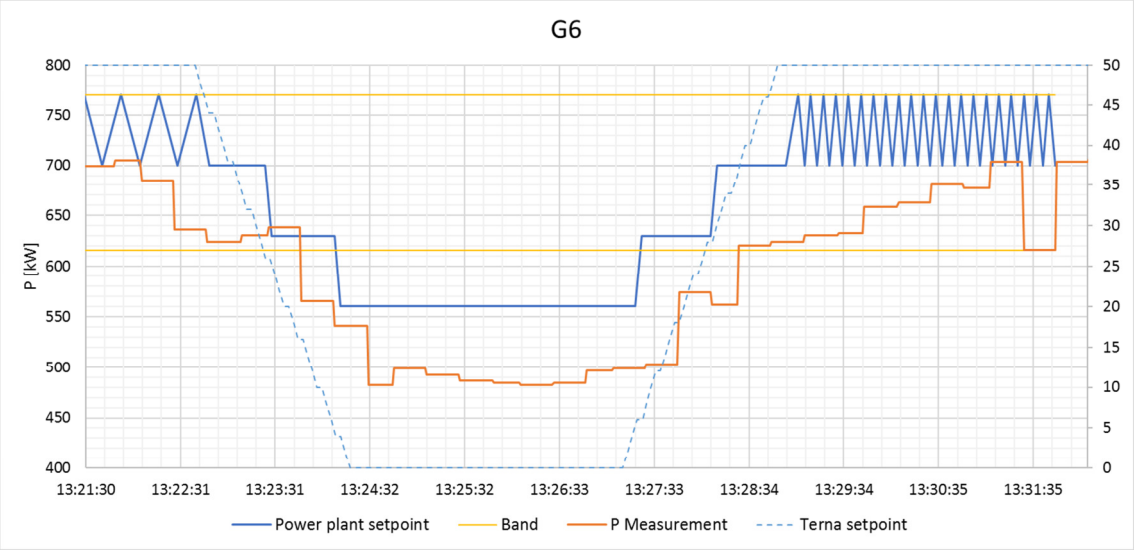

Figure 163: Performance of G6 connected at red transformer - Test 2 13/03/2019

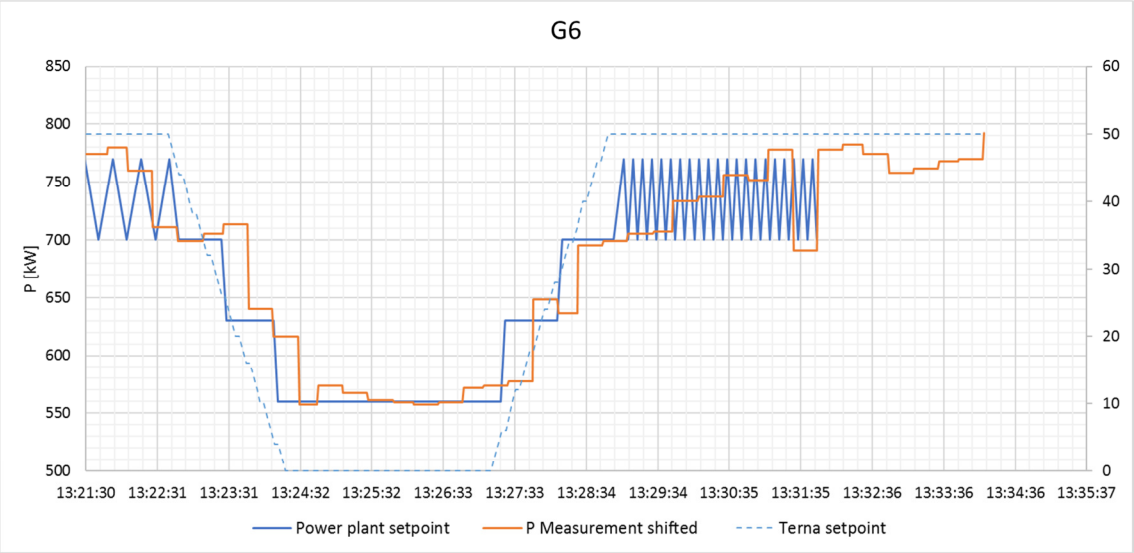

Figure 164: Trend of G6 contribution shifted to evaluate the dynamic response - Test 2 13/03/2019

As shown in Figure 165 and Figure 166, also Generator 4 followed the level calculated sent by the MVRS with a trend similar to the previous test; in particular it follows quite well the setpoint when it is constant at 0 or 50 % and during the ramp-up, while it shows an irregular dynamic response in the step-down phase, that can be explained by technical limits of the dynamic operation of the generator or technical difficulties of the local control logics.

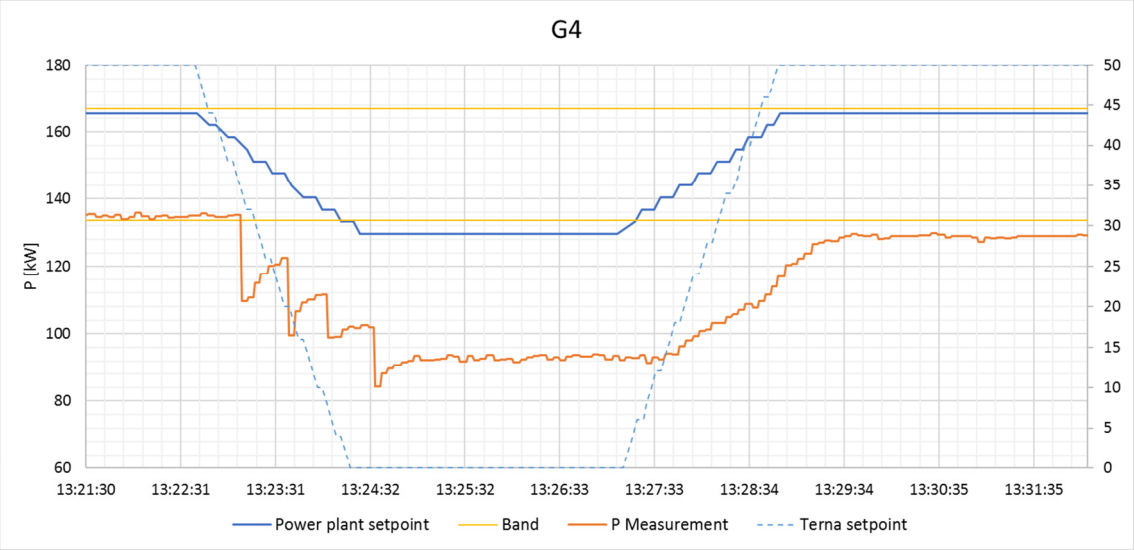

Figure 165: Performance of G4 connected at red transformer - Test 2 13/03/2019

Another factor that affect the quality of the service that is highlighted in particular in Figure 166 in the final regulation phase is that the power plant is not able to return to the initial reference value: this aspect is strictly connected to the non-programmability of the primary energy resource of the hydro power plants, that, generally, cannot guarantee the productivity forecast and then a complete control of the plant real power, especially for the restoration of the initial power.

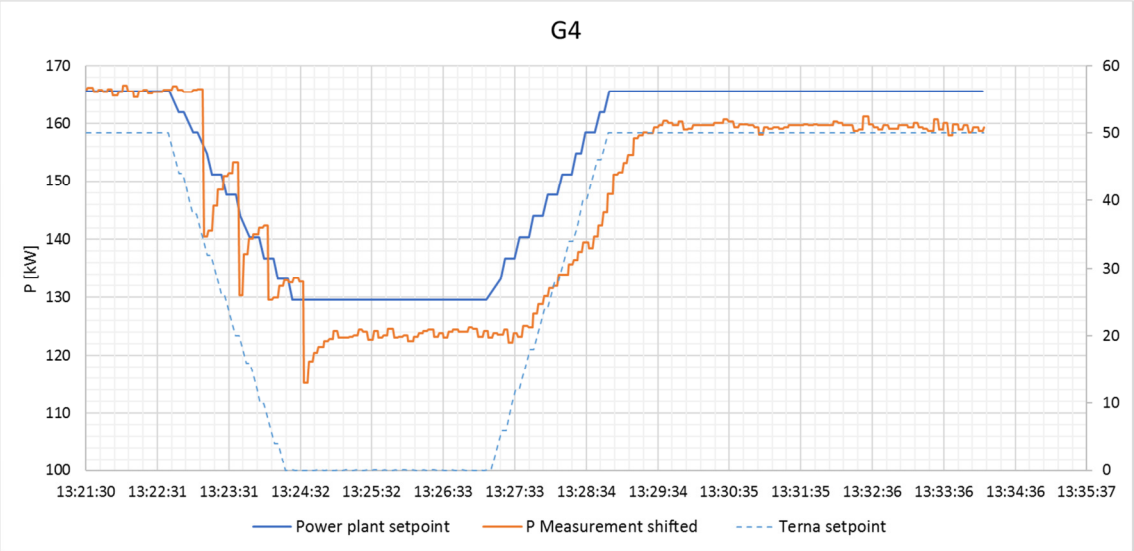

Figure 166: Trend of G4 contribution shifted to evaluate the dynamic response - Test 2 13/03/2019

Generator 5 (Figure 167) did not follow the setpoint sent by the MVRS even in this test and it maintained an almost constant production.

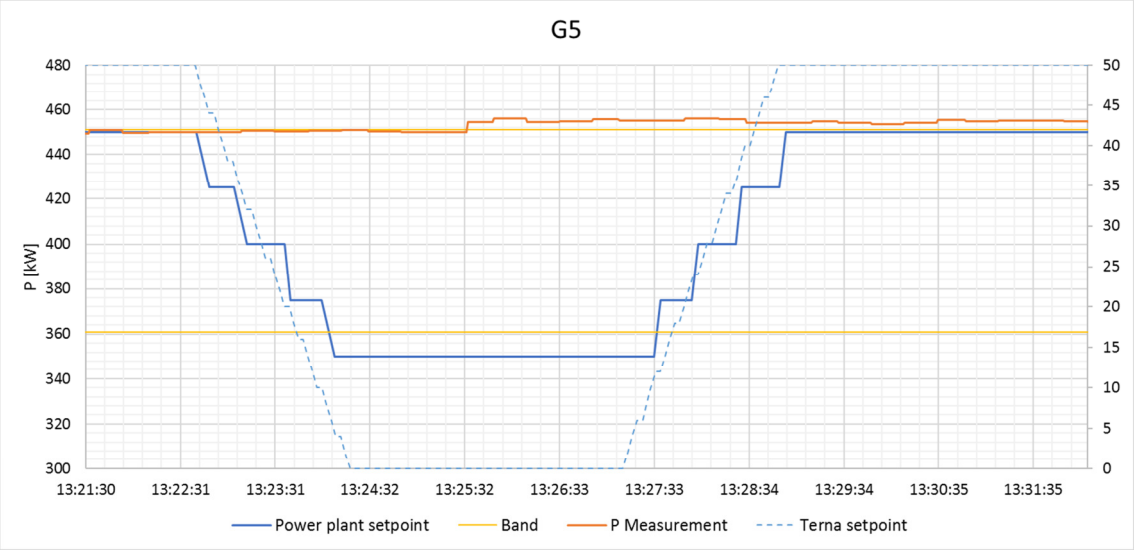

Figure 167: Performance of G5 connected at green transformer - Test 2 13/03/2019

In conclusion, Figure 168 shows the comparison between the sum of the single setpoints calculated by the MVRS and the sum of the production of the power plants involved in the regulation; the calculated production has been reduced from 1838 kW to 1411 kW with a variation of 427 kW. The half-band declared to Terna was 720 kW while the sum of the requirements calculated by MVRS for the regulating power plant was 532 kW: the real response complies the amount required but Generator 5 did not participate in the regulation and the other power plants reduced their production more than had been foreseen by MVRS.

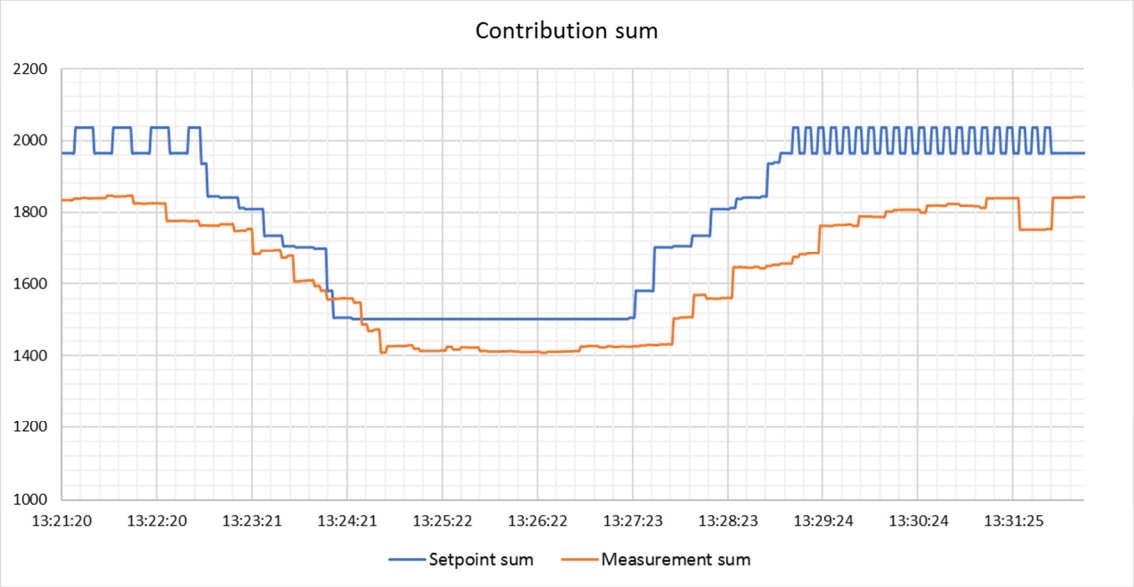

Figure 168: Calculated response of the aggregation with respect to the sum of the setpoints – Test 2

6.4.2.3 Test 3

The next test involved 3 MV plants connected on the red HV/MV transformer: generator 1, generator 6 and generator 4. The minimum power value declared available from each power plants for the f/P regulation was configured considering the 60 % of the reference power of the power plant itself, i.e. the step-down regulation band transmitted to Terna is 40 % of the reference power. The total half-band declared for the VPP was 550 kW. The comparison between the expected contribution corresponding to the half-band declared and the real response of the aggregation and the dynamic error calculated as percentage error during the ramp are represented in Figure 169. The data considered are the active power measurement of the non-solar aggregation. On one hand, the production started to diminish before the start of the signal ramp-down and this is due to an unforeseen program of the RES. On the other hand, the performance at the interconnection point during ramp-up led to an error of 60 % because the MV plants were not able to go back to the reference power.

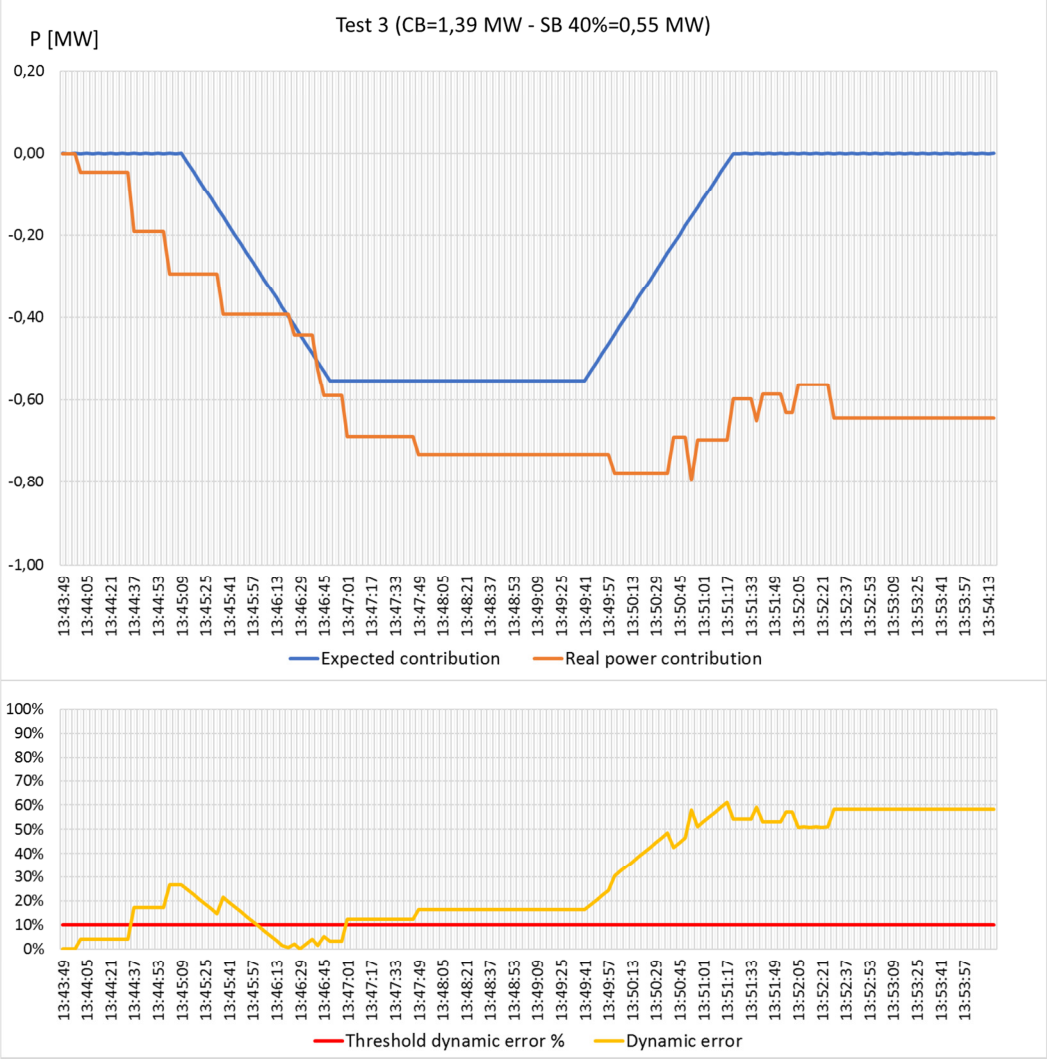

Figure 169: Analysis of the HV contribution of the VPP - Test 3 13/03/2019

In order to analyze the behavior of each MV plant, in the following figures the graphs obtained from data acquired from PCR at the terminals of power plants in regulation are reported. The results are in line with the outcomes of the previous tests and this indicates that the response of the power plants is completely linked to the characteristics of each plant and changes in the VPP configuration and in the bands made available for regulation do not affect the trend of the shape of the plant response.

In particular, generator 1 (Figure 170) and generator 6 (Figure 171) show clearly how the final power that could be restored is different from the initial power reference. Comparing the trends obtained in the three tests (Figure 156, Figure 161 and Figure 170), G1's response has the same shape: the orange lines that represent the active power measurements is always below the calculated setpoint of about 100kW and a delay of just over 30 seconds. G6 shows in all three tests that it follows the ramp quite well, even if in this case it cannot return to the initial production value even after more than 6 minutes from the end of the ramp to climb.

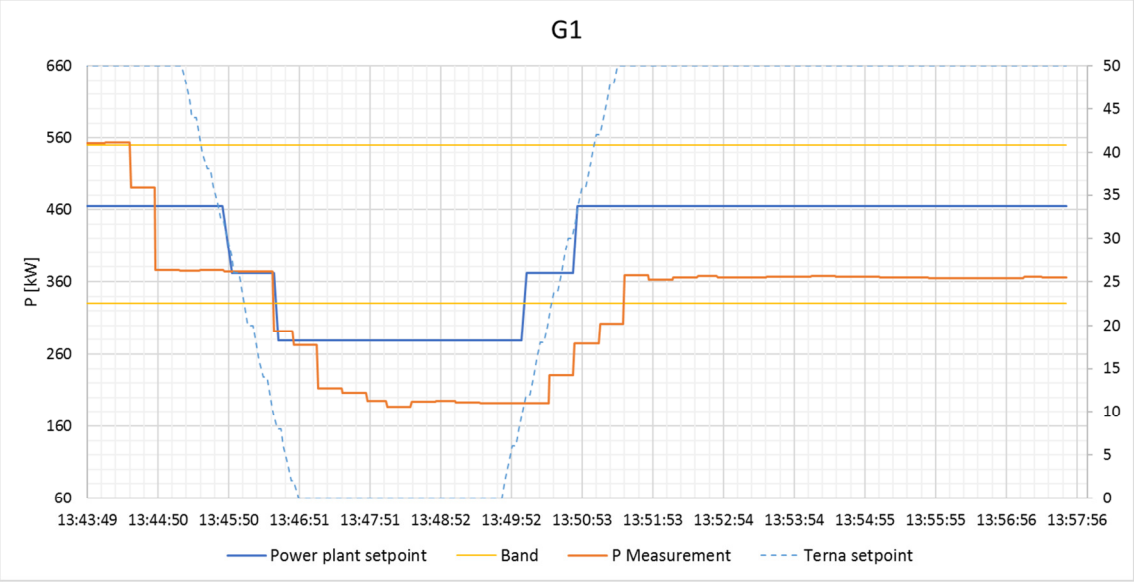

Figure 170: Performance of G1 connected at red transformer - Test 3 13/03/2019

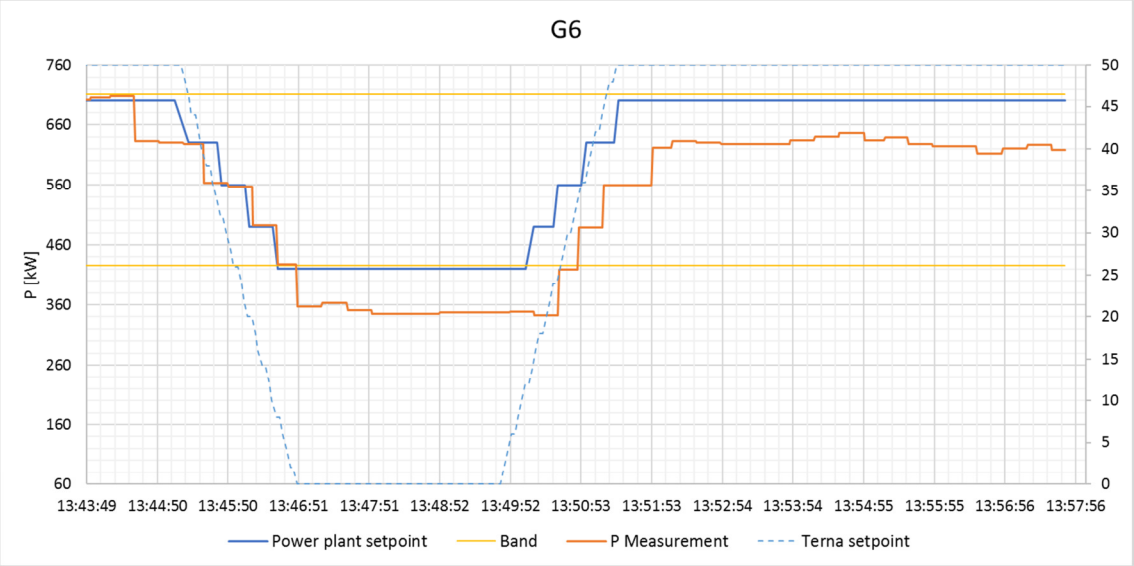

Figure 171: Performance of G6 connected at red transformer - Test 3 13/03/2019

Generator 4 (Figure 172) showed the same oscillating trend during the downward ramp, while did not follow at all the setpoint to move back to the reference power.

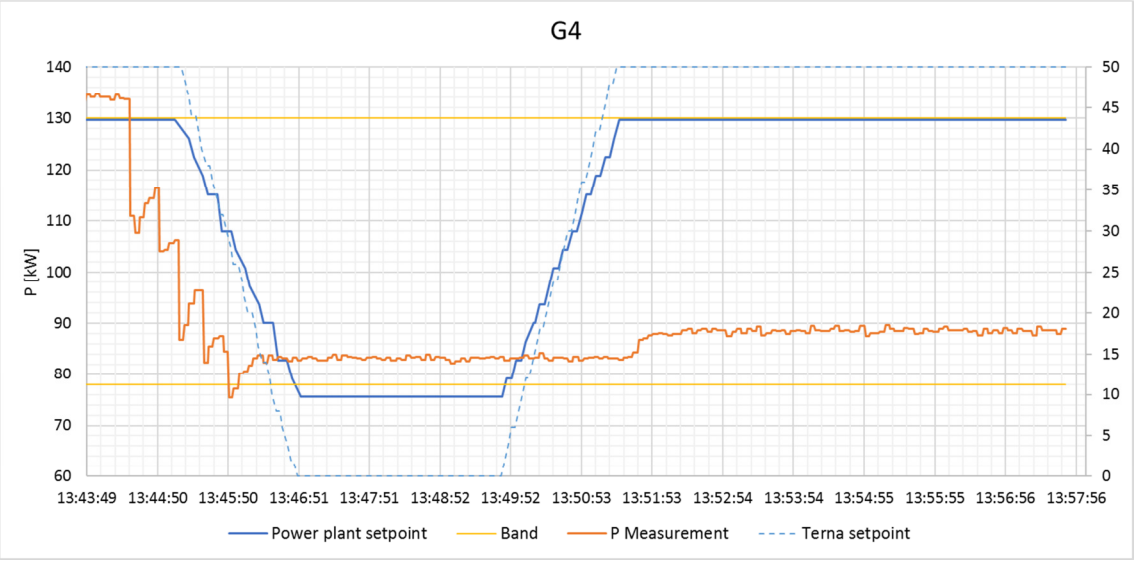

Figure 172: Performance of G4 connected at red transformer - Test 3 13/03/2019

In Figure 173 is represented the comparison between the sum of the single setpoints calculated by the MVRS and the sum of the active power of the only power plants involved in the test: the declared available half band was 550 kW and the MVRS distributed a total reduction command of 520kW (blue line) while the VPP production decreased from 1395 kW to 614 kW during the ramp-down (ΔP=771 kW) but it reached only 1082 kW at the end of the ramp-up because none of the power plants was able to return at the program value.

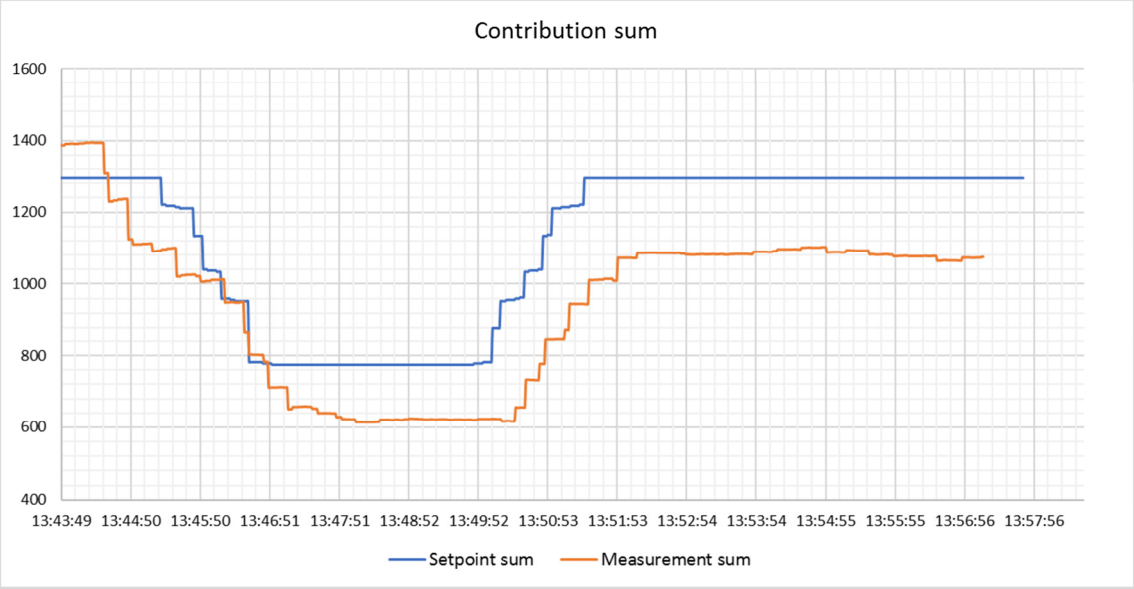

Figure 173: Calculated response of the aggregation with respect to the sum of the setpoints – Test 3

6.4.2.4 Test 4

The last test carried out involved four MV plants connected on the red HV/MV transformer: the four generators (G1, G6, G4 and G2) made available the 60 % of the last active power measurement for a total real power step-down regulation available for TSO service equal to 1900 kW. The trend of the real contribution of the aggregation (orange line) is compared with the ramp of the required contribution (blue line) in Figure 174. The dynamic error calculated shows high inaccuracy during the whole test: during the ramp-down the error seems to depend mainly on the delay in the response (33 %) while during the ramp-up MV plants do not seem to follow the trend of the expected contribution and when fully operational the aggregation has not reached the value of the program.

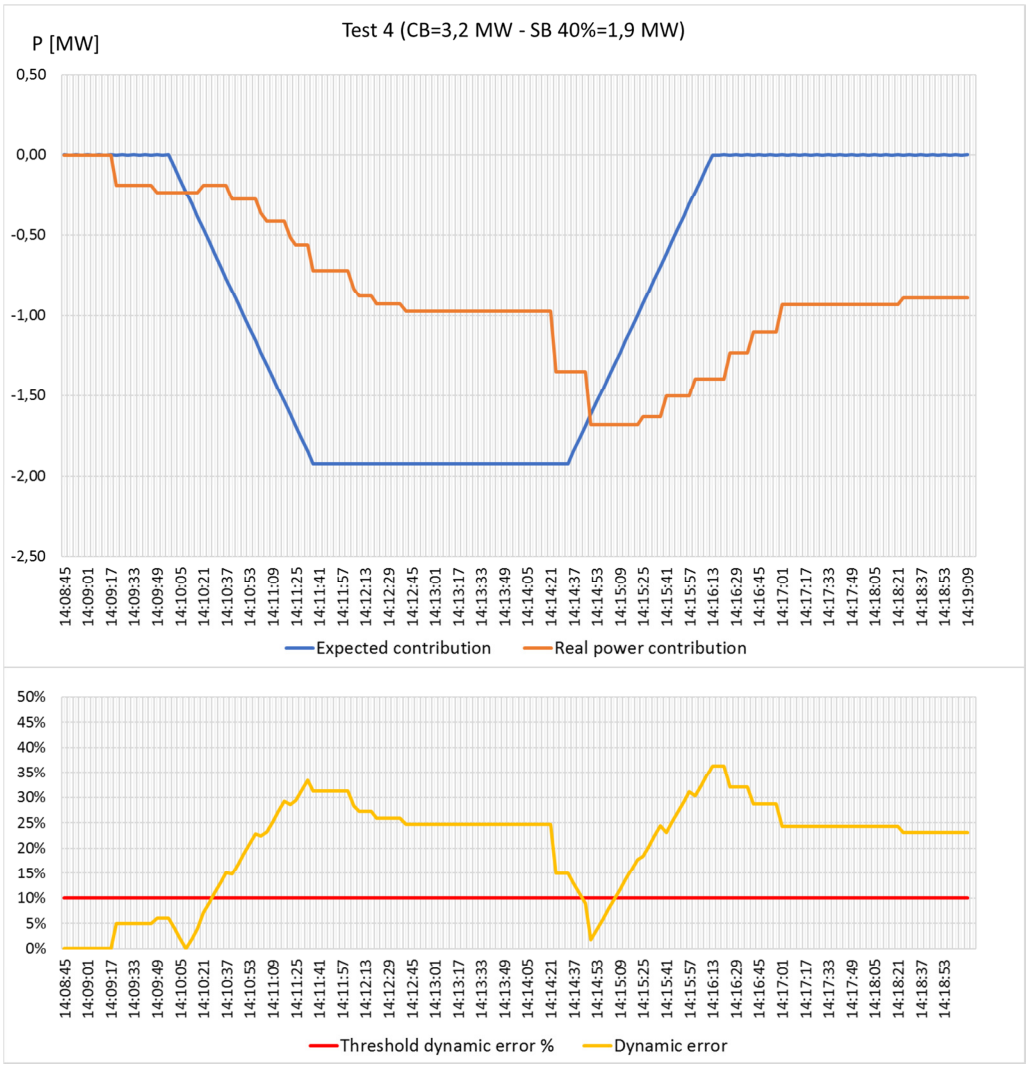

Figure 174: Analysis of the HV contribution of the VPP - Test 4 13/03/2019

Considering the response of each MW plant, generator 1 (Figure 175) and generator 4 (Figure 176) have the best ramp pattern and the shapes of the response are in line with the results of the previous test. In particular G4 shows that it is able to return near the declared program value, unlike what occurred in the previous test, where it could not follow the ramp-up (Figure 172).

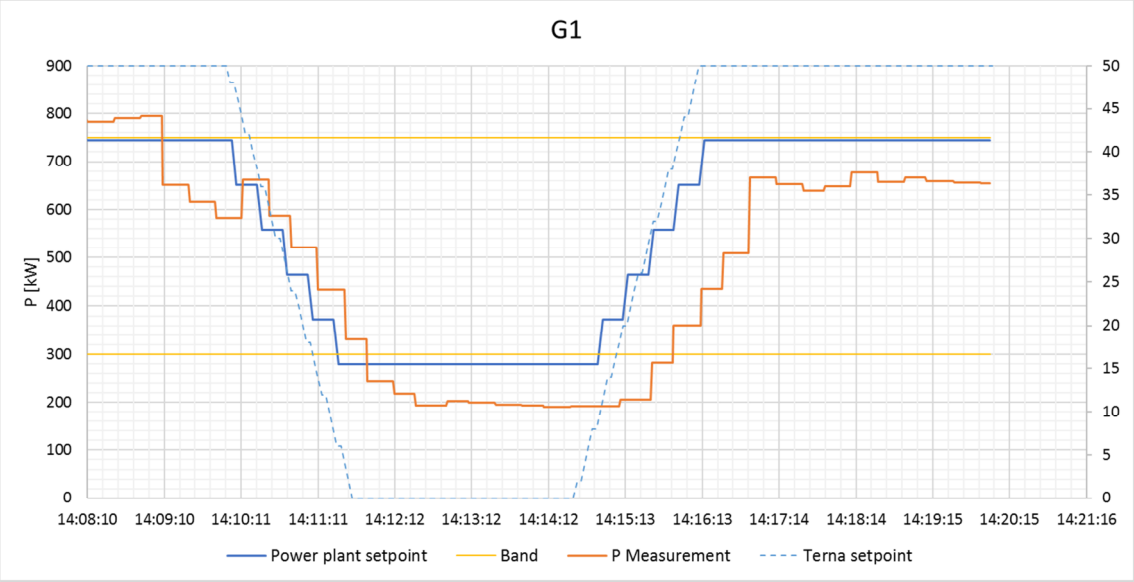

Figure 175: Performance of G1 connected at red transformer - Test 4 13/03/2019

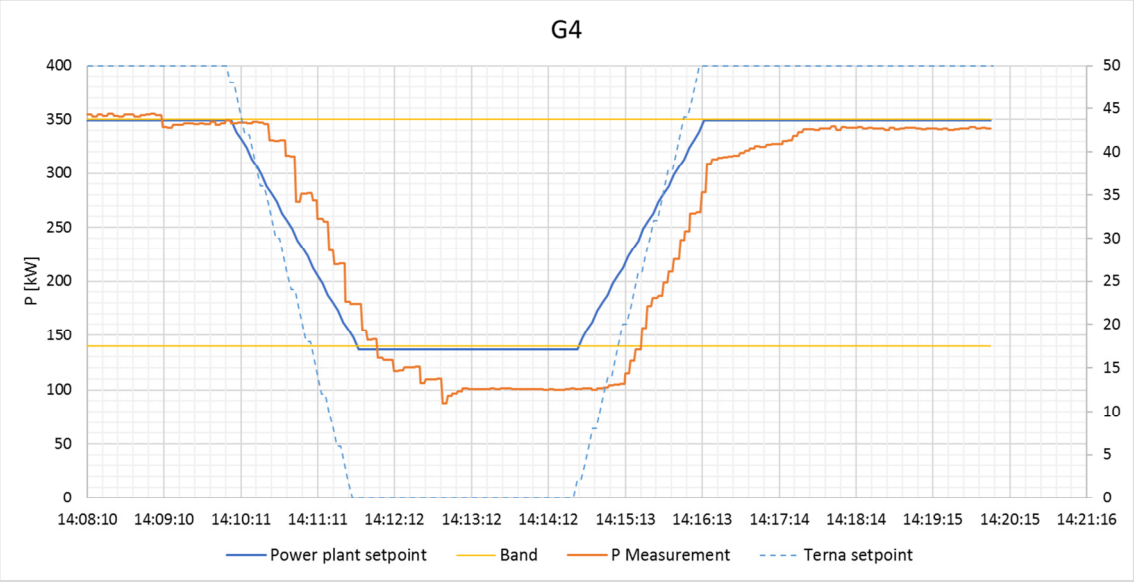

Figure 176: Performance of G4 connected at red transformer - Test 4 13/03/2019

Generator 6, as shown in Figure 177, performed a small step downwards an then turned off completely; this response can be explained considering that actually this power plant is powered by the same water flow as another power plant and its production depends on the production of the upstream hydro power plant that is not actively involved in the regulation test. When the upstream power plant was switched off, G6 stopped producing by resetting the active power measured at the terminals. This case shows how the specific characteristics of hydro generators can limit the effective involvement of the plants in an ancillary service that requires to guarantee a reliable provision.

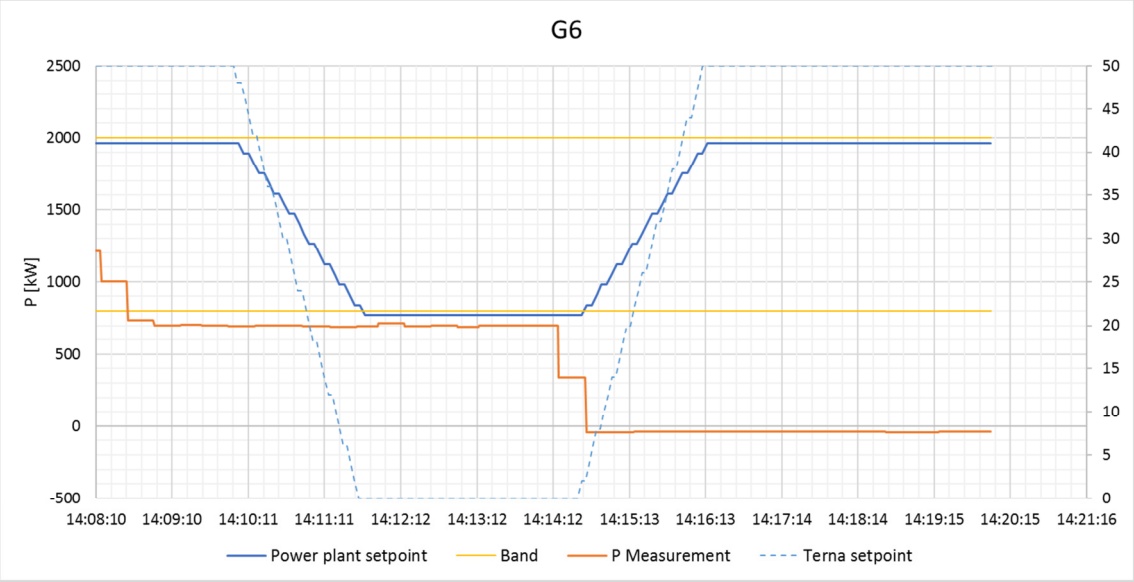

Figure 177: Performance of G6 connected at red transformer - Test 4 13/03/2019

The response of the last generator in regulation, G2, is reported in Figure 178. After having followed the ramp-down reducing the produced active power by about 45 kW, the power plant reaches the technical minimum and switches off, zeroing its production (in the central part of the graph); during the ramp-up, when the setpoint reaches again a value above the technical minimum (51 kW) it starts to adjust its production in steps to restore the power production trying to go back to the reference power.

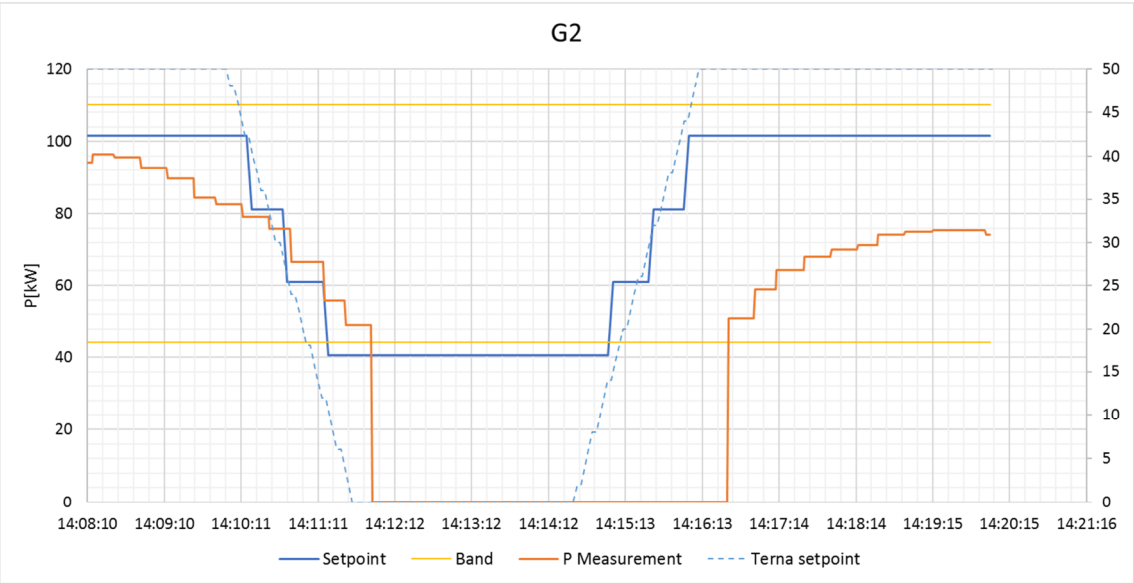

Figure 178: Performance of G2 connected at red transformer - Test 4 13/03/2019

The issues in the provision of the regulation are evident also in Figure 179, where it is represented the comparison between the sum of the single setpoints calculated by the MVRS and the sum of the active power measurements of the power plant involved in the regulation.

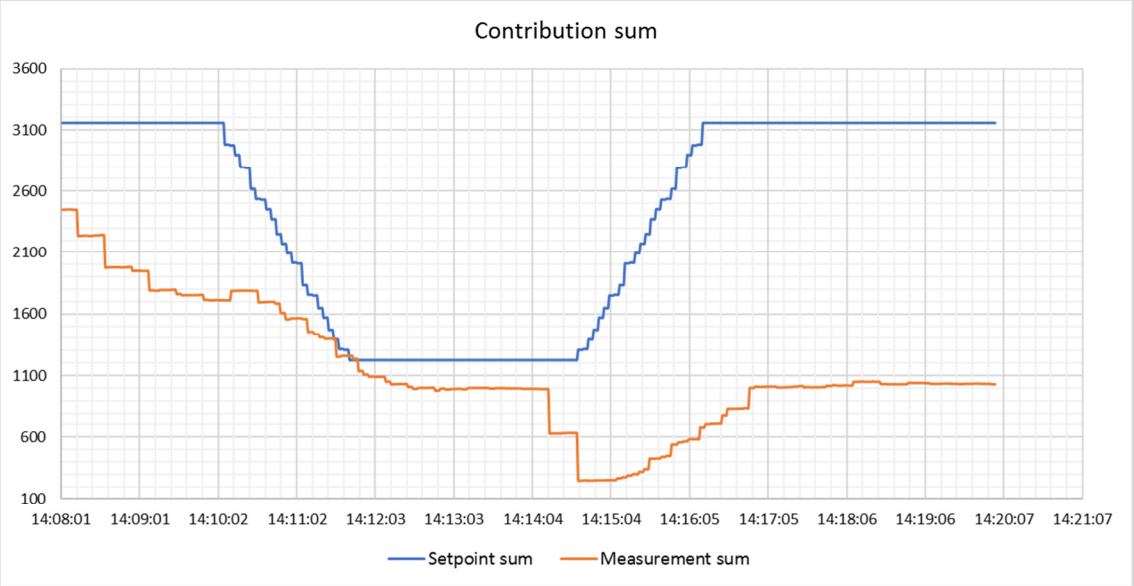

Figure 179: Calculated response of the aggregation with respect to the sum of the setpoints – Test 4

7 Challenges and lessons learnt

7.1 HVRS

The HV part of project aimed to evaluate the technical feasibility of the coordinated voltage regulation through power plants connected at the sub-transmission grid (132 kV) that at the moment are not involved in the hierarchical voltage regulation.

In fact, the Italian Grid Code provides that only relevant programmable power plants, i.e. thermal and programmable hydro power units, which have nominal power greater or equal than 10 MVA, are required to provide local voltage regulation (called primary voltage regulation). This service is mandatory and non-remunerated. Furthermore, the coordinated hierarchical voltage regulation is provided only by large power plants equipped with specific devices that enable to participate in the hierarchical control voltage. In particular, it is an obligation for traditional plants with a generator with a size of more than 100 MW or where required explicitly by the TSO

The evolution of the electrical system leads to extend the involvement of non-programmable renewable generating facilities in the operation of electric power system and the SmartNet project offered the chance to technically implement an equipment to provide a coordinated voltage regulation (the HVRS).

During the SAT (Site Acceptance Test) carried out with the HVRS, the technical feasibility of controlling the reactive production/absorption of hydro power plants in a coordinated manner was proved. As aimed, the HVRS cabinet allows the TSO to control the involved plants as a unique plant sending a single command from remote and automatically split the command among the controllable resources.

The experimentation highlighted critical issues to be taken into account in the implementation of this kind of the devices.

Firstly, **the communication chain plays a fundamental role:** the data flow, needed for the control of the plants, involves the TSO OC, the SAS, the HVRS and the power plant control systems (both the SCADA and the exciter or inverter). Besides, the communication must respect TSO's safety and quality standards.

The SAT detected initial communication problems that have been overcome by acting on the interface between the devices and improving the telecommunication channel with the power plants: **although the communication protocol adopted was the same, it has been evident the need to introduce dedicated assessments between devices of different manufacturers to obtain a reliable communication among devices**. The availability of the telecommunication accessibility is also necessary, which it is not obvious, considering that the controlled power plants are located in remote isolated places.

Once fixed the communication issues, the experimentation showed the possibility to coordinate the reactive contribution of different plants connected at the same substation, also of different technology (RES units and traditional generators), in order to contribute to the management of the grid. It also demonstrated the correct distribution of the command among the power plants involved in order to require the same contribution in term of percentage of available capability.

Regarding the implementation of the regulation command, **it was evident that the dynamic response of the generators strongly depends on the characteristics and the configuration of the local control equipment. The response, especially during the first tests, showed delay in the response and biases, mainly initial overshoots and fluctuations.**

The manufacturer of the plant's AVR has been involved in the project, both to realize the proper communication with the HVRS and to assess the configurations of the AVR to improve the dynamic response of the generators. An example is shown in Figure 180. The assessment aimed to optimize the control parameters reducing the delay and the overshoot, but the system shows a dependence between the two parameters and reducing the delay within certain limits the fluctuation increases. **The devices have been set using the best compromise between the two phenomena.**

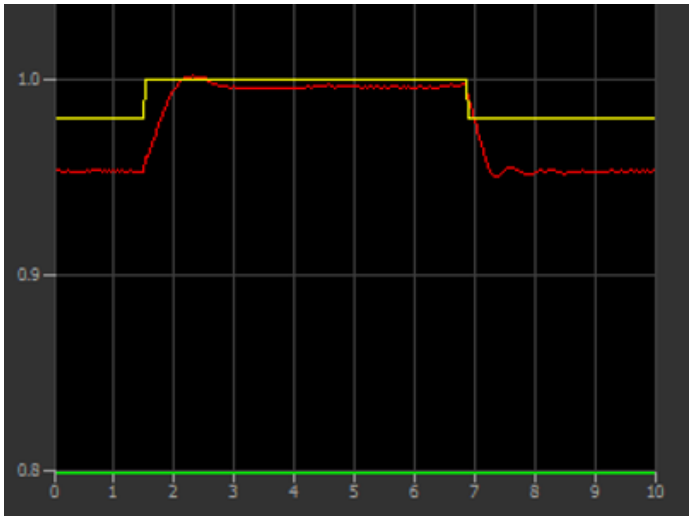

Figure 180: Interface of the AVR manufacturer to test the response of the system controller

Regarding the HV busbar voltage regulation, the influence of the reactive power modulation on the voltage at the transmission side of the substation is well represented in Figure 43. The tests showed a lower impact in reducing the voltage, due to both the asymmetrical nature of the generator's capability and the high short-circuit power level of the node of the grid.

It is clear that **the contribution of sources connected to the sub-transmission grid help to avoid reactive power internal loop and a regional coordination of their behavior with the regulation of the plants involved in the secondary voltage regulation could help to support the reactive power management.**

At the moment, this type of power plants cannot replace the ancillary services provided by big-sized traditional plants connected at the transmission level of the grid (380 kV and 220 kV) **both for the influence on the voltage modulation at the HV side of the transformer and for the quality of the dynamic response, that can hardly comply with the requirements of the service.**

In future applications, it will be possible to improve the response of the power plants acting on the coefficients of the HVRS correlation law to increase the reactive response for the same amount of voltage deviation from measured value at the busbar. **Another improvement will be the implementation of the proportional integral controller in order to refine the contribution required to the plants: instead of considering a fixed amount of reactive power variation following a change in measured voltage, a closed-control loop allows to compensate continuously the deviation from the target.**

7.2 MVRS

The MV part of the project aimed to involve, with a centralized control scheme, the DG in the management of the grid by the TSO, always respecting the DSO network constraints (voltage and overload).

As detailed in the report, a precondition for the integration of DERs in the system is the accuracy of the monitoring of the DSO grid. All data are collected by MVRS equipment and the distribution grid is represented at the TSO's HMI as nodal aggregations at the MV side of the interconnection point. In order to have an accurate and reliable awareness of the actual functioning of the grid needed to guarantee a safe and efficient management of the grid, in this application, the observability of the grid is obtained by a quite total measurement of the grid production and of the net power exchange with subtended DSO grids. The estimation algorithms implemented by Siemens and Selta have been tested with an offline analysis, because the real-time aggregations are mainly composed by measured sources in order to satisfy the accuracy and the reliability required for an ancillary service.

Both approaches were useful for understanding how to properly deal with the task and it is important to investigate the challenges/limits in the operation phase. On the one hand, the estimation algorithm of Selta based on sentinel measurements revealed the need to monitor a large quantity of power plants to reach the target accuracy. In addition, the choice of which plants to measure is based on an optimization problem and it does not seem easy to find standard rules to define the power plants where to install the meters. On the other hand, this allows to avoid measuring some generators. The accuracy of the estimation strongly depends on the kind of source and the location of each meter.

The estimation of the PV production proposed by Siemens has led to similar conclusions. The algorithm is based on real-time weather prediction acquired by solar radiation and temperature meters.

The analyses carried out showed that the estimation of the PV component is more accurate than the hydroelectric one.

In this case, the application of this approach has faced problems in the real-time acquisition of meter data and the experimentation has therefore demonstrated the necessity for further technological developments to have the access to this data.

On the technological point of view, the installed modules of Selta and Siemens showed positive outcomes regarding the collection and the correlation of different type of data.

The availability of continuous monitoring of the DG opens up the possibility to experience the provision of ancillary services from power plants connected in distribution grids. In particular, the project aimed to prove the technical feasibility of the hierarchical voltage control and the frequency/power regulation through aggregated MV plants, commanded as single VPPs. The MVRS implements the connection between the TSO OC and the MV power plants involved in the pilot and the coordination of the sources. **The project has enabled the successful handling of active and reactive power in the distribution grid, but the operational performance is not in line with TSO's technical requirements for these services yet.**

Regarding the frequency/power regulation, one of the most important aspect has been the relationship with the producers, that, in absence of remuneration, have only voluntarily participated in the test sessions.

During the tests, the activation of the MV sources (7 generators) caused a variation of the production of more than 6 MW and the regulation had effect also at the HV/MV transformer of the primary substation. The dynamic response of the power plants, as illustrated in paragraph 6.4, did not comply with the technical requirements of the service, due to delays in the communication and the inaccurate regulation of the AVR. In addition, the contribution in the service has to be evaluated at the HV side of the interconnection point, and the error at the transformer level is usually greater than the errors at the terminal of the MV power plant, probably due to overlap of errors. Moreover, the tests described in the report showed that the reliability and the quality of the regulation at the interconnection point does not depend solely on the power plant controller performance, but the trends are influenced by other elements of the network that are uncontrolled and unforeseeable. **In future developments, it should be important to improve the regulation of the controller of the power plants and to figure out how to avoid the indeterminateness due to the independence between the single power plant performance and the response at the interconnection point to comply with the technical requirements.**

In addition, the non-programmability of the hydro power plants involved in the project maintains uncertainties in the possibility to reach the setpoint. In fact, the aFRR requires that the power plant is able to maintain a constant production at the scheduled value and change the trend in accordance with the level sent by national regulator. The aleatory nature of the source can lead the TSO to require to the power plant an unreachable value or a value that is no longer reachable due to the reduction of water

level or the emptying of a small reservoir. Improvements on this aspect allowed for refining the value, by considering the last measurement available at the beginning of the ramp as the initial point, but the tests highlighted that this measure is not sufficient to completely remove the offset error.

On the other hand, the process showed an important aspect in the safe management of the grid: in the calculation of the active power capability of the VPP for the regulation, the MVRS takes account of the real-time operational point of the grid and the constraints also of the distribution grid. In this way, the amount of availability for the activation is already limited by potential network violations. In addition, during the regulation, the system automatically and continuously evaluates the operational condition and, in case of violation in the DSO grid, the MVRS interrupts the regulation and gives priority to the resolution of the potential violation. It allows the TSO to manage the available DER with respect to the DSO operation and network security.

The analyses carried out on the test results also revealed issues with the sampling of measurements and signals. As can be seen from the Figure 181, the 20-second update of the aggregated measurements at the interconnection point is not coherent with the 4-second setpoint and it is not compatible with safety assessment and closed-loop regulations, such as the aFRR, that require a response that varies rather quickly.

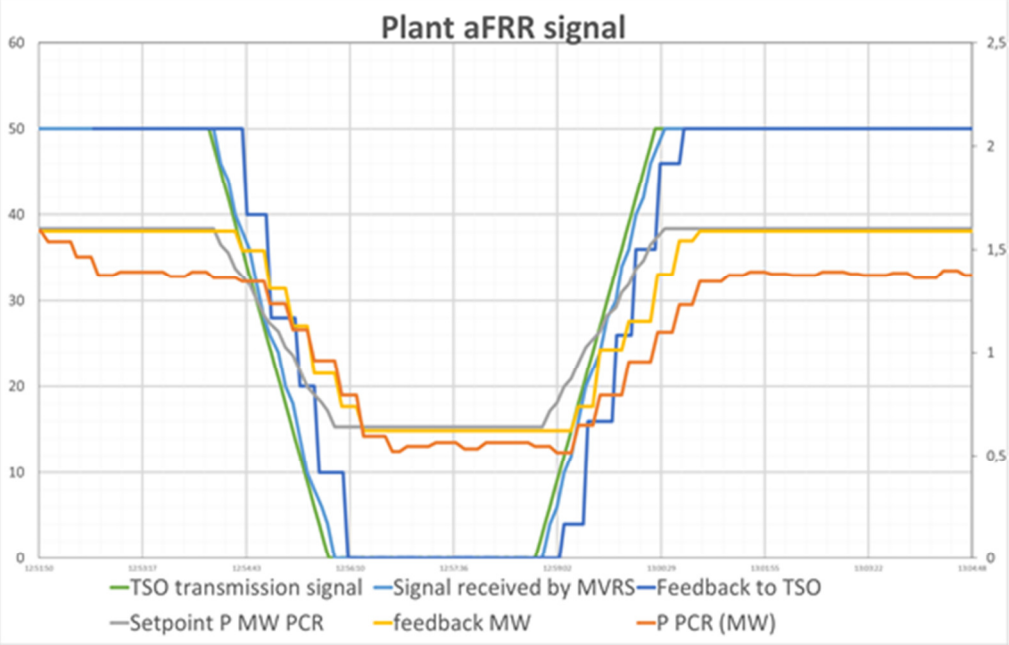

Figure 181: Time comparison of the signals exchanged during the f/P adjustment

The last functionality of MVRS tested is the voltage regulation. As detailed in paragraph 6.3.1, **the activation of reactive sources at the distribution grid showed benefits along the feeders of the DSO grid in order to maintain the overvoltage within defined limits. Regarding the effect on the voltage at the HV side of the primary substation, the outcomes showed little influence**: it is evident the

prevalent effect of the behaviour of power plants connected at the transmission grid. The modification in the absorption/production of reactive power of these last types of plants annul the contribution of the DG and the voltage trend follow the behaviour of the HV power plants.

As for the HVRS, the importance of this regulation is the possibility to coordinate the behaviour of the DERs with the rest of the controllable sources in order to avoid wasting reactive power due to loop of reactive power. In addition to the HVRS issues, in case of MV power plants it is also necessary consider the limited capability, particularly in under-excitation operation. Future improvements should aim to improve the technical performance of the controller installed to act on the power plant excitation.

8 Conclusions

This report presented in detail the Italian pilot within SmartNet project with the aim of explaining the experimentation context, the technical details of the devices implemented and the outcomes of the testing.

The purpose of the pilot was to experience in field new technologies in order to explore new approaches for the management of the grid, considering also the distributed generation (DG), the amount of which are supposed to grow in the near future.

The project included the development and the implementation in field of two innovative devices to control active and reactive power production of renewable energy sources (RES) connected at the sub-transmission and distribution grids in a coordinated way. The objective was to control this kind of power plants as a virtual power plant from the TSO point of view and to assess the extent to which DG and power plants connected at 132 kV grid could provide voltage regulation and automatic Frequency Restoration Reserve (aFRR).

The execution phase of the project allowed to collect important resulting data to evaluate both the functioning of the devices realized and the contribution of RES in ancillary services. The outcomes showed interesting results regarding the possibility of control in real-time the reactive exchange of high-voltage (HV) power plants and the active and reactive production of DG, through a centralized scheme controlled by the TSO but always taking into account the constrain of the distribution grid.

The devices here described represent tools that allow the TSO to manage and dispatch non-programmable power plants connected at lower voltage level of the grid[1]. This would result in an extension of the amount of power plants involved in the real-time management of the grid, with a view to the possible future replacement of big-sized traditional power plant with small-sized RES.

The first outcome of the pilot is the importance of an accurate and a complete monitoring of the distribution grid, which allows a safe and efficient centralized activation of resources at the distribution grid by the TSO. The observability part of the pilot implies the transmission of the measurement aggregations differentiated by source to the TSO control system, updated every 20 seconds. In this application, the required accuracy has been reached measuring almost all the interconnection points of all the MV power plants and the interconnection points of the subtended distributors. **The reverse engineering exercise, aimed at comparing the available measurements with the results of the estimation algorithms that were run simulating a reduction of the installed meters, showed that this accuracy is guaranteed by a high coverage-rate of direct measurements in field, to estimate the power production characterized by high unpredictability (at least the 60% of the**

[1] Please consider that when the SmartNet pilot project started in Italy the DG were still not allowed to play in the market.

installed production in case of hydro power plants). The outcomes also showed the dependence of the accuracy on the type of estimated resource (solar production seems easier to be estimated based on weather data) and on the choice of the sentinel measurement that significantly influences the result and is not based solely on the size of the power plants.

In the provision of the ancillary services, it is also evident that the data update rate of 20 seconds is not adequate to evaluate the dynamic response when DER are providing active power services like aFRR, since in the provision of aFRR, the power production varies rather quickly (about each 4 seconds and the calculation of the closed-loop amount of the aFRR activation is updated every 2 seconds).

Regarding the contribution to the provision of ancillary services, the tests proved the technical feasibility to control the aggregated production and the reactive power exchanged by power plants with a unique setpoint sent directly by the TSO, but the results also showed difficulties in the regulation on the HV side of the grid:

- Regarding the voltage regulation, the effect of the behaviour of big-sized plants connected in the area prevails over the small-sized hydro contributions, but the advantage is the possibility to reduce the recirculation of reactive power among generators and the waste of regulating resources. The project proved the possibility to coordinate the reactive power between TSO and DSO through coherent reactive power activations. In any case, further studies are necessary to improve the dynamic response of these power plants to meet what is currently required for the service.
- Regarding the f/P regulation, the tests have led to the activation of 6 MW in distribution grid and, thus, the experimentation has verified the possibility to activate services from DG in accordance with network constraints. However, the dynamic response does not comply with an aFRR service in terms of both delay and accuracy. The project highlighted future opportunities for manufacturers to improve the performance of the regulation and of the communication chain (for instance, regarding information and communication technologies, as well as power plant controllers). Furthermore, it is evident the need to find a way to overcome the unpredictability of RES: it is not possible to guarantee a contribution in the service without a production plan or without considering the combination with other types of flexibility capable of compensating the performance errors presented during the tests.

In conclusion, the pilot provided an interesting preliminary study to evaluate feasibility of the project and it opened the door to future improvements to understand how to exploit new flexibilities of the electrical system to support the TSO in the grid management.

9 References

[1] Grid Development Plan 2019 - http://download.terna.it/terna/0000/1188/36.PDF

[2] ARERA Resolution 646/2015/R/eel

[3] ARERA Resolution 300/2017/R/eel

[4] G. Guida, G. Bruno, L. Ortolano, M. Poli, M. Palleschi, G. Migliavacca, D. Moneta, C. Arrigoni, F. Zanellini, G. Della Croce, A. Bridi, "Smart TSO-DSO interaction schemes and ICT solutions for the integration of ancillary services from distributed generation", 2018 Cigre Session

[5] SmartNet website: http://smartnet-project.eu/

[6] Italian Network Code: www.terna.it/it-it/sistemaelettrico/codicedirete.aspx